DISS. ETH NO. 29805

Disrupted Lifelines

Modelling natural hazard risks to basic services through interdependent critical infrastructure

A thesis submitted to attain the degree of

Doctor of Sciences
(Dr. sc. ETH Zurich)

presented by

Evelyn Mühlhofer
MSc ETH MTEC, ETH Zurich
born on 5 April 1994

accepted on the recommendation of

Prof. Dr. David N. Bresch
Prof. Dr. Elco E. Koks
Prof. Dr. Giovanni Sansavini
Prof. Dr. Erin Coughlan de Perez

2023

When the winds and the storms subsided, the sheer scale of the catastrophe was on display. Glass shards littered the roads. Trees, entangled in electrical wires, obstructed entrances to homes.†

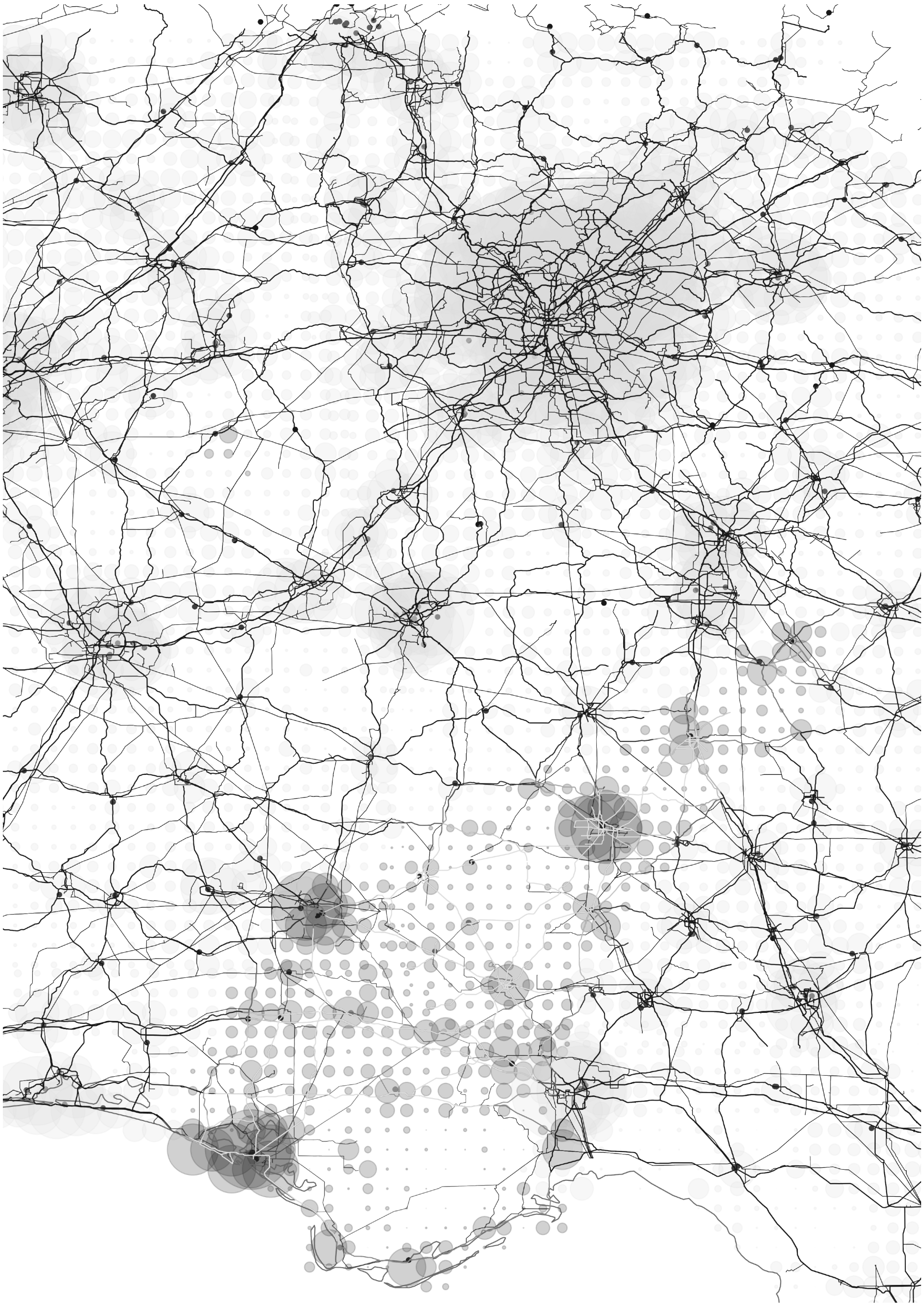

† Jonathan Moens, Inside Climate News, March 22, 2022. *Hurricane Michael Hit the Florida Panhandle in 2018 With 155 MPH Winds. Some Black and Low-Income Neighborhoods Still Haven't Recovered*

Figure: Infrastructure damages and healthcare service disruptions from Hurricane Michael across the Florida Panhandle. Shown are power lines, primary roads, hospitals and population clusters. Computed using the infrastructure network module in CLIMADA.

Abstract

Critical infrastructure ensures essential functions in every-day life. It enables access to power, healthcare, education, and other basic services, and contributes to the attainment of all 17 Sustainable Development Goals. However, while infrastructure investments have reached unprecedented levels globally, infrastructure exposure to natural hazards has equally risen. Climate-related direct damage to critical infrastructure surpasses 730 billion USD yearly, and is projected to increase in a changing climate. Risk to critical infrastructure must be understood as risk to people's well-being and to sustainable development, and it is crucial to recognize challenges towards climate-resilient infrastructures and services. While critical infrastructure is ubiquitous, knowledge on locations, vulnerabilities, and potential exposure to relevant natural hazards is not. Further, critical infrastructure comprises networked, interdependent systems, in which asset damages can lead to cascading failures along these connections. Services may consequently be disrupted far beyond physically affected areas. These disruptions may affect different parts of society in different ways. Currently, practices in natural hazard risk assessment, technical system understanding, and social vulnerability considerations do not interlink adequately, which hampers service-centred and equitable adaptation of infrastructure to a changing climate.

This thesis aims to understand natural hazard-induced critical infrastructure risks at national scales, mindful of interdependencies between these systems and their embedding in society. Conceptually, this is approached in three stages: I first develop a harmonized modelling framework from natural hazard impacts to interdependent critical infrastructure and basic service disruptions. I then use this modelling framework for in-depth single event and large-scale comparative studies in various world regions; to explore drivers of service disruption risk and resilience by exposing models of real-world infrastructure systems to diverse hazards, and to evaluate adaptation options under a service-centred perspective.

The central tool of this research, a flexible, spatially explicit infrastructure risk modelling framework, integrates representations of interdependent infrastructure systems into the open-source natural hazard risk assessment platform CLIMADA. The event-based computation engine simulates infrastructure damage from hazard, infrastructure asset and vulnerability data, triggers failure cascades along network dependencies, and estimates resulting basic service disruptions experienced by the population. This modelling framework relies on two major developments. First, I show that that incorporating high-resolution exposure data, for instance from crowd-sourced data platforms such as OpenStreetMap, is a prerequisite for (direct) infrastructure risk assessments; it also opens doors for any multi-faceted climate risk assessments beyond coarse-scale monetary asset and population layers. To facilitate access to this data universe, as a light-weight, Python-based data extraction tool (OSM-flex) was developed for use within CLIMADA. Second, the modelling framework generically represents infrastructure and population as elements of an interdependent network, and incorporates book-keeping on infrastructure functionality and services delivered. Drawing on infrastructure modelling approaches and graph theory, I devised a set of simple logical and spatial heuristics to infer dependencies between different infrastructure assets, and between end-users and infrastructures, from geo-spatial data. This allows to portray the same high-resolution exposure layers used for risk assessments mutually as directed topological networks with functional states, service sources, and service sinks. The method requires comparatively little additional system knowledge, and caters to efficient analyses at large spatial scales. A validated case study on hurricane Michael across the Florida Panhandle demonstrated that the hence-developed modelling framework reproduces important failure dynamics among infrastructure networks, can be re-calibrated with available impact data, and provides a novel spatial population map of service disruptions.

Large-scale trends from over 700 tropical cyclone and flood events in 30 countries indicate that physical infrastructure damages and directly exposed population - core metrics of classic risk assessments - are insufficient predictors for service disruptions. I find that in 84% of floods and 65% of tropical cyclones, service disruptions spread well beyond the area directly affected by the hazard. These broader disruptions are shown to result from functional failure cascades triggered by infrastructure interdependencies and physical access constraints. I further show that services in richer and more infrastructure-dense regions tend to be more resilient, yet even there, certain event constellations can trigger failure cascades.

Analyses also show that services are subjected to hazard-specific vulnerabilities. These are based on infrastructure-specific vulnerabilities, but are further amplified along system dependencies: floods particularly impact road-access dependent services, strong winds power-dependent services. Resolving flood, surge and wind sub-hazards in a case study on tropical cyclone Idai in Mozambique further revealed the importance of considering the joint impacts of compound events on infrastructure systems, as system functionality thresholds or service access conditions may only jointly be surpassed.

The multiple, entangled constituents of infrastructure risks have implications for devising resilience-enhancing strategies: Climate-proofing basic services cannot solely focus on avoiding asset damages, as adaptation options which avoid structural damage may not (linearly) translate into service resilience. In a suggestion to visualize high-level strategic trade-offs, I show that service resilience, contribution of indirect failures to disruptions, and base-line service access rates may be considered to decide among investing in protecting existing infrastructure, enhancing system redundancy, or building more infrastructure.

This thesis shows the need to explicitly consider system interdependencies and spatially resolved, real-world hazard and exposure data to adequately comprehend service disruption risks, and provides a tested modelling framework for doing so. By exploring impacts of natural hazard to basic services, this research bridges academic silos, and contributes to a more holistic and systemic focus on risk beyond monetary perspectives. The network-based approach further allows for a deeper understanding of the failure-triggering processes behind observed impacts, instead of purely aggregating loss metrics. This contributes a readily-applicable tool to scenario-based stress testing principles for resilient infrastructures, and may enable decision-makers to plan infrastructure investments with a priority on service resilience.

Zusammenfassung

Kritische Infrastrukturen sind essenziell für einen funktionierenden Alltag. Sie stellen den Zugang zu Strom, Gesundheitsversorgung, Bildung und anderen Dienstleistungen der Grundversorgung sicher und tragen zum Erreichen aller 17 Ziele für Nachhaltige Entwicklung (engl.: *Sustainable Development Goals, SDGs*) bei. Globale Infrastruktur Investitionen haben einen Höchststand erreicht, was auch mit einer entsprechenden Exposition gegenüber Naturgefahren einhergeht. Klimabedingte Direktschäden an kritischen Infrastrukturen überschreiten jährlich 730 Milliarden USD und werden aufgrund des Klimawandels voraussichtlich weiter steigen. Infrastruktur Risiken müssen als Risiken für menschliches Wohlergehen und nachhaltige Entwicklung gesehen werden; ein besseres Verständnis der Herausforderungen hinsichtlich Klima-resilienter Infrastrukturen und Grundversorgung ist daher unabdingbar. Kritische Infrastrukturen sind allgegenwärtig, das Wissen um deren geografische Lage, Verwundbarkeit und potenzielle Gefährdung jedoch nicht. Kritische Infrastrukturen bestehen zudem aus netzwerkartigen, wechselseitig abhängigen (*interdependenten*) Systemen, innerhalb welcher Schäden zu Kaskadenversagen führen können. Dadurch kann es zu Störungen und Versorgungsengpässen in der Grundversorgung kommen, welche weit über direkt betroffene Gebiete hinausgehen. Versorgungsengpässe können wiederum unterschiedliche Auswirkungen für Betroffene verschiedener Bevölkerungsschichten haben. In gegenwärtigen Vorgehensweisen zur Risikobeurteilung von Naturgefahren knüpft das technische Systemverständnis jedoch nicht ausreichend an die Beurteilung von sozialen Verwundbarkeiten an, was eine gerechte Anpassung von Infrastrukturen an den Klimawandel erschwert.

Diese Arbeit hat zum Ziel, Naturgefahren bedingte Risiken kritischer Infrastrukturen auf nationalen Skalen zu verstehen, unter Berücksichtigung von Interdependenzen und deren Einbettung in die Gesellschaft. Konzeptuell wird dies in drei Abschnitten getan: Zunächst entwickle ich ein Rahmenwerk für die harmonisierte Modellierung von Naturgefahren Auswirkun-

gen auf interdependente kritische Infrastrukturen und Grundversorgungsausfälle. Dieses Modell verwende ich dann für detaillierte Ereignisstudien sowie für grossangelegte Vergleichsstudien in unterschiedlichen Weltregionen; einerseits, um Treiber von Risiko und Resilienz hinsichtlich der Grundversorgung auszumachen, indem ich Modelle realer Infrastruktursysteme Naturgefahren aussetze, andererseits, um Anpassungsmassnahmen unter einem Versorgungsblickwinkel zu evaluieren.

Das zentrale Werkzeug dieser Forschungsarbeit, ein flexibles, räumlich explizites Infrastruktur Risikomodell, integriert Darstellungen von Infrastruktursystemen anhand komplexer Netzwerk Theorie in das öffentlich zugängliche Naturgefahren Risikomodell CLIMADA. Das Ereignis-basierte Modell simuliert Infrastrukturschäden aus einer Kombination von Daten zu Gefährdung, Exposition und Verletzlichkeit. Es setzt Störkaskaden entlang Abhängigkeiten in Bewegung und berechnet daraus resultierende Ausfälle der Grundversorgung für die Bevölkerung. Diesem Modell liegen zwei nennenswerte Entwicklungen zugrunde. Erstens zeige ich, dass die Berücksichtigung hochaufgelöster Expositionsdaten, etwa von Plattformen wie OpenStreetMap, eine Vorbedingung für die Beurteilung von (direkten) Infrastruktur Risiken ist; es öffnet zudem den Zugang zu facettenreichen Risikobeurteilungen für jegliche Grössen jenseits grobaufgelöster monetärer und bevölkerungsbasierter Grundraster. Um Daten effizient zu extrahieren und in CLIMADA zu verwenden, wurde eigens ein Python-basiertes Tool (OSM-flex) entwickelt. Zweitens stellt das Modell jegliche Infrastrukturen-und Bevölkerungsdaten als zusammenhängendes Netzwerk dar, und führt Buchhaltung über Funktions- und Versorgungszustände. Basierend auf Methoden in Infrastruktur Forschung und Graphentheorie habe ich simple logische und räumliche Heuristiken entwickelt, um Abhängigkeiten zwischen verschiedenen Infrastruktur Komponenten und der Bevölkerung anhand derer Geo-Daten zu erschliessen. Dies erlaubt es, dieselben Expositionsdaten, welche zur Risikobeurteilung verwendet wurden, als topologische, gerichtete Netzwerke mit Funktionalitäts-, Versorgungslieferung- und Versorgungsnachfrage Attributen zu repräsentieren. Die Methode benötigt relativ wenig weiterführendes Systemwissen und eignet sich für effiziente Analysen über grosse räumliche Skalen.

In einer validierten Fallstudie zu Hurrikan Michael in Florida wurde aufgezeigt, dass das entwickelte Modell wichtige Ausfalldynamiken zwischen Infrastruktur Netzwerken wiedergibt, mit verfügbaren Auswirkungsdaten re-kalibriert werden kann und neuartige räumliche Karten von Versorgungsausfällen aufzeigt.

Eine Studie über 700 tropische Zyklone und Fluten in 30 Ländern veranschaulicht, dass physische Infrastrukturschäden und Anzahl Direktbetroffener - Kernzahlen in der klassischen Risikobeurteilung - unzulänglich sind, um das Ausmass von Grundversorgungsstörungen hervorzusagen. Ich zeige auf, dass in 84% aller Fluten und 65% aller tropischen Zyklone Versorgungsausfälle über die direkt betroffene Region hinausgehen. Diese Störungen können auf Kaskadenversagen und physische Zugangsbeschränkungen zurückgeführt werden. Zudem zeige ich, dass die Grundversorgung in reicheren und dichter bebauten Regionen in der Regel widerstandsfähiger ist, jedoch selbst dort in gewissen Fällen Kaskadenversagen zu beobachten sind.

Resultate beleuchten zudem, dass verschiedene Basisdienstleistungen unterschiedlich stark verletzlich sind durch unterschiedliche Naturgefahren. Dies beruht auf Gefährdungs-spezifischen Verletzlichkeiten gewisser Infrastruktur Komponenten, welche durch Systemabhängigkeiten weiter verstärkt werden: Fluten beeinträchtigen besonders Dienstleistungen, welche auf Strassentransport angewiesen sind, Stürme hingegen Dienstleistungen, welche Strom benötigen. In einer Fallstudie zum tropischen Zyklon Idai in Mosambik, in welcher Flut, Sturmflut und Sturm explizit behandelt wurden, wurde zudem verdeutlicht, dass Untergefahren und Mehrfachgefahren signifikante Auswirkungen auf Infrastruktursystem haben können, da diese potenziell nur unter gemeinsamer Betrachtung System-oder oder Zugangsschwellen überschreiten.

Die verschiedentlichen und verwickelten Treiber von Infrastruktur Risiken haben wichtige Implikationen für Strategien zur Resilienzverbesserung: Klimaresiliente Grundversorgung kann nicht einzig auf strukturelle Anpassungen zur Vermeidung physischer Infrastruktur Schäden zurückgreifen. In einem Vorschlag zur Visualisierung von Trade-Offs zeige ich auf, dass die Resilienz verschiedener Basisdienstleistungen, Anteil indirekter Kaskadenausfälle, und Grundversorgungsrate zusammen betrachtet werden können, um zwischen folgenden Strategieoptionen abzuwägen: Investition in den Schutz bestehender Infrastruktur, Verbesserung der Netzwerkredundanz, Investition in neue Infrastruktur.

Diese Arbeit zeigt die Notwendigkeit auf, Systemabhängigkeiten und räumlich explizite, reale Naturgefahren-und Expositionsdaten zu berücksichtigen, um

Grundversorgungsrisiken adäquat abzubilden. Hierfür wurde ein getestetes Modell bereitgestellt. Durch die Ausleuchtung von Auswirkungen verschiedener Naturgefahren auf unterschiedliche Basisdienstleistungen wurden Brücken geschlagen zwischen akademischen Disziplinen, und ein Beitrag geleistet zu einer ganzheitlichen Betrachtung von Risiko abseits monetärer Blickwinkel. Die Netzwerk-basierte Methodik ermöglicht zudem, Störprozesse hinter den beobachteten Auswirkungen zu verstehen, anstatt auf aggregierten Schadenssummen zu verbleiben. Als ein einfach anwendbares Werkzeug für Szenario-basierte Stress-Tests im Infrastrukturbereich kann es Entscheidungsträgern helfen, Infrastrukturinvestitionen mit einem Fokus auf resilientere Grundversorgung zu tätigen.

Contents

Acknowledgements

This thesis would unlikely have been written, if it were not for the sometimes eccentric, mostly refreshing, and always challenging views of David on the role of academia in society, which inspired me to pursue a PhD. This thesis would be a different one without Elco and his incessant generosity in supervising and mentoring, his capability to do splendid research while being also just a very pleasant person, dedicated father, and role model. Giovanni did not only introduce me to the world of reliability engineering, but also to a world that can be encountered with a bigger smile and curiosity than I ever imagined. Erin generously accepted to evaluate this work and its implications.

A PhD is, as David puts it, a journey of personal development, yet one that has been majorly influenced by my colleagues at the Weather and Climate Risks group: Simona Meiler, who's stare of ultimate focus and determination has not only reminded me countless times to work, but also earned her the doubtful honour to be the bouncer at my wedding; Samuel Lüthi, who is a great conversation partner irrespective of my moods and the best Berlin conference accompaniment; Carmen Steinmann, who's empathetic way of interacting has made us all more aware of non-violent communication and of Indian wedding series; Zélie Stalhandske, who has shared not only student supervisions, but also many wonderful days in Sweden and in France; Chahan Kropf with his brilliant analytical mind and gin stash; Lukas Riedel, who opened Pandora's box to GitHub worklflows; Alessio Ciullo, who took understatement of his value as a colleague to the next level; Timo Schmid, Leonie Villiger, and Dahyann Araya, who will make my future work easier; Mannie Kam, who increased the tea quality in our coffee-centric group; and Jamie McCaughey, who provided direly needed perspectives from social sciences and good command of the English language. Sarah Spitzauer has gone out of her way as administrative assistant by also organising Japanese lunches and helping to reserve cars in Kazakhstan. Emanuel Schmid has prevented CLIMADA from drowning in failure messages. As my research career has started long before this thesis, former members made a significant contribution to my remaining in this group: Thomas Röösli, Samuel Eberenz, Marius Zumwald, Benedikt Knüsel, Maurice Skelton, Luise Fischer, Gabriela Aznar-Siguan, Rachel Bungener, and Chris Fairless.

My work was broadened by the contribution of Bachelor and Master students, who shed light on aspects of this research which might else have remained unexplored: Dewi Westra, Annina Wiher, Michelle Ammann, Jakob Burkhardt and Gabriela Espejo.

Pursuing a PhD is also a lonely task over significant stretches, and exchanges and collaborations with fellow infrastructure risk researchers a treat. Roman Schotten and Alex Chatzistefanou merit particular mentioning, together with Elco's team at the Infrastructure Risk and Resilience group, especially Sadhana Nirandjan, Mengqi Ye, and Siyu Gao, who contributed to Amsterdam becoming a second academic home.

Andrés has had infinite patience and accompanied me tirelessly through the four Novembers which have passed since starting this journey. My entire family has laid - consciously or unconsciously - many of the foundations for this work; specifically my parents, Sandra and Mike, my grandmother, Traudl, and my brothers, Valentin and Sebastian. Lastly, my friends did their best to ensure that the ratio of work to free-time was healthily skewed to the latter; members of the Nomadic Mountain WG and the atomic garbage are particularly to be credited with this.

List of Abbreviations

CI	critical infrastructure
CIN	critical infrastructure network
ECA	Economics of Climate Adaptation
FL	flood
GCF	Green Climate Fund
IFRC	International Federation of Red Cross and Red Crescent Societies
IPCC	Intergovernmental Panel on Climate Change
NH	natural hazard
OSM	OpenStreetMap
SDG	Sustainable Development Goal
TC	tropical cyclone
UNDRR	UN Office for Disaster Risk Reduction

CHAPTER 1

Introduction

1.1 Motivation

In July 2021, parts of Western Europe experienced a 1-in-400 years rainfall event that led to severe flooding. It caused over 5 billion Euros in damage to property and infrastructure, and over 200 fatalities (Kreienkamp et al. 2021). The severity of impacts took many local governments and citizens by surprise, despite prior weather warnings (ibid.). Evacuations, emergency response, and repairs were hampered due to power outages, telecommunication disruptions, and a dysfunctional transport systems, which left some villages inaccessible for days (Koks, van Ginkel, et al. 2022). Restoration of services proceeded slowly in the worst-hit area, with schools and hospitals remaining closed, and gas supplies being cut for months (ibid.). Climate change had made the occurrence of this event up to nine times more likely compared to pre-industrial times (Kreienkamp et al. 2021).

This incident was drastic for the region. However, many similar accounts across the globe contribute to a body of systematic evidence: As infrastructure investments are at an all-time high (Thacker, Adshead, et al. 2019), infrastructure systems and services are more exposed than ever to natural hazards. 25% of the world's busiest airports are located at less than 10 metres above sea level (Yesudian and Dawson 2021); around 27% of all road and railway assets, almost 95% of all ports, and power generation plants in nearly every country of the world are exposed to at least one natural hazard (Koks, Rozenberg, Zorn, et al. 2019; Nicolas et al. 2019; Verschuur, Koks, and Hall 2022).

Global damages from natural hazards to infrastructure are considerable, with average annual estimates around USD 3.1 - 22 bn (road and rail), 4 bn (ports), 15 bn (power plants), and 732-845 bn (total) (Cardona et al. n.d.; Koks, Rozenberg, Zorn, et al. 2019; Nicolas et al. 2019; Verschuur, Koks, and Hall 2022). By 2030, this risk is projected to increase for all sectors in transportation, telecommunications, energy and water (McKinsey Global Institute 2020).

As critical infrastructure provides society with basic services such as access to power, healthcare, and education, they ensure the most essential functions in every-day life and contribute to the attainment of all 17 Sustainable Development Goals (SDGs) (Thacker, Adshead, et al. 2019). The wider socio-economic consequences of critical infrastructure disruptions are therefore even more detrimental. Future coastal and extreme flooding could disrupt up to 20% of global flights and 66% of inter-urban road trips (Y. He et al. 2022; Yesudian and Dawson 2021); unstable electricity supplies cost firms in low and middle income countries nearly USD 200 bn (Rentschler et al. 2019) and port disruptions put at least USD 122 bn of economic activity at risk - each year.

Protecting critical infrastructure and ensuring continuous, high-quality basic services is of importance in policy-making on many levels: as a target of the Sendai Framework for Disaster Risk Reduction (UNDRR 2015, §25 e, f), within the the European Programme for Critical Infrastructure Protection (European Commission 2008), as key representative risk and major accumulator of global adaptation costs until 2050 in the IPCC's latest assessment report (O'Neill, van Aalst, et al. 2022; Thacker, Adshead, Daniel, et al. 2021), and within climate-resilient implementation principles of multilateral donors such as the Green Climate Fund.

Significant challenges are on the way to climate-resilient infrastructure and services. While infrastructure is ubiquitous, knowledge on locations, building quality, vulnerabilities and potential exposures to all relevant natural hazards is unevenly distributed across the globe. Critical infrastructure consists of networked systems, which depend on each other to provide services; such interdependencies can enhance tolerance to failures if well managed or lead to cascading failures, spilling beyond physically affected areas, and hampering recovery (Guidotti et al. 2016; Nan and Sansavini 2017; Zorn, Pant, et al. 2020). Yet, infrastructure interdependencies are often poorly understood (cf. *SWD(2013)318* 2013) and systemic approaches for analysis are encouraged (Bresch, Berghuijs, et al. 2014; Zio 2016), but constrained by silo-thinking in specialized (research) communities (Pant, Hall, and Blainey 2016). Even in civil protection, daily emergency management or humanitarian aid, awareness of the dependency on infrastructure services has been hardly integrated into existing concepts (Fekete 2019). It is further not well understood which differential impacts critical infrastructure failures may have on different parts of the society, as the gap between technical system understanding, social vulnerability and equity considerations remains large (Garschagen and Sandholz 2018).

Risks to critical infrastructure are risks to basic services, and a deeply intertwined socio-technical problem. Understanding the role of infrastructure during natural disasters can only be done jointly, considering interdependencies between infrastructure networks, their embedding within the natural and built environment, and society (Thacker, Adshead, et al. 2019).

1.2 Aim of this thesis

This thesis aims to

> understand natural hazard-induced critical infrastructure risks, mindful of the interdependent, networked nature of the systems, and their consequences on society in which they are embedded.

By exploring spatially explicit risks from natural hazards to structural assets, and evaluating those impacts on service disruptions experienced by the population, in a globally consistent manner, this research contributes to an enhanced understanding of how basic services can be made more resilient in a world affected by climate change.

1.2.1 Research questions

RQ1 How to capture the impacts of natural hazards on interdependent critical infrastructure, and their consequences on basic service disruptions, at national scales, in a globally consistent and open-source manner?

- RQ 1.1 · · · How do critical infrastructure components depend on each other for delivery of basic services to end-users; can dependency heuristics be devised?
- RQ 1.2 · · · Can complex network modelling and natural hazard risk modelling be aptly combined to build an end-to-end framework from physical infrastructure impacts to service disruptions?
- RQ 1.3 · · · How do resolution, quality, and spatial availability of data on infrastructure assets, end-users, dependencies, hazard-specific vulnerabilities, and functional performance affect the representation of these socio-technical systems?

RQ2 What drives risk and resilience of basic services during natural hazard events?

- RQ 2.1 · · · Do spatial patterns of physical infrastructure impacts differ from those of infrastructure failures and service disruptions?

RQ 2.2 ··· Do different hazards, multi-hazards and sub-hazards cause distinct impacts to interdependent critical infrastructure systems?

RQ 2.3 ··· How does the interplay of specific infrastructure system characteristics and hazard exposure influence the resilience of basic services?

RQ3 How do social vulnerabilities and adaptation interventions modulate basic service risks?

RQ 3.1 ··· How can adaptation measures for interdependent infrastructure be evaluated under a systemic lens, mindful of service resilience outcomes?

RQ 3.2 ··· How are different population groups impacted by the consequences of natural hazard-induced service disruptions?

1.2.2 Working hypotheses

In order to bridge research efforts across various communities, and to cater to the criteria of global consistency, large geographic scales, and open-source data and methods, three working hypotheses guided this research process:

Resolution hypothesis: A meaningful compromise can be found to reconcile the trade-off between model resolution demanded by the large scales at which natural hazards occur and the degree of model sophistication needed to represent the functional processes and interdependencies in critical infrastructure systems.

Interoperability hypothesis: Diverse layers of information, pertaining do different stages along a chain of impacts, can be tailored and harmonized to deduce a single framework from hazards to service disruptions.

Consistency hypothesis: There is ‘sufficient’ open-source data and generic enough heuristics to design a model which is coherent (standardized) in its way of computing global impacts, yet locally meaningful.

1.2.3 Data and Methods

The methodological centre-piece of this research consists of a multi-stage risk modelling approach; spatially explicit physical risk computations are performed on infrastructure assets, from which infrastructure failures and service disruptions are then derived (Fig. 1.1). This framework is developed and tailored in various alterations to the scales and problems posed in the research questions above. All input data used and code produced within this research are publicly available.

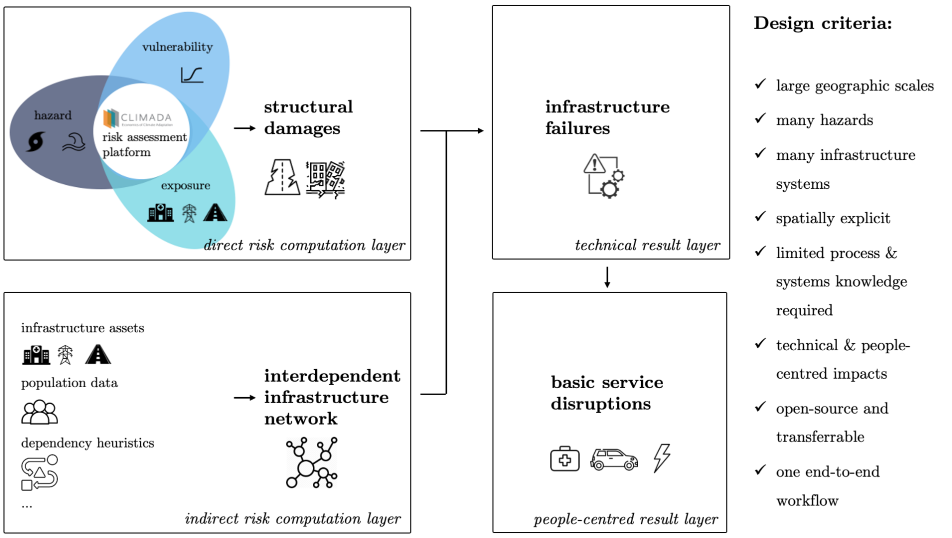

Figure 1.1: The methodological framework of this research, a multi-stage risk modelling approach combining physical impact computations on infrastructure assets using the risk modelling platform CLIMADA, and a complex-network based representation of interdependent infrastructure systems and their users. Results are reported along a technical (infrastructure functionality) dimension, and a people-centred (service disruption) dimension.

Physical risk computations. The open-source software CLIMADA (CLImate ADAptation Aznar-Siguan and Bresch 2019) is a globally consistent multi-hazard risk modelling platform which allows for spatially explicit, event-based and probabilistic risk assessments in line with the IPCC's definition of risk. Data on exposure - here, infrastructure assets and population -, hazard and vulnerability can be ingested in a fully user-defined manner. Risk (or impact) is computed as a convolution of these three layers, and expressed in the value metric assigned to the exposure (i.e., affected population counts, fraction of assets damaged, etc.).

Infrastructure failures, failure cascades and service disruption computations. Within CLIMADA, a complex network-based module represents infrastructure systems, population, and dependencies between them as hierarchical networks featuring nodes and edges. From this topological representation, functional states of infrastructure components and service access of end-users are computed. Physical damage calculations on infrastructure assets (see above) are fed into this module as disruption trigger, from which infrastructure failures, failure cascades, and service disruptions are simulated.

Data. This work is based on a plethora of different data, notably geo-spatial data on hazards, infrastructure asset, and population counts; secondary data on service quality, demand, and supply (e.g., road speeds, energy access, power generation, etc.), academic literature on vulnerability curves and infrastructure dependencies; and unstructured print media accounts, utility provider and government reports for verification purposes.

1.3 Scientific Background

1.3.1 Definitions around critical infrastructure and basic service risks

Critical infrastructure. Most governments and organizations have a working definition of critical infrastructure which share important features of the one provided by the European Commission:

> Critical infrastructure is an asset or system which is essential for the maintenance of vital societal functions. The damage to a critical infrastructure, its destruction or disruption by natural disasters, terrorism, criminal activity or malicious behaviour, may have a significant negative impact for the security of the EU and the well-being of its citizens. - *European Commission, 2023*

Critical infrastructure systems secure essential functions in society, they mitigate negative effects during adverse events, their failure is detrimental to economic security, health and safety, and they are systems consisting of physical assets, processes and people. Despite the absence of a unique classification, and the fact that criticality of an infrastructure may vary according to geographic scope and impact metric (Kröger and Zio 2011), infrastructure sectors frequently considered critical are transportation, information and communication, energy, water, public health, public safety, public administration, finances, food and agriculture, and waste disposal[1].

Infrastructure interdependencies. (Inter-)dependencies refer to (bi-)directional relationships between components of infrastructure systems (Ouyang 2014)[2]. Interdependencies can be of different nature (e.g., physical, logical, geographic and cyber, as categorized in the seminal work of Rinaldi et al. 2001), strength, and coupling behaviour.

[1] cf. classifications from Switzerland (`https://www.babs.admin.ch/en/aufgabenbabs/ski/kritisch.html`) and the United States (`https://www.cisa.gov/topics/critical-infrastructure-security-and-resilience/critical-infrastructure-sectors`) featuring 9 sectors with 27 sub-sectors and 16 sectors, resp.

[2] In the following, no strict distinction will be made with respect to the use of the word (inter-)dependency for enhanced readability.

Basic service (access). Basic services, also: essential services, refer to "public service provision systems that meet human basic needs including drinking water, sanitation, hygiene, energy, mobility, waste collection, health care, education and information technologies. [...] Access to basic services implies that sufficient and affordable service is reliably available with adequate quality" (UNSTATS 2023). Sufficient and adequate are highly context-specific characteristics, and many governments have their own target metrics; as a reference and starting point, the access criteria developed for SDG indicator 1.4.1 (Proportion of population living in households with access to basic services) may be considered.

Natural hazard risk. According to the IPCC, *natural hazard risks* emerge through the interplay of weather and climate-related hazards, the exposure of assets and people to those hazards, and their specific vulnerabilities (Field et al. 2014). Risk is the convolution of severity and probability, and can be expressed as an expected level of 'impacts' associated with a certain return period (Kaplan and Garrick 1981). Frequently, but less standardized, *direct risk* refers to the expected physically caused impacts on the exposure, and *indirect risks* is used as a collective term for of any secondary, cascading, 'consequently resulting' impacts.

Dimensions of critical infrastructure risk. Critical infrastructure systems are exposed to multi-faceted risks with diverse consequences. Efforts to understand and mitigate these risks are equally diverse. Traditionally, *critical infrastructure protection* from natural hazards and man-made causes has been the concern of governmental institutions[3] (Fekete 2019). Informed by advances in structural and civil engineering, critical infrastructure protection has retained a predominantly technical focus on reliability and system performance, and notably on system interdependencies, with their potential for failure cascades and knock-on effects (Ouyang 2014; Rinaldi et al. 2001). In natural hazard risk management and risk modeling, risk assessments and the appraisal of adaptation measures frequently feature an infrastructure dimension, albeit at varying degrees of explicitness (Hallegatte et al. 2019;

[3]see, for instance, the European Commission's framework - European Programme for Critical Infrastructure Protection (EPCIP).

Pant, Thacker, et al. 2018). Owed to the provision of services to people and businesses and their consequences on livelihoods, the societal dimensions of critical infrastructure risks have entered international policy frameworks and evoked interest in economics, human geography, and sociology (Cutter et al. 2006; Garschagen and Sandholz 2018; Thacker, Adshead, et al. 2019).

In an effort to systematize dimensions of critical infrastructure risks, Dawson et al. (2018) suggest a categorization into *asset scale risks*, stemming from physical damages to individual infrastructure components, *network* scale risks, referring to a reduction in service provision of an infrastructure due asset damages, *infrastructure (inter-)dependency* risks, referring to a reduction in service provision of other infrastructure due to dependencies on damaged infrastructure, and *systemic risks*, stemming from revenue losses incurred by industries due to supply chain disruptions, etc.

Hallegatte et al. (2019) suggest a *people-centred* and an *economy-centred* view on impacts from critical infrastructure damages and service disruptions, spanning direct and indirect dimensions: examples include repair costs, lost sales, traffic congestion, immediate effects on health, education and livelihood, and extensive consequences such as coping costs of forgone services, market investment barriers, reduced competition and innovation, long term economic prospects, quality of life, mortality and morbidity.

Distinct research communities in this interdisciplinary field rely on domain-specific methodologies, terminologies and foci. The resulting silo-thinking is increasingly criticized (Thacker, Pant, et al. 2017) and interdisciplinary approaches which better cater to the complexities of the problem space are encouraged (Zio 2016). The following paragraphs provide an overview on research developments along the introduced dimensions of critical infrastructure risk with a predominant focus on natural hazard risk modelling; research directions in civil engineering and social sciences are pointed out where feasible and necessary for the scope of this work.

1.3.2 Direct risks to critical infrastructure from natural hazards

Empirical risk. Natural hazard-induced direct risk is frequently expressed in metrics such as monetary damages to asset stocks or the number of dead and affected people. Empirical loss and damage databases in (re-)insurance and academia primarily report on these figures: for instance, Swiss Re's sigma explorer[4], Munich Re's NatCatSERVICE[5], and the University of Louvain's EM-DAT (CRED / UCLouvain 2023). Analogous risk metrics for critical infrastructure, i.e. damaged or exposed infrastructure components, are increasingly monitored, for instance through respective indicators to the Sendai Framework[6]. However, empirical data on infrastructure impacts trails far behind more established economic loss and mortality records. This reporting asymmetry reflected by similar tendencies in risk management and research, where critical infrastructure is a comparatively new field (Fekete 2019), despite such knowledge being crucial for evaluation, funding allocation and operational planning.

Modelled risk. On the modelling side, risk assessment studies have computed direct risk from various natural hazards to several infrastructure sectors at sub-national (ibid.), national (Thacker, Pant, et al. 2017), regional (van Ginkel et al. 2021), and even global (e.g. road, rail, ports and airports; Koks, Rozenberg, Zorn, et al. 2019; Verschuur, Koks, S. Li, et al. 2023; Yesudian and Dawson 2021) level. However, quantification of direct risk to critical infrastructure assets faces bottlenecks along all components of the risk equation (i.e., hazard, exposure and vulnerability), which contributes to the scarcity of regional and global studies for a wider range of infrastructure sectors.

Challenges and Gaps. Most critical infrastructure consists of diverse structural assets. Geospatial location information, however, varies widely depending on world region and infrastructure type. Primary roads, for instance, are relatively well mapped globally on crowd-sourced platforms such

[4] `https://www.sigma-explorer.com/`

[5] `https://www.munichre.com/en/solutions/for-industry-clients/natcatservice.html`

[6] `sendaimonitor.unisdr.org`

as OpenStreetMap (Barrington-Leigh and Millard-Ball 2017) and through advancements in remote sensing technologies (Lu et al. 2022). On the contrary, geospatial information on small-scale or under-ground infrastructure such as water and sanitation assets (Stip et al. 2019), or on highly sensitive infrastructure, such as power assets in high resolution, is scarce. Some governments in predominantly wealthy regions provide official, publicly accessible infrastructure data[7], while many lowest-income countries are reliant on humanitarian mapping efforts following disasters (Herfort et al. 2021). The high complexity of some infrastructure sectors which are made up of numerous different components additionally complicates comprehensive risk assessments[8]

Information on age, structural deterioration or design standards of infrastructure components significantly impact the vulnerability to natural hazards, but are virtually absent at larger scales (Mahmoud et al. 2023). Increasing efforts are dedicated to collect, for instance, number of floors and construction materials of healthcare facilities and schools[9], or surface material of roads, but this remains a laborious task . Even with significant asset information, obtaining adequate vulnerability functions (impact functions, fragility curves), which relate hazard intensities to the expected damage sustained by infrastructure components, remains a challenge. While extensive work has been done in structural engineering disciplines to devise such vulnerability functions for diverse infrastructure components, as for instance within the widely used (US-specific) manuals from the FEMA's Hazus Program, limited empirical damage records for calibration, and doubtful transferrability, require assumptions and simplifications (Koks, Rozenberg, Zorn, et al. 2019; Nicolas et al. 2019).

Lastly, globally available hazard models do not necessarily resolve highly enough to adequately capture impacts on all critical infrastructure compo-

[7] e.g., the Swiss federal geoportal `www.geo.admin.ch`, or the US-American Homeland Infrastructure Foundation-Level Data `https://hifld-geoplatform.opendata.arcgis.com/`

[8] e.g., power and telecommunication infrastructure, consisting of numerous types of power plants, substations, towers, poles, lines; submarine, fibre optic and co-axial cables, data centres, cell towers, landlines, etc. (Nicolas et al. 2019; Sandhu and Raja 2019).

[9] cf. the World Bank's Global Library for Schools Infrastructure `https://gpss.worldbank.org/en/glosi`

nents. While for spatially extensive infrastructure such as roads or rails, imprecision on damage computations from low-resolution hazard sets may cancel out over larger stretches, this might not hold for sparse, local infrastructure components such as power substations. Further, infrastructure components may be vulnerable only to certain sub-hazards, which is not captured adequately when the entire hazard phenomenon is proxied by one, even though dominant, sub-hazard (e.g. for tropical cyclones, wind is used as a proxy for the subset of wind, surge and rain sub-hazards, which can strain infrastructure components in a different manner). Further, research on physical infrastructure impacts is often dominated by earthquakes (Mahmoud et al. 2023), in spite of floods and tropical cyclones being similarly damaging[10].

1.3.3 Indirect risks of natural hazard-induced damages to critical infrastructure

Modelling indirect infrastructure risks. To derive indirect infrastructure risks resulting from natural hazard events, researchers have coupled direct infrastructure risk computations with a variety of models capturing risk propagation: For instance, input-output and agent-based models for supply chain and welfare losses from telecommunication interruptions (Colon et al. 2019), bespoke maritime transport and input-output models for trade and logistics disruptions from port interruptions (Verschuur, Koks, S. Li, et al. 2023), flight routing data for flight disruptions and economic losses (Yesudian and Dawson 2021), network models for trip delays and cancellations (Y. He et al. 2022), and theoretical frameworks for infrastructure as 'winnowing device' to consider multi-hazard risks (Raymond et al. 2020).

While the importance of systems-thinking in natural hazard risk modelling is increasingly recognized (Bresch, Berghuijs, et al. 2014), much academic work at the intersection of critical infrastructure and natural hazards focuses either on network scale risks (i.e., from within a single infrastructure network), or on system scale risks (i.e., on coarse cross-sectoral impacts). The middle ground, interdependency scale risks, (i.e., consequences of impacts to

[10]As a first orientation, global total damages between 2000 and 2023, as reported in the EM-DAT database, amount to $\sim$ USD bn 5 000 (TC), 6 300 (FL) and 4 600 (EQ), resp.

infrastructure assets as part of interdependent infrastructure systems), are rarely treated in natural hazard risk modelling, despite interdependent infrastructure systems being a central element of research in many engineering disciplines. The following paragraphs hence focus on this type of risk.

Identifying infrastructure interdependencies. With the recognition of the existence and importance of interdependencies between infrastructure components, numerous typologies have been developed (e.g., Lee II et al. 2007; Rinaldi et al. 2001; Zimmerman and Restrepo 2006). While they may provide a common mental framework, utility of these classifications has been debated in practical terms. To identify and quantify such infrastructure interdependencies, simple empirical approaches have counted occurrences of infrastructure disruptions from print media and outage databases, and tracked which sectors were at initiating and receiving ends, resp. (Luiijf et al. 2009; Zimmerman and Restrepo 2006). Other approaches have relied on participatory methods (e.g. 'Preliminary Interdependency Analysis' (Bloomfield et al. 2017), expert surveys (Mitsova, Sapat, et al. 2020) and focus group discussions (Schotten and Bachmann 2023a)), or conducted in-depth case studies of past events (Chang, Pasion, et al. 2012; Gao et al. 2023). More quantitative approaches have deduced interdependencies from critical infrastructure restoration curves after disasters (e.g. Cimellaro 2016; Dueñas-Osorio and Kwasinski 2012; Zorn and Shamseldin 2016).

Network-based modelling of interdependent infrastructure. Approaches for modelling interdependent infrastructure systems are equally diverse as those for identifying interdependencies. A comprehensive overview on the dominating approaches, including their benefits and shortcomings, is provided in Ouyang (2014), who categorizes them into empirical, agent-based, system dynamics-based, economic theory-based, network based, and other approaches.

Critical infrastructure are large, spatially distributed, complex systems, and share many typical attributes of complex networks (Kröger and Zio 2011). While network-based approaches do not replace more detailed reliability analysis methods, they offer a tool to represent systems at different levels of complexity, are easily generalizable and transferable, and can serve as a first large-scale screening analysis to identify hot-spots for further in-depth investigation (Pant, Hall, and Thacker 2017). Modelling interdependent critical infrastructure as hierarchical networks is furthermore intuitive and illustrative (Pant, Hall, and Blainey 2016). Due to the versatility of the modelling approach, complexity and resolution between different network model implementations varies considerably. Purely topological representations model infrastructure and their interdependencies as graphs consisting in nodes and edges, while network flow models add supplies, demands, capacity constraints and flow rates to the graph elements, allowing to capture and optimize the system's performance at continuous levels (Guidotti et al. 2016; Lee et al. 2009).

Challenges and Gaps. As this thesis relies on a network modelling approach for interdependent infrastructure, a comprehensive literature review was conducted on research at the intersection of interdependent critical infrastructure, network modelling approaches, and natural hazards, between 2005 and 2021 to scope for common challenges and gaps in the field. 80 relevant publications spanning the water, electricity, oil and gas, road, rail and air transport, mobile, internet and land-line communication, education, healthcare and emergency service sectors. Supplementary SM1 provides search and inclusion criteria, and an information flow diagram according to the PRISMA method. Fig. SM1.1 illustrates findings from the meta-analysis, Table SM1.1 gives an overview on identified infrastructure interdependencies.

Most network studies on interdependent critical infrastructure investigate only two systems. The power system is most often studied, especially in connection with the water or the telecommunication system. Healthcare and education systems are nearly absent.

Most studies do not explicitly investigate natural hazards as disruptive scenarios. Frequently, disruption effects are studied from the removal of individual nodes and edges (component criticality studies), from the random removal of an increasing amount of edges and nodes (percolation studies), or from the failure of all infrastructure components within the area of stylized polygons (e.g. Fang, Pedroni, et al. 2016; Jenelius and Mattsson 2012; D.

Li et al. 2015; Mooney et al. 2018; Zorn, Pant, et al. 2020), within which all infrastructure components are concurrently failed. The studies which investigate real-world hazards often focus on earthquakes, and to a smaller degree on floods, tropical cyclones and severe winds.

Most studies model systems at local scales, i.e. communities or districts. The typical study object is a mid-sized city in the US, where all needed infrastructure data is either available, or a similarly-sized test-bed environment which reproduces artificially generated, but representative conditions (cf. 'Clarc County' in Loggins and Wallace (2015) or 'Centerville' in X. He and Cha (2020)). Resolution of the modelled critical infrastructure is typically inversely correlated with the geographic scale at which they are studied. The few national-scale, real-world infrastructure system studies are restricted to well-delimited islands, such as the UK and New Zealand (Pant, Thacker, et al. 2018; Zorn, Pant, et al. 2020). Apart from few studies in Korea, mainland China and Nigeria, no studies investigate on infrastructure systems in Asia, Africa or Latin America and the Caribbean.

Most studies evaluate impacts on a technical system performance level. Typical metrics are number of disrupted nodes in relation to the overall supply of a system (e.g., number of generators vs. power remaining in the system) or in relation to recovery times, sometimes evaluated against various network configurations. Few studies look at economic impacts, such as monetary loss, business interruption, and even fewer at impact on population, such as number of people affected by disruption of a service.

1.3.4 Basic service disruptions and social vulnerability

As natural hazards affect the well-being of people (Dargin and Mostafavi 2020), various factors and characteristics among population groups can modulate the degree of severity of potential impacts (Cutter et al. 2006). While research has been relatively conclusive on the broad variables contributing to social vulnerability, such as demographics, socio-economic condition, living situation, ethnicity and health status (ibid.), it is widely unclear how critical infrastructure failures and service disruptions interact with social vulnerability conditions, and how these differential impact patterns relate to different hazard and crisis scenarios (Garschagen and Sandholz 2018).

This lack of understanding is problematic as socially vulnerable population groups tend to be more often exposed to natural hazards, and seem to experience more and longer-lasting resulting service disruptions (Liévanos and Horne 2017; Mitsova, Esnard, et al. 2018; Yu et al. 2020). Understanding such differential needs is crucial for adequate response in the instant aftermath of a disaster (Dargin and Mostafavi 2020), for equitable restoration, and adaptation (Karakoc et al. 2020).

To counter this gap, empirical research has screened print media accounts to relate infrastructure failure mechanisms to social impacts (Chang, McDaniels, Mikawoz, et al. 2007), built a systematic database (Chang, McDaniels, and Beaubien 2009, though discontinued), and conducted surveys on subjective well-being due to post-disaster service disruptions (Dargin and Mostafavi 2020).

While modelling approaches have captured service disruptions and analysed them with respect to certain social vulnerability metrics (e.g. Chang, Pasion, et al. 2012; Karakoc et al. 2020; Lan et al. 2023; Tariverdi et al. 2023), a recurring challenge lies in relating physical damages to service quality despite lack of data on post-disaster service performance (Chang, Pasion, et al. 2012), which further complicates the task of capturing differential impacts to differently vulnerable groups. The emerging discourse on implementing minimum supply standards of services in situations of major infrastructure failures is commendable, but has been found to neither link adequately to a technical infrastructure dimension nor to a social vulnerability dimension (Garschagen and Sandholz 2018).

1.3.5 Adapting critical infrastructure and basic services

As infrastructure damages and service disruptions take a toll on the well-being of individuals and firms alike, investing in more resilient infrastructure is not only critical from a humanitarian perspective, but in many cases even profitable: Hallegatte et al. (2019) estimate that in lower and middle income countries, every USD invested in infrastructure returns a four-fold benefit.

However, resources to implement resiliency measures are generally limited, and indiscriminate expansion of infrastructure conflicts with environmental considerations, such that prioritization of options is indispensable (Trejo and Gardoni 2023). While prioritization is often thought spatially, decisions should essentially reflect on the type of resilience to be achieved (Lewin et al. 2023): of infrastructure assets, of infrastructure services, or of infrastructure users (Hallegatte et al. 2019).

While resiliency measures can also target prevention, preparedness, recovery, general risk management principles, and long-term adaptive capacity (Almoghathawi and Barker 2019; Bresch, Berghuijs, et al. 2014; Pant, Zorn, et al. 2018), (structural) adaptation option appraisal at asset-level is still the traditional approach seen in most Economics of Climate Adaptation (ECA) studies (Bresch 2016) and in large-scale studies on sectoral risks (e.g. Koks, Rozenberg, Zorn, et al. 2019, for global road and rail assets): In line with a direct risk perspective on infrastructure, adaptation measures are evaluated in terms of their potential to avert infrastructure asset damages, and contrasted against their implementation costs.

Enhancing service resilience and avoiding adaptation asynergies (de Ruiter et al. 2021) requires multi-sectoral and multi-organizational commitments and hence face challenges which usually span many interdependent infrastructure systems at once (Lewin et al. 2023; Pant 2022). More systemic ways of thinking about infrastructure and service resilience are being taken up in the discussions on minimum standards of service that are tolerable (Garschagen and Sandholz 2018), on ‘chains of resilience’ (Lewin et al. 2023) and on adaptive pathways (Koks, Le Bars, et al. 2023), which acknowledge the need to include not only climate change, but also socio-economic developments to plan and invest into the decade to century-long lifespan of infrastructure assets.

Adaptation studies hence increasingly evaluate the response of entire infrastructure networks to a range of asset-level and network-level interventions, as research has shown that investment in a few critical components may have large impact on the overall network performance (Pant 2022). For instance, physical hardening of individual critical assets or the effect of changing the network structure can both be evaluated in terms of avoided service losses (Oh et al. 2019; Stürmer et al. 2023). Nevertheless, appraisal of concrete adaptation measures to natural hazards at asset-level, network-level or even interdependent networks-level for multiple interdependent infrastructure and services is scarce, despite considerable research on restoration and recoverability of interdependent infrastructure systems (e.g. Almoghathawi and Barker 2020; Almoghathawi, Barker, and Albert 2019).

1.4 How to read

This cumulative thesis consists of four first-authored papers submitted to scientific journals and conferences, which are included as stand-alone chapters. Further co-authored papers and notes which organically add to the synthesis of this research are included in the supplementary materials. Fig.1.2 provides an overview on the thesis structure in relation to the research questions.

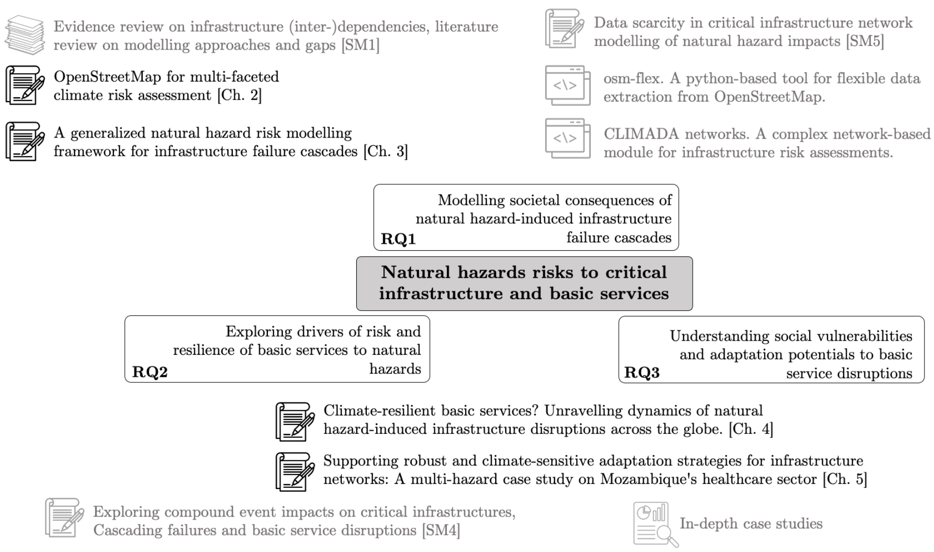

Figure 1.2: Research content in relation to the posed research questions (RQs). Black - main chapters, gray - not included or included in supplementary materials of this thesis.

Chapter 2 motivates the use of diverse, high-resolution exposure layers for risk assessments, notably from crowd-sourced public databases such as OpenStreetMap, thereby setting a necessary pre-condition for exploring infrastructure risks. It is accompanied by the open-source software OSM-flex, which was developed as light-weight Python based tool to enable efficient extraction of geo-spatial data from OpenStreetMap.

> Mühlhofer, E., C. M. Kropf, L. Riedel, D. N. Bresch and E. E. Koks, 2024: OpenStreetMap for multi-faceted climate risk assessments. *Environmental Research Communications*, **6**, 015005, doi:10.1088/2515-7620/ad15ab

Evelyn Mühlhofer, Elco Koks, Lukas Riedel, & Chahan M. Kropf. (2023). osm-flex/osm-flex: v1.0.1 (v1.0.1). Zenodo. https://doi.org/10.5281/zenodo.8083066

Chapter 3 develops the central methodology of this thesis, an end-to-end framework from natural hazard impacts on interdependent critical infrastructure to basic service disruptions over large geographic scales. The methodology is accompanied by a network module within the open-source CLIMADA risk assessment software, which was developed to technically enable this research and to provide useful tools to fellow researchers.

Mühlhofer, E., E. E. Koks, C. M. Kropf, G. Sansavini, and D. N. Bresch, 2023: A generalized natural hazard risk modelling framework for infrastructure failure cascades. *Reliability Engineering & System Safety*, **234**, 109 194, doi:10.1016/j.ress.2023.109194

Chapter 4 uses the developed methods and tools to explore impacts and drivers of infrastructure failures and basic service disruptions from multiple hazards, in diverse regions across the globe. By expanding the study horizon to a global perspective, a comparative view on broad risk trends, failure mechanisms and resilience-enhancing strategies is obtained.

Mühlhofer, E., D. N. Bresch and E. E. Koks, under review: Climate-resilient basic services? Unravelling dynamics of natural hazard-induced infrastructure disruptions across the globe. *One Earth*

Chapter 5 examines impacts from a single event in detail. It explores the importance of considering sub-hazards for resolving all impact dynamics, and evaluates trade-offs in adapting infrastructure systems under a holistic, service-centred focus. In Supplementary SM4, a complementary study explores how large-scale infrastructure may lead to compounding impacts of (un-)connect hazard events.

Mühlhofer, E., Z. Stalhandske, M. Sarcinella, J. Schlumberger, D. N. Bresch, E. E. Koks, Supporting robust and climate-sensitive adaptation strategies for infrastructure networks: A multi-hazard

> case study on Mozambique's healthcare sector. *14th International Conference on Applications of Statistics and Probability in Civil Engineering (ICASP14), Dublin, Ireland, 2023*, doi:10.25546/103336

> Mühlhofer, E., E. E. Koks, and D. N. Bresch, 2022: Exploring Compound Event Impacts on Critical Infrastructures, Cascading Failures and Basic Service Disruptions, *61st ESReDA Seminar On Technological disruptions triggered by natural events: identification, characterization, and management, September 22 – 23, 2022, Politecnico di Torino, Italy.*

Chapter 6 synthesises the findings of this research along the initially posed research questions. It further reflects on two cross-cutting issues: (i) the heavy reliance on (unavailable) data and information throughout this research, and the implications of replacing them with implicit and explicit assumptions and heuristics; (ii) the trade-off between global consistency and local specificity, and how this influences the adequacy of hence-obtained insights for different decision-making contexts. It ends with an outlook for future research.

The cross-cutting issue on data and information challenges was further expanded upon in a collaborative reflection process with fellow researchers at the intersection of critical infrastructure and natural hazard modelling, and is provided as manuscript in Supplementary SM5.

> Schotten, R., E. Mühlhofer, G. A. Chatzistefanou, D. Bachmann, A. S. Chen, E. E. Koks, 2024: Data for Critical Infrastructure Network Modelling of Natural Hazard Impacts: Needs and Influence on Model Characteristics. *Resilient Cities & Structures.*

CHAPTER 2

OpenStreetMap for multi-faceted climate risk assessments

Evelyn Mühlhofer, Chahan M. Kropf, Lukas Riedel, David N. Bresch and Elco E. Koks; published in *Environmental Research Communications*

Abstract. Natural hazards pose significant risks to human lives, infrastructure, and ecosystems. Understanding risks along all these dimensions is critical for effective adaptation planning and risk management. However, climate risk assessments mostly focus on population, economic asset values, and road or building infrastructure, because publicly available data on more diverse exposures are scarce. The increasing availability of crowd-sourced geospatial data, notably from OpenStreetMap, opens up a novel means for assessing climate risk to a large range of physical assets. To this end, we present a standalone, lightweight, and highly flexible Python-based OpenStreetMap data extraction tool: OSM-flex. To demonstrate the potential and limitations of OpenStreetMap data for risk assessments, we couple OSM-flex to the open-source natural hazard risk assessment platform CLIMADA and compute winter storm risk and event impacts from winter storm Lothar across Switzerland to forests, UNESCO heritage sites, railways, healthcare facilities, and airports. Contrasting spatial patterns of risks on such less conventional exposure layers with more traditional risk metrics (asset damages and affected population) reveals that risk hot-spots are inhomogeneously and distinctly distributed. For instance, impacts on forestry are mostly expected in Western Switzerland in the Jura mountain chain, whereas economic asset damages are concentrated in the urbanized regions around Basel and Zurich and certain train lines may be most often affected in Central Switzerland and alpine valleys. This study aims to highlight the importance of conducting multi-faceted and high-resolution climate risk assessments and provides researchers, practitioners, and decision-makers with potential open-source software tools and data suggestions for doing so.

2.1 Introduction

Natural hazards affect humans, human-made structures, and nature. Impacts and consequences of such events may therefore be as diverse as the exposed assets. Understanding these multiple dimensions of disaster risk across economic, social, health, educational, environmental, and cultural heritage is also a main priority within the Sendai Framework for Disaster Risk Reduction (UNDRR 2015, § 24 f). While capturing many facets of risk incurred by natural hazard events can allow for better and more informed risk management practices, capabilities to do so are often severely constrained by data availability within all stages of the risk assessment chain - not least on the exposure side.

The Sendai Framework, therefore, stresses the importance of access to reliable data, including geographic information systems (GIS), to "strengthen technical and scientific capacity to capitalize on and consolidate existing knowledge and to develop and apply methodologies and models to assess disaster risks, vulnerabilities, and exposure to all hazards" (ibid.). As the research community and decision-makers are urged to move towards more diverse analyses of natural hazard-induced risks in a changing climate, open-source tools are needed to facilitate these in an equitable manner that is accessible to a wider range of stakeholders.

Responding to this need, models to capture risk—defined as the product of hazard, exposure and vulnerability by the IPCC (Field et al. 2014)—are increasingly developed in an open-source manner (e.g., Aznar-Siguan and Bresch 2019; Koks 2022; Paulik et al. 2022). However, many off-the-shelf input data sets for risk computations may not have global coverage, and bespoke models frequently focus on a single component of the risk equation, especially on the hazard side (cf. Bloemendaal, Haigh, et al. 2020; Lüthi et al. 2021; Pagani et al. 2022; Yamazaki et al. 2011). Moreover, interoperability between models and data sets covering different risk components is often not straightforward, reducing usability for non-experts despite their (theoretical) availability.

Nevertheless, the advancement of remote sensing has greatly aided the development of spatially explicit global exposure layer data, such as building footprints (Microsoft 2023), population counts (Center for International Earth Science Information Network (CIESIN), Columbia University 2017; WorldPop 2020), land use and land cover (Potapov et al. 2022) or economic asset value concentrations (Eberenz, Stocker, et al. 2020). While this offers obvious potential for natural hazard risk assessments, the aspects of risk which can be explored with these data sets are inherently constrained to economic values and population numbers.

The increasing level of detail with which the visible environment is mapped in OpenStreetMap (OSM) offers different and less conventional opportunities for natural hazard risk assessment (Nirandjan et al. 2022). As a freely available and open-source resource for geo-referenced exposure data, OSM has been used as an input layer in a number of studies in the wider area of natural hazard risks, spanning direct damage assessments (Koks, Rozenberg, Zorn, et al. 2019), service disruptions (Mühlhofer, Koks, Kropf, et al. 2023), emergency response (Gultom et al. 2021) and adaptation planning (Schotten and Bachmann 2023a). Many of them focus predominantly on general building stocks (Bloemendaal and Koks 2022; Cerri et al. 2021) and major transportation assets such as roads and railways (Koks, Rozenberg, Zorn, et al. 2019; Mulholland and Feyen 2021; van Ginkel et al. 2021), and to a lesser degree on other (critical) infrastructure assets such as airports (Yesudian and Dawson 2021), social facilities (Mühlhofer, Koks, Kropf, et al. 2023; Nirandjan et al. 2022) or power generation and distribution assets (Nirandjan et al. 2022). However, as it is not limited to modern human-made structures, the OSM data supports the study of other risk areas of the built-up and natural environment, such as forests, agricultural land, UNESCO heritage sites, and ecosystem services (Ruckelshaus et al. 2020).

Although a number of Python tools have been developed for the retrieval of certain high-resolution exposure data from OSM (e.g., Boeing 2017; Tenkanen 2020), there is no versatile linkage to access the entire data universe and efficiently perform natural hazard risk assessments on these data on a large scale.

The aim of this study is thus three-fold: first, to bridge a data access gap by presenting the lightweight, stand-alone, and highly flexible Python module OSM-flex (Mühlhofer, Koks, Riedel, et al. 2023) that enables users to efficiently and consistently retrieve geospatial exposure data from OSM with all available information; second, to demonstrate seamless integration within the open-source natural hazard risk assessment platform CLIMADA (Aznar-Siguan and Bresch 2019) to perform end-to-end risk assessments; and third, to show that more diverse perspectives of natural hazard-induced risks, and hence risk management strategies, may be explored when opening up to the potentials of non-conventional exposure data.

Within a brief case study on winter storm impacts to railroads, hospitals, UNESCO heritage sites, airports, and forests in Switzerland, yet without loss of generality, we illustrate the major implementation steps, assumptions, limitations, and decision-making implications involved in computing event impacts and natural hazard risks from high-resolution exposure data obtained through OSM. By providing these open-source tools and perspectives, we aim to raise awareness and broaden the means for exploring non-monetary facets of climate risk.

2.2 Methods

2.2.1 Obtaining Geospatial Data from OSM with OSM-flex

Features can be extracted from OSM and converted into geographical tabular format for use in Python in two ways: either by reading data directly from the Overpass API[1] or by downloading regional data dumps as Protocolbuffer Binary Format (PBF) files[2] from dedicated online repositories such as GeoFabrik (2023), from which the desired data can then be parsed.

Two well-known Python packages, Pyrosm (Tenkanen 2020) and OSMnx (Boeing 2017), excel at opposite ends of this retrieval spectrum. Both packages are well maintained and easily installable using standard package managers. While a core functionality of both packages is the selective parsing of geographical features from OSM into Python-based tabular formats, OSMnx features additional integration with graph-analysis packages and common plotting libraries. Because OSMnx relies on API queries for data retrieval, it is limited by restrictions on query sizes and requires a

[1] See `https://overpass-api.de/`

[2] See `https://wiki.openstreetmap.org/wiki/PBF_Format`

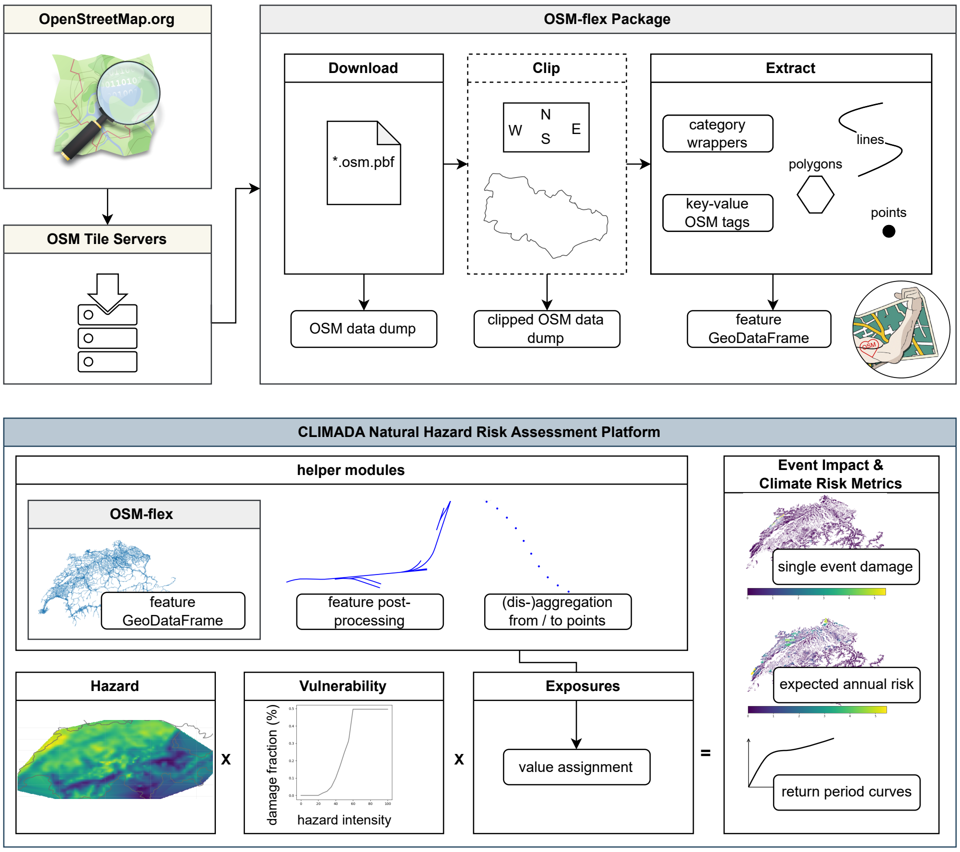

Figure 2.1: Schematic representation of a climate risk assessment workflow for OSM features using the OSM-flex package and CLIMADA. Top panel: basic steps for OSM feature extraction in the OSM-flex module: an OSM data dump is downloaded in *.osm.pbf format; optionally the area is clipped to an arbitrary polygon shape; the elements of interest are extracted using pre-written or custom queries with OSM tags; the data is converted into a GeoDataFrame. Bottom panel: integration of OSM data into the CLIMADA risk assessment workflow. The helper modules within CLIMADA conveniently allow users to directly derive point-based CLIMADA Exposures by accessing the OSM-flexmodule and dissaggregating lines and polygons exposure elements to points. The obtained point exposure can then be combined with the hazard and vulnerability models to compute point impacts (risk). Finally, point-based impact and risk data can be re-aggregated to the original OSM feature geometries.

constant internet connection for this process. Pyrosm circumvents this by parsing downloaded data dumps, yet relies on OSMnx in the background for other functionalities. Both come with a range of non-standard package dependencies and vary in customizability of the queries in terms of spatial areas and specification of filtering attributes.

Here, we introduce the lightweight Python-based package OSM-flex (Mühlhofer, Koks, Riedel, et al. 2023), which efficiently parses large sets of OSM data based on user-specified queries from PBF data dumps within arbitrary and fully user-defined geographical boundaries, such as cities, states, multi-country regions or bounding boxes. This provides the computational efficiency and user flexibility required to perform multi-faceted risk analyses. Its availability on common software distribution channels (PyPI and GitHub) and its low dependency requirements make it suitable for integration within larger and more complex software packages such as the CLIMADA risk assessment platform discussed in section 2.2.2. The package repository features a test suite that is executed in an automated testing pipeline. 2.A.2 provides an in-depth comparison of all three above-mentioned packages to guide interested researchers in the selection process for the most-suited tool given their research ambitions.

The general workflow of the OSM-flex package includes four steps, as illustrated in the upper panel of Fig. 2.1:

1. **Download** a country, regional or planet data dump (PBF file) from an online repository
2. **Clip** the data dump to the area of interest (optional)
3. **Extract** the desired features from OSM into tabular format using the OSM tagging syntax
4. **Post-process** the extracted data set (optional)

OSM-flex favors the one-time download of PBF data dumps over the direct query of individual features from the Overpass API, as feature extraction does not require a constant internet connection nor is constrained by query size limitations. 2.A.1 provides details on what access points and (regional) versions of data dumps are readily obtainable within OSM-flex.

The optional step of clipping a larger data dump to specific bounding boxes or (multi-)polygons is useful when dealing with regions or small islands that are not available as dedicated files on one of the OSM data repositories, or when wanting to clip from, for example, the global level along own predefined borders. It currently requires manual installation of the small command-line executable `osmconvert`[3] which facilitates the clipping commands within OSM-flex. In future iterations of OSM-flex, this step may be further simplified. See 2.A.1 for details on clipping options and these tools.

While OSM-flex is built to be lean and accessible, its use requires some familiarization with the syntax of keys and values in OSM, that is, the attributes that characterize geolocated data and allow it to be queried. For increased user friendliness, common exposure data categories can also be retrieved with pre-written extraction wrappers, such as road and railway assets, healthcare and education facilities, or power infrastructure. Additional details are provided in 2.A.1.

The desired geospatial information with point-, line-, and polygon-based object geometries and attribute columns is provided as a GeoDataFrame, a data type defined by the GeoPandas Python package (Bossche et al. 2023). After obtaining the data, further post-processing may be required, such as filtering out very small, yet numerous polygons belonging to large natural areas, removing duplicates, or simplifying transportation network geometries. See 2.A.1 for helpful post-processing resources and steps.

More extensive code documentation and detailed tutorials featuring usage examples are available at `https://osm-flex.readthedocs.io` to guide users. Starting from the possibility of extracting a wide range of exposure data from OSM, the following paragraph outlines how this data can be efficiently integrated into a climate risk assessment workflow.

2.2.2 Using OSM Features in Climate Risk Assessments with CLIMADA

CLIMADA is an open-source Python platform for natural hazard impact computations, climate risk assessments, and adaptation option appraisal

[3]See `https://wiki.openstreetmap.org/wiki/Osmconvert`

(Aznar-Siguan and Bresch 2019; Bresch and Aznar-Siguan 2021). It computes risk according to the IPCC risk definition as the product of exposure, vulnerability, and hazard (Pörtner et al. 2022). Hazard represents events as spatially explicit footprints with an associated hazard-specific intensity metric such as flood depth or wind speed. Each event can be assigned an occurrence probability to form a probabilistic set. Exposures are a spatially explicit representation of the elements potentially at risk, including their (non-)monetary value such as population clusters with population counts or infrastructure assets with their production capacity. Vulnerability is the linking element between hazard and exposure, and is modeled as an impact function relating the hazard intensity to the expected impact, expressed in a ratio of exposure value.

Exposure data which represents the spatial distribution of monetary asset values (Eberenz, Stocker, et al. 2020) or population counts most commonly forms the basis of climate risk assessments. CLIMADA is flexible with regard to input data, thus allowing arbitrary exposure inputs, vulnerability function definitions, and hazard footprints.

To perform such a risk analysis on OSM features, exposure data must first be extracted into a GeoDataFrame as described in Section 2.2.1. As CLIMADA's engine is designed only for pointwise data, line- and polygon-based data must be interpolated to points before the impact computations, and re-aggregated afterwards, which can be done with a dedicated utility module (see 2.A.3 for the logic of this helper module and (dis-)aggregation options). Similarly, dedicated hazard and vulnerability data must be provided and can be obtained via the CLIMADA data API for several hazards (Schmid 2023) or be ingested from users' own resources.

2.3 Application: A Multi-Faceted View on Winter Storm Risk

On December 26, 1999, winter storm *Lothar* swept across France, Germany and Switzerland, leaving a trace of destruction. In Switzerland, the event is among the top three most impactful winter storms, with significant tolls on human lives, critical infrastructure, building damage, forest loss, and wildlife

(Gaillard et al. 2003; Jordi 2019; Niemeyer and Albisser 2001).

In the following sections, the methodology presented above is explored by computing the wind impacts of Lothar on OSM-extracted built-up and natural assets across Switzerland. The results are compared with more conventional metrics such as the total value of physical assets damaged and the number of people affected, and validated with event reports. Furthermore, the average annual risk of winter storms to these exposures, obtained from a probabilistic hazard set representing today's climate, is reported.

2.3.1 Winter Storm Impact Calculations with OSM and CLIMADA

OSM Exposure Data Extraction

Using OSM-flex, OSM data from Switzerland was downloaded from `https://geofabrik.de` on March 13, 2023. Points, lines and polygon data were extracted into GeoPandas GeoDataFrames for 1155 major healthcare facilities (hospitals, clinics, and doctors' practices), 20 100 km of railways (individual rails, incl. trams and narrow gauge rails), 15 airports, 12 500 km^2 of forests, and 11 UNESCO heritage sites, see Fig. 2.4. The exact queries (OSM tags) are noted in Table 2.5. Geo-spatial data were post-processed to eliminate very small areas ($< 100\text{m}^2$) of forest, and duplicates for healthcare facilities and airports.

Wind Impact

The wind field of storm Lothar was prepared by Welker et al. (2020) as the maximum 3-second sustained wind speeds at a height of 10 m above ground over 72 h at a spatial resolution of approximately 4.4 km, based on the Windstorm Information Service (WISC) of the Copernicus Climate Change Service. These data were obtained via the CLIMADA Data API and stored as a CLIMADA Hazard object, see Fig. 2.3. OSM data were stored as CLIMADA Exposure objects, together with a general asset value exposure for Switzerland based on the product of nightlight intensity and population count data at 30 arcsecond resolution (LitPop, (Eberenz, Stocker, et al. 2020)), and a population exposure at the same resolution based on the

SEDAC GPW v4.0 dataset (Center for International Earth Science Information Network (CIESIN), Columbia University 2017); see Fig. 2.5). Impact functions (vulnerability curves) relating hazard intensity to damage extent were obtained from (Welker et al. 2020) for wind-induced general asset damages, which were calibrated to the Swiss context. For all other exposures, step functions were employed that mirror warning categories issued by the Swiss Federal Office of Meteorology and Climatology (Blass et al. 2022; MeteoSwiss 2023). For population, railways, healthcare facilities and airports, wind intensities above 30.5 m/s (110 km/h, warning category 4) were considered critical based on the warning rationales provided by official sources, whereas for forests, wind intensities above 38.9 m/s (140 km/h, warning category 5) were considered more adequate to capture tree snapping (Virot et al. 2016). See Fig. 2.6 for the plots of all impact functions used. Impacts were computed for all exposures within the CLIMADA, whereby line and polygon-based data (i.e. railways and forests) were interpolated to a 100 m resolution and re-aggregated (by summation) afterwards into their original shapes. The impact data are shown in Fig. 2.2.

Wind Risk

In addition to the extreme storm Lothar, we also considered the general winter storm risk in Switzerland following the IPCC definition of risk as the probability of occurrence of an event multiplied by its severity. To this effect, we used the WISC probabilistic extension hazard event set, available through the CLIMADA Data API (Röösli and Bresch 2020; Welker et al. 2020). This hazard set is based on historic records, but features an additional 29 synthetic hazards per historic hazard occurrence from 1940 to 2014. It was calibrated on the years 1990–2010, which can be seen as representative of climate conditions today. Furthermore, for the physical asset and population exposure layers, we used the reference year 2020 instead of 1999.

2.3.2 Results

Table 2.1 summarizes the impacts of storm Lothar computed for different exposures. Although affected by varying absolute and relative degrees, the impacts are considerable across all studied dimensions. An important dis-

Table 2.1: Impacts from winter storm Lothar (1999) across Switzerland for general asset values, population counts, and five categories of OSM-retrieved exposures.

Exposure type	Absolute	Relative
Asset Values[a]	US $179.4 mil.	0.01%
Population[a]	4.17 mil. people	57.2%
Healthcare Facilities[b]	649 units	56.2%
Airports	6 units	40.0%
UNESCO Sites	3 sites	27.3 %
Railways[c]	6 951 km	50.4%
Forests	464.6 km^2	3.7%

[a] reference year: 2000; [b] hospitals, clinics and doctors' offices; [c] all individual lines counted separately, also for parallel tracks.

tinction must be made with regards to what these impact figures stand for: For forests and general asset values, physical losses and damages are modelled; for the remaining exposure categories, the numbers of items *exposed* to a certain hazard intensity are modelled without direct implications of the extent of loss or damage, as no such impact functions were available in the concrete case.

Comparison with print media accounts, official records, insurance reports, and the compilation by Niemeyer and Albisser (2001) confirms the severity of the event across many dimensions of (public) life and strengthens the picture of multi-faceted impacts obtained from the computations presented in this study: reported impact metrics tend to revolve around (insured) building damages (in the case of Lothar, around CHF 600 mil.) and affected population or fatalities (15 people died during the storm, and roughly the same amount afterwards during clean-up and reconstruction efforts). The standard impact computations within CLIMADA capture these metrics as asset damages (though under-estimated with US $179 mil. or CHF 113.3 mil. at the time), and affected population (4.17 mil., a number that is inherently difficult to track and verify, as reports tend to focus on the well-reported number of fatalities instead). However, other dimensions of societal importance were equally captured, such as rail transportation - mapped here as affected to roughly 50 % - was indeed interrupted on many lines across the German-speaking part of Switzerland (covering approximately 65 % of Swiss territory); estimated forest losses (amounting to CHF 750 mil. in economic worth, and 4.3% of the Swiss forest area), is close to the modelled 3.7% of

Table 2.2: Average annual risk from winter storms across Switzerland for general asset values, population counts and five categories of OSM-retrieved exposures.

Exposure type	Absolute	Relative
Asset Values[a]	US $4.8 mil.	0.0003%
Population[a]	91'200 people	1.3%
Healthcare Facilities[b]	14.4 units	1.3%
Airports	0.5 units	1.2%
UNESCO Sites	0.08 sites	0.7%
Railways[c]	17.3 km	1.3%
Forests	9.83 km^2	0.08%

[a] reference year: 2020; [b] hospitals, clinics and doctors' practices; [c] all individual lines counted separately, also for parallel tracks

the area. It was not possible to retrieve explicit reports on the impacts to airports (apart from flight cancellations), healthcare facilities or UNESCO heritage sites. Not modelled within the scope of this illustrative case-study, but frequently mentioned in reports were impacts on the power grid and road transportation (Niemeyer and Albisser 2001). While structural impacts on the latter may be easily computed with the presented approach, modelling systemic impacts on the energy sector is not only restrained by power line mapping quality on OSM, but would also require consideration of the cascades of failing infrastructures (Mühlhofer, Koks, Kropf, et al. 2023). The results highlight that, when using multiple exposure layers, important aspects of a natural hazard event beyond conventionally reported (undifferentiated) asset damages can be captured relatively effortlessly, and guide risk management efforts.

As introduced in Section 2.3.1, it may be insightful to consider probabilistic risk metrics apart from single-hazard event impacts, to gauge the potential risk landscape and to adequately place the occurrence of historic events therein. Various metrics may be relevant, such as the risk associated with a one-in-a-hundred-year event or the average annual risk. Table 2.2 presents the latter, modelled from the probabilistic winter storm set. Evidently, since most winter storms are less extreme than Lothar (cf. Table 2.1), the average annual risk values are much lower (less than 1.5% of the total count or value for all exposure categories). The extremes of Lothar's impacts are even more strikingly illustrated when locating these impact figures on return period curves generated from the probabilistic hazard set (Fig. 2.7). With

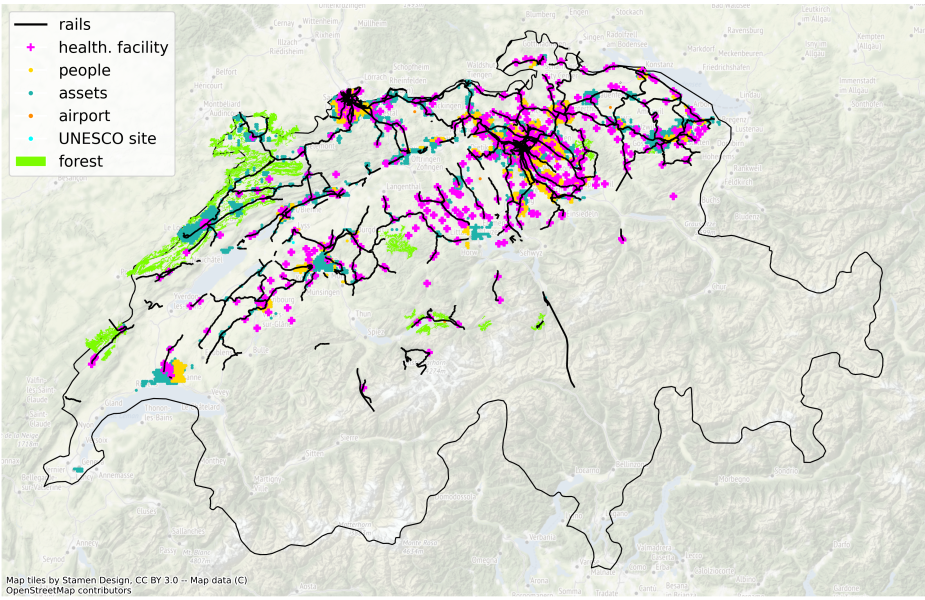

Figure 2.2: Geographical representation of all impacted elements by storm Lothar (c.f. Table 2.1). For visual clarity, only asset value grid cells and population grid cells with impacts above 10 000 $ and 1 000 persons, respectively, are shown. Note that in certain areas (e.g. around the city of Zurich in the North-East) many impacts overlap.

return periods between roughly 80 and 150 years depending on the choice of exposure category, this highlights the potential for disastrous consequences of tail risk events as compared to the average, in particular for non-monetary elements. Furthermore, as shown in Fig. 2.8, the average annual expected impacts are inhomogeneously distributed, with distinct patterns for the different exposure types. For instance, regular impact on forestry is mostly expected in Western Switzerland in the Jura mountain chain, whereas asset damages are concentrated in the regions around Basel and Zurich, and certain train lines in central Switzerland and alpine valleys may be often affected.

Studies have also demonstrated that, under a rapidly changing climate, winter storm risk, as measured in losses to general asset values, may increase by up to 50% between 2020 and 2050, both for average events and for more extreme events (Severino et al. 2023). This increase might bring significant economic challenges, yet does not provide a full picture of the potential for disruption of the railway system, or the losses to vital forest ecosystems and irreplaceable cultural sites, which may hence be explored using the demonstrated workflow.

2.4 Discussion

We showed how OSM-flex, a flexible OSM feature extraction package, can be seamlessly integrated into the CLIMADA risk modelling framework, and how this can provide a basis for multi-faceted natural hazard impact and climate risk assessments on a variety of exposure types. The case study, though brief and mainly illustrative of the major steps and processes of using OSM for climate risk assessments, demonstrated that the readily computed event impacts from winter storm Lothar on rails and on forests in Switzerland came remarkably close to the actual event estimates, which were collected in meticulous survey work at the time (Niemeyer and Albisser 2001), hence providing an efficient way to quickly estimate damages also to sectors which are not closely and easily monitored. Probabilistic estimates for winter storm risks further revealed that risk hot-spots differ spatially for different exposure categories, which may hence guide more targeted adaptation planning. Moreover, contrasting impacts derived from less conventional exposure layers such as UNESCO world heritage sites and natural landscapes with more traditional impact metrics on population and economic assets illustrated that judgment on the severity of an event strongly depends on the exposure considered.

However, the risk modelling approach based on OSM exposure data has several limitations. The suitability of OSM for certain research purposes, as well as OSM data quality and data completeness have been discussed extensively (e.g., Zhang et al. 2022; Zheng et al. 2021). There is a large disparity in OSM coverage between countries and world regions, and between different types of assets (Herfort et al. 2023; Ludwig and Zipf 2019) and attributes further describing these assets (Biljecki et al. 2023). Furthermore, as a crowd-sourced project, not all entries are checked for their accuracy (Xie et al. 2019; Q. Zhou et al. 2022). Even for Switzerland, the extracted features are therefore by no means complete. While the rail network on OSM is mostly congruent with the official geospatial records[4] publicly provided by the Swiss government, only 11 of the 13 UNESCO World Heritage Sites in Switzerland were listed, and of the 58 prehistoric pile dwellings around the Alps, only five were included.

There are no future projections or reliable tracking of past exposure changes within OSM, which is predominantly a snap-shot of a moment in time. Thus, an assessment of past events or future risks can only be made with respect to current exposure or requires additional modeling techniques beyond the OSM realm[5]. Hence, the quality of the risk analysis based on OSM exposure data can vary significantly. Nevertheless, it is often the only freely available resource, and its catalog is continuously growing and improving.

On the technical side, the disaggregation step from OSM polygons and lines to CLIMADA point exposures, as well as the reaggregation of the impact values to these original polygon and line shapes, introduces imprecision owing to the finite resolution of the interpolation algorithm. The uncertainty re-

[4]See `https://geo.admin-thefederalgeoportal`

[5]The Swiss Federal Office for Spatial Development, for instance, reports that settlement and forest areas have grown by >10 % and >2 %, resp., between the early 1990s and 2004, with a slowdown thereafter, at the expense of agricultural land (Bundesamt für Raumentwicklung ARE 2023). Those changes are moderate in absolute terms (e.g. for settlements, an increase from 7% to 7.7% of total Swiss land area)

lated to the resolution can be assessed using Monte Carlo approaches (Kropf et al. 2022). The relative importance of this uncertainty with respect to all other risk model uncertainties from unknowns in the hazard, exposure, and vulnerability model must in general be assessed case by case and can be quantified with sensitivity analysis. Note that it is not possible to make a generic statement on the effect of resolution uncertainty on the risk model, as this depends strongly on the purpose of the study, the chosen output metrics, and the chosen set of modeled input uncertainties (Meiler, Ciullo, et al. 2023).

Extracting features from OSM beyond the pre-written exposure category wrappers in the OSM-flex module can be cumbersome, as the required keys and values need to be identified, and often requires some back-and-forth iterative consultation of the OSM wiki [6] or OSM taginfo databases [7]. The extracted features may further need to be post-processed to eliminate duplicates or simplify complex shapes. This may limit their wide use to non-expert practitioners in the field of climate risk modelling. However, these difficulties are inherent also to the few other open-source and well-maintained OSM feature extraction packages, of which we presented advantages and drawbacks for the use of natural hazard risk assessments. We showed that OSM-flex particularly excels for the use case of repeated, large-scale and highly customized spatial feature extraction within complex software environments where efficient dependency management is key.

Several other works seamlessly integrate OSM data for natural hazard risk calculations. For example, Koks, Rozenberg, Zorn, et al. (2019) combined state-of-the-art global hazard mapping of cyclones, floods and earthquakes with approximately 50 mil. kilometer of transport network data included in OSM to study multi-hazard infrastructure risk and the viability of protection measures. And Nirandjan et al. (2022) extracted, categorized, and rasterized the world's main critical infrastructure systems into a global database, from which the Critical Infrastructure Spatial Index (CISI) is developed, which expresses the global spatial intensity of critical infrastructure and is used in several natural hazard risk studies ((e.g., Gnyawali et al. 2023) for

[6] See `https://wiki.openstreetmap.org`
[7] See `https://taginfo.openstreetmap.org`

landslides). Both studies draw on the extraction and processing source code for OSM data presented in section 2.2.1, which is now packaged into the OSM-flex module, and available to an even wider research audience.

More generally, this may open up complementary possibilities for areas of study that traditionally rely on other types of data sources such as satellite imagery (Stritih et al. 2021). In recent years, there has been a trend towards more holistic, quantitative views of the consequences of extreme weather events as opposed to focusing on monetary asset losses alone. Exemplary studies investigate, e.g., displaced population (Kam et al. 2021) or basic service disruptions (Mühlhofer, Koks, Kropf, et al. 2023). Wider quantitative perspectives will allow decision-makers to not inherently prioritize monetary elements because of the absence of other quantifiable criteria. Thus, the diverse indicators of natural hazard risk, towards which the here-presented approach contributes, can form the basis of multi-criteria adaptation decision frameworks (Bowen 2002; DiStefano and Krubiner 2020; Haque 2016; Velimirović et al. 2023), leveling the playground with economic interests and allowing us to tackle questions such as the role of social inequalities, urban-land divides, and environmental justice (Gerber et al. 2012) in a (semi-)quantitative way.

2.5 Conclusion

OSM is a potent data source for informing multi-faceted climate risk analysis, and can support decision making with respect to climate adaptation, going beyond the common focus on (coarse-resolution) monetary asset values and population counts. Despite the limitations inherent to crowd-sourced open data, OSM can be used to freely retrieve a large variety of exposures with world-wide coverage. In this manuscript, we showcase risk assessment on healthcare facilities, railways, UNESCO World Heritage Sites, forests, and airports, but OSM can be used to retrieve an even larger variety of features: A non-exhaustive listing includes urban assets at single building scale; different land uses such as agriculture, forestry, or pastures; assets for different economic sectors such as mining, industrial manufacturing, commerce, energy or tourism; culturally relevant sites and regions; road networks; critical infrastructures for, e.g., education, water management, communication, energy supply; and ecological regions important for ecosystem service provision, biodiversity preservation, and leisure. We present OSM-flex as light-weight Python-based OSM extraction tool for any of these features. The seamless integration of OSM-flex into the established open-source risk modelling framework CLIMADA promises that the methodology is applicable in academia, public institutions, the private sector, and the humanitarian sector.

Acknowledgement

This project received funding from the European Union's Horizon 2020 Research and Innovation Program (grant agreement No 101003687). Elco Koks received funding from the Dutch Research Council (NWO), Grant No. VI.Veni.194.033.

The authors also thank Emanuel Schmid (ETH Zürich) for their generous technical support.

Data Availability

All the data and source code are publicly available as mentioned in the manuscript. Scripts to reproduce results and result figures can be found at `https://github.com/Evelyn-M/osm-climate-risks`.

2.A Appendix

2.A.1 OSM-flex module

The main steps in the OSM feature extraction process using the OSM-flex package, introduced in section 2.2.1, are explained in more detail in the following paragraphs. The OSM-flex package is available on GitHub (`https://github.com/osm-flex/osm-flex`) and as PyPI package (Mühlhofer, Koks, Riedel, et al. 2023). The modules available within the OSM-flex package are structured according to the previously introduced fours steps.

Download

OSM data is downloaded in Protocolbuffer Binary Format (PBF; see `https://wiki.openstreetmap.org/wiki/PBF_Format` for further description). Automated download options are currently available for the entire planet file (retrieved from `https://planet.openstreetmap.org/pbf/planet-latest.osm.pbf`), for world regions (Africa, Antarctica, Asia, Australia and Oceania, Central America, Europe, North America, South America) and for all countries available on, for example, `download.geofabrik.de`. If the desired region or country is not available via the download-API, it is recommended to clip the desired area from a larger source file (see next step).

As OSM is a crowd-sourced and living project, mapped data constantly evolves. To prevent data sources from becoming outdated when working on them for a longer time span, it is recommended to update the source files occasionally. Two options are conceivable: re-downloading the entire data dump of concern (allowing for existing files to be overwritten in the respective command) or updating the already downloaded files on a recurring basis, using diffs (*.osc.gz). Such diffs are provided at various timestamps from different extract providers, for instance daily via `download.geofabrik.de` or minutely via `download.openstreetmap.fr`.

Clip

This optional step of clipping (cutting) larger source files to any user-defined area requires a one time installation of either osmconvert (Weber 2020) or osmosis (OpenStreetMap contributors 2023b). More command line executables for handling *.osm.pbf files exist, some of which are available via pip and conda distribution channels, such as pyOsmium (Hoffmann and contributors 2023; Topf 2023). However, not all of those currently support all operating systems, which is why the OSM-flex package gives preference to osmconvert and osmosis.

There are three ways to specify the area to which to clip: by passing a bounding box (the corners of a geographical rectangle), passing a shapely (multi-)polygon, or passing a Polygon filter file (*.poly; see `https://wiki.openstreetmap.org/wiki/Osmosis/Polygon_Filter_File_Format` for further description) containing the (multi-)polygon outline information.

Convenience functions are available to obtain country and admin-1 shapes within the OSM-flex package, and there are several ways to obtain .poly files externally (for example, `https://github.com/jameschevalier/cities` for a good description of how to find and obtain them via `http://polygons.openstreetmap.fr/`, and for a .poly file collection of many cities of the world). It should be noted that clipping to (multi-)polygons requires the creation of a temporary .poly file under the hood, and that OSM-flex provides a simplification method for complex shapes owing to file size restrictions. Clipping may take a while, and this process is faster if the source file is smaller (e.g. when taking a region file instead of the entire planet file to clip a contained sub-region).

Extract

There are two broad ways to extract OSM features into tabular (Geo)Pandas (Jordahl et al. 2022) format: via predefined wrappers for some frequently-used exposure categories, or via defining user-specific queries. Extraction wrappers are currently available for assets of many critical infrastructure sectors such as road, rail and air transportation, power, telecommunication, gas, healthcare and education. For user-defined queries, keys, key-value pairs or logic concatenations of these are allowed, together with a specification of which additional attribute keys should be parsed as columns the output table, and which geometry types should be considered. Finding suitable OSM keys or key-value pairs can be challenging at first, yet useful information may be obtained via the OSM wiki map feature documentation (`https://wiki.openstreetmap.org/wiki/Map_features`) or the OSM tag-info webpage (`https://taginfo.openstreetmap.org/`). There are some particularities when extracting uncommon features with may not yet be "registered" in the osmconf.ini file, which comes with the distribution. In such cases, the unknown keys must be manually added in the corresponding sections of the file.

Post-process

The following is a non-exhaustive list of common post-processing tasks which may be needed. Some are already part of this package, with more methods in development:

- simplifying networked geo-data (e.g. roads, rails, power lines): see for instance the "trails" package (Koks, Dickens, et al. 2022)
- removing duplicates (same amenities with slightly different names) and near-duplicates (e.g., amenities may be marked as points, but building-shapes of the same amenities are also collected as multi-polygons): for example GeoPandas sjoin with a certain buffer tolerance (e.g. 100m, ..)
- removing small multi-polygon shapes in large multi-polygon based results (e.g. forest outlines) by filtering polygon area (a built-in shapely geometry attribute)

2.A.2 Comparison of OSM-flex with other OSM-based tools

A plethora of helper tools exist to handle OSM data. Low-level command line tools such as osmosis (OpenStreetMap contributors 2023a), (Py)Osmium (Hoffmann and contributors 2023; Topf 2023), and osmconvert (Weber 2020) have basic functionalities for getting information about an OSM file, converting OSM file formats (such as .xml, .pbf, and .o5m), merging change files (diffs) or clipping geographical areas from an OSM file to a new OSM file.

On the side of maintained, well-documented and user-friendly Python-based parsing tools for OSM features, OSMnx and Pyrosm are two frequently used packages. Table 2.3 presents a brief comparison between these and OSM-flex, to guide potential users in selecting the adequate tool.

Table 2.3: Comparison of OSM-flex V1.0.1 with commonly used Python-based OSM parsing tools Pyrosm V0.6.1 and OSMnx V1.6.0

	OSM-flex	Pyrosm	OSMnx
Source of OSM data	.osm.pbf data dumps	.osm.pbf data dumps	overpass API
Continuous integration & testing	yes	yes	yes
Documentation	yes	yes	yes
Active development	yes	no[a]	yes
License	GPL-3.0	MIT	MIT
Distribution channels	GitHub, pip	GitHub, pip[b], conda	GitHub, pip[b], conda
Package dependencies	Geopandas, cartopy	Geopandas, Pygeos, Cython, Pyrobuf and Cykhash, OSMnx	Geopandas, igraph, networkX, and many others
Feature cleaning & simplification	yes[c]	no	yes
Graph analysis	no	no[d]	yes
Parsing from bounding boxes	yes[e]	yes[f]	yes
Parsing from polygons	yes[e]	no	yes
Parsing from address	no	no	yes
Suitable for large queries	yes	yes	no
Suitable for queries on any user-defined tags	yes	yes	yes
Availability of pre-written common queries	yes (many infrastructure sectors)	yes (streets, buildings, POIs, landuse)	yes (buildings, many road classes)
Integration in risk model	yes[g]	no	no

[a] no code development within past 365 days; [b] limited guarantee of success due to complex package dependencies; [c] simple filtering and duplicate removal, [d] util functions for export to igraph or networkX graphs via OSMnx available; [e] python-based wrappers requiring pre-installation of osmosis or osmconvert; [f] inefficient for very large data sets; [g] seamless integration with CLIMADA (Aznar-Siguan and Bresch 2019) and DamageScanner (Koks 2022).

OSM-flex is closer in its implementation logic to Pyrosm. Two main advantages are the lower dependency requirements and the possibility to clip arbitrary user-defined geographical shapes from the data dumps (i.e. pre-perform a geographical filtering). Due to its implementation in Cython, Pyrosm might on the other hand be slightly faster in parsing data where no geographical filtering is applied. If only few OSM features are queried, or (road) network analysis should be performed, OSMnx is likely the best tool at hand.

2.A.3 Lines and Polygons utility module

This utility module disaggregates line and polygon geometries into points, which, for instance, is necessary to spatially overlay (or, essentially, point-match) hazard footprints and exposures in CLIMADA impact calculations.

The desired disaggregation resolution can be specified in units of either the original coordinate reference system (crs) or in metres. In the latter case, geometries are automatically re-projected to a metre-based cylindrical projection centered around the object's central coordinate, to minimize distortions from the re-projection. For polygons, a regular raster of the chosen resolution is created and all points of the raster inside of a polygon are assigned to it. For polygons smaller than the raster resolution, at least one single point inside the polygon is assigned (even if this point is not part of the raster). Note that one does thus not have a common raster for all polygons, but one raster per object (since each object uses its own centered projection). Users that want to use a common raster can define one for the disaggregation (the re-projection must then be performed by the user). Lines are divided into segments equal in length in such a way that the total length of all lines is preserved. This is achieved by first computing the number of points N per line by dividing the line length by the resolution and rounding the result. The minimum number of points is one. Second, the line is divided into corresponding $N + 1$ equal-length segments, and the points are placed in the middle of the segments.

More precisely, the number of points a line is divided in is

$$N = \max\left[\mathrm{round}[(l/r) - 1)], 1\right] \tag{2.1}$$

with l the total length of the line and r the resolution. The effective resolution of the line is then

$$r_e = \frac{L}{N}. \tag{2.2}$$

These N points are then distributed on the line at fractions of the line lengths starting from $r_e/2$

$$f_1 = r_e/2 \; ; \; f_2 = r_e \; ; \; f_3 = 3r_e/2 \; , \; \ldots . \tag{2.3}$$

Several examples are listed in Table 2.4.

Table 2.4: Disaggregation examples for lines of varying lengths and target resolutions.

Length	Resolution	Number Points	Effective resolution	Fractions
l=1	r=2	N=1	$r_e = 1$	$f_1 = 0.5$
l=1	r=0.8	N=1	$r_e = 1$	$f_1 = 0.5$
l=1	r=0.6	N=2	$r_2 = 0.5$	$f_1 = 0.25, f_2 = 0.75$
l=1	r=0.4	N=2	$r_e = 0.25$	$f_1 = 0.25, f_2 = 0.75$
l=1	r=0.2	N=5	$r_e = 0.2$	f_1=0.1, f_2=0.3, f_3=0.5, f_4=0.7, f_5=0.9

The exposure value associated with each original line or polygon geometry can then either be divided equally among all points or be assigned wholly to each point. The former is typically used to disaggregate quantitative values such as the number of people, or to compute relative affected areas by disaggregating the value 1 over each geometry. The latter can be used to assign the area of the corresponding raster cell to each raster point, or the length of the corresponding line element to each line point, or to propagate qualitative values such as an ecosystem type. Note that the disaggregation leads to a certain distortion of the values, in particular, due to boundary effects, and the user should carefully choose the resolution of the raster to fit the purpose of the study. One way to check the approximation resulting from the disaggregation step is to re-aggregate the values by geometry and compare.

2.A.4 Application: Input data and method details

OpenStreetMap queries

The exposures used for the impact computation reported in Table 2.1 and 2.2 were based on the GeoDataFrames retrieved with the OSM-flexmodule using the OSM tags (keys and values) as described in Table 2.5. Note that for the critical infrastructures 'Healthcare facilities' and 'Airports', a single-line helper function is implemented within the CLIMADA OpenStreetMap module, which facilitates common queries.

Table 2.5: OSM tags (keys and values) and geometry types, which were extracted from the osm.pbf data dump for the respective exposure types, using the OSM-flexpackage

Exposure Type	OSM Keys	OSM Values	Geometry Type
Healthcare facilities	'amenity' 'building' 'healthcare'	'hospital' or 'doctors' 'hospital' or 'clinic' 'hospital' or 'clinic' or 'doctors'	points, multipolygons
Railways	'railway'	'rail' or 'tram' or 'light_rail' or 'narrow_gauge'	lines
Airports	'aeroway'	'aerodrome'	multipolygons
UNESCO sites	'heritage_operator'	'whc'	points, multipolygons
Forests	'landuse'	'forest'	multipolygons

Hazard, Exposure, and Vulnerability Data

Fig. 2.3 displays the winter storm hazard footprints retrieved from the CLIMADA data API (Schmid 2023). Fig. 2.4 displays exposures for Switzerland, retrieved using the OSM-flex module, and fig. 2.5 asset value distributions from LitPop (Eberenz, Stocker, et al. 2020) and gridded population density (Center for International Earth Science Information Network (CIESIN), Columbia University 2017). Fig 2.6 displays impact functions (vulnerability curves) wind storm intensity to expected exposure impacts.

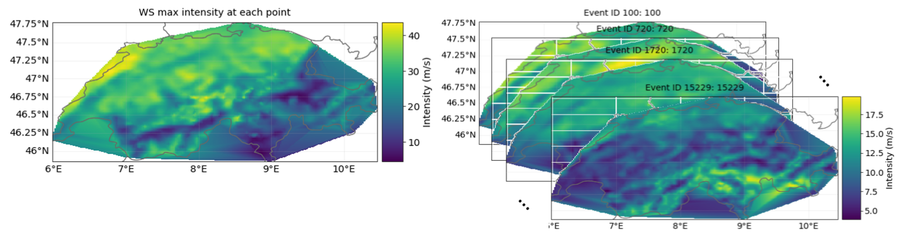

Figure 2.3: Winter storm hazard footprints (maximum 1-minutes sustained wind speed over 3-days) of Lothar (left) and of the WISC probabilistic extension hazard set for current climate (right) from (Röösli and Bresch 2020; Welker et al. 2020).

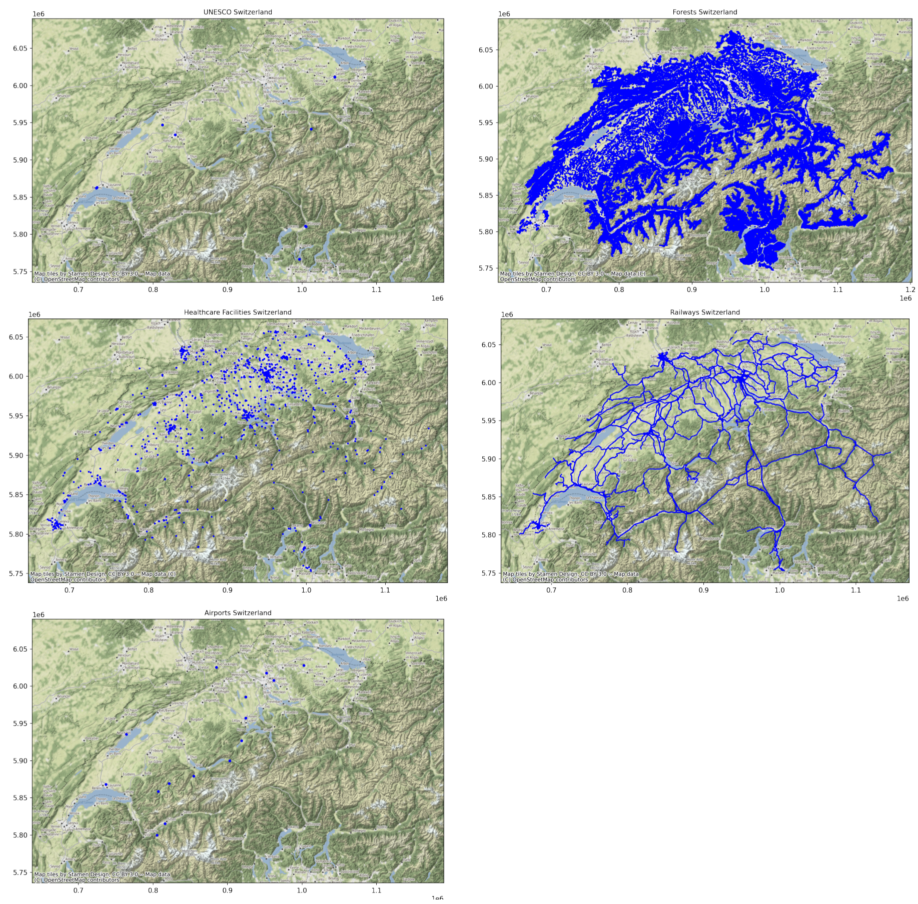

Figure 2.4: Exposure data extracted with the OSM-flexmodule (UNESCO heritage sites, forests, healthcare facilities, railways, airports) after post-processing (removal of duplicates, removal of polygons with area below 1 000 m^2)

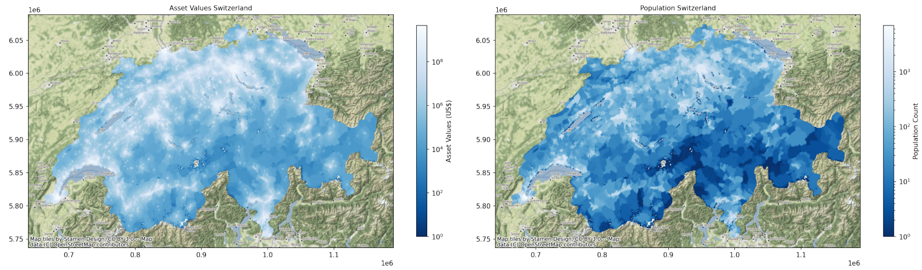

Figure 2.5: Exposure data often used for climate risk assessment: asset value distributions from LitPop (Eberenz, Stocker, et al. 2020), and gridded population density (Center for International Earth Science Information Network (CIESIN), Columbia University 2017).

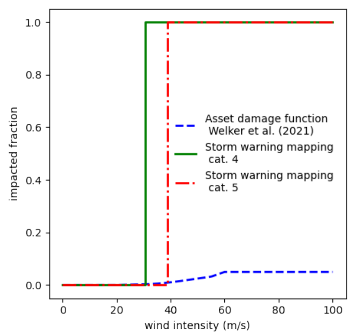

Figure 2.6: Impact functions employed for event impact and risk computations from winter storms for asset damages (blue, based on (Welker et al. 2020)), for affected healthcare facilities, UNESCO heritage sites, population and railways (green, based on the Federal Office for Meteorology and Climatology's warning category 4 wind-speed threshold (110 km/h or 30.5 m/s), and for forest loss (red, based on the warning category 5 wind-speed threshold (140 km/h or 38.9 m/s)).

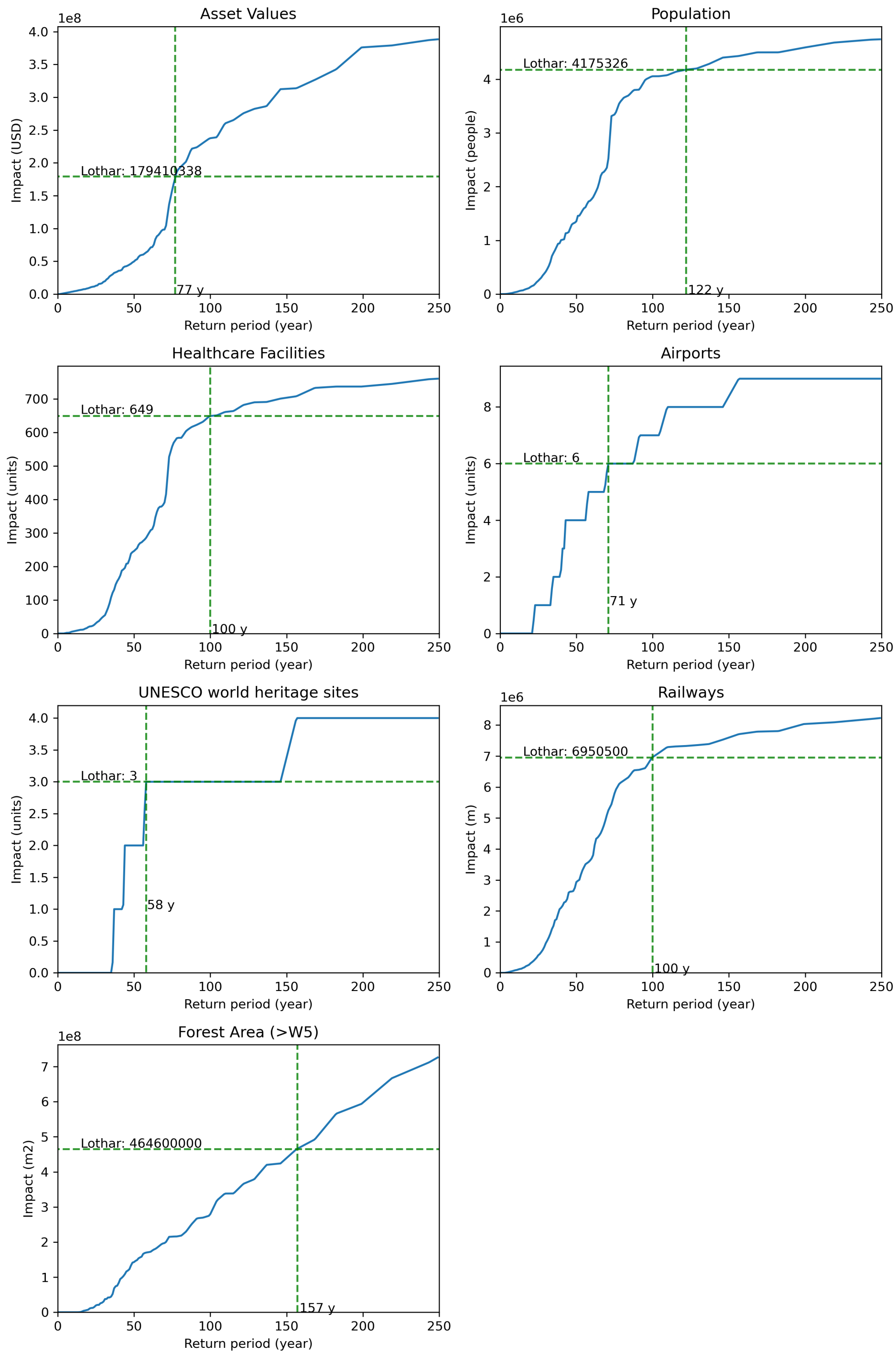

Figure 2.7: Return period curves of winter storm impacts for all exposure data categories used in this work's climate risk assessment, computed from the WISC probabilistic extension hazard set for current climate from (Röösli and Bresch 2020; Welker et al. 2020). Historic impacts from winter storm Lothar are indicated on the vertical axis, the corresponding computed return period values of these impacts are indicated on the horizontal axis.

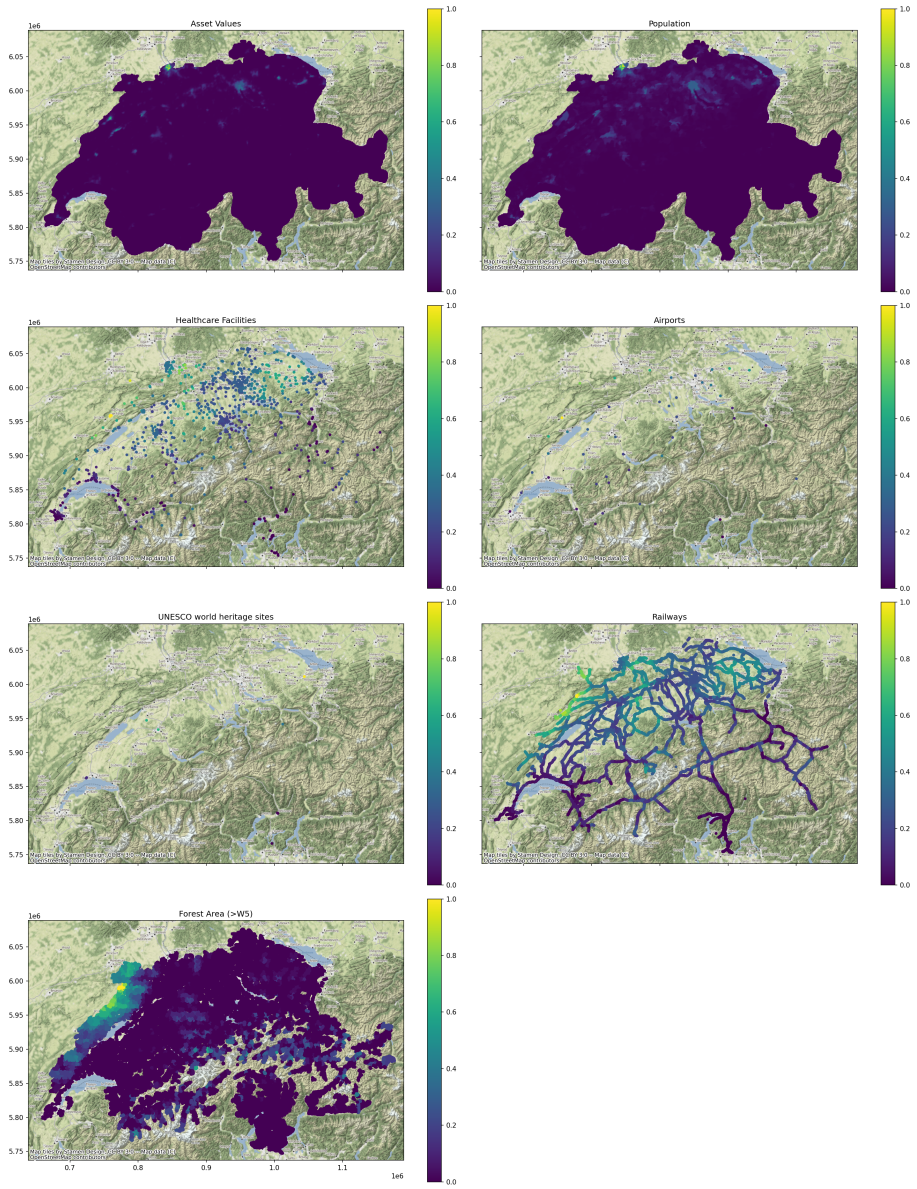

Figure 2.8: Normalized average expected annual impact derived from the probabilistic winter storm set (c.f. Fig.2.3) for all exposures (c.f. Figs. 2.4, 2.5). For each exposure type individually, the impacts are normalized by the maximum impact over all points. The relative value highlights the impact hotspots for all exposure types.

CHAPTER 3

A generalized natural hazard risk modelling framework for infrastructure failure cascades

Evelyn Mühlhofer, Elco E. Koks, Giovanni Sansavini and David N. Bresch;
published in *Reliability Engineering and Systems Safety*

Abstract. Critical infrastructures are more exposed than ever to natural hazards in a changing climate. To understand and manage risk, failure cascades across large, real-world infrastructure networks, and their impact on people, must be captured. Bridging established methods in both infrastructure and risk modelling communities, we develop an open-source modelling framework which integrates a network-based interdependent infrastructure system model into the globally consistent and spatially explicit natural hazard risk assessment platform CLIMADA. The model captures infrastructure damages, triggers failure cascades and estimates resulting basic service disruptions for the dependent population. It flexibly operates on large areas with publicly available hazard, exposure and vulnerability information, for any set of infrastructure networks, hazards and geographies of interest. In a validated case study for 2018's Hurricane Michael across three US states, the model reproduced important failure dynamics among six infrastructure networks, and provided a novel spatial map where people were likely to experience disruptions in access to healthcare, loss of power and other vital services. Our generalized approach allows for a view on infrastructure risks and their social impacts also in areas where detailed information and risk assessments are traditionally scarce, informing humanitarian activities through hotspot analyses and policy frameworks alike.

3.1 Introduction

When natural hazards disrupt critical infrastructures (CIs), their failure can be detrimental to public health, safety, security, well-being and economic activities. Whether due to an earthquake in Japan, a flooding across Western Europe or a hurricane hitting the US, lifeline disruptions are ubiquitous: loss of power and telecommunication services may compound with a dysfunctional transport system and damaged hospitals, preventing emergency responders to intervene timely, rendering villages inaccessible for days, cutting off evacuation routes, or leaving school children without access to education for up to weeks (Bay District Schools 2022; Beven II et al. 2019; Burlew 2018; Price and Glenn 2018).

As infrastructure investments are at an all-time high (Thacker, Adshead, et al. 2019), CI systems around the globe are more than ever exposed to natural hazards, a trend which is further exacerbated in a changing climate (McKinsey Global Institute 2020). This poses a threat to air, road and rail transportation alike (Koks, Rozenberg, Zorn, et al. 2019; Yesudian and Dawson 2021), puts power generation at risk (Nicolas et al. 2019) and causes losses of billions of US dollars annually in several CI sectors (Koks, Rozenberg, Zorn, et al. 2019; Nicolas et al. 2019).

Since societal impacts of CI failures tend to reach far beyond the technical sphere, managing resilient infrastructure has become a prime area of concern for policy makers: CIs "directly or indirectly influence the attainment of all of the SDGs" (Thacker, Adshead, et al. 2019) and may accrue up to 88% of all climate adaptation costs until 2050 (Thacker, Adshead, Daniel, et al. 2021). Reducing CIs damages and basic service disruptions forms part of the agendas of the Sendai Framework for Disaster Risk Reduction, the European Commission's Programme for Critical Infrastructure Protection (EPCIP) and the 26th UN Climate Change Conference (COP26) alike. Though different in scope and nature, three key challenges of CIs in a socio-technical context are recurrent: Knowledge on the extent to which CIs are exposed to natural hazards is insufficient, especially in the Global South (cf. §25 e and f in UNDRR 2015); interdependences between different CIs are often poorly understood, and cascading effects from CI failures are difficult to analyse and hence manage systematically (Rinaldi et al. 2001; *SWD(2013)318* 2013); the experienced hardship from CI failures depends on the degree and duration to which basic services are disrupted (Mitsova, Esnard, et al. 2018), yet the link between infrastructure damages, resulting service outages and affected population is not straightforward.

Capturing the response of interdependent CI systems to natural hazards, and studying the impacts of their failures onto the population, is an endeavour residing at the intersection of natural hazard (NH) risk modelling, infrastructure modelling and social vulnerability research. Traditionally, those problems have been approached with community-specific research questions and methods: NH risks emerge through the interplay of weather and climate-related hazards, the exposure of (infrastructure) assets, goods and people to those hazards and their specific vulnerabilities (IPCC 2014). Event-based impact modelling therefore commonly relies on those three components to calculate expectable asset damages to CIs as a proxy of direct risk (Group 2009). Efforts to capture risk levels for CIs globally are often challenged by data availability (cf. Stip et al. 2019), yet have been undertaken for a few hazards and CI sectors such as road, rail, airports and power generation (Hallegatte et al. 2019; Koks, Rozenberg, Zorn, et al. 2019; Yesudian and Dawson 2021). Despite acknowledging the importance to embrace a systems-thinking approach for resilience (Bresch, Berghuijs, et al. 2014; Dawson et al. 2018), NH risk modelers' predominant focus on 'asset scale risk' (Dawson et al. 2018) often runs short of capturing CI interdependencies and 'network scale risks'. As such, the community's risk assessment methods are not yet tailored to the specificities of CIs.

In infrastructure research, CI interdependences and failure cascades have received much attention since the seminal work of Rinaldi et al. (2001) and approaches to model them have converged to several state-of-the-art methods, comprehensively summarized in Ouyang (2014). Especially in studies employing network (flow) approaches (cf. Lee et al. 2009), research on failure cascades is often motivated by NH events as triggers (Goldbeck et al. 2019; Loggins and Wallace 2015; Nan and Sansavini 2017; Pant, Hall, and Blainey 2016; Pant, Thacker, et al. 2018; Zorn, Pant, et al. 2020). Yet, most research in this domain shares some of the following tendencies: Investigated systems are mostly small-scale, representative of mid-sized towns or single community districts and illustrate dynamics for a sub-system of two infrastructure types (Banerjee et al. 2018; Dueñas-Osorio, Craig, et al. 2007; Goldbeck et al. 2019; Guidotti et al. 2016; Ouyang and Dueñas-Osorio 2011) (see Pant, Hall, and Blainey 2016; Thacker, Pant, et al. 2017; Zorn, Pant, et al. 2020, for counter-examples) where power, transport and telecommunication systems are investigated much more often than social facilities such as schools or hospitals. CI data is frequently based on artificial, well-defined test-beds (Guidotti et al. 2016; X. He and Cha 2020; Loggins and Wallace 2015; Masoomi et al. 2020) or tailored to the (sometimes proprietary) data at hand, which is overwhelmingly based in the US, Europe and Oceania (Hernandez-Fajardo and Dueñas-Osorio 2013; Ouyang and Dueñas-Osorio 2011; Tootaghaj et al. 2019; Zorn, Pant, et al. 2020). Failure scenarios often focus on random or component-wise removals (Beyza et al. 2020; Fotouhi et al. 2017; Thacker, Pant, et al. 2017) or feature stylized shapes in lack of realistic hazard footprints (Masoomi et al. 2020; Zorn, Pant, et al. 2020). Study scopes and trigger mechanisms in existing CI research are hence not necessarily tailored to capture the magnitude and spatial extents of real-world NH events and CI systems.

Lastly, the technical discourse on CI failures, where impact metrics focus predominantly on functional performance benchmarks, does not link adequately to the domain of social vulnerabilities (Garschagen and Sandholz 2018). Apart from empirical case-studies using print media accounts (Chang, McDaniels, Mikawoz, et al. 2007), only few modelling studies have explored consequences of CI failures for (socio-economically different groups of) people (Chang, Pasion, et al. 2012; Karakoc et al. 2020). Despite advances in tackling this common problem space, silos persist which have inspired several stylized and theoretical frameworks on systemic CI risks at a national analysis level (Dawson et al. 2018; Pant, Hall, and Thacker 2017). Following this logic, our aim is to practically implement a flexible and open-source end-to-end impact model which estimates spatial patterns of people experiencing basic service disruptions caused by natural hazard-induced CI failure cascades. In line with Zio (Zio 2016), who stresses the need to integrate different modelling perspectives to capture complexities of CI system failures, we showcase how synergies can be yielded by combining established methods and platforms used by CI researchers and NH risk modellers alike. The design focus of this seamless impact model is put particularly on the rapid analysis of large, interdependent, real-world infrastructure systems and the dependent population in diverse geographical regions, which are exposed to different types of natural hazards and where only limited process knowledge and data may be available. Impact estimates produced with this approach are hence thought to inform rapid hotspot assessments during emergency responses, or as a cross-national, human-centric measure of risk for policy purposes in international frameworks.

Section 3.2 describes the conceptual framework which was constructed to meet above-mentioned design criteria and its concrete implementation as a 'system-of-systems' (Pant, Hall, and Thacker 2017) formulation for infrastructure networks embedded in the open-source risk modelling platform CLIMADA (Aznar-Siguan and Bresch 2019). Section 3.3 exemplarily illustrates how the model can provide information services in the aftermath of disaster using a real-world case study of Hurricane Michael hitting the Florida Panhandle. A scenario analysis is performed and model outputs are validated using official reports and print media accounts, to facilitate a wider discussion on the merits and trade-offs of this approach in section 3.4, and to examine its adequacy for use in risk assessments, emergency response, adaptation planning and policy making.

3.2 Methods

The framework in Figure 3.1 illustrates the major conceptual stages developed to calculate basic service disruptions from natural hazard-induced infrastructure failure cascades, with required inputs and main outputs.

In stage I an infrastructure system model calculates functional states of interdependent critical infrastructures using georeferenced information on infrastructure components, dependent population, dependency heuristics and supply and demand data. The employed modelling approach relies on a 'system-of-systems' formulation logic (cf. Pant, Hall, and Thacker 2017; Thacker, Pant, et al. 2017; Zorn, Pant, et al. 2020), where CI systems are treated as hierarchical topological networks interconnected through depen-

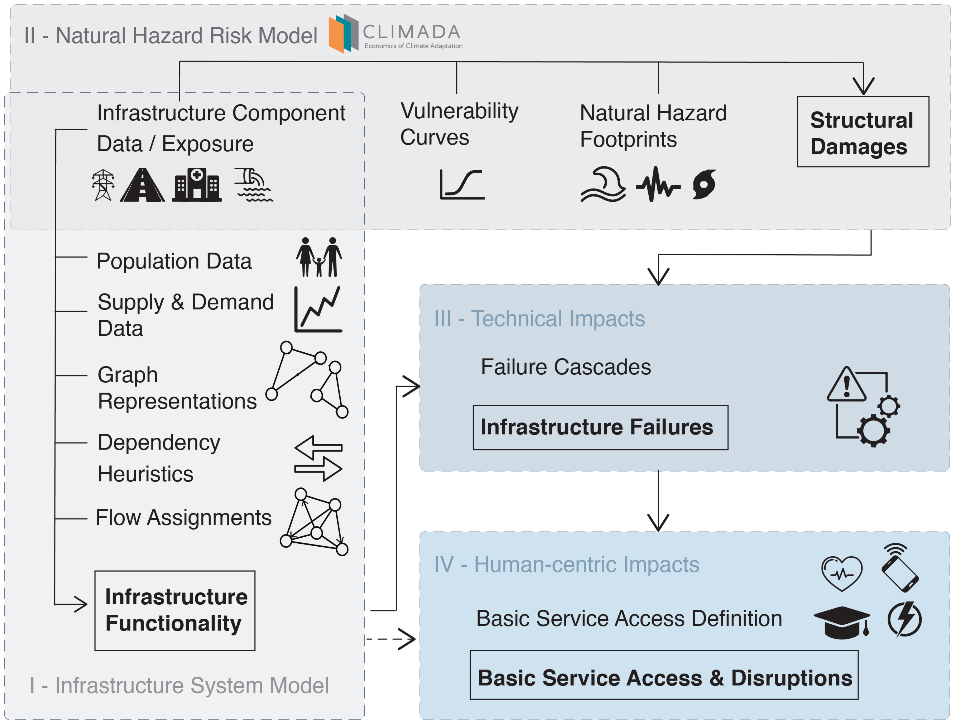

Figure 3.1: Developed framework to model the population experiencing basic service disruptions from natural hazard-induced infrastructure failure cascades. The four stages are linked within a single platform and encompass infrastructure system modelling (I), natural hazard risk modelling (II), and two spatially explicit results layers - impacts to infrastructure components (III) and to the dependent population (IV). Main outputs of each stage are in bold within a box.

dencies between each other. The reliance on complex network theory and simpler flow calculations reduces the complexity of full-fletched physical models, yet has been demonstrated as a versatile, illustrative and data-efficient alternative capable of capturing large-scale dynamics across big system scales (Zorn, Pant, et al. 2020). In stage II, structural damages to infrastructure components are computed from spatially- explicit hazard footprints and tailored vulnerability curves, using the risk assessment platform CLIMADA, which was in turn chosen for its state-of-the art performance in hazard modelling, global consistency and open-source character. Stage III feeds results from structural damage calculations back into the infrastructure system model, which triggers failures cascades along infrastructure dependencies. Results of this stage are technical failures at the infrastructure systems level. In stage IV, technical impacts of CI failures are translated to human-centric impacts. Resulting disruptions to basic service access are computed for all services provided by the CI systems under study, for the dependent population.

The following sections describe the implementation details of the framework. While emphasis is put on the conceptual choices that were made to unite models from natural hazard risk and infrastructure modelling communities, specific technical explanations referring to the practical open-source code base implementation are provided where necessary. For a list of abbreviations used throughout the text and a condensed formal description of the entire algorithm, see Appendix 3.A.1.

3.2.1 Stage I: Infrastructure System Model

Data Requirements: Infrastructure Components, Population, Supply and Demand

Geographic data of CI networks - henceforth referring to the spatial representation of real-world infrastructures such as the location of schools, roads or electrical power plants - and of population must be procured at component (i.e. asset) level for the area of interest, such as a country, state or greater metropolitan area. Within the modelling framework, user-provided data sources may be ingested or high-resolution data can be obtained via automatized queries from open-source data providers such as OpenStreetMap and the WorldPop project(WorldPop and Center for International Earth Science Information Network (CIESIN), Columbia University 2020). A first step of complexity reduction and standardization then consists in limiting the diverse structural components per CI network to a few main building blocks or components. For instance, the road network could be reduced to intersections (nodes) and streets (edges), without differentiating further between road types, bridges or tunnels (cf. Table 3.4 for a non-prescriptive component selection example for six main types of CI networks at various resolutions). Further, supply and demand data of the CI networks and their end-users, e.g. electricity generation and consumption statistics for the power network, as provided by the International Energy Agency (IEA), may be collected as available. This is, however, not imperative for the presented approach, as will be demonstrated throughout the method sections.

As a stylized example throughout the remainder of the model description, we consider the mobile communication (c), electric power (e) and health (h) networks represented through their most crucial components (respectively, cell towers, power plants, transmission lines, poles, and hospitals) and population grid cells (p) representing end-users as illustrated in Figure 3.2, panel BS.1. Fictitious power plant generation values and per capita electricity consumption statistics are included to demonstrate a case of demand and supply data availability, whereas such statistics are here supposed to be unavailable for all other CI networks.

Graph Representations

Infrastructure components are hence transformed into directed graphs consisting in nodes and edges. Within the modelling framework, corresponding cleaning and conversion algorithms are provided. In our example, the power network's plant and poles are represented by nodes and power lines as edges, while the graphs for communication and healthcare networks are made up of nodes only (see Figure 3.2, panel BS.1 (centre)). These formal representations will henceforth be referred to as CI graph G^j , where j is the system type (e.g. Ge for the electric power CI graph). In addition, geographical location L, initial functional state F_0 and the infrastructure-specific damage threshold D^j are set as attributes for all elements (nodes and edges) in each CI graph. F_0 is set to 1 for all elements. D^j indicates the structural damage fraction beyond which a component will lose its functionality and is a simplifying concept to derive functional states from damages. Thresholds are set arbitrarily in this example for purely illustrative purposes. The population network similarly is represented by a node-containing graph with people counts and geographical location as node attributes.

Dependency Heuristics

Departing from an extensive review on CI interdependence models, a list of 120 functional and logical dependencies between components of 11 different CI networks was collected (see Supplementary SM2) and consolidated within six generic rules, referred to as dependency heuristics:

i. Most CI networks depend on electric power supply, (cooling) water supply and information and communications technology (ICT)

ii. People-hosting facilities (e.g. hospitals, schools, power plants) depend on road access

iii. Dependencies can be categorized into either having redundant character, where several sources can provide necessary support (e.g. telecommunication access from any reachable cell), or being unique, where support is provided from a unique source (e.g. power from the single closest power line).

iv. Dependencies are distance-constrained (e.g. a cell tower located 500 km away will not provide relevant service, neither will a hospital which is 1500 km across the country).

v. Dependencies may entail a continuous, physical flow between source and target (e.g. water, electricity), yet can be approximated through a binary, logical connection.

vi. Population (end-users) depends on CIs for services, but not vice-versa.

These rules serve as a first starting point to identify sets of CI networks between which functional dependencies likely exist, and to sketch out a set of variables which can be fed into a quantitative dependency-search algorithm: source, target, distance threshold, redundancy, road access and flow. These dependency-search variables, described in more detail in Table 3.1, can be parametrized and manually adjusted to the case study at hand. The modelling framework's algorithm then places directed edges e^{jk} (dependencies) between any nodes of CI graph pairs (G^j,G^k) which fulfil the dependency conditions specified in the parametrizations of the described variables. In the stylized example of Figure 3.2, panel BS.1 ('Interdependent CI Graph'), a dependency list indicates CI network pairs which are generally hypothesized to exhibit dependencies (white underlaid). For instance, hospitals (target) are likely dependent on electric power (source), which for hospital node 6 is supplied uniquely from power node 3 (no redundancy), given that the supply point was close enough (distance $<$ distance threshold).

The dependency-search algorithm equally allows assignment of end-users to CI networks in the absence of more detailed, yet often proprietary utility

Table 3.1: Required variables for the dependency-search algorithm between CI graphs. 'Source' and 'Target' are CI network components of different systems, previously identified from the heuristics explained above. Specific values for the variables may be filled in as adequate for the case study at hand.

Variable	Description
Source	Supporting CI component
Target	Dependent CI component
Distance Threshold	The maximum distance for establishing a link between two nodes is determined by a circle around the target with respective radius if road access is not required, else the shortest path via road edges connecting source and target nodes must not exceed the specified threshold.
Redundancy	Whether a target node is connected to all CI nodes of type source within a specified distance threshold (TRUE) or only to the single closest one (FALSE).
Road Access	Whether a road path must exist between source and target.
Flow	Whether the flow through the dependency edge is informed by a physically informed, continuous variable ('physical', such as power cluster capacity), or by a binary ('logical') variable, indicating if supply can be provided or not based on the functional state of the source.

providers' customer data; the population graph is then the target of infrastructure - end user pairs (G^j,G^p) for any relevant infrastructure type j. The algorithm hence results in the creation of one interdependent CI graph G from all CI graphs and the population graph. This is illustrated in Figure 3.2, panel BS.1 ('Interdependent CI Graph'); population cluster node 12 (source), for instance, is dependent on any (redundancy) of the cell towers (target) within the set distance threshold for the provision of mobile communications, which is fulfilled by cell tower node 12.

Next, for each combination of source-target pair jk for which edges e^{jk} were created in the interdependent CI graph, the attributes capacity C^{jk} and capacity threshold T^{jk} are assigned to all nodes. C^{jk} is initialized to discrete values, depending on whether a node is a source (1), a sink (-1) or neither (0) for the flow from CI network of type j to type k. T^{jk} ([0,1]) indicates what percentage of a standardized flow unit from j needs to arrive at a component of type k for it to remain functional. Bespoke hospital node 6 in Figure 3.2, panel BS.1 ('Interdependent CI graph') depends on electric power (e) and telecommunications (c), and provides healthcare services to people (p), and hence C^{eh} and C^{ch}=-1, while C^{hp}=1. For the hospital to remain functional in this example, it needs to receive at least 0.6 standardized units of power through its dependency link(s) (T^{eh}=0.6), 1 unit of telecommunications access (T^{ch}=1), and no unit of healthcare access, since it is the provider of this service (T^{hp}=0). Geographic dependencies (Ouyang 2014; Rinaldi et al. 2001) are implicitly accounted for in the framework through the spatial explicitness of all representations.

Flow Assignments and Infrastructure Functionality

Incorporating commodity flows in addition to a system's topology has been argued as crucial for capturing system performances adequately (Guidotti et al. 2016). Yet, interdependent CI networks entail flows within individual networks (e.g. power in the power grid), and across networks (e.g. power to hospitals). Flows are furthermore of different natures, involving physical commodities (water, electricity, etc.) as well as logical dependencies (connectivity to mobile communications). To deal with this diversity, internal flows in CI networks and flows along dependencies between CI networks are treated separately. Results are then translated into binary functional states and normalized capacity values for coherence across all networks. Formally, those calculations are performed on subgraphs of the previously established interdependent CI graph G, henceforth denominated as G'^{j} and G'^{jk}. Subgraphs span all elements of infrastructure type j, and of types j, k, and linking edges e^{jk}, respectively, yet also retain their reference to the overarching graph G, which is hence updated. Figure 3.2, panel BS.2 provides a visual illustration of such subgraphs.

Flows within networks For networks with internal flows between sources and sink elements, infrastructure type-specific flow assignment algorithms, flexibly tailored to the data and knowledge available, are employed to update all capacity attributes C^{jk} on the corresponding subgraphs G'^{j} (for examples on flow calculation approaches, see (Gauthier et al. 2018) for road networks, (Chmielewski et al. 2016) for water networks and (ibid.) for power networks). Figure 3.2, panel BS.2 (left) illustrates this procedure for the power network, which is the only network involving internal commodity flows in this stylized example. In absence of further system knowledge apart from demand (per capita consumption data), supply (power plant generation data) and

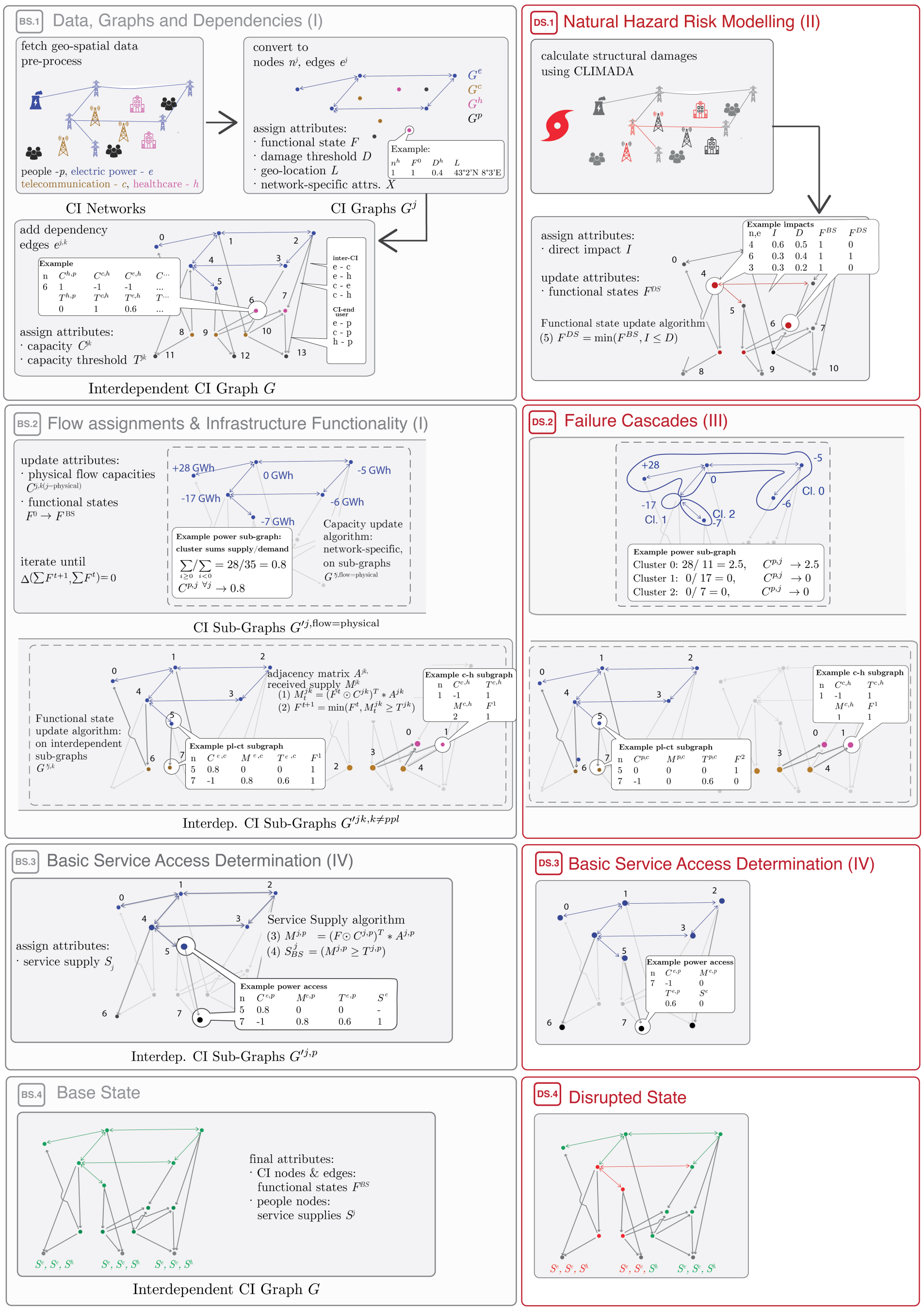

Figure 3.2: Stylized illustration of the entire modelling chain for 3 CI systems, people and a tropical cyclone event. Panels BS.1-4 (left) show the setup of the infrastructure systems model given infrastructure data, population data and dependency heuristics (BS.1), flow assignments and infrastructure functionality determination (BS.2), and basic service access determination for the population (BS.3), which hence represents the base state of the system (BS.4). Panels DS.1-4 (right) demonstrate the effects of structural damages caused by a natural hazard event (DS.1) triggering CI failure cascades (DS.2) and causing basic service disruptions to the population (DS.3). Roman numbers in brackets refer to the corresponding stages in overview Figure 3.1. Detailed explanation is given in sections 3.2.1-3.2.4. For a list of abbreviations and formal treatment, see Appendix 3.A.1.

network topology, a cluster approach is employed. For each cluster in G'^e (here there is only one cluster), the ratio of supply (28 GWh) to demand (35 GWh) is computed, and assigned as a new relative capacity value C^{ek} (here 0.8) to all nodes in that cluster. This can be read as the power system operating at C*100% of its required capacity. Functional states F of the components remain unaltered in this mechanism.

Flows across networks The goal of this step is to determine the functionality F of each dependent infrastructure node in the interdependent CI graph based on the available capacities from other supporting infrastructure nodes. For each unique type of dependencies jk (e.g., power-communication, j=e, k=c) in G, subgraph G'^{jk} is extracted. A received supply variable M^{jk} is computed for each node in G'^{jk}. M^{jk} amounts to the sum of capacities C^{jk} received at target nodes k from functional source nodes j via an edge e^{jk}, and is hence 0 at nodes of type j. Technically, this flow propagation is computed on the adjacency matrix using matrix multiplication only, which is computationally efficient even for large networks. If M^{jk} is smaller than a previously set capacity threshold T^{jk}, a node loses functionality ($F = 0$). Figure 3.2, panel BS.2 (right) illustrates this procedure formally (Eqs. (1) and (2)) and graphically on the electric power-mobile communications subgraph, which entails a physical, continuous variable flow, and on the mobile communications-healthcare subgraph, approximated by a binary (logic) variable flow: The cell tower node #7 receives a total of $Mec = 0.8$ normalized units of power from the power sources it is connected to, which is greater than the capacity threshold (here set to $T^{ec} = 0.6$). It hence remains functional ($F = 1$). Hospital node #1 receives $M^{ch} = 2$ logical units of supplies from both cell towers it is connected to. As this exceeds the needed (logical) units of cell tower supply ($T^{ch} = 1$), the hospital also remains functional ($F = 1$).

Since dependency loops (inter-dependencies) can exist among CI networks, internal and inter-network flow assignment procedures are iteratively repeated until there are no more functional variable changes across any elements in the interdependent CI graph G.

3.2.2 Stage II: Natural Hazard Risk Model

While several platforms for natural hazard modelling exist, the open-source and -access software CLIMADA (CLImate ADAptation) (Aznar-Siguan and Bresch 2019) is the only globally consistent and spatially explicit tool which is freely available to assess the risks of natural hazards and to support the appraisal of adaptation options (Bresch and Aznar-Siguan 2021). The event-based modelling approach of CLIMADA has been used, among others, to conduct risk studies of tropical cyclones on assets across the globe (Eberenz, Lüthi, et al. 2021), to discern impacts from river floods in a changing climate (Sauer et al. 2021) and on people displacement (Kam et al. 2021), and in the wider context of Economics of Climate Adaptation studies (Souvignet et al. 2016). The framework allows for a fully probabilistic risk assessment based on the IPCC risk definition (Field et al. 2014) as a function of hazard, exposure and vulnerability.

Hazard

Hazard is a spatially explicit representation of the intensity of a natural physical event, such as geo-referenced wind speed for storms or water height for floods. Hazard footprints can, for instance, be based on historic records, forecasts or climate projections, or be synthetically generated to create probabilistic event sets. In CLIMADA, hazard modules are available for tropical cyclones, floods, wildfires, earthquakes, landslides, avalanches and heatwaves in different stages of maturity, yet can also be provided through user-ingested raster or vector data.

Exposure

Exposure refers to the geo-referenced assets or population data that are located in the area of interest. In CLIMADA, exposure modules are available to retrieve a global gridded asset dataset (LitPop Eberenz, Stocker, et al. 2020), critical infrastructures from OpenStreetMap, and high-resolution gridded population data out-of-the-box. User-provided data in raster or vector formats can equally be ingested. Exposures require a value assignment to capture the value potentially at risk, such as pre-computed economic (Dollar) values for LitPop, and lengths, areas or simply unity for infrastructure components (e.g. 100 m for a road section or 1 for 'a' healthcare facility).

Vulnerability

Vulnerability, also termed impact function or fragility curve, is an exposure-specific mapping of hazard intensity to expectable damage extent. Vulnerability curves for tropical cyclone winds on general economic asset stocks have been calibrated in CLIMADA for nine world regions (Eberenz, Lüthi, et al. 2021), while the dedicated impact function module also allows to specify hazard- and infrastructure-component specific functions taken from literature, such as the HAZUS technical manuals provided by the US Federal Emergency Management Agency (FEMA).

Risk (Structural Damages)

Risk calculations are performed in CLIMADA by spatially overlaying hazard and exposures and mapping impacts via the corresponding impact function. Since most infrastructure exposures originally come in line or polygon formats, such shapes are interpolated to centroids at user-defined resolutions, and re-aggregated into their original shape after impact calculations. Here, risk is hence measured in terms of estimated structural damage to all infrastructure exposures, which in turn is expressed according to the respective value metric (either as damage fraction or total length/area affected). Computed structural damage values are then assigned as attribute I ('impact') to each corresponding element in the interdependent CI graph G. See Figure 3.2 panel DS.1 for an illustration of tropical cyclone risk calculations on power lines, cell towers and healthcare facilities.

3.2.3 Stage III: Technical Impacts (Infrastructure Failures)

For each element in the interdependent graph, the impact to the corresponding component computed with CLIMADA is assigned as attribute I. Functional state F of an element is set to zero if the impact I exceeds the damage threshold D^j as illustrated in Figure 3.2, panel DS.1.

This change in functional states can set off a failure cascade within the graph, through both internal and dependency-induced flow changes. In order to propagate the disruption, the capacities and functional attributes of all CI components are updated by applying the algorithm described in section 3.2.1 iteratively until a new steady state is obtained. In our example illustrated in panel DS.2 in Figure 3.2, several cascades occur: The power graph is split into three clusters as a consequence of the initial failure of a node and an edge element, whereby two clusters (Cl. 1 and Cl. 2) remain without capacity as they are cut off from connection to the power plant ($C^{ek} = 0$). Interdependencies among CI networks further propagate those disruptions (cell tower #7 is connected to a capacity-less power node, hence becoming dysfunctional; hospital #1 still receives 1 unit of supply - instead of previously 2 - from supporting cell towers, which prevents its failure).

3.2.4 Stage IV: Human-centric Impacts (Basic Service Access & Disruptions)

The final step is to compute basic service access (and disruptions, correspondingly) for a range of services at population nodes. Basic service access, according to the United Nation's definition , is ensured through the confluence of two factors:

i. functionality of the CI (component) responsible for the provision of a service

ii. a notion of accessibility to the CI (component)

Here, we define functionality through the functional states of the infrastructure graph elements. Accessibility is defined either through literal road path availability between end-user and infrastructure (e.g. hospitals for healthcare services) or through coverage of an area around an infrastructure's location (e.g. cell towers for mobile communication services). A qualitative summary of basic service access parametrizations for six services examined in this work is given in Table 3.2.

The quantitative basic service access algorithm is implemented in analogy to the flow assignment and functionality determination algorithm in the previous step. For each unique infrastructure-population pair combination jp, for which dependency edges e^{jp} exist in the interdependent CI graph G, the subgraph G'^{jp} spanning G'^{p}, G'^{j} and e^{jp} is extracted. Received services M^{jp} are hence computed as the sum of capacities from source infrastructure

Table 3.2: Examples for basic service access conditions which can be implemented in the infrastructure system model.

Basic Service	Description
Mobility	Functional connection to an intact road element within a certain distance threshold.
Power	Functional connection to an intact power cluster which runs above a certain capacity ratio.
Healthcare	Existence of an intact road-path below a certain distance threshold to a functioning facility.
Education	Existence of an intact road-path below a certain distance threshold to a functioning facility.
Mobile communication	Functional connection to an intact cell tower within a certain distance threshold.
Drinking water	Functional connection to an intact wastewater treatment plant within a certain distance threshold.

nodes arriving at population nodes (see eqs. 3 and 4 in Figure 3.2, panel BS.3). Each population (target) node is then assigned a service attribute S^j, indicative of the service provided by CI type j. The service is accessible ($S^j = 1$) if M^{jp} exceeds the capacity threshold Tjp and, additionally, fulfils the access conditions (c.f. Table 3.2), else $S^j = 0$. While the coverage-based access conditions are implicitly accounted for through the (non-)existence of a dependency edge, the literal (road-access) condition is checked for explicitly in the interdependent CI graph G through a shortest path algorithm, calculating the distance of the path between population node and facility node. Panel BS.3 in Figure 3.2 illustrates the procedure with the example of electric power access, where population node #7 receives $M^{ep} = 0.8$ normalized units of power, which exceeds the capacity threshold ($T^{ep} = 0.6$) and hence the service is accessible ($S^e = 1$).

The interdependent CI graph with functional state attributes F at infrastructure elements and service attributes S at population nodes hence defines the base state. Panel BS.4 in Figure 3.2 illustrates this for the three infrastructure networks and the corresponding three service types at the population network (electric power access Se, basic information access Sc and healthcare access S^h).

Once CI component failures are determined, basic service access is re-computed as hence described. See illustration in panel DS.3 in Figure 3.2 for the given stylized example on population's power access, leading to a new, disrupted

Table 3.3: Drivers of model uncertainties throughout all stages in the modelling chain.

Stage	Source	Explanation
I	CI System Representations	Choices on CI components included or excluded, simplifications (for instance, no differentiation between transmission lines of different voltages, approximating the communication network by cell towers, water network by water treatment plants)
	Dependency Identification	Choice of dependency rules (i.e., heuristics, between which CI systems dependencies exist)
	Dependency Parametrization	Choice of conditions for dependency establishment (i.e. distance thresholds between components identified through heuristics, path requirements, etc.)
II	Hazard Footprint	Resolution, spatial accuracy and representational validity, when in- or excluding sub-hazards (e.g. wind-fields, storm surge and torrential rainfall for tropical cyclones) or multi-hazard phenomena (compound events).
	Vulnerability Curves	Assumptions on (deterministic) relationship between hazard intensity and component damages.
	Damage-Functionality Thresholds	Assumptions on the (deterministic, threshold-based) relationship between structural damages and resulting component functionality levels.
III	Cascading Algorithm	Deterministic (strict) propagation of failures along dependencies, assumption on target becoming strictly dysfunctional due to failure at source.
IV	End-user Dependencies Basic Service Parametrization	Uncertainties are analogous to stage I.

state (panel DS.4 in Figure 3.2).

3.2.5 Model Uncertainties and Sensitivity Testing

Due to the amount of consecutive stages featured in the presented modelling chain, model assumptions and representational choices in one stage may greatly influence end-results. In order to allow for evaluation of such sensitivities, Table 3.3 provides a brief discussion on the main points where model uncertainties are introduced.

Owing to the complexity of the presented approach, a one-at-the-time analysis obtained by constructing scenarios, where only one set of parameters are varied within plausible bounds at a time (such as parametrizations of dependency conditions, vulnerability curves and functional thresholds), is a good starting point for identifying key sensitivities in the system responses. More in-depth characterization of the uncertainties can then be carried-out by focusing on the identified sensitivities (see Pianosi et al. (2016) for a comprehensive discussion on best practices and recommendations, catering specifically to the field of environmental modelling, and (Tabandeh et al. 2022)for an exemplary computational workflow designed for uncertainty propagating in and multi-level sensitivity analysis of hierarchical systems, particularly interdependent CI networks). Much can be done directly in CLIMADA using the ‘unsequa’ module that provides readily usable methods for state-of-the art global uncertainty quantification and sensitivity analysis based on quasi-Monte Carlo sampling (Kropf et al. 2022). In addition, the probabilistic hazard modelling approach may help estimating representational uncertainties on the trigger side.

3.3 Application: CI Failures and Basic Service Disruptions from Hurricane Michael

Tropical Cyclone Michael made landfall in the Florida Panhandle on the 7th of October 2018, and caused severe impacts across Florida, Alabama and Georgia, both in terms of direct asset damages (over US$ 25 billions) and lives lost (at least 43) (Beven II et al. 2019), as well as in terms of CI failures (power and mobile communication outages affecting millions, among others). It was selected for demonstration based on two reasons. Ample documentation of the event permits result validation and provides a reality check on quality and information content of the developed model. Further, Michael’s severity was dominated by strong winds and storm surge as opposed to torrential rainfalls (Bloemendaal, Moel, et al. 2021). The hazard can therefore be approximated by modelling only its wind-field, lending itself as an illustrative, yet simple enough example.

3.3.1 Model Demonstration

Stage I: Infrastructure System Model (Infrastructure Functionality)

We delimit the system of study to the states of Florida, Alabama and Georgia which were directly hit by hurricane-strength winds. Besides population, infrastructure systems considered are main roads, transmission power lines, power plants, cell towers, wastewater treatment plants, healthcare institutions and public schools (see Figure 3.3 column 'CIs' for geographical maps of the CI networks). Details on data sources, pre-processing and individual CI graphs generation, can be found in Appendix 3.A.3. Generation sources and demand sinks within the power network are obtained from power plant generation and energy consumption statistics (Appendix 3.A.3). To generate the interdependent CI graph, twelve distinct dependencies are identified in between CI networks (6) and between CI networks and population (6), and parametrized as indicated in Appendix 3.A.3. The established interdependent CI graph consists of nearly 80'000 nodes and 500'000 edges, with dependencies making up the majority (59%) of links (see Figure 3.6for detailed graph statistics). Network flows are computed and functional states assigned to all infrastructure components in this pre-disaster configuration (termed 'base state'), resulting in all elements of the interdependent CI graph being functional. Population's basic service access rates surpass 99% for all service types considered in the base state (access to mobility, power, education, healthcare, mobile communications and drinking water).

Stage II: Natural Hazard Risk Model (Structural Damages)

Track data for tropical cyclone Michael is obtained from the International Best Track Archive for Climate Stewardship (IBTrACS) project (Knapp, Kruk, et al. 2010) . The wind field (see Figure 3.7) is computed from the CLIMADA tropical cyclone module, according to the parametrization in (Holland 2008). CI-type specific impact functions for structural damages from winds are taken from literature (see Figure 3.8 in Appendix 3.A.3) and ingested into CLIMADA for all infrastructures except power plants, which are not designed to fail. All CI networks are converted to CLIMADA exposure layers for impact calculations. Structural damages are computed using the CLIMADA impact module, yielding direct impact figures as displayed in Figure 3.3, column 'Component Damages'.

Stage III: Technical Impacts (Infrastructure Failures)

Structural damages fractions of all infrastructure components are translated into binary functionality states by applying infrastructure-specific threshold values (Appendix 3.A.3). Component failures hence initiate the failure cascade algorithm in the infrastructure systems module, both within individual CI networks and along dependencies across CI networks. Under the given system specifications, only the power network features an internal cascading mechanism, as it contains designated source nodes (power plant), sink nodes (power line nodes with customer demands) and transition nodes (all other power line nodes). A cluster approach was chosen to capture this failure behaviour, where all components in a remaining functional cluster become dysfunctional once generation capacity falls below a certain fraction of demand (here set to 60% for demonstrative purposes). Dependency-induced failure cascades are experienced across all CI networks within the interdependent CI graph. Results are displayed in Figure 3.3, 'CI failures', where initial, structural damage-induced failures and cascaded failures are marked with the respective colour code.

Stage IV: Human-centric Impacts (Basic Service Disruptions)

Following the failure cascade algorithm, access to basic services are computed for all population nodes within the interdependent CI graph. For road-path constrained dependencies (access to healthcare and education, resp.), this involves re-calculation of path availability and travel distances. Figure 3.3, 'Basic Service Access' shows the disruption results for access to mobility, power, healthcare, education, mobile communication and drinking water.

3.3.2 Scenario Analysis

To obtain first insights on how strongly results depend on assumptions along the modelling chain, seven modelling scenarios are constructed (see Table 3.8). We explore the role of interdependencies, and of parametrization de-

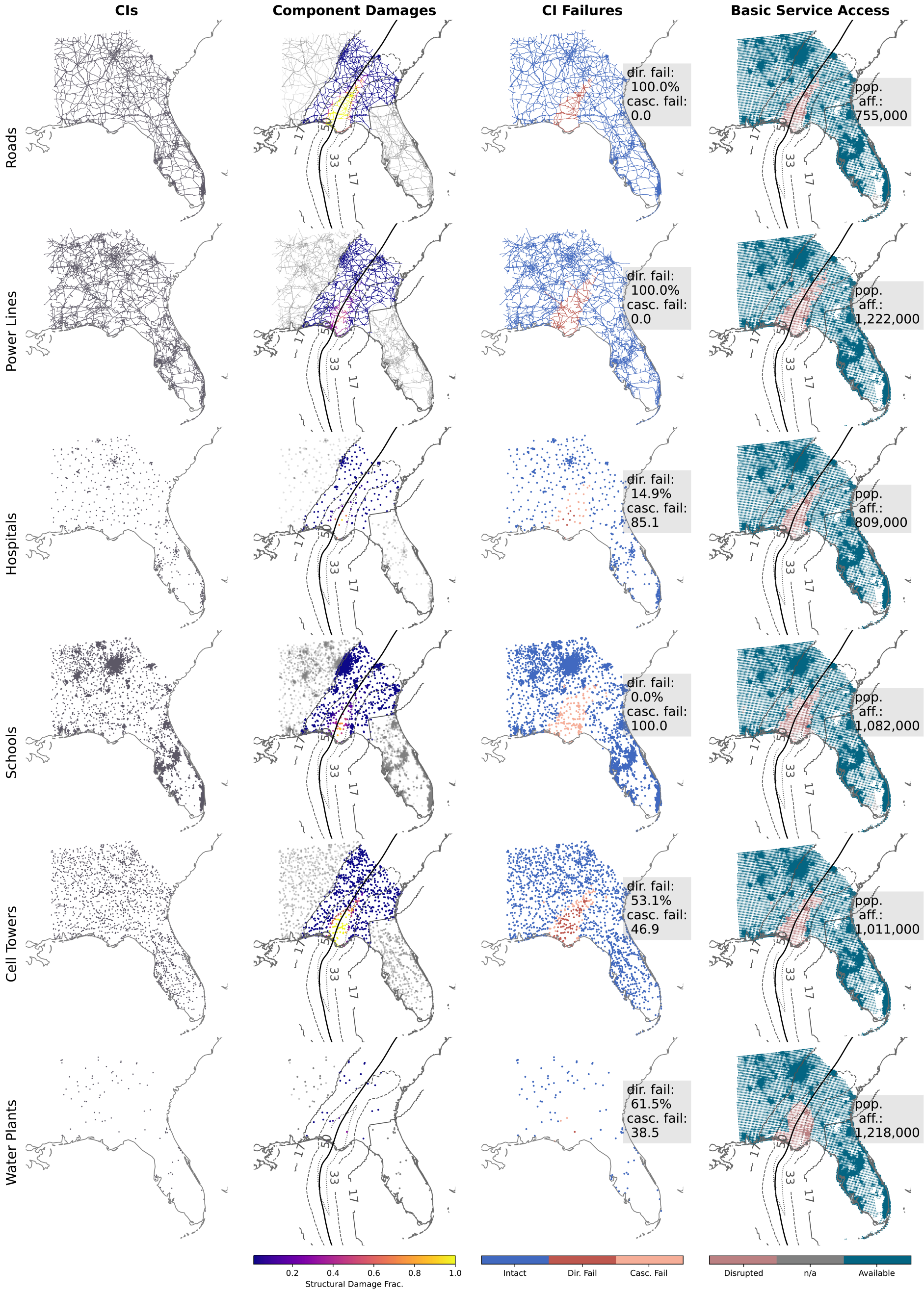

Figure 3.3: From natural hazard to basic service disruptions in four stages. Demonstration for Hurricane Michael '18 hitting the Florida Panhandle: Asset data for 6 CIs across FL, AL & GA used in the CI model (column 'CIs'), wind-induced structural damages calculated with CLIMADA ('Component Damages'), CI failure cascades triggered by the initial disruption, resulting in functional, dysfunctional and cascaded dysfunctional components ('CI failures'), population impacted from basic service disruptions following CI failures ('Basic service access', a: access to mobility, b: power, c: healthcare, d: education, e: mobile communication, f: drinking water. TC track and wind-field contour lines (m/s) are plotted in columns 2 & 4 for reference.

cisions for impact functions and for functionality thresholds on result outcomes (see Table 3.9 for numeric results). The above presented case, referred to as 'original' parametrization henceforth, is taken as a reference.

Results are greatly influenced by the inclusion of CI interdependencies: As cascaded failures account for a significant part of all infrastructure failures in the base scenario, the removal of this impact driver drastically reduces component failures across all CI types but roads, with strong consequences for projections of service disruptions. Numbers of affected people decrease for all basic services apart from access to mobility (see Figure 3.4, gray). While the inclusion of dependencies itself plays a great role in determining the magnitude of impacts, the exact parametrizations of establishment conditions thereof (such as path distance thresholds) affect end results less strongly (see Figure 3.4, blues). Parametrization of impact functions directly and strongly influences estimates of structural damages, which has far-reaching consequences on the entire impact chain from immediate CI failures over cascades to basic service disruptions. Shifting impact functions by 15 m/s in either direction compared to the base scenario (i.e.same level of structural damage at wind intensities of 15 m/s more or less, resp.) can lead to a divergence in services disruption estimates between millions of people and almost none (Figure 3.4, reds).

Due to the resolution of the hazard footprint (360 arcsec, ca. 11 km), which exceeds most CI component lengths, results are less sensitive to the threshold assumptions between structural damage fractions and functional performance of components, since components are mostly entirely affected or not at all (see Table 3.9). This may change and become increasingly important, though, at higher hazard resolutions.

3.3.3 Validation

The aim of this validation is to collect evidence on whether the showcased impact cascades - from CI damages to affected people - do happen, and whether predicted impacts, even when drawing on coarse assumptions and a set of heuristics, are in the right order of magnitude. The multiple impact stages calculated within the underlying approach are reflected in the breadth of validation sources taken into account, and span official government re-

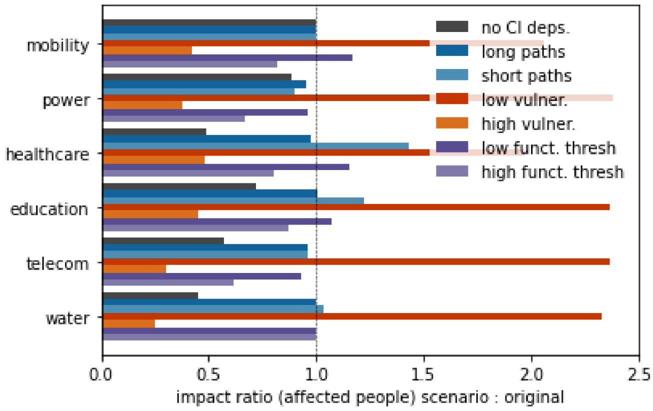

Figure 3.4: Number of people affected by basic service disruptions for seven scenarios, relative to original parametrization presented in section 3.3.1. Blue: no CI interdependencies, blues: allowing for shorter and longer road travel paths to social facilities, reds: higher and lower CI component vulnerability, purple: higher and lower structural damage thresholds until reaching component dysfunctionality.

leases, utility providers' reports and newspaper articles (see Supplementary SM2 for a comprehensive overview).

Even for the case study region, where information sources after natural hazard events are ample and accessible, documentation on the entire impact cascade is incomplete: structural damages are only incidentally reported across all infrastructure types, comprehensive functional outage reports are limited to the power and telecommunication sector, while accounts on basic service disruptions remain anecdotal. Figure 3.5 synthesizes this evidence, contrasting quantitative outage statistics against model outputs (panels b and e for power and telecom), and mapping qualitative service-related incidents against areas of modelled access disruptions (panels a, c, d and f for healthcare, education, mobility and drinking water).

Loss of power access is captured well, both in terms of impacted people (ca. 1.65 million reported vs. 1.22 million modelled), and in terms of spatial distribution (compare Figure 3.3 and Figure 3.5 (a) for a more detailed visual reference). Loss of mobile communication access is not reported as such, yet documented occurrences of cell site outages coincide well with spatial model predictions on failed cell towers (see Figure 3.5 (e), aggregated at county level); most county predictions lie well within a 50% margin of error, even though the impact severity is overestimated in hurricane-hit counties located further inland.

Documented incidents related to the loss of service access and infrastructure damages, such as hospital evacuations, structural damages and fatalities due to untimely care in the case of healthcare access, all lie within the modelled area of concern (Figure 3.5). Yet, road damages and mobility-related incidents were reported far less inland than model predictions (Figure 3.5 (a)), a tendency which is less pronounced, yet shared for access to healthcare and education (Figure 3.5 (c, d)), and most drastic for evidence on drinking water issues (Figure 3.5 (f)). The divergence in projected and actual disruptions to mobility confirms the importance of choosing adequate impact functions, as pointed out also in the section on scenario analysis. The road impact function used in this study was designed for disruptions from tree blow-down, which may have provided an overly pessimistic picture on (longer-lasting) structural damages.

Validation results for mobile communications, healthcare and education access highlight the importance of incorporating dependencies and failure cascade into the model, yet also show caveats of adequate parametrization: The relatively accurate projection of people affected by cell site outages could not have been reproduced without power interdependencies, as the scenario analysis showed above. Similarly, several hospitals which were not directly damaged reported evacuations due to water and power supply issues, while many of the indirect deaths were linked to either patients or emergency workers not getting physical access to healthcare facilities in time. This confirms the general validity of incorporating such CI dependencies into infrastructure functionality calculations, and the importance of people's road path availability into bespoke service access computations. Such dependency specifications can, however, also propagate errors and over-estimate disruptions, as seen with access to education: The estimated 45'000 students reported to be missing school due to closures (Price and Glenn 2018) fall short of the approximately 145'000 projected by the model. This is partly due to the non-redundancy between end-users and educational facilities: Contrary to hospitals, where any facility within reach can be chosen, people are assigned to one fixed school. When damages to such facilities or their supporting CIs are hence over-estimated, this will transmit directly to over-estimations of education access disruptions throughout the entire assignment surroundings.

Lastly, the case of water access disruptions demonstrates that a high degree of system simplification can become problematic: In absence of better data, the drinking water system was proxied by water treatment plants only. As a consequence, the model projected large areas of disruption from a single failing facility, which seems not to be the behaviour observed in those real-world water systems. Similarly, caution should be taken when approximating the telecommunications network - consisting in more and more resilient subnetworks than mobile communication structures only - through cell towers.

Despite the fact that some service disruptions were less extensive than modelled, the integration of a hazard model and a CI model based on relatively simple dependency heuristics and readily available open-source data allowed to capture important failure dynamics within one interoperable calculation chain. The model reproduces impacts in the correct order of magnitude, allows to trace back impact drivers to parametrization decisions in each stage of the impact cascade, and to re-calibrate mechanisms. It further gives a social dimension to technical CI failures, mapping out areas of disruption for basic services which are not consistently monitored by official sources. While those are promising features, there is demand for an even more refined picture, as remarked by a reporter in the aftermath of TC Michael: *"While the coastal devastation has become obvious, some disaster experts are most concerned about the conditions farther inland. [...] These are some of the most socially vulnerable places in the entire country, low-income counties with high proportions of older adults, and many people with disabilities and chronic illnesses"* (Fausset et al. 2018).

3.4 Discussion

The developed modelling framework was designed for interoperability, transferability and scale. Interoperability is achieved though the embedding of an infrastructure system model into the risk assessment platform CLIMADA, allowing for a streamlined workflow from natural hazards to social impacts. The linkage to an event-based hazard simulation engine is a way forward

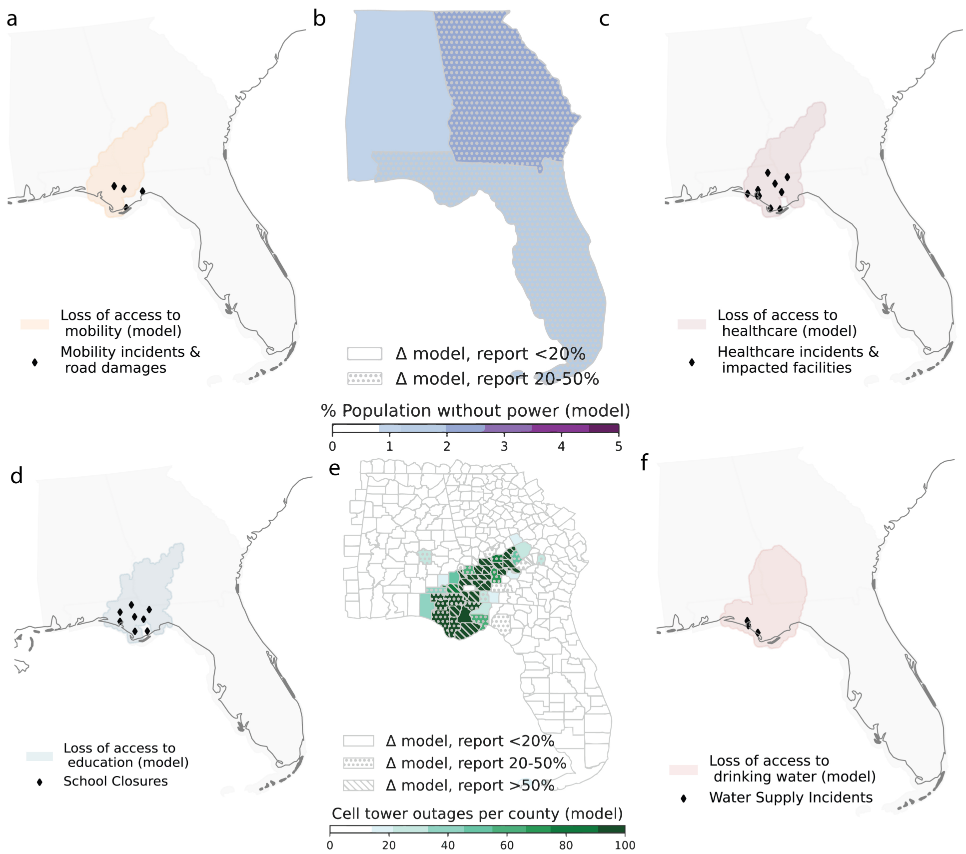

Figure 3.5: Validation results for road blockages, structural damages and mobility incidents (a), power outages (b), healthcare-access related incidents and hospital damages (c), school closures (d), cell site outages (e) and water supply issues (f).

from the use of stylized polygons in absence of physically-informed hazard footprints (Jenelius and Mattsson 2012; Zorn, Pant, et al. 2020), hypothetical events (Loggins and Wallace 2015) or return period maps which are not representative of individual events (Bruijn et al. 2016). Transferability is ensured both theoretically and practically: While we provide readily available suggestions on infrastructure and population data sources, dependency heuristics, impact functions and hazard models, the framework can handle both proprietary and/or other open-source data (e.g. regional or national-level developed data). This allows to investigate other infrastructure types, hazards, dependencies and case study regions of interest to the user: For instance, vulnerability functions may be altered to capture the important effect of deterioration through ageing of infrastructures (Iannacone et al. 2022), or dependencies re-parametrized with different distance thresholds to account for locally specific cell tower ranges (Holma et al. 2011) or travel speeds (De Leonardis et al. 2018). The scale criterion is integrated in the design of the infrastructure system model, which requires few technical specifications, and relies mainly on network topology and a set of heuristics for dependency and flow assignment procedures, enabling the study of large systems.

The results simulated must be interpreted as a first indicator on impact hotspots and peak disruptions from the angle of people at risk. The simplifying nature of network-based approaches has been recognized earlier as a necessary trade-off against capturing large system scales at which natural hazards can occur (Bresch, Berghuijs, et al. 2014; Loggins and Wallace 2015). The merit of the developed system model's approach therefore lies in the possibility of working at a globally consistent basis with several interdependent CI systems, yet does not replace specialized system models (Gauthier et al. 2018; Guidotti et al. 2016; Ouyang, Hong, et al. 2009) for detailed local analyses and individual infrastructure system optimizations.

The three information levels on infrastructure risk which the model provides (structural component damages, failure cascades, and service disruptions), align well with the highly diverse nature of real-world impact data, which is often anecdotal and encompasses several of those risk layers. This offers the versatility to calibrate and adjust parameters in the model based on evidence, such as tailoring impact functions to match print media coverage on structural damages, or amending dependency heuristics to fit utility provider's outage reports. To the best of our knowledge, only few quantitative modelling studies (Zorn and Shamseldin 2016) incorporate such feedback possibility. Obtaining results on direct and cascading infrastructure failures further allows to quantify the role of infrastructure dependencies in causing wide-spread impacts: Validation in the presented case study empirically confirmed that the extent of observed impacts could not be reproduced without the inclusion of dependencies between infrastructure networks, which is in line with findings from other research on infrastructure interdependencies (Luiijf et al. 2009; Zorn, Pant, et al. 2020).

The scenario analysis highlighted that structural damage functions and dependency parametrizations are sources of considerable uncertainties in the model. How to capture the diverse nature of interdependencies, which adequately accounts for the varying 'coupling strengths' (Nan and Sansavini 2017; Rinaldi et al. 2001) between CI networks observed in reality, is a topic of ongoing research. The presented use of capacities, capacity thresholds, redundancies and road-path availability checks in the parametrization of infrastructure dependencies (Appendix A) is a pragmatic compromise between elaborate mathematical frameworks with many conditionalities (for instance (Sharma and Gardoni 2022)) and implementation feasibility for large networks with limited process knowledge and data availability. We refine commonly employed user-assignment procedures relying purely on geospatial conditions (e.g. Voronoi tessellations) or on shortest path algorithms without alternative targets (Poljansek et al. 2017; Thacker, Pant, et al. 2017). Yet, modelling of back-ups for failing dependencies (such as generator availability for power-dependent components (Zorn and Shamseldin 2016)), changing demand patterns for infrastructure-related services among end-users as a reaction to natural hazard occurrences (Naqvi and Monasterolo 2019; Otsuka 2019) or the reduction in functionality as opposed to binary failures (Sharma and Gardoni 2022) upon dependency disruptions may improve currently implemented cascading dynamics. Furthermore, the threshold approach employed to relate structural damages to loss of component functionality is a simplification for the notoriously challenging task of developing consistent performance indicators (Ghosn et al. 2016; Nan and

Sansavini 2017), for which research in the engineering community may lead to future insights.

Our approach does not feature an explicit notion of time. Since the modelled structural damages to infrastructures need to surpass a certain threshold for the components to become dysfunctional, this implies that the model captures rather longer-lasting disruptions. Yet, since impact severity is a function of time and timing (Devanandham and Ramirez-Marquez 2012), making it an explicit variable can be insightful: While for healthcare access a few hours of disruptions in the immediate aftermath of a natural hazard event may be extremely relevant, they may be less so for access to schools, especially if occurring on a weekend. Introducing time could further provide an informative indication on restoration and recovery dynamics (Almoghathawi, Barker, and Albert 2019; Lee II et al. 2007) when introducing repair times and 'snapshots' of the interdependent CI network at various moments, and capture oscillating or non-convergent functional behaviours which interdependent systems can exhibit.

Lastly, our estimates of post-disaster basic service disruptions add an often-neglected human-centric dimension to the discourse on infrastructure risks (Hasan and Foliente 2015), which both academic models, utility providers or government post-disaster reports do not usually capture systematically (cf. Karakoc et al. (2020) as a rare exception); the holistic approach further allows to include under-represented sectors in CI research such as healthcare (Chang, Pasion, et al. 2012) and education. This can offer valuable information to emergency responders with limited resources, and decision makers facing multi-criteria investment decisions alike (Hasan and Foliente 2015; Karakoc et al. 2020; Mitsova, Sapat, et al. 2020). However, and especially as research on social vulnerability is still in its infancy (Garschagen and Sandholz 2018), it will be important to take a closer look at the differential impacts of basic service losses on different parts of the population, such as the poor, the elderly or non-native speakers, which have repeatedly been shown to dispose of fewer coping mechanisms (Cutter et al. 2006; Mitsova, Esnard, et al. 2018).

3.5 Conclusion

Critical infrastructures such as powerlines, roads, telecommunication and healthcare systems across the globe are more exposed than ever to the risks of extreme weather events in a changing climate. CI failure models often operate at local scales with high data requirements and low transferability, focusing on the technical performance side. Natural hazards are often not explicitly modelled as a disruptive scenario therein. Natural hazard models, in turn, frequently focus on direct damages to assets, which neglect the networked and interdependent character inherent to critical infrastructure systems.

To bridge those gaps between infrastructure modellers and natural hazard risk modellers, we draw on well-established methods in both communities to develop an interoperable, coherent and open-source modelling framework for assessing spatially explicit, large-scale risks from infrastructure failure cascades and their social impacts induced by natural hazards. Embedded into the risk assessment platform CLIMADA, a state-of-the-art tool for natural hazard impact calculations and adaptation options appraisal, we demonstrate a network theory-based infrastructure systems model designed to require few technical details apart from commonly available asset location and population data, which can handle many types of infrastructure networks and captures interdependencies among them based on a set of heuristics. The framework hence offers a three-layered view on infrastructure risks in terms of on infrastructure component damages, technical failure cascades, and human-centric basic service disruptions. It is readily transferable across geographies, and can be tailored to include CI systems, interdependencies and hazards of interest to the user.

The validated case study on Hurricane Michael across the US states of Florida, Georgia and Alabama for six interdependent CI networks showed that the established modelling chain captures impact hotspots and reproduces failure cascade dynamics, which could not be obtained when looking at structural infrastructure damages alone. It also showed how real-world impact data, such as outage reports and print-media accounts, can be used to iteratively refine and calibrate the model. Projecting spatially explicit locations of service disruptions experienced by the dependent population as a result of infrastructure failures further adds a novel layer of risk information, which is usually not available on the ground.

While we do not offer the one single "comprehensive methodological approach with a platform of linked models and data interoperability for modelling infrastructure interdependencies for a range of different stakeholder concerns and decision contexts" (Hasan and Foliente 2015) our approach takes a step into this direction. We provide a tool apt for decision making-contexts involving large geographic scope and the effects of several interdependent CI systems' responses to disruptions for the population: The global consistency of the approach permits a comparative view of risk across countries, relevant for international policy frameworks; adaptation planning and infrastructure investments for resilience can be evaluated under their aversion potential for different types of human-centric impacts and under trade-offs amongst different CI sectors; post-disaster hotspot analyses can lead to more targeted humanitarian relief and recovery activities.

Acknowledgements

This project has received funding from the European Union's Horizon 2020 research and innovation programme under grant agreement No 821010 and under grant agreement No 820712. Elco Koks was further supported by the Netherlands Organisation for Scientific Research (NWO; grant no. VI.Veni.194.033).

Data Availability

CLIMADA risk assessment platform is accessible on GitHub (`https://github.com/CLIMADA-project/climada_python` for impact calculations, `https://github.com/CLIMADA-project/climada_petals` for the infrastructure system model). Code for reproducing case study results and figures is accessible under `https://github.com/CLIMADA-project/climada_papers/tree/main/202208_critical_infrastructure_nw_risks`. All raw data sources needed for reproducing calculations are mentioned in the text and appendix.

3.A Appendix

3.A.1 Formal treatment of the developed modelling chain

G^j	graph of CI network j
n_i^j	ith node in G^j
e_{mn}^j	directed edge from n_m^j to n_n^j
G	interdependent CI graph, spanning all graphs G^j,G^k,... of investigated CI networks and all e^{jk}
e_{mn}^{jk}	directed dependency edge from n_m^j to n_n^k
G'^j	subgraph of G spanning all elements of G^j
G'^{jk}	subgraph of G, spanning all elements G^j, G^k and e^{jk}
A^{jk}	adjacency matrix of G'^{jk}
L_i	geo-spatial location of graph element i (node and edge attribute)
F_i	functional state (0,1,) of graph element i (node and edge attribute)
I_i	structural damage ('impact') of graph element i (node and edge attribute)
E_i	exposure value of graph element i (node and edge attribute)
D_i	damage threshold of graph element i from which I $F_i \rightarrow 0$ (node and edge attribute)
C_i^{jk}	capacity for node i for type of flow passing between CI types j and k(node attribute)
T_i^{jk}	capacity threshold for node i for type of flow passing between CI types j and k (node attribute)
M_i^{jk}	capacity supply at node i for type of flow passing between CI types j and k (node attribute)
S_i^j	service supply at node i for type of flow delivered by CI type j (node attribute)
$H(L)$	hazard intensity at geographic location L
$V(H)$	hazard intensity-dependent vulnerability curve

Initialization

1. $\forall$ j create G^j with n^j (nodes only) or n^j, e^j (nodes and edges) and set attributes $L, F(\rightarrow 1\ \forall n^j, e^j \in G^j), D, E, X$

2. Create interdependent CI graph $G = \Sigma_j G^j : \forall\ (jk)$ in list of identified CI dependencies:

   (a) Create e_{mn}^{jk} between n_m^j and n_n^k if linking conditions (distance, redundancy criterion, etc.) fulfilled

   (b) Assign node attributes $C^{jk}, T^{jk} \forall n \in G$:
   C_i^{jk}: (-1 if n_i^j; 1 if n_i^k; 0 else)
   T_i^{jk}: ([0,1] if n_i^k; 0 else)

Flow Assignment & Functional State Update

3. $\forall j$ where $G^j \in n^j, e^j$:
   (a) extract G'^j from G.
   (b) perform internal flow calculations according to adequate algorithm.
   (c) update $C^j k, F \forall n^j$ in G, where required.
4. $\forall$ combinations of (jk) where $k \neq$'people', extract G'^{jk} from G; update $F \forall n^k$:
   $M^{jk} = (F \cdot C^{jk})^T * A^{jk}; F = \min(F, M^{jk} \geq T^{jk})$
5. Repeat 3. and 4. until $\Delta F = 0$

Basic Service Access Determination

6. $\forall$ combinations of (j,people), extract $G'^{j,people}$ from G. Assign attribute S^j to n^{people}:
   $M^{j,people} = (F \cdot C^{j,people})^T * A^{j,people}$
   $S^j = (M^{j,people} \geq T^{j,people})$

Natural Hazard Impact Calculation & Functionality State Update

7. Assign structural damage attribute $I \; \forall \; n, e \in G$:
   $I = H(L) * V(H) * E$
8. Update $F \forall n, e \in G$:
   $F = \min(F, I \leq D)$

Cascade & Functional State Updates

9. Update $C^{jk}, F \; \forall \; n, e \; \forall (jk, k \neq people)$ in G according to 3. - 5.

Basic Service Access Update

10. If road access is a linking condition for dependency combination $(j, people)$: Re-check path existence and length of path between $n^j, n^{people} \; \forall e^{j,people}$; else delete $e^{j,people}$from G
11. Update $S^j \; \forall \; n^{people}, \forall (j, people)$; see step 6.

3.A.2 Modelling Choices for CI Networks

Table 3.4: CI networks and their components, in edges (E) and nodes (N). First column suggests a simple sub-selection of network components to represent the systems in a standardized low-complexity setting, second column proposes additional components if data is available.

CI system	Simplified representation	Extension possibilities
Road	N: intersections E: streets	N: tunnels, bridges E: -
Electric Power	N: power generation plants E: transmission lines	N: transmission & distribution substations, power poles E: low-voltage distribution lines
Tele-communication	N: cell towers E: -	N: internet exchange points, data centres, central offices, base stations, poles E: landlines, fibre-optic cables, submarine transmission lines
Wastewater & Water Supply	N: water treatment plants E: -	N: wells, reservoirs, tanks, cisterns, pumps, water bodies E: water pipelines, water tunnels, rivers
Healthcare & Emergency Serv.	N: hospitals, clinics E: -	N: doctors' practices, dentists, pharmacies, nursing homes
Educational Facilities	N: schools E:	N: universities, childcare centres, kindergartens
End-users	N: people clusters E: -	

3.A.3 Case Study

Infrastructure System Model Inputs

Infrastructure Component Data

Infrastructure	Source	Data description, Pre-processing
Roads	OpenStreetMap	Data: Retrieved from data dump at geofabrik.de for states FL, AL, GA matching tags highway= motorway, motorway_link, trunk, trunk_link, primary, primary_link using the OpenStreetMap module in CLIMADA. Pre-processing: Line merging, roundabout cleaning, duplicate removal, linking unconnected cluster
Hospitals	HIFLD*: Hospitals	Data: All amenities in states FL, AL, GA incl. 20kms buffer around outer borders Pre-processing: -
Power lines	HIFLD: Electric Power Transmission Lines	Data: All lines in in states FL, AL, G Pre-processing: Line merging, duplicate removal, linking unconnected cluster
Power plants	HIFLD: Power Plants	Data: All amenities in states FL, AL, GA incl. 20 km buffer around outer borders Pre-processing: -
Educational facilities	HIFLD: Public Schools	Data: All amenities in states FL, AL, GA incl. 20 km buffer around outer borders Pre-processing: -
Cell towers	HIFLD: Cellular Towers	Data: All amenities in states FL, AL, GA incl. 20 km buffer around outer borders Pre-processing: -
Wastewater	HIFLD: Wastewater Treatment Plants	Data: All amenities in states FL, AL, GA incl. 20 km buffer around outer borders Pre-processing: -
People	WorldPop Gridded Population Count	Data: United States of America, 1km UN-adjusted, 2020. Pre-processing: Re-gridded raster data on population counts to resolution of 10 km x10 km, vectorized, cropped at outer borders of states FL, AL, GA

Table 3.5: Geo-coded infrastructure asset data used in the case study, section 3.3. *) HIFLD: Homeland Infrastructure Foundation-Level Data

Power Supply & Demand Data

Table 3.6: Population data, energy supply and demand data used for case study in section 3.3.

Variable	Source	Data description
Supply	HIFLD: Power Plants	Same data source as for geo-location data of power plants in the region of interest. Electric energy supply taken from power plants net annual generation, given in column NET_GEN.
Demand	International Energy Agency (IEA) World Energy Balances	Total electric energy consumption for entire USA, all sectors, 2019.

Calculation of electric power demand per people cluster (cf. Table 3.5): Total electric energy consumption / total US-population * population count of cluster

Calculation of electric power supply per power plant (cf. Table 3.5): Directly taken from data source.

Supply / demand balancing in undisrupted state: Addition of an import/-export element to the power plant data frame with supply amounting to difference between total power plants supply in region of interest and total energy consumption in region of interest.

Dependencies

Table 3.7: Dependencies identified between CI networks (1-6) and between CI networks and end-users (7-12). Dependency parametrizations are used to link individual CI graphs and population graph into one interdependent CI graph. Decisions for certain parameter settings are discussed in the paragraph below.

Dep	Source	Target	Redundancy	Road access	Dep. type	Flow type	Func. Thresh	Dist. Thresh. [m]
1	power line	celltower	TRUE	FALSE	funct.	physical	0.6	
2	power line	education	TRUE	FALSE	funct.	physical	0.6	
3	waste-water	education	TRUE	FALSE	funct.	logical	1	
4	power line	health	TRUE	FALSE	funct.	physical	0.6	
5	waste-water	health	TRUE	FALSE	funct.	logical	1	
6	power line	waste-water	TRUE	FALSE	funct.	physical	0.6	
7	cell-tower	people	FALSE	FALSE	end user	logical	1	30000
8	education	people	TRUE	TRUE	end user	logical	1	40000
9	health	people	FALSE	TRUE	end user	logical	1	100000
10	power line	people	TRUE	FALSE	end user	physical	0.6	
11	road	people	FALSE	FALSE	end user	logical	1	30000
12	waste-water	people	TRUE	FALSE	end user	logical	1	

Selection of distance thresholds: A combination of sophisticated guess (such as 30 km being a generous diameter for cell tower reach (Holma et al. 2011) or hospitals being at most 100 km from persons, which equals a travel time of little more than the “golden hour” crucial in medical emergencies, when considering average travel speeds on a highway (De Leonardis et al. 2018)), and iterative refinements such that service access levels in stage IV were >99% for all basic services across the area of investigation in a base state simulation with undamaged CIs. For instance, setting cell tower ranges to 15 km would have resulted in 6.7 M customers without mobile communication access in the base state, whereas the hence chosen range (30 km) resulted in only a few hundred persons without coverage. For dependencies where no distance thresholds are set, target elements are linked to the closest element of the respective source type, irrespective of its distance. This is the case for all non-redundant dependencies where it is obvious that such a link must exist (e.g. educational and healthcare facilities having power and water access).

Selection of redundancy specification: Water and power are modelled to be supplied through a single source per dependent target. Mobile communication is modelled to be provided from any source within distance thresholds, as connectivity can be established through any reachable cell site. Healthcare can be provided from any reachable healthcare facility, but school enrolments are usually fixed, hence each population clusters dispose of only one non-substitutable education link. Road access is assumed to be provided by any reachable road within the given distance threshold.

Selection of flow types and functionality thresholds: Physical variables for power demand and supply across the modelled area were available and capacity in the network is hence calculated as the ratio of power demand to power supply in each network cluster. Functionality thresholds for power dependencies could therefore be expressed as a continuous fraction with regard to the capacity ratio. It was set here to 0.6 in absence of any component-specific information, to interpreted as "if demand-to-supply ratio in the power network cluster to which the dependent component is linked, drops below 0.6, the component will turn dysfunctional". All other dependencies are, in absence of physically informed flow metrics, logical dependencies. As such, they either provide supply from a functional source, or they do not, if the source is dysfunctional. Functionality thresholds for logical dependencies are hence trivial and set to 1. Road paths between population nodes and social facilities (hospitals, schools) were computed based on a Dijkstra's shortest path algorithm.

Infrastructure Interdependent CI Graph Specifications

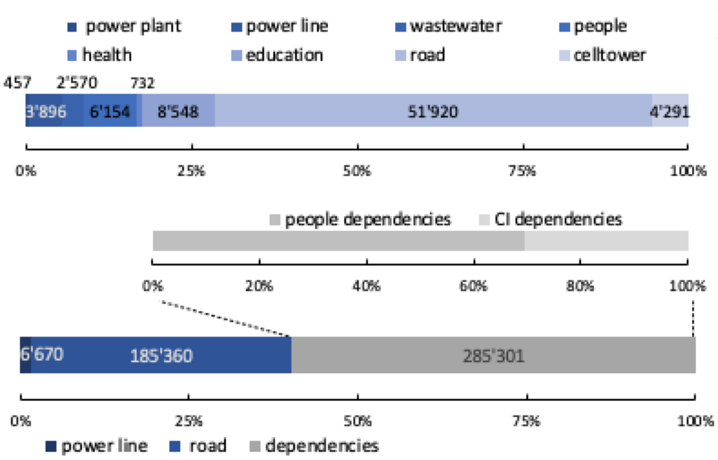

Figure 3.6: Specifications of node (1st bar plot) and edge elements (2nd bar plot) in the interdependent CI graph, constructed for the case presented in section 3.1.

Natural Hazard Risk Model Inputs

Hazard Footprint

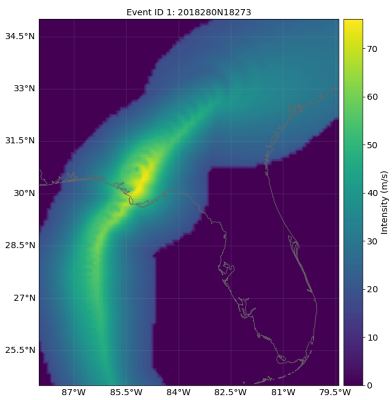

Figure 3.7: Map of Hurricane Michael wind-field intensity, computed with CLIMADA from Michael's hurricane track. Track data from IBTrACS, implemented wind field algorithm from [85]

Vulnerability Curves

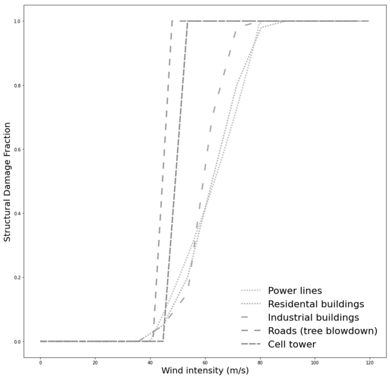

Figure 3.8: Impact functions used for structural damage calculations from hurricane wind field in section 3.3.1, for all CI types. Note that y-axis represents fraction of structural damage to components for all CIs except power lines, for which it is failure probability. Sources: power lines in (Pianosi et al. 2016), residential building and industrial building (both for z=0.35) in [87], roads in (Koks, Rozenberg, Zorn, et al. 2019), cell towers: step function taken from interview with cell tower provider stating they are "built to withstand winds of up to 110 miles per hour".

Scenario Analysis

Scenario Selection and Results Overview

Table 3.8: Scenarios to study the sensitivity of end results (number of people experiencing basic service disruptions) to assumptions throughout the modelling chain. For parameterizations details, see Supplementary SM2.

Scenario	Description	Stage
No CI inter-dependencies	Removing any functional dependencies between CI networks.	I
Longer path threshold	Increasing allowed distance thresholds for end-user travel paths	I / IV
Shorter path threshold	Decreasing allowed distance thresholds for end-user travel paths	I / IV
Low component vulnerability	Shifting impact functions to withstand higher hazard intensities.	II
High component vulnerability	Shifting impact functions to withstand lower hazard intensities.	II
Low functionality threshold	Decreasing damage thresholds for component dysfunctionality.	II
High functionality threshold	Increasing damage thresholds for component dysfunctionality.	II

Table 3.9: Results of scenario analysis: Amount of people experiencing service disruptions in each scenario due to hazard-induced failure cascades, relative to disruption numbers in the originally chosen parametrization as described in section 3.3.1. The 7 selected scenarios are described in Table 3.8 and discussed in section 3.3.2. Parametrizations of the scenarios are listed in Supplementary SM2.

Access to Basic Service	original	No CI Inter-dep.	Longer path thresh.	Shorter path thresh.	Low vulner-arbility	High vulner-ability	Low funct. thresh.	High funct. thresh.
Mobility	100	100	100	100	205	42	116	81
Power	100	88	95	90	238	37	96	66
Healthcare	100	48	97	142	196	48	115	80
Education	100	72	100	121	236	45	106	87
Mobile Comms.	100	57	95	96	236	30	92	61
Water Supply	100	45	100	103	232	24	100	100

Scenario Parametrizations

Provided in Supplementary SM2.

Validation Sources

Provided in Supplementary SM2.

CHAPTER 4

Climate-resilient basic services? Unravelling dynamics of natural hazard-induced infrastructure disruptions across the globe

Evelyn Mühlhofer, David N. Bresch and Elco E. Koks; under review in *One Earth*

Abstract. Critical infrastructure underpins daily societal functioning. However, severe weather events can inflict damages to infrastructure and cause basic service disruptions. Here we explore how real-world infrastructure network designs, interdependencies, population distribution, wealth, and hazard characteristics jointly drive regional risk of disruptions to power, healthcare, education, mobility, and telecommunication services. We couple an open-source risk model with a complex network-based infrastructure module to simulate spatially explicit service disruptions from 700 historic flood and tropical cyclone hazards in 30 countries. We find that in 84% of flood and 65% of tropical cyclone events, service disruptions spread beyond the hazard footprint, impacting up to ten times the directly affected population. 64-89% of all service disruptions stem from failure cascades triggered by infrastructure interdependencies and physical access constraints. Implications are that strategies for resilient, equitable and climate-proof basic services must consider the dynamic interplay of system interdependencies, spatially-resolved hazard and exposure data, instead of merely avoiding asset losses

4.1 Introduction

When natural hazards occur, access to healthcare, electricity, mobility, and many other services may be severely compromised and threaten the functioning of society (Tariverdi et al. 2023). Yet, the severity of an event, as well as current and future risks from natural hazards, are often predominantly judged based on actual or potential asset damages and fatalities (Fekete 2019). While such direct impact metrics form the core of classic risk assessments, they render an incomplete picture of the wider impacts on people's livelihoods. Understanding how critical infrastructures cease to function during disasters, and how this leads to loss of critical services, can uncover complex systemic, socio-technical dimensions of natural hazard-induced risk. It may explain economic losses incurred by firms through service-outage related business interruptions (Braese et al. 2019), guide more holistic adaptation planning (Koks, Le Bars, et al. 2023; Schotten and Bachmann 2023a), and pinpoint social (in-)equity and vulnerability (Garschagen and Sandholz 2018; Karakoc et al. 2020).

As both infrastructure investments and occurrences of extreme weather and climate events are at an all-time high (Hallegatte et al. 2019; Thacker, Adshead, et al. 2019), a plethora of (non-)governmental initiatives are pushing for more climate-resilient infrastructure and critical services to mitigate societal risks. The Sendai Framework for Disaster Risk Reduction aims to substantially reduce disaster damage to critical infrastructure and disruption of basic services (target D); the UN Sustainable Development Goals explicitly aim to build resilient infrastructure (goal 9), and implicitly rely on such for attainment of all 17 goals (Thacker, Adshead, et al. 2019); the Intergovernmental Panel on Climate Change (IPCC) identified risk to critical physical infrastructure and networks as a Representative Key Risk in their Sixth Assessment Report (O'Neill, van Aalst, et al. 2022). Many multi-stakeholder organisations, such as the Coalition for Disaster Resilient Infrastructure (CDRI), the World Bank, and the Green Climate Fund actively build on these frameworks in their implementation agendas, driving the need for actionable science. In response to this need, the UNDRR's Principles for Resilient Infrastructure hence propose a set of more concrete principles, key actions, and guidelines to create national scale infrastructure resilience and improve the continuity of critical services (UNDRR 2022) - starting with the goal to understand infrastructure and service resilience within its interconnectedness between sectors, and its exposure to historic, current and future (multi-)hazards (Principle #1).

Academic efforts have captured exposure of critical infrastructures to natural hazards at various scales (Hallegatte et al. 2019; Koks, Rozenberg, Zorn, et al. 2019; Mühlhofer, Kropf, et al. 2023; Nirandjan et al. 2022), and pointed out the cost-effectiveness of implementing resilience-enhancing adaptation measures in many cases (Hallegatte et al. 2019). The need to model critical infrastructures as interdependent systems is increasingly acknowledged (Buldyrev et al. 2010; Rinaldi et al. 2001; Zio 2016), and the critical role of system interdependencies has been recognized when evaluating the impacts of natural hazard onto infrastructure failure cascades (Thacker, Pant, et al. 2017; Zorn, Pant, et al. 2020), for recovery dynamics (Almoghathawi, Barker, and Albert 2019; X. He and Cha 2020; Zorn and Shamseldin 2016), and for adaptation and adaptive resilience (Espada et al. 2015; Koks, Le Bars, et al. 2023; Prothi et al. 2023). As critical infrastructures are key to the provision of basic services, an increasing number of studies are also exploring the relationships between infrastructure destruction and critical service disruptions. These often focus on mobility disruptions (Y. He et al. 2022; van Ginkel et al. 2021), inaccessibility of important sites - particularly, healthcare and emergency services (Tariverdi et al. 2023; Yu et al. 2020; Zhang et al. 2022), and on utility provision failures, such as telecom and power outages (Zorn, Pant, et al. 2020). However, few studies (Mühlhofer, Koks, Kropf, et al. 2023; Schotten and Bachmann 2023b) consistently cover the entire impact chain, i.e. the evaluation of real-world hazard events onto the behaviour of several interdependent infrastructure systems, and their consequences for service provisions across the dependent population. To the best of our knowledge, there is to date no study which systematically quantifies and compares natural hazard-induced risk of basic service disruptions from an infrastructure perspective across large and diverse regions.

Here we fill this gap with a comparative study on over 700 historic tropical cyclone and flood events in 30 countries and provinces. Using a high-resolution network-based infrastructure model, integrated within the open-source risk modelling platform CLIMADA, we draw solely on publicly available data. We quantitatively explore the populations' risk of losing access to power, healthcare, education, mobile communications and mobility services in a spatially-explicit manner. We examine how the interplay between physical impacts to infrastructure assets, infrastructure system designs, and socio-economic characteristics either contribute to failure cascades or enhance system resilience. By analysing multiple drivers behind service disruptions, we show that service disruption risks are hazard and place-specific, and can substantially diverge from direct impacts due to infrastructure interdependencies. We highlight geographic hotspots of service disruption risks, and derive a framework for regionally tailored and service resilience-focused adaptation planning. Providing such insights at national scales and in a transferrable manner may contribute, for instance, towards the UNDRR's Principles for Resilient Infrastructure.

4.2 Results

4.2.1 Methods Summary

Figure 4.1 provides a flowchart of the modelling approach to compute basic service access, and event-based infrastructure damages and service disruptions. The approach, developed in (Mühlhofer, Koks, Kropf, et al. 2023), combines network modelling and spatially explicit natural hazard risk modelling. For each study region (mostly countries, see Supplementary SM3.1), geo-spatial infrastructure and population data is transformed into topological networks and combined into a single interdependent network based on dependency heuristics between components of different infrastructure systems, and between end-users and infrastructure system components (see section 4.4.1). Such network-based approaches have proven valuable for capturing interdependencies between large-scale infrastructure systems and their end-users, to compute population's access to services, and to mimic functional failure cascades and service disruptions from severe events (Pant, Hall, and Thacker 2017). Structural damage computations from floods and tropical cyclones are performed within the core part of the CLIMADA risk assessment platform (Aznar-Siguan and Bresch 2019; Mühlhofer, Kropf, et al. 2023) by spatially overlaying hazard footprints, exposures (infrastructure components), and respective vulnerability curves (see section 4.4.2). Resulting failure cascades from these disruptive events are propagated through the network set-up and allow to model service disruptions at the population level (see section 4.4.3), which forms the main metric of interest for event-based, regional, and cross-regional risk and resilience analyses (see section 4.4.4).

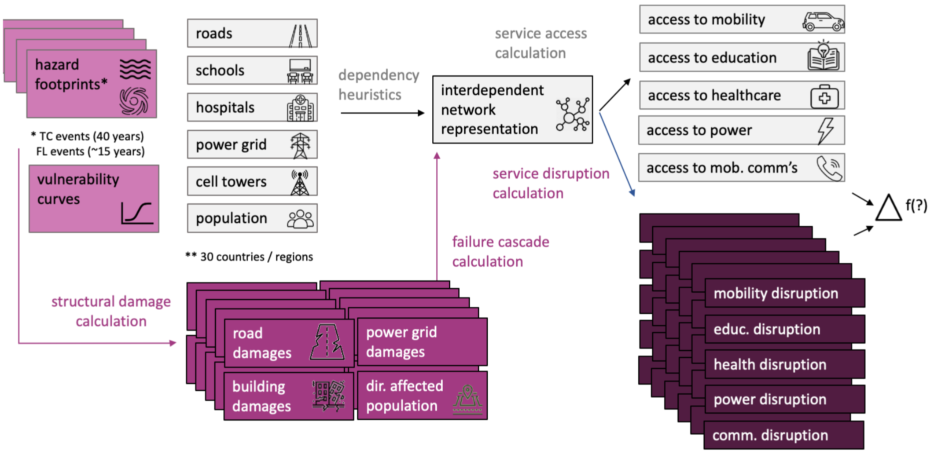

Figure 4.1: Schematic of the workflow to compute infrastructure damages and service disruptions in 30 countries / regions from historic records of tropical cyclones and floods. In grey: Geo-located infrastructure and population data is fed into an infrastructure network model, from which infrastructure functionality and population's access to basic services are modelled. In pink: Disruptive scenarios are introduced from structural damages computed using spatially explicit flood and tropical cyclone footprints, which perturb the network model and cause functional failures, failure cascades, and service disruptions. The computation chain strictly uses open-source and -access data and the CLIMADA risk modelling platform.

4.2.2 Tropical cyclones and floods cause distinct patterns of infrastructure damages and service disruptions

Floods and tropical cyclones result in distinct infrastructure damage patterns. Figure 4.2 (left panel) shows that the average destruction magnitude of a flood event across all computed events and regions is up to two orders of magnitude lower than that of a tropical cyclone event. Many small-scale flood events occur in scarcely populated and built-up areas; 36% of all studied floods caused no physical damage. This contrasts with the high intensity and spatial extent typical tropical cyclone events, where 100% of the events directly impacted people or damaged infrastructure assets. Clear differences emerge in which infrastructure sectors are most affected. Cell towers and the power grid are particularly vulnerable to the impacts of tropical cyclone winds (Figure 4.2, left panel) which often cause large-scale destruction to lines and towers through snapping and toppling, respectively (see section 4.4.2). Substations and other power-generating elements may be inundated, but as these components are more sparsely distributed, physical exposure and hence damages from floods are less frequent. Roads on the contrary are much more often exposed to flooding due to their spatial ubiquity and density, and often sustain severe damage. Following the same line of argumentation, roads are also highly spatially exposed to tropical cyclones, but accumulation of debris and trees tends to cause relatively fewer modelled physical damages than to other infrastructures.

Patterns of service disruption are also hazard-specific (see Figure 4.2, right panel): Floods disrupt healthcare and mobility services most severely, whereas tropical cyclones disrupt power and education access most frequently. These cross-regionally observed damage and service disruption patterns can also be observed at an individual study region scale (see Figure S4 of Supplementary SM3.1, exemplarily selected for Great Britain, Serbia, Cambodia, Puerto Rico and Florida). Tropical cyclone-induced service disruptions further tend to affect 1-2 orders of magnitude more people than floods, which is consistent with the typically larger structural damage magnitudes. However, service disruption patterns do not fully correspond with physical damage patterns of infrastructures; median rates of tropical cyclone-induced service disruptions to healthcare, education, and mobile communications are, for instance, much more similar to power disruption rates than physical damage fractions of hospitals, schools and cell towers are to power line damage rates. Further, for either hazard, shares of population affected by service disruptions mostly surpass shares of physically destroyed infrastructure assets. This large-scale perspective on impact patterns underscores the complex relationships between natural hazards, infrastructures and services.

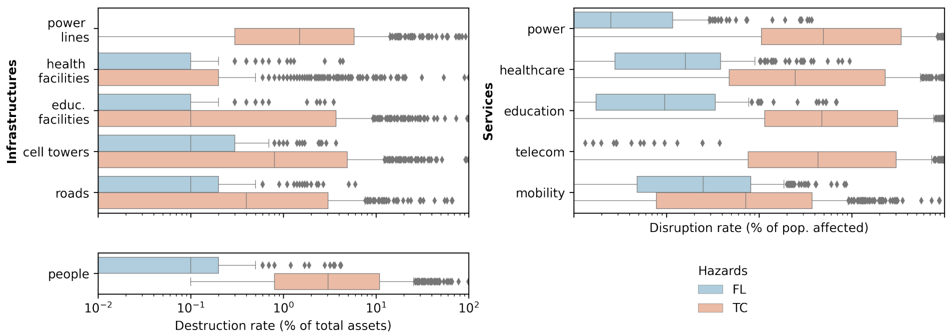

Figure 4.2: Impact patterns of flood and tropical cyclone events: Impact magnitude, most affected infrastructures, and most disrupted basic services differ between both hazard types. Left: Structural damages to infrastructure components (in % of region's assets). Right: basic service disruptions (in % of population affected). Based on all tropical cyclone (TC, red, N=479) and flood (FL, blue, N=242) events across all studied regions (N=30). Share of directly affected population (physically exposed to a flood or TC-grade winds) is included in the left panel for reference.

4.2.3 Physical impacts are not indicative of the severity of service disruptions

Hazard events which cause higher infrastructure damages tend to also cause larger service disruptions, but we find outlier events across most study regions and hazard types (see Figures S5 and S6 in Supplementary SM3.1). In study regions belonging to the US and the Caribbean (Florida, Louisiana, Texas, Cuba, Puerto Rico, Antigua and Barbuda) correspondence between damage rank and disruption rank of tropical cyclone events is generally very high (Spearman rank correlation coefficient > 0.9), whereas in other regions (e.g., Mozambique, the Philippines, Vietnam and Hainan (CHN)), up to 60% of all events cause significantly larger (or smaller, resp.) service disruptions than expected given the rank of physical damages. In some study regions which are exposed to floods and to tropical cyclones, the outlier effect is much more pronounced for one hazard type (e.g., only for tropical cyclones in the Philippines and Vietnam).

We further observe that in 65% of all tropical cyclone events and in 84% of all flood events, at least on type of service is disrupted for more people than those which are physically affected. However, this 'multiplier effect' strongly depends on the type of service, regional characteristics, magnitude and type of the hazard (see upper panels of Figure 4.3 and S7 (Supplementary SM3.1) for tropical cyclones and for floods, resp.). For instance, tropical cyclone-induced power and mobile communication disruptions often spread beyond the impacted population, but flood-induced disruptions do not. Mobility and healthcare disruptions tend to affect less people than those physically affected by floods and tropical cyclones, but only in wealthy regions.

Similarly, the extent of physical infrastructure damage is not highly indicative of the service disruption extent (see lower panels of Figure 4.3 and S7 (Supplementary SM3.1) for tropical cyclones and floods, resp.). This non-correspondence between asset damages and service disruptions is particularly pronounced for education and healthcare services, which depend on other services to function (i.e., power and road access), and power, which has many internal power-grid dependencies and localized supply clusters. Only mobility disruptions, as the only service modelled without significant road network-internal or external dependencies, correlates with the number of damaged roads.

4.2.4 Drivers of service resilience are regional, systemic, and hazard-specific

To gain an understanding of what drives above-seen patterns and tendencies of service disruptions in different study regions, we examine spatially-resolved and coarse averaged region characteristics, processes behind disruptions retrieved from the graph-based modelling approach, and an in-depth case study for selected events.

Quantifying the spread of service disruptions. We quantify above-mentioned multiplier effects of physically impacted to 'service-disrupted' population per study region and basic service, by means of *resilience factors (RF)* and *spatial cascade factors (SF)* (see section 4.4.4 for method details and Figures S8 and S9 in Supplementary SM3.1 for results). The *RF* measures the spread of service disruptions relative to directly impacted population, and incorporates awareness to locally specific pre-disaster service access rates. This is crucial in regions with low service access rates, as services can only be disrupted to those who were served . The *SF* measures the degree of spatial containment of disruptions within (or beyond)

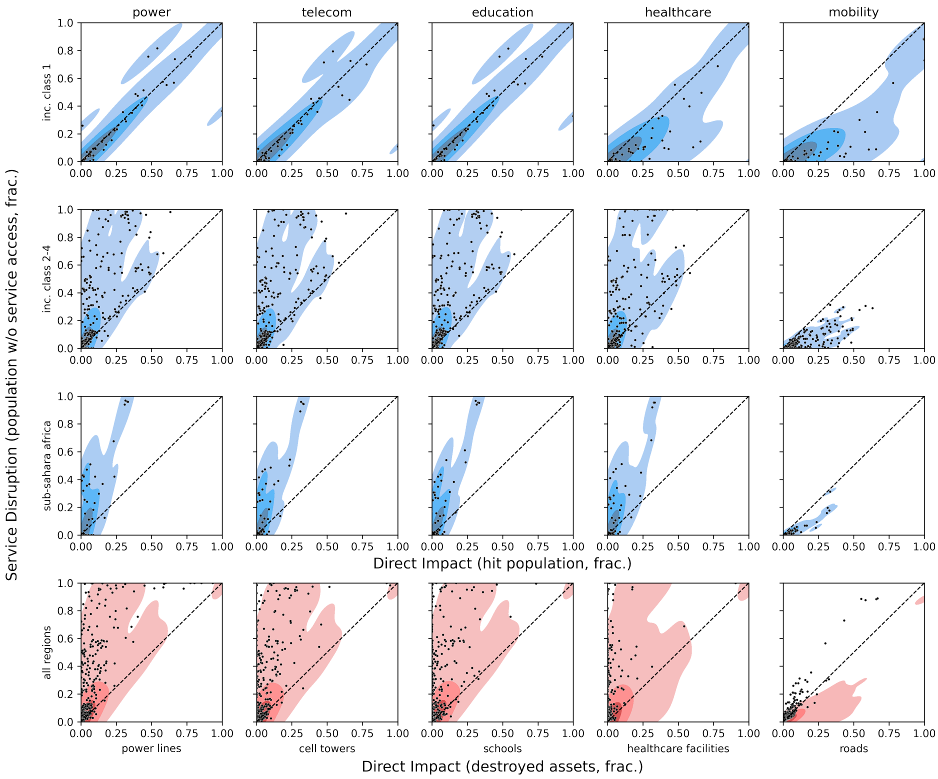

Figure 4.3: Disruptions to power, telecom, education, healthcare and mobility access are not concurrent with physical impacts. Upper panel: Directly affected population (located within the tropical cyclone-hit area) vs. population without access to the respective service, split by income / geographic groups. Lower panel: Destroyed assets vs. population without access to the respective service, for all events and regions. Colour shades represent point density. Normalizations (frac.) are with respect to the corresponding study regions' total populations or assets.

the directly affected region.

Services in wealthy, densely built-up, and small regions tend to be resilient (RFs<1): In Louisiana, Florida, and Texas (USA), for instance, median RFs across all tropical cyclone events are between 0.2 and 0.8 for all services, meaning only about 20-80% of the physically affected population tends to experience service disruptions. Analogously, services in poor and sparsely built-up study regions tend to be non-resilient; in Mozambique, services are frequently disrupted for a ten-fold larger number of people than directly impacted (RFs>10). However, the spread of service disruption in poorer regions also varies much more strongly between events; as observed through the large interquartile ranges of RFs in Haiti, Mozambique and Madagascar. Due to (very) low baseline service access rates in poor regions and the stark spatial concentration of infrastructure assets and service availability to confined, urbanized areas, we observe a 'hit-or-miss dynamic' for service disruptions: Non-serviced areas cannot be disrupted, and failure of infrastructure assets in the few serviced areas may cause large disruptions. This highlights the sensitivity towards the exact location of the hazard occurrence for causing service disruptions impacts. The importance of spatially resolved access statistics in predicting service disruptions also explains why regionally-averaged metrics such as population density, infrastructure density per capita, and income class have limited explanatory power for RFs of most regions' services (see Figures S9 - S11 in Supplementary SM3.1). Figure 4.4 exemplifies these results for Louisiana (USA) and Madagascar; the separate documents in Supplementary SM3.1, providing spatially explicit maps of baseline service access rates and disruption patterns for each study region.

Mechanistic drivers of service disruptions. Harnessing the graph-based modelling approach, the analysis of functionality, damage, and service access attributes in the network representation of the study regions allows to infer the mechanisms leading to service disruptions in each simulated event. We distinguish four mechanisms: direct damages (services are disrupted due to sufficient physical damage of service-providing core infrastructure asset, e.g. hospitals for healthcare), access disruption (services could not be accessed due to physical access path constraints), cascading failures (services

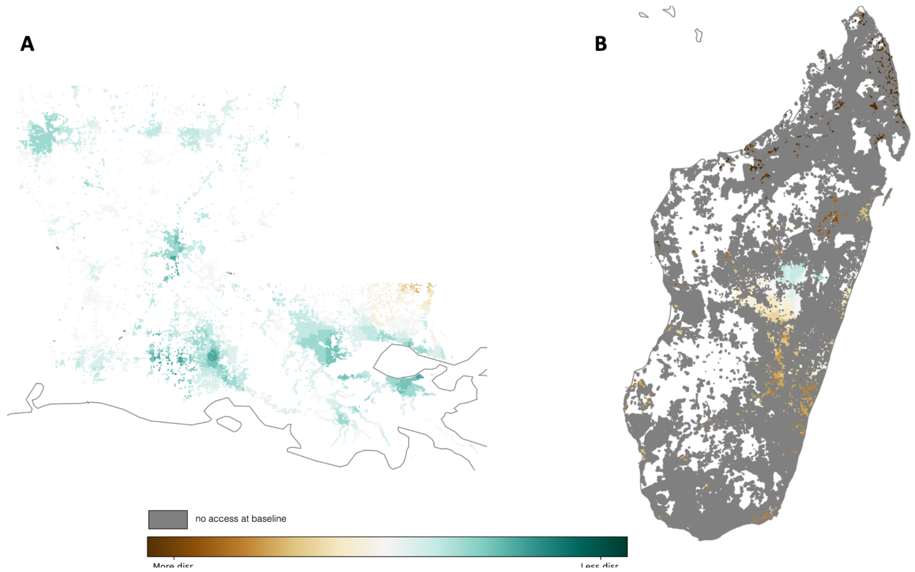

Figure 4.4: Spatial distribution of healthcare disruptions relative to physical tropical cyclone exposure in Louisiana (USA, panel A) and in Madagascar (panel B). 'More disrupted' refers to services being lost in areas not directly impacted, 'less disrupted' to services being retained despite physical impact. Scale normalized to hypothetical maximum number of disruptions (i.e. total number of events).

are disrupted due to loss of another supporting infrastructure functionality) and capacity failures (for power only; the shut-down of services after falling below a certain supply capacity).

Figure 4.5 shows population-averaged statistics of disruption mechanisms per study region and type of basic service, for tropical cyclones (upper panel) and floods (lower panel). For tropical cyclone-induced disruptions, physical damages are important (causing 14(+/-14) % of healthcare, 27(+/-22) % of education, 36(+/-27) % of mobile communications, and 23(+/-17) % of power disruptions, resp.). However, the main driver of service losses for tropical cyclone-induced services losses are cascading failures (83(+/-15) % of healthcare, 73(+/-23) % of education, and 64(+/-27) % of mobile communications disruptions) and capacity failures (power, 71(+/-20) %), which render the undamaged service-providing infrastructure dysfunctional. Remarkably, the drivers differ starkly for flood-induced service disruptions. Restriction of physical access, i.e. blockage or unmanageable prolongation of paths, is a major driver of healthcare and education disruptions (36(+/-36) % and 89(+/-23) %, resp.). For education, physical damages of school facilities further play a more prominent role than damages to healthcare facilities for healthcare access: Healthcare services may be sought from any functioning facility, but schools are allocated uniquely. It is hence less likely that all hospitals within a reasonable distance are damaged by (mostly localized) floods. However, as the average journey to a hospital is often longer than to a school, access paths are more likely to be disrupted. Functional failure cascades, the dominant driver for most tropical cyclone-induced service disruptions, play a minor role, owed to the fact that the power system, which initiates most of these cascades, is generally less affected by floods.

Drivers of service disruptions are also sensitive to event size and to infrastructure network density/redundancy: Event-wise analysis of mechanisms reveals that failure cascades are crucial for a wide range of 'medium-sized' events. For small events, damage to local access roads (i.e. physical access-based disruptions) or the occasional destruction of a core infrastructures drives destructions. For large events, wide-reaching physical damage to most infrastructure assets is enough to drive disruptions. In dense networks, access-related disruptions and failure cascades are reduced. These observations are substantiated by service disruptions in smaller and wealthier regions being more influenced by direct damages (cf. small-island states in upper panel of Figure 4.5) compared to larger and less affluent regions.

Case study deep-dive. We exemplarily select the study regions of Hainan, province of China, and Florida, USA, to examine intermediary modelling outputs of the service disruption computation chain from two tropical cyclones each, which were similar in hazard strength but had very different consequences on the respective regions. Further, Supplementary SM3.2 contains many of the intermediary outputs discussed in the following for all 30 study regions.

Hainan is highly exposed to tropical cyclones, with 40 records in the studied 40-year period. The region's area is relatively small ($\sim$ 33k km^2), urbanisation rate low (58%), and access to most basic services relatively high (computed baseline access rates range between 84% for healthcare access and 100% for power access). Florida is equally exposed to tropical cyclones (31 storm records). The region's area is considerably larger ($\sim$ 170 km^2), urban-

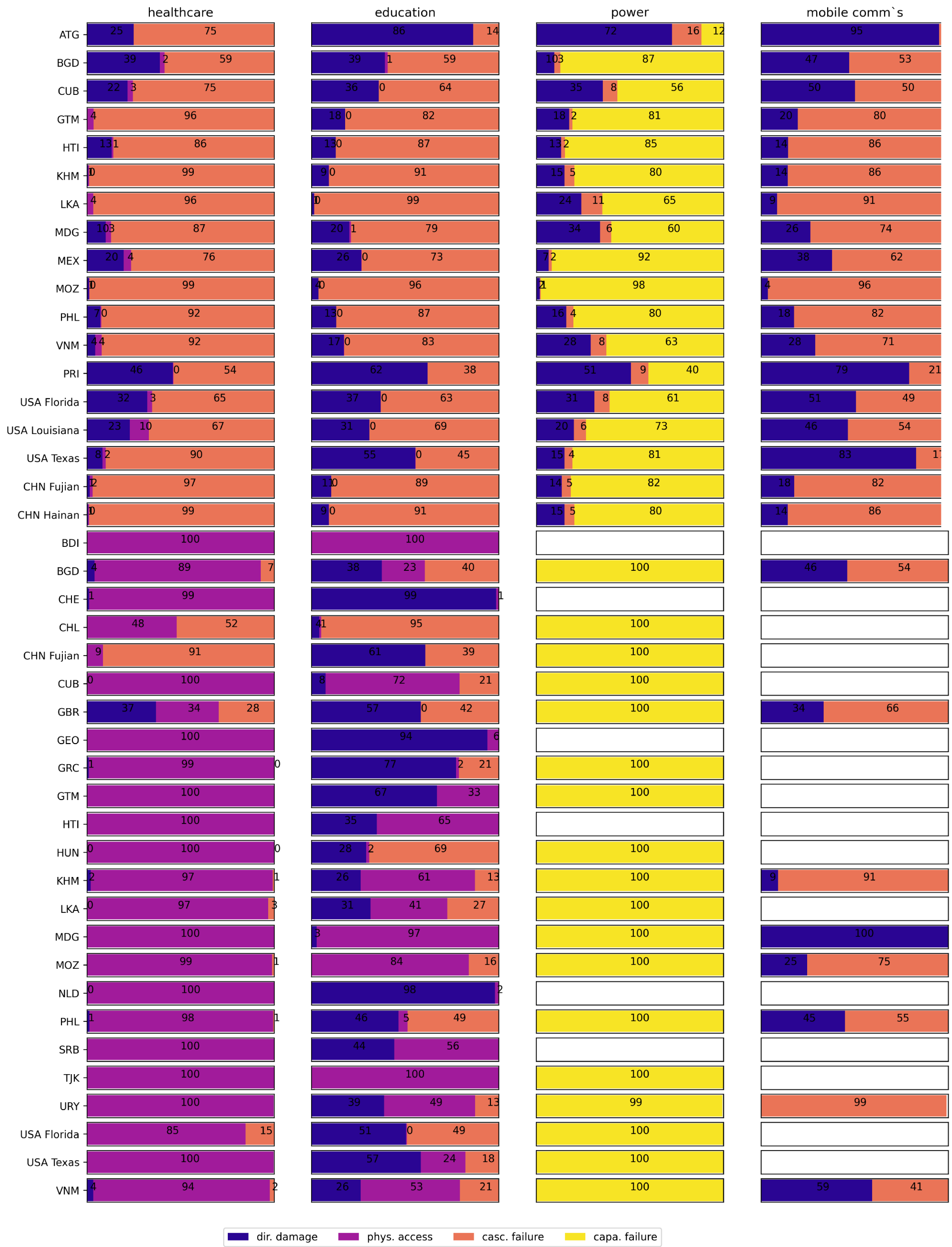

Figure 4.5: Population-weighted service disruption drivers of tropical cyclone (above) and flood (below) induced healthcare, education, mobility and mobile communication disruptions across all events, per study region. Empty bars: no disruptions.

isation rate high (91%), and baseline access rates to all services near 100%. In Hainan, modelled service disruptions are distinctly grouped into events where disruptions are either significantly worse given the extent of physical damages, or vice-versa. In Florida, event ranks ordered by service disruption severity mostly coincide with event ranks of physical damage severity (see Figure S5 (Supplementary SM3.1) for the respective rank plots).

Panels A in Figure 4.6 and S13 (Supplementary SM3.1) display the aggregate spatial service disruption patterns for the populations of Hainan and Florida, resp., over all events. In Florida, direct impact patterns spatially coincide over wide areas with service disruptions, whereas in Hainan the North-Eastern half of the island suffers over-proportionally from disruptions. Panels C-E in Figure4.6 and S13 (Supplementary SM3.1) illustrate these dynamics on four individual events: Typhoon Lois and hurricane Mitch hit 12.5% and 17% of the populations in Hainan and Florida, resp., typhoon Vera and hurricane Charley hit 49% and 53% of the population. Despite its lower physical impact, typhoon Lois caused much larger service disruptions in Hainan, while the contrary applies to hurricane Mitch in Florida. Analysing the disruption causes (see panel E of Figure 4.6), it is evident that failure cascades, induced by large-scale power grid failures, are responsible for the majority of the wide-spread service disruptions during typhoon Lois. Reasons for the extensive power outage in the physically less destructive event become evident in the structural damage and power grid failure computations illustrated in panel D of Figure 4.6: In Hainan, power-generating assets are concentrated in the South-West of the island; damages in the North (e.g., typhoon Vera) hence remain geographically contained, whereas damages in the South (e.g., typhoon Lois) spread across the entire island due to the non-resilient grid design. In Florida, power assets are distributed across the entire state and many power clusters hence retain functionality even if others are lost. Further, a generally higher infrastructure density in Florida (for instance, of healthcare facilities) creates redundancy even in the case of blackouts and physical destruction, and leads to less pronounced disruptions than in Hainan at similar hazard intensities.

While it is not feasible to perform in-depth validation of more than 700 individual events and multiple modelled result layers from physical asset damages to service disruption impacts , the case studies on Hainan and Florida provide opportunities for anecdotal comparison with real-world evidence. While reports specifically for typhoons Vera and Lois were difficult to obtain in English language, print media, technical reports and scientific studies unanimously confirm the low power supply security and high risk of massive outages of Hainan's energy infrastructure, which is driven by a combination of exposure to tropical cyclones and, until recently, its insufficiently backupped and weak power grid structures which are isolated from the Chinese mainland (X. Zhou and Yan 2008). Our model captures the non-resilient power grid architecture as well as the frequent exposure of assets to tropical cyclones. Many of the modelled damage and disruption dynamics were also confirmed in event reports of hurricane Charley's aftermath in Florida: Power pole toppling and line snapping caused power outages for more than 2 mio. residents, fallen trees and debris resulted in extensive road blockages and isolated some communities, public schools closured in the counties where our model predicted heaviest education disruptions (FEMA 2005). Real-world evidence further provides interesting aspects for future studies: Power outages affected the supply of clean drinking water in the aftermath of Hurricane Charley (Messina 2004). Due to insufficient data availability of water and sewage assets at global scale, these infrastructure systems were not included in the current model runs, but have been considered in a US-specific study (Mühlhofer, Koks, Kropf, et al. 2023). Pre-emptive action may influence the extent of structural damages and propagation of failure cascades (in southern Cuba, for example, the power grid was shut down in the wake of Charley to avoid accidents (Messina 2004). Adaptation, socio-economic development, and infrastructure system changes may drastically alter an interdependent infrastructure system's exposure and resilience to natural hazards: For instance, in Hainan, strong population and GDP growth, the increase in power transmission capacity, and the shift to a decentralized, renewables-based power grid are projected for the near future (De Zotti 2020; XinhuaNet 2019).

4.2.5 Quantifying services-at-risk

Natural hazard-induced risks are predominantly expressed in terms of asset value damages or economic losses, derived the product of likelihood and

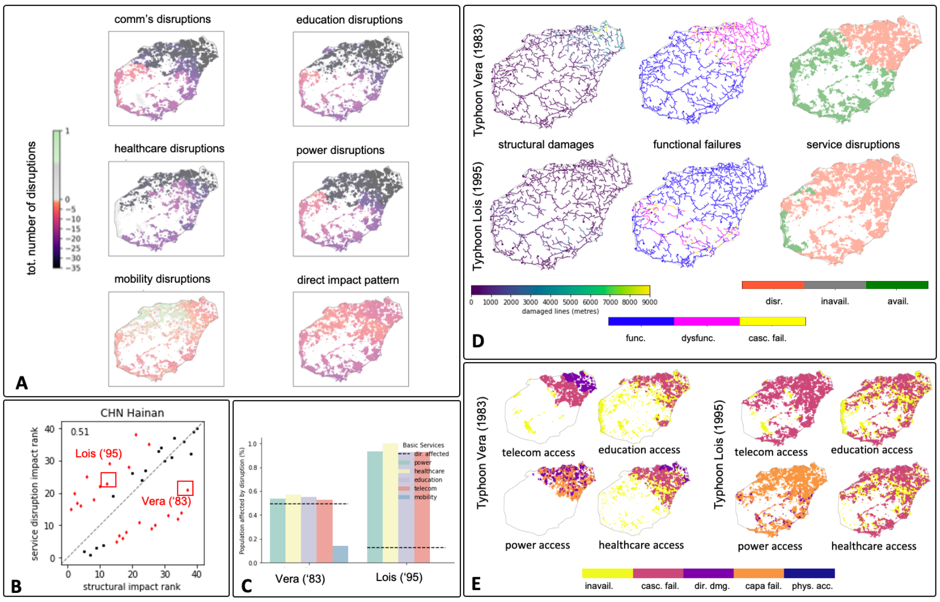

Figure 4.6: Case study on the drivers of tropical-cyclone induced service disruption patterns in Hainan, Province of China. A - spatial distribution of modelled service disruptions and direct impact patterns on the population based on historic hazard events (<0: # disruptions experienced by population cluster during study period; 1: undisrupted service; 0: population cluster generally has no access to service). B - event rank plots of service disruptions vs. damages (from Fig. S5, Supplementary SM3.1). C - service disruption numbers and directly impacted population statistics for case study events; D - physical destruction of the power grid (in metres of power lines destroyed), functional failures of the power grid (according to driving mechanisms of failure), and resulting power disruption map for population clusters; E - Population clusters experiencing service disruptions, according to disruption driver.

consequences of events (Kaplan and Garrick 1981). Our results allow us to express services-at-risk in terms of expected annual percentage of population affected. For tropical cyclone-exposed study regions, relative average annual power disruption risk is largest in Hainan, province of China (67% of the population) and the Philippines (62% of the population), but also Florida, USA, carries a considerable risk (11%). Healthcare disruption risks are similar (67% in Hainan) to considerably lower (52% and 6%, resp.). Figure S14 (Supplementary SM3.1), left panel, details the complete risk statistics for all services and study regions. The spatial explicitness of the approach further allows to consider service disruption risk at the level of individual population clusters, which reveals large inner-regional disparities (see risk maps as in Figure S14 (Supplementary SM3.1), right panel). In Mexico, for instance, service disruption risks are concentrated around the coast-line, and in the Philippines, the Northern island of Luzon, where Manila is located, is more at risk of disruptions than the Southern island of Mindanao.

While the availability of over 40 years of tropical cyclone records allows estimation of regional risks by attributing event frequencies to hazard records, incomplete event records and attribution of occurrence frequencies to (sparse) historic events are common challenges involved in risk quantification. The flood hazard data used throughout this study is a prime example, as the hazard footprints are based on a short time record of less than 15 years, and events are not consistently captured due to the inherent shortcomings of remote-sensing based event detection (see Tellman et al. 2021, for details). We hence refrain from risk computations in the classic sense for flood-induced service disruptions.

4.3 Discussion

Studies which explore systemic impacts on critical infrastructures and services across large geographic areas mostly focus on the transportation sector. Y. He et al. (2022) demonstrate in a global study on road transport disruptions from flooding that the number of interrupted routes correlates positively with direct impact and negatively with network density, a trend which we equally observed. While high percentages of built-up area are often found to reduce transport disruptions (Koks, Rozenberg, Tariverdi, et al. 2023), we showed that direct impacts and asset density nevertheless have limited explanatory power for actual service disruption magnitudes - phrased differently, the “underlying relationship between failure rate and potential causal factors is complex and varies across space” (Y. He et al. 2022). Findings that South-East Asian, Central African and Latin American are particularly vulnerable to transport disruption even during low-intensity events (ibid.) are consistent with our results: Vietnam, Cambodia, Haiti, Cuba, Mozambique and Madagascar are amongst the regions with lowest mobility resilience to flooding, often due to critical road crossings in the country with few alternatives (Hallegatte et al. 2019; Koks, Rozenberg, Tariverdi, et al. 2023).

Studies which examine the response of more than two interdependent infrastructure systems to (natural) hazard events commonly focus on spatial scales at community or province level (Lan et al. 2023; Montoya-Rincon et al. 2023; Tariverdi et al. 2023). To the best of our knowledge, we provide the first comparative study involving many country-level systems. Several single country-level studies with a similar network-based approach observe similar larger trends in failure cascade dynamics as we presented: In a New Zealand-based study, Zorn, Pant, et al. (2020) find that the electricity grid is particularly vulnerable, leads to largest-scale user disruptions and triggers most frequent failure cascades among all infrastructure system (31%), while the road network initiates much fewer (9%) of the combined average disruptions. These figures and the finding that indirect failures constitute a majority of all service disruptions experienced by end users (46% of disruptions ibid.) are comparable with similarly wealthy and built-up regions in our study, such as Florida, Texas or Puerto Rico.

While service risk and resilience patterns have been broadly identified according to hazard type and region income class, many of our results emphasize the need to consider the intricacies of interdependent infrastructure and population networks with the spatial and mechanistic specificities of the triggering hazard on a case-by-case basis: Generally, failure cascades contribute substantially towards service disruptions, though not in very large-scale events which anyways cause ‘sufficient’ physical damage; this behaviour was also observed in a study on regional failure cascades from flood impacts

(Lan et al. 2023). In regions with very low baseline access rates to services, disruption patterns largely mirror urban population, as services are mostly only available - and disrupted - there (e.g., tropical cyclones in Madagascar). In regions with very high baseline access rates to services, disruptions patterns often mirror overall population patterns (e.g., tropical cyclones in Florida). However, we also find cases of disruptions concentrating on the peripheries of urban agglomerates rather than on the urban areas themselves, single 'unfortunate' areas, or entire physically unaffected regions which are affected through the spread of failure cascades due to non-resilient infrastructure designs. This leave us to conclude that no simple, univariate spatial rules of thumb can be derived to predict largest disruption potentials.

4.3.1 A tiered, process-oriented perspective on service disruption risk

Adding service disruption to the conception of natural hazard-induced risks yields a picture which is not necessarily congruent with a focus on direct, physical asset damages. Packaging this impact layer into commonly used risk metrics, such as expected annual service disruptions per population, allows for regional comparability and coarse screening of risk hotspots. While such aggregate metrics can guide first directions of in-depth investigation, we argue that the systemic, multi-stage and event-based nature of our model provides the largest advancement, as this allows to gain an in-depth understanding of the responses of interdependent infrastructure systems under stress.

As the underlying network modelling approach is computationally intense, its use for probabilistic risk calculations is limited; rather, it lends itself particularly to complementary approaches such as story-lines (Ciullo, Martius, et al. 2021; Koks, Le Bars, et al. 2023; Shepherd et al. 2018), where probabilistic hazard sets are either unavailable, or where the focus lies explicitly in evaluating a broad scope of complex and multi-faceted consequences derived from carefully selected scenarios. The case studies on Florida and Hainan, for instance, helped to understand how in the two study regions, despite both being hotspots for service disruptions at an aggregate level, impacts were driven mostly by extreme physical exposure in the one, and by a non-resilient infrastructure design in the other instance.

This scenario-based thinking and process-understanding forms a vital component of tiered risk and resilience approaches (Linkov et al. 2018), where after a coarse screening of risk hotspots, one may delve into the intricacies of iteratively understanding the drivers behind potentially vulnerable systems. This staged process is encouraged for stress testing not least by the UNDRR's Resilient Infrastructure Tool (UNDRR 2023).

4.3.2 Informing adaptation strategies for resilient basic services

The identification of risks in a socio-technical system and the understanding of the drivers behind these, provide crucial foundations into guiding adaptation strategies. Given financial constraints and significant environmental impacts of infrastructure construction (Hallegatte et al. 2019; Trejo and Gardoni 2023), resilience-enhancing measures must be prioritized on a spatial dimension and on the type of resilience which should be achieved: the resilience of infrastructure assets, of infrastructure services, or of infrastructure users (Hallegatte et al. 2019).

Concurrent with the different levels of service risk perspectives presented above, we suggest that higher and lower-level adaptation strategies can be derived from our study results: As our first quantitative basis is a physical impact layer, asset-level prioritizations are easily derived following structural damage hotspots. One might, for instance, allocate funds for structural reinforcements of roads in central Cambodia due to frequent flood-exposure, or suggest wind-proofing of the hospitals in northern Philippines due to frequent physical damage from tropical cyclones. However, harnessing the result layers on functional failures of infrastructure systems and on end-user service disruptions, adaptation strategies may be guided along these components of resilience.

As Hallegatte et al. (ibid.) suggest that skilful prioritization may come at a tenth of the expenditures of a system-wide strengthening, considering these layers makes not only a strong case from a humanitarian and a sustainability perspective, but also from an economic one. High-level adaptation strategies have been devised in earlier system-spanning studies (Hallegatte et al. 2019; Koks, Rozenberg, Tariverdi, et al. 2023; Zorn, Pant, et al. 2020) and often revolve around the following actions: Maintaining or hardening specific key infrastructures, decreasing system dependencies through diversification, decentralization or back-ups and increasing redundancy in the systems, usually by increasing infrastructure density.

Based on these considerations, we can derive a qualitative decision framework for adaptation strategy planning which is informed by baseline service access computations, resilience factor computations and failure mechanisms analyses. Figure 4.7 illustrates this on the tropical cyclone-exposed study regions, exemplified on healthcare access resilience.

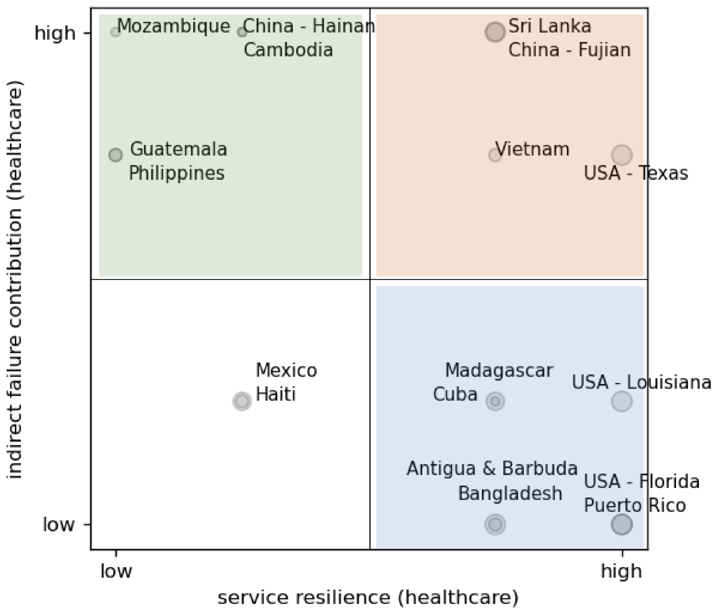

Figure 4.7: Qualitative decision framework for devising high-level adaptation strategies which focus on enhancing systemic service-resilience. Different quadrants indicate different adaptation priorities, derived from service resilience to disruptions (x-axis), contribution of indirect failures to disruptions (y-axis) and baseline access rates (marker size).

If resilience of a service is high, and indirect failures contribute little to the disruptions (blue shaded quadrant), it may be most effective to invest in better protecting the already existing most hazard-exposed service-providing key infrastructure (in this case, hospitals). However, in case of low baseline access rates (as in Madagascar), this measure would do little to the population already left out of the system; such equity considerations in adaptation decisions are an important component in achieving sustainable development and are crucial to make explicit. If service resilience is generally high, but failures are mostly driven by the failure of supporting infrastructures (red shaded quadrant), it may be most beneficial to reinforce existing highly exposed secondary infrastructure, such as power lines in a particular area. The green quadrant shows regions where service cover is generally low, services are not resilient and disruptions are strongly driven by failing support infrastructure. In such cases, a combined approach of investing into more key infrastructure (building hospitals) and decentralizing and diversifying supporting infrastructures (architecture of the power grid), may help increase baseline accessibility and strengthen the resilience to failure cascades. The case of Hainan has been discussed earlier and illustrate this scenario well.

For regions affected by several hazard types, potential asynergies (de Ruiter et al. 2021) might arise when priority strategies to avoid wind-induced disruptions do not align with avoidance strategies for flood-induced disruptions. For instance, in Bangladesh flood-induced healthcare disruptions would mostly be avoided by reducing access path disruptions, i.e., investing in better roads, whereas wind-induced healthcare disruptions would be best avoided by wind-proofing existing healthcare facilities. Both the spatial resolution of this approach and the impact computations may help resolve such conflicts, since these strategies may affect entirely different sub-regions, or be orders of magnitude apart in terms of absolute risk and hence priority.

4.3.3 The importance of locally specific, spatially explicit, and physically consistent data

In our study we examine impacts based on real-world natural hazard footprints. Several comparative studies point out the added value of physically consistent hazards for infrastructure network studies: Loreti et al. (2022) demonstrate that for understanding the resilience of transportation networks, a realistic high-resolution flood simulation may provide different criticality judgements of certain road sections than the commonly used framework of percolation. Wang et al. (2019) conclude that floods are more locally destructive and more strongly affect a community than random damage and are more globally destructive than localized damage because they can affect entire river basins, which may further lead to prioritization of different adaptation strategies. According to our best knowledge, no comparative studies exist between service disruption outcomes of explicitly simulated tropical cyclones and such employing percolation theory or generic hazard cells. As the geographic and spatial characteristics of tropical cyclone occurrences are arguably vastly different from such approaches, we suggest that our results yield novel insights into the actual spatial extent and magnitude of cyclone-induced service disruptions.

A growing body of evidence on the nature of dependencies between infrastructure systems, and between infrastructure systems and end-users suggests that certain relationships are ubiquitous but locally specific in its manifestation. While healthcare facilities for instance generally require power, backup generator requirements and factual generator availability may be highly site-type and region specific (Chawla et al. 2018); similarly, patients choice preferences may be an important factor in adequately capturing healthcare accessibility (Tariverdi et al. 2023; Zhang et al. 2022), and travel times considered "adequate" may equally vary. In our approach, we incorporate locally-specific knowledge as far as available at the globally consistent basis required by the scope of our research, such as terrain-dependent driving and walking speeds and global power production estimates, yet also make necessary simplifications compared with specialized, mono-thematic engineering fields (e.g. patient surge and demand models (Mahmoud et al. 2023) or power flow analyses (Beyza et al. 2020). While an extensive discussion is out of scope here, Supplementary SM3.1 provides details on the rationales behind our heuristics.

Similarly, deriving tailored vulnerability functions and high-resolution exposure data are recurring concerns not only when relying on crowd-sourced data such as OpenStreetMap where quality and coverage are known to be unknown for certain types of infrastructure and regions (Herfort et al. 2023). While for local adaptation implementation designs it is crucial to iterate this type of analysis with increased contextual knowledge, we argue that at the presented level of analysis, where the goal is to identify large-scale risk hotspots and to compare dynamics and patterns of regions relative to each other, those are necessary trade-offs.

4.3.4 Conclusion

In this study we quantified structural damages, infrastructure failure cascades, and service disruptions on a range of critical infrastructure sectors across 30 countries and provinces due to historical tropical cyclone and flood events, computed risk metrics and discussed high-level adaptation strategies for service resilience, leveraging publicly accessible data and a high-resolution network-based infrastructure model integrated into the open-source risk modelling platform CLIMADA.

We demonstrated that distinct hazard-specific destruction and service disruption patterns exist, where tropical cyclones have a major impact on power and power-dependent services across expansive areas that surpass the direct hazard footprint, and floods predominantly disrupt road access-dependent services and remote but smaller areas. However, relationships between physical destruction and service disruptions cannot be narrowed down to simple spatial rules; outlier events emerged in all examined regions, and neither asset damages, exposed population or economic wealth are satisfactory predictors of modelled disruption impacts, as disruptions are often driven by failure cascades through system interdependencies. Our results underscore the complex interplay of event size, network density, hazard type, baseline access rates and service category which drives disruptions and hence the importance to consider systems in their contextual embedding, using spatially explicit exposure and hazard data, to understand service risks.

By transitioning from a physical-impact to a service-resilience centred view on natural hazard risks, we highlight disparities within regions that may else remain concealed. We showed how understanding drivers of service risk can form the basis for more systemically-informed adaptation strategies to enhance service resilience. Our derived qualitative decision framework offers a first suggestion on ways forward, which could also incorporate equity implications of such strategies. As our approach is based on open-source code, it can easily be applied to other study regions and hazards, and may guide future risk and adaptation studies at various spatial scales and levels of detail across the globe.

4.4 Experimental Procedures

The employed modelling set-up is illustrated in the flow chart of Figure 4.1, and based largely on the generalized modelling framework developed in Mühlhofer, Koks, Kropf, et al. (2023), which is hence scaled up to cover diverse regions and natural hazard types. We additionally develop novel metrics to capture cascading behaviour and resilience indicators of (national) interdependent infrastructure systems and service disruption potential in a condensed format.

4.4.1 Modelling Infrastructure Interdependencies and Basic Service Access

Infrastructure and Population Data. 30 study regions (25 countries, 3 US states and 2 Chinese provinces) which are either affected by floods, tropical cyclones, or both hazards, were chosen such as to cover all continents, all World Bank income classes, and wide ranges of population density (20 people/km2 - 1'265 people/km2), urbanisation rate (3% - 95%), and region area (27'000 km2 - 2'000'000 km2). See Table S4, Supplementary SM3.1 for the full list. For all study regions, gridded population count data was retrieved from the WorldPop project (WorldPop 2020) and geospatial data was obtained for roads, healthcare facilities, educational facilities, power plants, high-and medium voltage transmission lines, and cell towers from OpenStreetMap (OSM) and other publicly available data sources. Section S1 of Supplementary SM3.1 provides details on extraction queries from OSM, data sources, and post-processing of geospatial exposure data.

Dependence Heuristics for Infrastructures and Service Access. Critical infrastructures frequently depend on other critical infrastructures (dependencies), or even mutually depend on each other (interdependencies), to ensure their functionality (Rinaldi et al. 2001). Similarly, end-users depend on the (simultaneous) usage of a range of critical infrastructures to obtain access to the services which they deliver. Capturing these (inter-)dependencies is therefore essential to adequately map the functionality and disruption of the systems under study. While the identification, parametrization and quantification of infrastructure (inter-)dependencies is at the centre of investigation of numerous studies (e.g. Chou and Tseng 2010; Cimellaro 2016; Gao et al. 2023; Hernandez-Fajardo and Dueñas-Osorio 2013), there is no universally applicable approach which reliably predicts dependencies at component level with scarce data. We therefore use a heuristics-based approach (see Figure 4.8, explained in depth in Mühlhofer, Koks, Kropf, et al. (2023), which combines a set of regionally adjustable rules and (spatial) data to infer where components of one infrastructure system may depend on support the component of another infrastructure system. Similarly, such rule sets are employed to infer where population clusters depend on the provision of which (jointly) functioning infrastructure systems to obtain certain basic services.

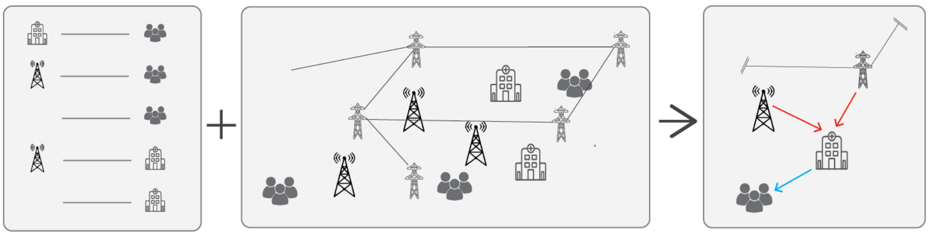

Figure 4.8: Based on geo-spatial infrastructure and population data, and using a set of dependency heuristics, a complex network-based graph is formed representing assets, end-users, and dependencies as edges and nodes.

Formally, these infrastructure dependence heuristics rely on a set of variables to quantitatively express and code them, such as the source (supporting infrastructure type) and target (dependent infrastructure type), the redundancy (whether a component can rely on several support sources) and the flow type (whether the dependency is manifested as a physical transmitting discrete, physical goods, or whether it is of a logical, binary type). For dependencies between end-users and infrastructures, which mimic the way how people access basic services, the same formal rules are applied, yet include further conditionalities to capture distinct aspects of service access: functional access, physical access and socio-economic access.

- Functional accessibility: The service-providing infrastructure must be in a (sufficiently) functioning state to do so.
- Physical accessibility: The service-providing infrastructure must be physically accessible (e.g. schools).

- Socio-economic accessibility: Even if physical and functional access are provided, socio-economic hurdles may prevent the effective access to a service (e.g. in low-income countries, physical distance to power infrastructure over-predicts actual electrification rates, and must be corrected for by using socio-economic proxies)

In this study, heuristics were applied to capture 8 distinct infrastructure dependencies as well as service access dependencies between the power grid, healthcare and educational facilities, the mobile communication infrastructure, the road network and population clusters. They are qualitatively described in Table 4.1. In-depth explanations of the applied dependency inference heuristics, data sources and data usage are provided in Supplementary SM3.1, section S2.

Graph Creation and Service Access Baseline Computation. Geospatial infrastructure and population data are transformed into directed topological graphs consisting in nodes and edges, where all prior attributes such as geographic location, element length and area, infrastructure type and population counts are retained as attributes. The above-described dependence inference heuristics are quantitatively implemented within a search algorithm across all graphs, which places directed dependence edges along their elements if respective conditions are fulfilled, creating a single multi-layered interdependent graph per study region. Upon completion, all infrastructure graph elements are checked for the existence of their required supporting dependences (resulting in a functional state), and all population graph elements are checked for the fulfilment of their service access dependences. Hence-computed basic service access rates for access to power, healthcare, education, mobile communications and mobility in the undisrupted (baseline) scenario are indicated in the region overview of Supplementary SM3.1, Table S4. The formal treatment of this algorithm is further described in Mühlhofer, Koks, Kropf, et al. (ibid.).

Table 4.1: Heuristics used in this study to infer infrastructure dependencies and service access rules. Data usage refers to secondary data (apart from geo-spatial information on infrastructures and population clusters) used to feed the search algorithm. An in-depth explanation of and justification for the applied dependency inference heuristics, and data usage is provided in section S2 of Supplementary SM3.1.

Infrastructure Dependencies		
Internal power grid dependences	*Heuristic:* Power plants connect to nearest substation; clusters must be running at a certain capacity	*Data usage:* power plant generation statistics (WRI), electricity consumption statistics (IEA)
Power-dependence of schools, cell towers	*Heuristic:* Nearest power substation to the facility must be running at a certain capacity	*Data usage:* power plant generation statistics (WRI), electricity consumption statistics (IEA)
End-user Dependencies (Basic Service Access)		
Access to electricity	*Heuristic:* Nearest power substation must be running at a certain capacity and population cluster must lie in an electrified area.	*Data usage:* night-light data-based electrification targets (Arderne et al. 2020), electrification rates (World Bank open data platform)
Access to healthcare	*Heuristic:* A functioning facility must be reachable within a certain time threshold by foot or road at terrain-dependent speed.	*Data usage:* global walking-only friction surfaces for non-motorized transport (Weiss et al. 2020); national mean road travel speeds (Moszoro and Soto 2022)
Access to education	*Heuristic:* The assigned facility must be reachable within a certain time threshold by foot or road at local speed.	*Data usage:* ibid.
Access to mobile communication	*Heuristic:* At least one cell tower must be located within coverage range.	*Data usage:* ibid.
Access to roads	*Heuristic:* Road section must be located within a certain distance threshold, depending on the road type.	*Data usage:* ibid.

4.4.2 Computing Infrastructure Damages from Floods and Tropical Cyclones

Impact computations were performed within the core modules of the CLIMADA risk assessment platform (Aznar-Siguan and Bresch 2019; Bresch and Aznar-Siguan 2021), which computes event-based damages according to the IPCC's risk definition as a convolution of hazard, exposure and vulnerability. CLIMADA is a spatially explicit, globally consistent open-source and open-access tool, and has been used in numerous risk assessment and climate adaptation studies (e.g. Ciullo, Strobl, et al. 2023; Lüthi et al. 2021; Meiler, Vogt, et al. 2022).

Hazard Data. Tropical cyclone wind fields were retrieved from the public CLIMADA data API at a 150 arcsec resolution, which are pre-computed based on IBTrACS track records (Knapp, H. J. Diamond, et al. 2018; Knapp, Kruk, et al. 2010) and the wind field computation algorithm by Holland (2008), for all events between January 1, 1980 and December 31, 2020 making landfall in the selected study regions. Events without any wind speed records above 30m/s were dropped. Flood extent data was obtained from the Global Flood Database (Tellman et al. 2021). 913 original events between 2002 and 2018 were downloaded and post-processed to regional hazard files. Minor events with fewer than 10 flooded grid cells a region area were dropped from the analysis. Number of event records hence obtained per region and hazard type is provided in the region overview of Table S4 (Supplementary SM3.1).

Exposure Data. Exposure refers to the assets and people potentially at risk, and their value. In this case, geospatial data of all previously obtained infrastructure systems were stored as *CLIMADA Exposure* objects. Since CLIMADA operates based on points (centroids), line-, raster- and polygon-based data (e.g. roads, large buildings and population grids) were interpolated to 500m resolution. Population centroids were valuated at their respective people count, and infrastructures at their segment length (500m) or area, respectively.

Vulnerability Data. Impact functions (fragility curves) which relate hazard intensities to structural damage fractions were obtained from literature review for all relevant combinations of infrastructure components and hazards. An overview is given in Supplementary SM3.1, section S3. Curves were stored as *CLIMADA ImpactFunc* objects.

Structural Damage Computations. Impact computations were performed for all exposures and events, returning structural damage fractions per infrastructure component and natural hazard event, stored as *CLIMADA Impact* objects. Impacts for interpolated objects were re-aggregated to their original shapes.

4.4.3 Computing Damage-induced Infrastructure Failure Cascades and Service Disruptions

After performing impact computations, resulting infrastructure damages were evaluated against pre-defined functionality thresholds, beyond which the components were defined to be dysfunctional. Those thresholds are difficult to quantify as no consensus exists in literature, yet were generally set at 50% structural damage. Functionality states of the infrastructure components were hence inserted into the interdependent infrastructure network model described above, initiating failure cascades along dependency edges throughout the multi-layered graph. This failure propagation was continued until obtaining a steady-state with regards to functionality states of all graph elements, after which service access states were re-evaluated for the population elements according to the specified access rules.

For each event and study region, structural damage fractions for all exposed infrastructures, infrastructure functionality states as well as access statistics to all basic service types for population clusters were hence computed and stored.

4.4.4 Analysing Regional Risk Patterns, Risk Drivers and Resilience Metrics

Event-based, region-wise analysis. Region-wise event statistics were analysed with respect to tendencies and correlations between spatial hazard event magnitudes (directly exposed populations), damage extents of infras-

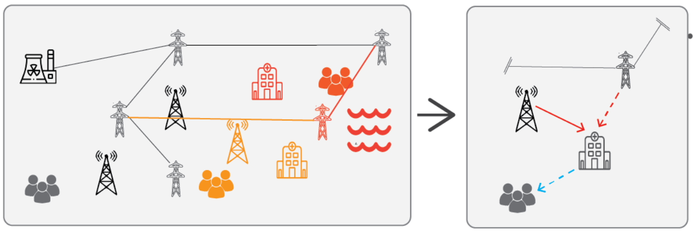

Figure 4.9: Physical damage computations on the infrastructure layer are introduced into the network model, which hence propagates functional failures along system interdependencies in the abstracted graph. Service access disruptions are computed analogously, as population clusters form part of the graph.

tructures, and service disruption magnitudes, according to service type and hazard type. Rank statistics of structural impacts and service impacts were computed, and contrasted. Regions where rank statistics were poorly correlated or had remarkable outliers were analysed further.

Resilience metrics definitions. To investigate the correlation between static region characteristics (such as income class, infrastructure density, etc.) and disruption dynamics, event-based cascade metrics were defined and aggregated, and hence examined for their explanatory power.

$$RF_S = \frac{P_{\not S}(t)}{P_S^X(t_0)}, SF_S = \frac{P_{\not S}(t)}{P_{\not S}^X(t)}$$

Resilience factor for service S (RF_S), Spatial cascade factor (SF_S), total population (P), population with access to service S (P_S), population without access to service S ($P_{\not S}$), directly hit area (X), post-disaster (t), pre-disaster (t_0).

The *resilience factor (RF)* captures overall levels of containment (or spread) of service disruption impacts. Values > 1 (service disruption impacts are larger than the number of people served within the directly hit area before the event) indicate cascading effects, values < 1 indicate resilience effects (less people observed disruptions than were directly hit by a hazard and previously had access to a service in that directly affected region). The *spatial cascade factor (SF)* focuses on the spatial containment aspect of the impacts, i.e. whether those impacts which occurred, occurred outside the area directly hit (values above 1), or whether they were all within the affected area.

Inference of failure mechanisms. Failure mechanisms for service disruptions were inferred from the graph-based information stored after service disruption computations; for all population nodes where a service-state was marked as disrupted, the service-providing nodes were checked for their internal damage state and total functional state, implying either direct damage, failure cascades or road-access to be the cause of disruption.

Deriving a service resilience-focused adaptation framework. Median RF-values for healthcare disruptions in tropical cyclone-affected study regions were grouped into quartiles (service resilience axis); population-weighted shares of indirect failure mechanisms leading to healthcare disruptions (i.e., failure cascades and physical access restrictions) were grouped into quartiles (indirect failure contribution axis). Baseline access rates to healthcare services were grouped into quartiles (size of markers).

Acknowledgements

The authors would like to thank Prof. Giovanni Sansavini (ETH Zürich) for his vital suggestions during conceptualization of this study, and for proof-reading of the manuscript, which greatly added to the quality of this research. The authors also thank Emanuel Schmid (ETH Zürich) for the generous technical support.

This project received funding from the European Union's Horizon 2020 Research and Innovation Program (grant agreement No 101003687). Elco Koks received funding from the Dutch Research Council (NWO), Grant No. VI.Veni.194.033.

Data Availability

All employed data are publicly available as mentioned in the manuscript. The CLIMADA platform is accessible under `https://github.com/CLIMADA-project`. Scripts to reproduce results and

figures can be found at
`https://github.com/Evelyn-M/gobal-service-disruptions`.

CHAPTER 5

Supporting robust and climate-sensitive adaptation strategies for infrastructure networks: A multi-hazard case study on Mozambique's healthcare sector

Evelyn Mühlhofer, Zélie Stalhandske, Margherita Sarcinella, Julius Schlumberger, David N. Bresch, Elco E. Koks; published in *Proceedings of the 14th International Conference on Applications of Statistics and Probability in Civil Engineering (ICASP14)*

Abstract. As climate change causes more intense and frequent natural hazard events, decision makers are tasked to climate-proof vital infrastructure systems against these challenges. Adaptation studies often evaluate benefits of different options in face of single types of natural hazards, and on their damage aversion potential to individual infrastructure components. In a proof of concept, we use the healthcare sector in Mozambique, which is highly affected by tropical cyclone winds and concurrent flooding, to showcase how packages of adaptation measures may be evaluated in their effectiveness on a systemic level, to mitigate basic service disruptions from multiple hazards, across various interdependent infrastructure networks. Using the open-source risk modeling platform CLIMADA on 2019's tropical cyclone Idai, we simulate five stylized adaptation strategies and their effects in reducing direct damages from wind and flooding to roads, power lines and healthcare facilities, their overall aversion of people's healthcare access losses, and synergies or trade-offs with other basic service supplies. ...

ctnd. Results illustrate the importance of considering multi-hazard phenomena and interdependencies between infrastructure systems in adaptation appraisals. We further provide an outlook on how to integrate probabilistic and climate-scenario driven hazard modeling into robust adaptation planning.

5.1 Introduction

Mozambique is among the countries most affected by weather extremes, and in 2019 suffered from two category 4 tropical cyclones (TC) Idai and Kenneth. Healthcare facilities were strongly damaged by wind and flooding and access was further hindered due to interrupted roads (Petricola et al. 2022). Since critical infrastructure components are usually embedded in a network of supporting infrastructure systems, structural damages can have unexpected and significant cascading impacts on the service levels provided by these infrastructures, as studies have shown in several countries on the African continent (Hallegatte et al. 2019). Despite this, healthcare infrastructures, their exposure to natural hazards, and their dependence on other critical infrastructure, have long been under-researched. This is in spite of the fact that resilient healthcare infrastructure is a critical component in achieving many health-related sustainable development goals (e.g. SDG indicators 1.4.1 and 3 Thacker, Adshead, et al. 2019), and that reducing damages to critical infrastructures and avoiding disruptions to basic services in general, is also a key goal of the Sendai Framework for Disaster Risk Reduction (UNDRR 2015). Adaptation strategies towards resilient infrastructure are shown to have multiple co-benefits, making them cost-effective in many cases (Hallegatte et al. 2019). To create robust adaptation strategies, it is however necessary to consider the effects and trade-offs on the entire interdependent infrastructure system and the service levels they maintain, as well as their effectiveness in mitigating threats from multiple hazard types.

While some studies have assessed the structural impacts caused by tropical cyclones on healthcare facilities (Deltares 2021), few have considered the potential for indirect impacts to lead to cascading failures (Petricola et al.

2022). Additionally, previous adaptation studies focused on the costs and benefits of different measures, yet only for mitigating structural impacts, neglecting the synergies and trade-offs across infrastructure systems. Furthermore, it is common for adaptation studies to look at single hazards, without accounting for the influence of compound events or sub-hazards (cf. Eilander, Couasnon, Sperna Weiland, et al. (2022) for a rare counter-example).

In this study on 2019's tropical cyclone Idai in Mozambique, we provide a proof-of-concept on how to simulate wind and flood-induced disruptions to the healthcare infrastructure, due to direct impacts and due to cascading failures from supporting infrastructure systems, taking on a service-level centered, multi-hazard perspective. We explore the mitigation potential of a set of stylized structural and system-changing adaptation measures aimed at reducing healthcare access disruptions. We discuss how to refine this end-to-end, generically applicable framework, which is based on open-source software and data. Finally, we provide insights on the challenges and ways forward for incorporating probabilistic event scenarios and climate change signals into more robust and systemic adaptation strategy planning.

5.2 Methods and Data

5.2.1 Risk Modeling Framework

The open-source and -access software CLIMADA is a globally consistent and spatially explicit tool to assess the risks of natural hazards and to support the appraisal of adaptation options (Bresch and Aznar-Siguan 2021). Its event-based modeling approach allows for a fully probabilistic risk assessment based on the IPCC risk definition as a function of hazard, exposure and vulnerability.

'Hazard' is a spatial representation of an intensity measure for the respective physical event. In this study, track data of Tropical Cyclone Idai was obtained from IBTrACS and wind fields were computed over Mozambique using CLIMADA's *TropCyclone* module based on the wind-field algorithm of Holland (2008) at a resolution of 150 arcsec. The flood footprint of the event, including the contributions from storm surge as well as fluvial

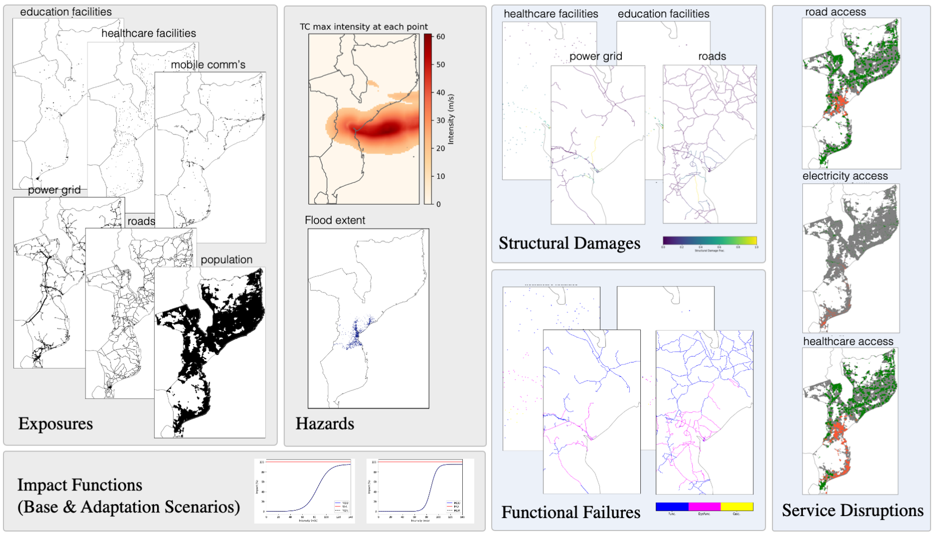

Figure 5.1: Schematic of the computation chain within CLIMADA. Gray - inputs to the systemic risk assessment and adaptation appraisal for Mozambique's healthcare sector, including six infrastructure and population exposure layers, flood and wind hazards from TC Idai, and various adaptation option parametrizations. Light blue - outputs metrics are structural damages to infrastructure components, functional infrastructure failures, and spatially explicit patterns service disruptions to the Mozambican population.

and pluvial flooding, was modeled based on Sentinel-1 SAR imagery. An automated-threshold classification (Otsu 1979) was applied to retrieve a binary surface water extent (flooded or not flooded) at a resolution of 10m. Hazard footprints are displayed in Fig. 5.1, left.

'Exposure' represents the geo-located critical infrastructures at component level which are potentially at risk, and their associated value (see Fig. 5.1, left). Data was obtained from OpenStreetMap for healthcare facilities, main roads, power plants, cell towers and school facilities. High and medium voltage power lines were obtained from the gridfinder project (Arderne et al. 2020); cell towers from an OpenCellID based rasterized map from the World Bank open data platform. Power towers were inferred and substation-locations were inferred along power lines. Gridded population count data was obtained from the WorldPop project (Center for International Earth Science Information Network (CIESIN), Columbia University 2017).

'Vulnerability' is a hazard- and infrastructure component specific function, relating hazard intensity to the degree of expectable structural damage. Vulnerability curves were obtained from literature for wind stress impacts on roads, power lines, power towers, cell towers, healthcare facilities and schools. Vulnerability curves for flood are constructed as binary step functions (damaged when flooded), and were applied to roads, substations, healthcare facilities and schools. Power plants are not designed to fail and hence not modeled as susceptible to either hazard.

The product thereof, ‘direct risk’ or ‘impact’, is measured in terms of the structural damages incurred by the infrastructure components. Direct impacts were computed for all exposures under three base scenarios (referring to the settings without adaptation assumptions): two single-hazard events, i.e. only flood and only wind, and one compound hazard event, where impacts from both flood and wind were summed on each exposure and capped at 100% of the respective values.

5.2.2 Failure Cascades and Service Disruptions Module

Indirect impacts - functional failures of infrastructure systems, failure cascades, and basic service disruptions - were computed using an interdependent infrastructure network model (Mühlhofer, Koks, Kropf, et al. 2023). The graph-based approach transforms spatial data of above-mentioned infrastructures and population clusters into directed edges and nodes. A set of rule-based and data-supported heuristics infer functional dependency links between components of different infrastructure systems, and service provision links between end-users and infrastructures. Qualitative examples of these link types and their generation approach are given below.

Functional infrastructure dependences

- **power supply** - A targeted edge is placed from the nearest substation node to hospital and school nodes. Functionality is upheld if the power grid runs at 60% or more of its normal capacity, else the dependent nodes fail. Not applicable to major hospitals (we assume generators to be available).

Service access dependences

- **access to healthcare** - Targeted edges are placed from healthcare facility nodes to population cluster nodes if they are reachable via functioning roads within one hour of driving at average speed, or if they are reachable by walking as the crow flies, at terrain-dependent speed, for less than one hour. Healthcare access is disrupted if no functioning facility is accessible according to those rules.

- **access to mobile communication** - Targeted edges are placed from cell tower nodes to population cluster nodes if they are located within a distance representative of typical rural cell site ranges. The service is disrupted if no single functioning link remains.

Structural damages from the previous risk computation stage introduce disruptions into the interdependent network, which may hence lead to functional infrastructure component failures upon surpassing design thresholds, which can cascade further across the systems along dependency links, leading to eventual service disruptions at population nodes.

5.2.3 Adaptation Appraisal

Adaptation measure packages for the healthcare sector were conceptualized in two categories: Structural adaptation measures (SAMs), reinforcing existing infrastructure components to withstand higher hazard intensities; and network adaptation measures (NAMs), reconfiguring the topology of the interdependent infrastructure network. Five different packages were parameterized.

Structural Adaptation Measures (SAMs)

- **SAM1** - Wind-and flood proofing of healthcare facilities (through roof-reinforcements and flood protections). This package acts only on the healthcare infrastructure itself, and is parametrized by shifting healthcare impact functions for flood and wind towards higher intensities in the Sofala province.

- **SAM2** - Flood proofing of primary and secondary roads, hardening of power infrastructure. This package acts only on supporting infrastructures, and is parametrized by shifting road, power line, power tower and substation impact functions for flood and wind towards higher intensities in the Sofala province.

- **SAM3** - Combination of SAM1 and SAM2, at a financial trade-off of implementing both measures only on half of the infrastructures in the Sofala province. Components receiving this measure were randomly sampled.

Network adaptation measures (NAMs)

- **NAM1** - Increasing primary healthcare facility density by 50% across the Sofala region. Six geo-located points were randomly sampled within the Sofala province to mimic newly constructed facilities.

- **NAM2** - Ramping up of generator capacities for all types of healthcare facilities within the Sofala province. This was implemented by removing the power dependence heuristic in the region.

To evaluate the effect of SAMs, structural impact calculations were performed with adjusted impact functions, and resulting failure cascades and service disruptions were re-computed on the interdependent infrastructure network as explained above. To evaluate the effect of NAMs, new interdependent infrastructure networks were computed, as these measures changed the topology of the initial graph, by introducing new network nodes (additional healthcare facilities) and by modifying dependency links. Direct impacts and cascades were simulated accordingly. All adaptation measure packages were evaluated under all three hazard scenarios (TC wind only, flood only and compound wind-and-flooding).

5.3 Results

5.3.1 Structural Damages and Service Disruptions

Fig. 5.2 shows simulation results for numbers of people experiencing basic service disruptions under non-adapted ("initial") conditions, per hazard scenario. It is evident that wind-induced disruptions are the dominant cause for most types of experienced service disruptions (apart from access to mobility), and that service disruptions tend to spread well beyond areas which are directly (physically) affected by hazard impacts, cf. dashed lines for reference.

Further, certain services are comparatively more prone to be disrupted by flooding than by winds, and vice-versa (cf. mobility and power, which are most and least affected depending on the sub-hazard). Lastly, the compound impact scenario reveals that sub-hazard impacts at the service level are not simply additive, but show escalating as well as redundant effects.

Fig. 5.3 explores these dynamics for healthcare disruptions in more detail: For each population cluster, the failure-causing hazard scenario is marked. While some clusters experience disruptions due to either wind or flooding (orange and blue, resp.), others experience disruptions in both scenarios (pink, 'TC & FL'). Interestingly, some clusters only suffer from service disruptions in the compound hazard scenario (yellow, 'TCFL'), i.e. the interdependent system only fails to deliver services under joint impacts of both sub-hazards.

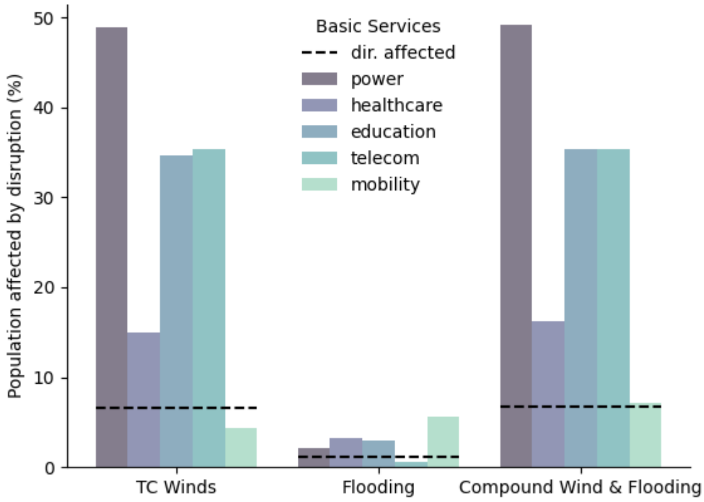

Figure 5.2: Share of Mozambique's population affected by service disruptions, depending on the sub-hazards considered. Share of directly affected population marked in dashed lines for reference. Wind-induced disruptions dominate in magnitude over flood-induced disruptions, yet are not fully additive under a compound-event scenario.

5.3.2 Evaluating Adaptation Measure Packages

Fig. 5.4 shows the effectiveness in reducing the number of people experiencing healthcare access disruptions according to measure and hazard scenario. Large differences are evident depending on which (sub-)hazard is considered: While package SAM2 (flood-proofing of roads and hardening of power in-

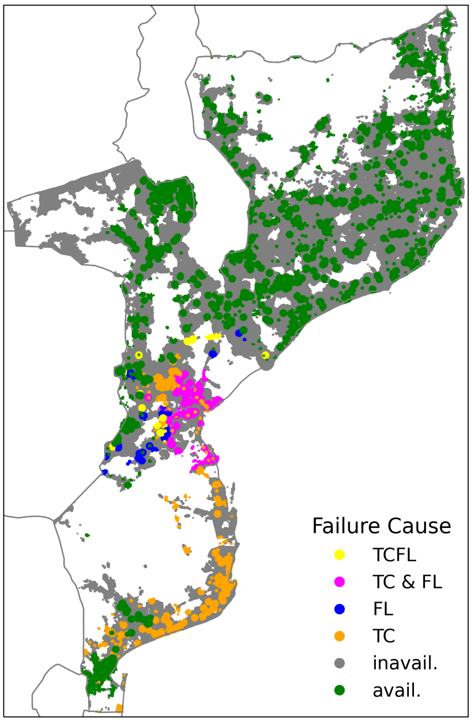

Figure 5.3: Population clusters experiencing healthcare access disruptions, according to responsible (sub-)hazard scenario which causes the failure. TC & FL refers to each sub-hazard independently causing access disruptions, whereas TCFL refers to the scenario in which only joint occurrence is significant enough to cause disruptions. avail. refers to undisrupted population clusters, inavail. to clusters which never had access to the service

frastructure), for instance, works well in reducing flood-induced healthcare disruptions by reducing road access disruptions, it is the least effective one to mitigate wind-induced disruptions. Addition of more healthcare facilities (NAM1) proved futile without any further structural or systemic resilience-enhancing measures, as half of these facilities were directly damaged, while access ways were blocked to the remaining ones. Removing minor healthcare facilities' dependence on the main power grid (NAM2), in contrast, consistently showed positive effects. Yet, all measures decrease in effectiveness when considering the 'real' compound wind & flooding event as opposed to single sub-hazard scenarios.

Fig. 5.5 demonstrates that some measures may feature substantial co-benefits in reducing other basic service disruptions (cf. SAM2 and SAM3, which have positive impacts on electricity and mobility). Lastly, the difference in aversion extents between Fig. 5.5 a) (structural damages) and Fig. 5.5 b) (service disruptions) highlight that, while adaptation measures may substantially reduce physical damages, this may not translate linearly into resilience at the service provision level. The opposite holds for network-based adaptation measures (NAMs), which have the potential to avert service disruptions, but do not reduce any physical damages.

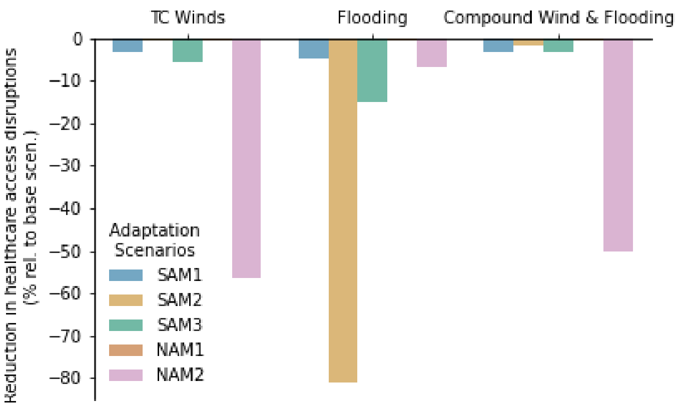

Figure 5.4: Reduction of healthcare access disruptions through implementation of structural adaptation measures (SAM1-3) and network adaptation measures (NAM 1 & 2), compared to a no-adaptation scenario, under different (sub-)hazard scenarios.

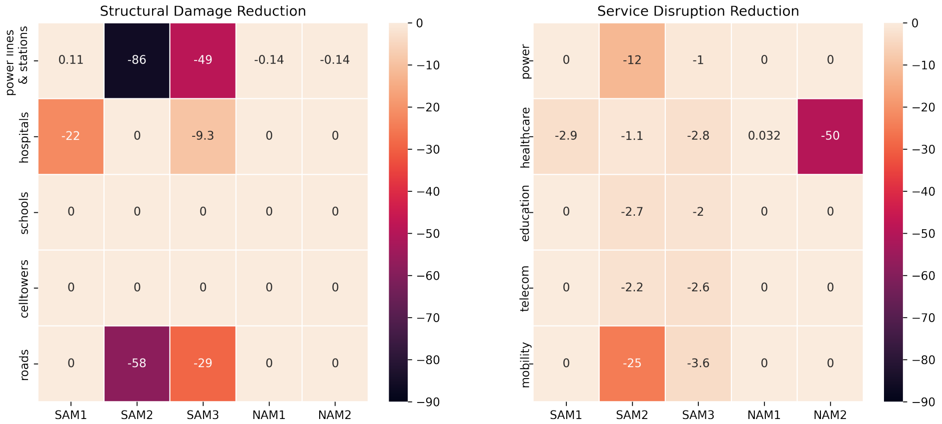

Figure 5.5: a) Co-benefits of the implementation of structural adaptation measure packages (SAM1-3), under the compound wind and flooding scenario: reduction of structural damages (%) to critical infrastructure components across Mozambique, compared to the no-adaptation scenario. b) - Co-benefits of the implementation of structural adaptation measure packages (SAM1-3), under the compound wind and flooding scenario: reduction of other basic service disruptions across Mozambique's population (%) compared to the no-adaptation scenario. SAM2 has most co-benefits, yet is not the most effective one in mitigating healthcare disruptions (cf. Fig. 5.4)

5.4 Discussion

This study provides us with some key insights in the modelling of systematic impacts of extreme events, based on the example of TC Idai in Mozambique. First, we find that most direct and indirect damages can be attributed to wind. However, some geographic areas are only affected by infrastructure failure when considering flood, and others only when considering the compounding effect of flood and wind. This demonstrates the importance of considering sub-hazards. Second, we find that system interdependences may lead to a different impact footprint of the event, with people losing access to healthcare infrastructure even in areas where no direct damage is observed. Third, we find that adaptation measures fare differently in mitigating direct and systemic (service-level) impacts. To protect the access to healthcare services, reducing facilities' dependence on the power system through generators seems to bring more benefits than flood and wind-proofing healthcare facilities, though latter fares better in reducing structural damages.

While interesting and unexpected dynamics can already be observed in this modeling prototype, three essential steps are required to make this framework suitable for robust decision-making: (1) Verifying the model assumptions and heuristics, (2) assessing the impacts of more events that better span the possibility space of current and future climate regimes and (3) considering the length of the disruption in the modelling.

As the results of this study are highly dependent on the heuristics used in the modelling, the first step would be to verify those. For example, we assume that smaller healthcare facilities do not have generators, which results in large disruption due to power failures. Reviewing event reports would allow us to compare modeled and observed impacts, and reverse-engineer some of the heuristics. Yet, while damage reporting on various infrastructure sectors was exceptional in the particular case of TC Idai (cf. Mutasa 2022; Williamson et al. 2023; Zimba et al. 2020), under- and non-reported impact dimensions, and impacts in remote locations, are difficult to verify. Consultations with stakeholders who have experienced the event, or the reconstruction phase would be crucial to verify and adapt some of the less observable modeling assumptions (Zischg et al. 2021).

The second step involves moving from analyzing one historical event to considering probabilistic event sets driven by different climatic conditions. Several methodologies allow for the creation of synthetic tracks for current or future climate. The TC module in CLIMADA creates a chosen number of tracks from historical tracks by applying a direct random-walk process to those and simulating future climates by modifying frequencies and intensities (Bresch and Aznar-Siguan 2021). Alternatively, the fully statistical STORM model can also provide present and future tracks (Bloemendaal, Haigh, et al. 2020). However, as demonstrated in the results for TC Idai, this is not sufficient to assess infrastructure risk, as a significant portion of people losing access to healthcare can be explained by flooding. A globally applicable framework has recently been developed to simulate storm compounds surge and river flood caused by a specific storm, using a local high-resolution 2D hydrodynamic flood model (Eilander, Couasnon, Leijnse, et al. 2022).

Finally, the time duration of the (partial) disruptions should be considered, as people may for instance temporarily lose access to healthcare facilities due to flooding of roads, yet experience longer lasting restrictions from destroyed facilities.

5.5 Conclusion

In this study, we examined the impacts of a compound wind and flood event (TC Idai) on critical infrastructure components (roads, power grid, healthcare facilities and schools), system functionality, and service provision levels in Mozambique. We highlighted the importance of considering all relevant sub-hazards of a disaster, as well as system interdependencies, to capture the potential for cross-system failure cascades and differential vulnerability patterns. Focusing on improving resilience of the healthcare sector, we evaluated several structural and network-changing adaptation measure packages in their effectiveness to reduce physical infrastructure damages as well as the number of people who experience service disruptions.

Results indicate that some measures may have substantial co-benefits in terms of reducing other service disruptions, yet that often, structural damage aversions fall short of translating linearly into service disruption aversion. We discussed pitfalls of our stylized proof of concept, and laid out an agenda to use the presented open-source model for probabilistic and hence more comprehensive adaptation measure appraisals which are capable of integrating climate change signals to support the development of robust adaptation strategies.

CHAPTER 6

Conclusion

6.1 Synthesis

This research aimed to better understand risk and resilience of basic services, as they are exposed to natural hazards and embedded in complex socio-technical constructs of interdependent critical infrastructures and people.

This aim was approached through what may conceptually be split into three stages: *Making the system, breaking the system* and *fixing the system*[1]. 'Making' an adequate system representation required conceptual work to understand how natural, technical and social systems interact, and technical work to translate this rich understanding into a simpler, transferable model which nonetheless retains spatial explicitness and some contextual knowledge, balancing computational and representational demands (RQ1; section 6.1.1). 'Breaking' the system, i.e., obtaining an understanding of service disruption risks, required exposing these interdependent critical infrastructures to diverse natural hazards, allowing to study how physical impacts are propagated through multi-layered networks systems to their end-users (RQ2; section 6.1.2). 'Fixing' the system, abstractly, demanded a better understanding of the variables which contribute to services in some systems withstanding disruptions better than in others, and concretely, was explored along the disruption mitigation potential of specific local adaptation measures; both perspectives must be regarded with caution on representational limits of and necessary extensions for just and equitable interventions (RQ3; section 6.1.3).

[1] Thanks to Dr. Raghav Pant (University of Oxford) for this useful problem framing suggestion.

6.1.1 Modelling societal consequences of natural hazard-induced infrastructure failure cascades

Interdependencies between assets of different infrastructure systems are ubiquitous and numerous, and failure cascades along these dependencies have empirical consequences on services; infrastructure dependencies on (electric) power, (cooling) water and information and communication technology are particularly pronounced (chapters 1 and SM1). To infer where interdependencies may exist between infrastructure networks on which this information is not readily available, generic heuristics were devised. These consist in a set of logical and geo-spatial rules which are based on infrastructure asset pairs identified from literature, distance constraints, redundancy constraints, physical access constraints, and capacity constraints (sections 3.2.1 and SM3.1). Basic service demands from end-users can be approximated using similar heuristics, but may be further constrained by socio-economic and regionally specific criteria (sections 3.2.4 and SM3.1).

The hence-developed modelling framework (chapter 3) captures people-centred consequences of natural hazard-induced infrastructure failure cascades, and is designed for interoperability, transferability and large geographic scales. Embedding a complex network-based infrastructure system model into the risk assessment platform CLIMADA allows for a single, streamlined and spatially explicit workflow from physically-informed natural hazard representations to basic service disruptions. Based on open-source code and data, and allowing user-defined, flexible inputs on infrastructures, hazards, dependencies and study regions, the modelling framework is readily transferable to diverse infrastructure systems, spatial scales and geographical regions. It further offers the versatility to calibrate and adjust parameters based on evidence (section 3.3.3). The choice of representing interdependent infrastructures as topological networks requires comparatively few technical specifications and heuristics, which is advantageous for the study of multiple large systems.

Problem design criteria, data, and information availability invariably influence the dynamics captured by the developed modelling framework: Translating physical infrastructure damages into infrastructure functionality, and lastly into end-users' service disruptions, is a cross-disciplinary venture between natural hazard risk modelling, engineering disciplines and social sciences. Breaking silos among disciplines requires conscious assumptions, simplifications and translations. The resulting compromise may not always cater to the (isolated) disciplines' state-of-the-art, but is indispensable. For instance, network-based approaches do not replace specialized system models for detailed local analyses and individual infrastructure system optimizations, but are a convenient means to reduce complexity. Similarly, reasons for which people do or do not seek healthcare and educational services may be multi-faceted and individual, but rule-based heuristics focusing on distance and facility availability provide a useful first estimate to model service access for entire countries.

Anecdotal case studies of individual events, drawing, among others, on print media accounts, typically focus on local to single-asset scales and people-centred impacts. This has proven a valuable complement to the generic modelling framework, as such insights allow to judge the *plausibility* of modelled heuristics, enriching this coarse-scale, mechanistic view[2].

Data and information scarcity are limiting factors in such a data-intense modelling approach. Advances in crowd-sourced data platforms such as OpenStreetMap have, nonetheless, proven valuable for high-resolution risk modelling (chapter 2). In a field where data protection is of great security concerns (Rinaldi et al. 2001), this is a common complication for researchers at the intersection of critical infrastructure and natural hazard modelling, as Supplementary SM5 shows: Lack of data has repercussions on the resolution, adequacy, communicability, and reproducibility of results. Systematizing a workflow, where commonly encountered stages in critical infrastructure network modelling of natural hazard impacts were classified, has helped to break down the data and information needs, can facilitate reaching out to potential providers of data, and has created a starting point for interacting with fellow academics through shared terminology in this relatively novel

[2]cf. a supervised thesis on healthcare impacts from Hurricane Irma (2017) in Florida (Wiher 2021) revealed that backup generators in hospitals may fail, justifying the modelled dependence of health facilities on the main power grid; similarly, surveys revealed that acceptable walking time to schools in Mozambique is up to six times as long as in Florida (USA), motivating flexible time thresholds to define access to certain services.

field.

Lastly, how much *must* be known of a problem before it can be modelled is deeply entangled with the purpose, societal context and ethical uncertainties involved in the consequences of the research output; for instance, an academic assessment of regional risk hot-spots may need to satisfy different standards in this regard than the planning of flood-protection measures of a provincial hospital.

6.1.2 Drivers of basic service risks and resilience to natural hazards

Economic wealth, physical damages, and exposed populations - core metrics of classic risk assessments - are insufficient for capturing the extent of service disruptions (section 4.2.3). Service impacts often spread beyond the physically affected area; disruptions frequently stem from failure cascades through system interdependencies rather than from direct damages, and resulting impact patterns are a complex interplay of hazard intensity, type, and location, network density, baseline access rates and service type (section 4.2.4). Wealthy and densely built-up regions tend to be less severely affected by service disruptions. However, rules of thumb do not sufficiently capture outlier events, which were omnipresent in all studied regions.

This incongruity between service disruptions and physical impacts makes a strong case for including more systemic risk assessment approaches into the concept of natural hazard risk modelling; the absence of simple, univariate predictors of service impacts further underscores the importance of considering systems in their contextual embedding, using spatially explicit exposure and hazard data.

Infrastructures and services are subjected to hazard-specific vulnerabilities, and dominant failure mechanisms strongly depend on the disruptive mechanism of the hazard: services reliant on road access are particularly vulnerable to floods, and power-dependent services are predominantly impacted by strong winds (section 4.2.4).

Resolving sub-hazards of an event, such as concurrent storm surge and pluvial flooding during a tropical cyclone, was shown as critical in estimating service impacts adequately: different infrastructure systems respond differently to the sub-hazards, and compound service disruption patterns do not always add up to the sum of their separate sub-hazard impacts, as infrastructure functionality thresholds or service access conditions may only jointly be surpassed (chapter 5).

A case study on whether spatially extensive, interdependent infrastructures may foster the occurrence of *connected events* (Raymond et al. 2020), tested on *spatially* compounding floods and tropical cyclones (SM4), showed that impacts do not necessarily escalate. However, as the occurrence of compound events - for instance, a devastating heatwave during tropical cyclone-induced power outages (a *temporally* compounding event, Feng et al. 2022) - are projected to become more frequent (Wu et al. 2022), the framework is adequate for further investigating the connection of events across the impact space, enhanced through (human-made) exposures.

For sufficiently long event records, service disruption impacts can be translated into risk metrics readily employed in risk management, such as expected annual fraction of population experiencing service disruptions or the disruption level associated with a 1-in-X year return period (section 4.2.5). Together with a quantification of the 'multiplier effect' (i.e., the service disruption spread, section 4.4.3) which can serve as a metric for service resilience, such aggregate figures allow for regional comparability and coarse screening of risk hot-spots with a service- and people-centred dimension.

However, as the developed network-based model allows to back-trace failure mechanisms on a per-event basis, this offers a richer understanding of the systemic drivers behind computed impacts. This caters to many scenario-based approaches, such as stress-testing procedures in tiered risk assessments (Linkov et al. 2018), climate story-lines (Shepherd et al. 2018) and downward counterfactual thinking, which promote in-depth investigations of single or few selective physically-consistent events to reveal "factors responsible for system failure, thus allowing the identification of robust decision options" (Ciullo, Martius, et al. 2021).

6.1.3 Understanding social vulnerabilities and adaptation potentials to basic service disruptions

Resilience-enhancing measures, and adaptation interventions in particular, are often cost-effective, but constrained resources require prioritization on the type of resilience which should be achieved, and where to implement options (Hallegatte et al. 2019; Trejo and Gardoni 2023). In this work, adaptation to natural hazards focused on high-level strategies from a basic service-perspective. Contrasting general service resilience, contribution of (indirect) failure cascades to service disruptions, and baseline service access rates across countries can inform a framework to prioritise actions: ranging between reinforcements of existing core and supporting infrastructures, management of dependencies and infrastructure network configurations, or the need for investing into more infrastructure (section 4.3.2).

Chapter 5 showed that adaptation strategies designed to reduce structural damages to infrastructure assets may not mitigate service disruptions, at least not to the same degree. Adaptation strategies which reduce service disruptions conversely may still incur substantial structural damages. Any strategy has the potential to feature substantial co-benefits on various services.

Adaptation asynergies (de Ruiter et al. 2021) may consequently be further amplified when considering not only structural, but also more systemic impact layers such as services protected (or disrupted). Service resilience-centred adaptation planning must cater to the interdependencies between infrastructures which deliver a service, bearing in mind the potentially differential vulnerabilities of supporting infrastructure systems. While high-level adaptation strategies derived from an interdependent infrastructure modelling approach can be useful to raise awareness on asynergies, and to shift the discourse from a purely structural to a service-oriented one, adaptation measures are implemented locally, and decision-making, depending on the ownership structure of the infrastructure sector (e.g., private or public), may effectively lie at individual sector or even single asset level (SM5). Constraints for systemic adaptation planning may hence not be solely knowledge-driven, but rather practically through sectoral silos and political aspects.

Adaptation strategies which reinforce the status quo may be far from equitable, as those left out of the system before will not experience any improvement afterwards; while obvious in theory, computing and mapping not only disruption potential, but also service access levels at baseline, allows to cover these blind spots (section 4.3.2). Even for those members of society covered by services, disruptions may have differential consequences depending on compounding social vulnerabilities. Adaptation strategies may want to include these in their devising. While not explicitly incorporated here, case studies have mirrored mainly what is already known from research on general social vulnerabilities: the elderly, the poor, those with medical needs and those without social and legal ties (e.g. (illegal) immigrants) are often most gravely impacted by the loss of services (Wiher 2021).

6.2 Implications of this research

Despite the aim of this work to bridge methods in classic natural hazard risk modelling and infrastructure systems modelling to derive basic service disruptions, there can be no one-stop-shop for the many conceivable problems and research questions at this intersection. The following paragraphs reflect upon a few of the fields to which this work may contribute in various manners.

Academia. This research adds knowledge to the academic literature on natural hazard-induced infrastructure risks, and also has contributed as an entry point for researchers in either risk modelling or engineering-related fields who seek to acquaint themselves with methods in the respective other field. Devising an interdisciplinary, conceptual framework can only approximate the complexity of the challenges which interdependent infrastructures pose, but similar approaches are gaining much traction as the increase in recent publications demonstrates (e.g., Brunner et al. 2024; Lan et al. 2023; Montoya-Rincon et al. 2023; Pittore et al. 2023).

Further, this work has greatly profited from the availability of open-source code and software, such as the CLIMADA project for facilitating direct risk computations, code for many general geo-spatial operations, network generation, simplification and data parsing. By equally providing much of the code developed in this research in an open-source, peer-reviewed and tested manner, within CLIMADA or as standalone OSM-flex, means that (network) risk studies can easily be performed on diverse exposure layers across the globe by fellow researchers, which is already done in various projects[3].

International donor funds & multilateral organisations. Large international donor funds, such as the Green Climate Fund (GCF) or the World Bank, fund infrastructure (adaptation) projects around the globe. Well-informed funding allocation decisions require screening at large geographic scales and for large portfolios. The global applicability and the focus on risk hot-spots of the developed approach may provide an apt tool which aligns with the needs for a relatively simple, yet systemic and coherent risk screening method[4]. Similarly, it aligns with Principle 1.4 of the Principles for Resilient Infrastructure (UNDRR 2023)[5].

Early warning & climate information services. Developing impact-based forecasts, i.e., shifting from forecasts and warnings about what the weather *will be* to what the weather *will do*, is currently of high priority in many National Hydrometeorological Services (Met Office et al. 2020). Many of the projects being developed under such premises revolve around impacts with an infrastructure dimension, such as the Met Office (UK) on wind and heavy precipitation on transportation (Hemingway and Robbins 2020), Météofrance (FR) on winter storms to power lines[6], the Bureau of Meteorology (AUS) on effects of East Coast Lows on built environment (Richter et al. 2018). While it is a matter of individual offices' decisions how

[3]cf. a global multi-hazard risk study on healthcare and education facilities, which finds that 48-93 % of buildings in all world regions are affected by at least one hazard (Ammann 2023)

[4]See, for instance, the implementation principles of the GCF result area on Infrastructure & Built Environment: "Deploy an infrastructure systems approach –a holistic approach reviewing investments that go beyond climate-proofing of assets by detecting potential for cascading failures affecting community resilience; Conduct climate risk assessments" (`https://www.greenclimate.fund/results/infrastructure-built-environment`, accessed 26.09.23)

[5]It recommends tiered stress-testing approaches using complex models which consider interdependent (sub-)systems and real (historic) hazards to generate knowledge on the performance of infrastructure systems and services under stress.

[6]cf. WIRE (winter risk for energy), `https://services.meteofrance.com/wire-prevision-de-neige-et-de-givre-sur-les-cables`, accessed 06.10.23

far on the systemic impact side such forecasts need to be, a flexible impact computation pipeline that can be user-tailored to the respective needs and data availability may add to this area of interest.

Humanitarian activities. Humanitarian organisations, such as the International Federation of Red Cross and Red Crescent Societies (IFRC), are moving towards anticipatory action, i.e., actions taken before a crisis hits (such as forecast-based financing, Coughlan de Perez et al. 2015). Those decisions are based on forecasts or predictions to prevent or reduce potential disaster impacts (IFRC 2022), and frequently rely on impact-based forecasts in collaboration with National Hydrometeorological Services, as discussed above. However, also in the aftermath of a disaster, it is crucial to rapidly estimate impacts on critical infrastructures. Currently, the IFRC Disaster Briefs[7] report on impacted critical infrastructure such as healthcare and educational facilities, roads, water and power utilities with varying degree of specificity, frequently based on surveys and remote sensing techniques. It does not automatically link to the number of people which might experience service disruption. A risk modelling approach on physical infrastructure damages and service disruptions may contribute such a first, rapidly available information layer.

[7] see the IFRC GO platform: `https://go.ifrc.org/`

6.3 Outlook for future research

A selection of ways forward, and of tangential, yet important research challenges are discussed in this loosely structured collection.

Time and timing. The generalized framework for infrastructure failure cascades presented in this work does not feature an explicit time component. However, recovery duration may greatly influence the severity of an event. In general, relations between structural damages and restoration times defy simple rules, owed to interdependencies and limited resources for reconstruction. Ample research has been conducted on restoration of services featuring network approaches (Fang and Sansavini 2019; González et al. 2016), albeit with similar gaps regarding scale and scope as discussed in section 1.3. It is further questionable whether network modelling is necessarily the most adequate tool to capture some of the crucial drivers of recovery (e.g. repair crew availability, institutional processes, funds, pre-emptive actions, community organisation, etc., Burkhardt 2022; Wiher 2021).

Equally, timing of the event may be crucial, as demand and supply patterns for services have daily, weekly, or seasonal cycles - such as power outages during heat waves in summer or cold waves in winter, transportation disruptions during morning commutes, or school interruptions during semester breaks. Whether such highly resolved and data-demanding time-awareness needs to be included in a globally applicable model or whether these consideration should rather be kept as pre-conditioning, situational awareness ('aggravating factors' in downward counterfactual thinking, Ciullo, Martius, et al. 2021) will depend on the final approach taken.

As infrastructures are built to last long time-spans of decades to centuries, the (co-)evolution of infrastructure degradation, population, and the built environment may be critical factors to bear in mind when thinking about risk and resilience in the future. While socio-economic and population projections (for instance, via via shared socio-economic pathways (SSPs), O'Neill, Kriegler, et al. 2014) are increasingly available also at sub-national resolutions (e.g. urbanisation trends, Merkens et al. 2016), projections for the built environment are scarce.

Social vulnerability and adaptation. Spatially resolved socio-economic population characteristics might improve predictions on baseline service access, as in this work, spatial distance to critical infrastructure assets served as the main proxy. While an important input factor into the computation chain for service disruption risk, it is a challenging task and area of research in itself (cf. Arderne et al. 2020; Mbungu et al. 2023, for power access).

Differentiating population exposure by socio-economic criteria can further elucidate if vulnerable people are disproportionately affected by the consequences of infrastructure failures, both in frequency and in severity. However, transitioning from differentiated exposures to differentiate vulnerabilities requires more research into variables contributing to coping capacities and resilience specifically for basic service disruptions (Cutter et al. 2006; Mitsova, Esnard, et al. 2018; Mitsova, Sapat, et al. 2020). Spatially explicit datasets on (potentially) relevant variables of vulnerability to basic service disruptions are scarce, and mostly confined to the United States (e.g. the SoVI, Cutter et al. (2003), or the CDC SVI[8]). The development of global datasets (e.g. the GlobE-SoVI, Reimann et al. 2023) may be a way forward, but urban inequality - an important locator of vulnerable people - is typically not resolved.

The importance of including social vulnerability variables for equitable (infrastructure) adaptation is generally recognized[9]. However, more work is required to include these equity considerations systematically, and to better connect them to current justice goals and policy discourses where policy-makers could access them as concrete planning support[10].

Probabilistic vs. scenario-based modelling for interdependent infrastructure risks. To quantify risk increments from climate change, and risk reduction from the implementation of adaptation measures, classical

[8] `https://www.atsdr.cdc.gov/placeandhealth/svi/data_documentation_download.html`, accessed 02.10.23

[9] Karakoc et al. (2020) investigate equitable restoration of infrastructure assets which are weighted according to importance determined from 8 variables of the SoVI; Montoya-Rincon et al. (2023) evaluate hurricane adaptation measures to the interdependent power and water system based on a social vulnerability index built on the CDC SVI

[10] A good discussion is provided in Lonergan, Suter, et al. (2023) specifically on justice in energy transitions, but many parallels can be drawn to the problem-setting presented here.

natural hazard risk modelling - and (re-)insurance practices - commonly apply probabilistic approaches, where impacts are computed over large numbers of hazard events, representing a 'satisfactory' range of future event realisations (Bresch and Aznar-Siguan 2021; Lonergan, Greco, et al. 2023). For a computationally expensive network model, as presented in this work, this currently pushes the limits of feasibility.

Aggravatingly, probabilistic event sets for compound, multi-hazard, or subhazards, which were shown to have significant impact on service disruption outcomes, are not yet available with sufficient geographic coverage and spatial resolution, despite considerable advances in this field (e.g., Claassen et al. 2023; Eilander, Couasnon, Sperna Weiland, et al. 2022).

Along a similar line, 'thorough' uncertainty and sensitivity quantification approaches often employ Markov Chain Monte Carlo methods which sample large numbers of parameter spaces. Despite mathematical frameworks being designed specifically for hierarchical interdependent networks (Sharma and Gardoni 2022), the ease of applicability and computational burden remains challenging.

It hence remains to be explored how scenario-based approaches can 'adequately' incorporate effects of climate change or adaptation in a non-probabilistic manner, as the probabilistic approach is no longer entirely suitable. While not yet entirely state-of-the-art in practice, scenario-based approaches may cater better to the intricacies of models designed for systemic risk and resilience, as they emphasise system performance in the face of a given challenge, and lend naturally to the exploration of particular system configurations where the data needed to conduct probabilistic assessments is sparse-to-unavailable (as, for instance, in mentioned context of multi-hazard threats) (Lonergan, Greco, et al. 2023).

Local knowledge and better data. As amply discussed, many of the current gaps are owed to a lack of data or information. A non-exhaustive list of items in which data scarcity is particularly pronounced, includes: identification and quantification of infrastructure dependencies, incomplete exposure data, simplistic damage-functionality relationships, lack of post-event validation data on infrastructure functionality and service levels. As a remedy, referring back to the conclusions in Supplementary SM5, more comprehensive impact data collection efforts beyond insured losses and fatalities, as driven, for instance, by the Sendai Monitor[11], data sharing platforms among critical infrastructure operators, and stakeholder interactions for information sharing - as a less problematic alternative to data sharing -, are conceivable future options, while maintaining good practices in sensitivity analyses, stocktaking of assumptions and, at least, anecdotal validations.

Modelling infrastructure system performance. The infrastructure model within the presented framework relies on a topological representation of infrastructure networks, i.e., on assets and their connections. This leads to a limited number of options for representing their functionality: mainly, internal functionality loss due to structural damages or functionality loss due to loss of supporting connections. Inclusion of flow models, representing physically informed metrics of supplies (sources), demands (sinks), and capacity constraints, or even bespoke system models, would allow to increase the granularity with which infrastructure system functionality is captured. The modular architecture of the framework allows for this incorporation, but most approaches would certainly not be feasible in a globally consistent manner.

[11] `https://sendaimonitor.undrr.org/`, accessed 06.10.23

6.4 Concluding remarks

This research took interdependent critical infrastructure networks as a lens to study how natural hazard risks are transmitted and escalate through systemic connections and 'indirect' layers of impacts. However, systems thinking approaches cater to many other phenomena in our environment, such as supply chains, ecosystems or migration flows.

In an interconnected world, problem solving strategies cannot be devised in silos - neither academically nor in practice. This is easier said than done, as connections are often far from obvious, and even once they have become salient, challenges lie in the readiness to compromise among methods and aims. Further, the obstacles encountered when intellectually motivating the need to act through large-scale, agnostic models, may differ vastly from the challenges encountered when practically deciding to act based on context-specific, local knowledge and real-world constraints. As both are needed, translational work between these worlds is a task that increasingly transdisciplinary projects may reconcile.

Lastly, while paradigms and problem frames are necessary preconditions for any (intellectual) activity, it is worth bearing in mind that

> *"[s]ometimes the best way to make an infrastructure resilient is not to build it."* (Hallegatte et al. 2019)

Supplementary Materials

SM1 Supplementary 1

Literature Review

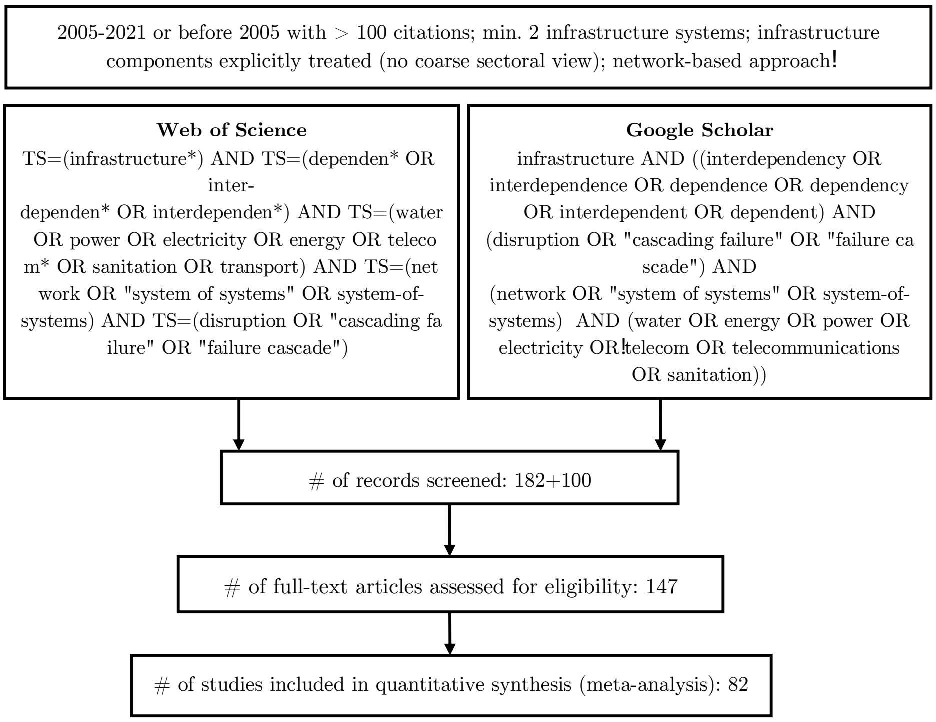

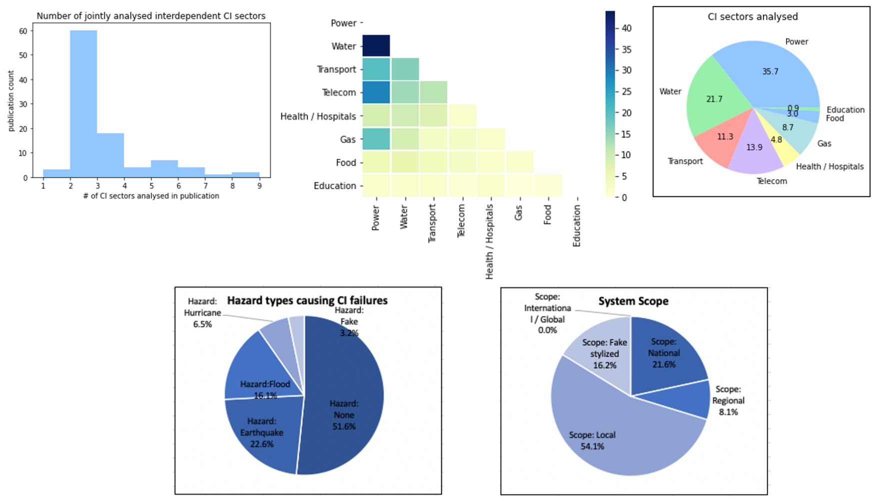

Figure SM1.1: Meta analysis of commonly analysed problems in research on network modelling approaches to natural hazard-induced impacts on interdependent critical infrastructures.

A collection of infrastructure dependencies

Table SM1.1: Dependencies between different infrastructure sectors (and components), as retrieved from an evidence research in literature.

source		**target**		**flow**
sector	**component**	**sector**	**component**	
electric power	substation	education	school	electricity
electric power	substation	emergency service	police	electricity
electric power	substation	food	retail	electricity
electric power	substation	food	distribution center	electricity
electric power	substation	gas	pumps	electricity
electric power	substation	gas	storage	electricity
electric power	substation	gas	SCADA	electricity
electric power	substation	gas	electric compressors	electricity

electric power	battery; backup generator	gas	n/a	electricity
electric power	battery; backup generator	healthcare	hospitals	electricity
electric power	substation	healthcare	hospitals	electricity
electric power	substation	oil	pumps	electricity
electric power	substation	oil	compressors	electricity
electric power	substation	oil	SCADA	electricity
electric power	substation	oil	storage	electricity
electric power	substation	oil	retail petrol stations	electricity
electric power	substation	telecom	fibre-optics backbone	electricity
electric power	substation	telecom	fixed lines	electricity
electric power	substation	telecom	mobile service network	electricity
electric power	substation	telecom	switches	electricity
electric power	substation	telecom	router	electricity
electric power	substation	telecom	fibre links	electricity
electric power	substation	telecom	switching office	electricity
electric power	substation	telecom	base station	electricity
electric power	substation	telecom	central office	electricity
electric power	battery; backup generator	telecom	both wired and wireless networks	electricity
electric power	substation	telecom	server	electricity
electric power	substation	telecom	cell tower	electricity
electric power	substation	telecom	transmitter	electricity
electric power	substation	transport	road	electricity
electric power	substation	transport	rail	electricity

electric power	substation	transport	rail	electricity
electric power	substation	transport	rail	electricity
electric power	substation	transport	airport	electricity
electric power	substation	waste water	plants	electricity
electric power	substation	waste water	pumps	electricity
electric power	substation	water supply	pumps	electricity
electric power	substation	water supply	SCADA	electricity
electric power	substation	water supply	treatment plants	electricity
electric power	substation	water supply	reservoirs	electricity
electric power	substation	water supply	controlling system	electricity
electric power	substation	water supply	pumps	electricity
electric power	battery; backup generator	water supply	wells and pump stations	electricity
natural gas	n/a	electric power	generator	natural gas
natural gas	pipeline	Electric power	gas-fired power plant	natural gas
natural gas	n/a	transport	rail	natural gas
oil	petrol backup supply	electric power	emergency generator	oil
oil	retail petrol stations	electric power	emergency vehicles	oil
oil	n/a	electric power	generator	oil
oil	retail petrol stations	healthcare	hospitals	fuel
oil	bulk petrol stations	oil	retail petrol stations	petrol
oil	petrol bulk supply	transport	ferry	petrol
oil	petrol bulk supply	transport	airport	petrol
oil	n/a	transport	rail	petrol

oil	retail petrol stations	transport	road	petrol
telecom	cell tower	electric power	generator SCADA	data
telecom	n/a	electric power	SCADA	data
telecom	router	electric power	substation SCADA	data
telecom	n/a	emergency service	Police	data
telecom	n/a	food	retail	data
telecom	n/a	gas	SCADA	data
telecom	n/a	healthcare	hospitals	data
telecom	n/a	healthcare	emergency vehicles	data
telecom	n/a	oil	SCADA	data
telecom	n/a	transport	rail	data
transport	air	electric power	transmission lines	data
transport	roads	electric power	employees	people (workers)
transport	roads	electric power	employees	people (repair crew)
transport	roads	electric power	n/a	physical components
transport	roads	electric power	emergency generator	oil, gas
transport	rail	electric power	employees	people (workers)
transport	rail	electric power	employees	people (repair crew)
transport	rail	electric power	n/a	physical components
transport	rail	electric power	emergency generator	oil, gas
transport	air	electric power	employees	people

transport	air	electric power	n/a	physical components
transport	rail	food	retail	groceries
transport	roads	food	retail	groceries
transport	rail	gas	n/a	train; gas
transport	roads	gas	n/a	truck; gas
transport	roads	gas	n/a	people (workers)
transport	roads	gas	n/a	people (repair crew)
transport	roads	healthcare	hospitals	people (patients)
transport	roads	healthcare	hospitals	medication
transport	roads	healthcare	emergency vehicles	emergency vehicles
transport	roads	healthcare	n/a	people (workers)
transport	roads	healthcare	n/a	people (repair crew)
transport	roads	natural gas	n/a	gas
transport	rail	natural gas	n/a	gas
transport	roads	oil	n/a	oil
transport	rail	oil	n/a	oil
transport	marine	oil	n/a	oil
transport	roads	oil	n/a	people (workers)
transport	roads	oil	n/a	people (repair crew)
transport	roads	port	n/a	people (workers)
transport	roads	power	power plant; substation	people (workers)
transport	roads	power	power plant; substation	people (repair crew)

transport	roads	solid waste	n/a	waste
transport	roads	solid waste	landfills	waste
transport	roads	solid waste	transfer station	waste
transport	roads	solid waste	n/a	people (workers)
transport	roads	solid waste	n/a	people (repair crew)
transport	roads	telecom	n/a	people (workers)
transport	roads	telecom	n/a	people (repair crew)
transport	roads	transport, air	airport	people (workers)
transport	roads	transport, air	airport	people (repair crew)
transport	roads	waste water	n/a	wastewater
transport	roads	waste water	plants	wastewater
transport	roads	water supply	n/a	people (workers)
transport	roads	water supply	n/a	people (repair crew)
waste water	n/a	healthcare	hospitals	wastewater
water supply	n/a	education	school	water
water supply	tanks, pumps	electric power	n/a	water
water supply	n/a	electric power	n/a	water
water supply	n/a	food	retail	
water supply	n/a	food	distribution center	water
water supply	backup supply	gas	vaporizers and fire suppression processes	water
water supply	pumping station	healthcare	hospitals	water

water supply	n/a	oil	n/a	water
water supply	tank	telecom	switching office	water
water supply	tank	telecom	central office	water
water supply	n/a	transport	rail	water

SM2 Supplementary 2

SM2.1 Infrastructure Dependencies

This file is provided in the online version of the manuscript, which can be retrieved at `https://ars.els-cdn.com/content/image/1-s2.0-S0951832023001096-mmc1.xlsx`. Table SM1.1 shows a simplified version.

SM2.2 Scenario parametrizatios and validation sources

Case study scenario parametrizations

i. Scenario Specifications ‘Higher and lower component vulnerabilities’

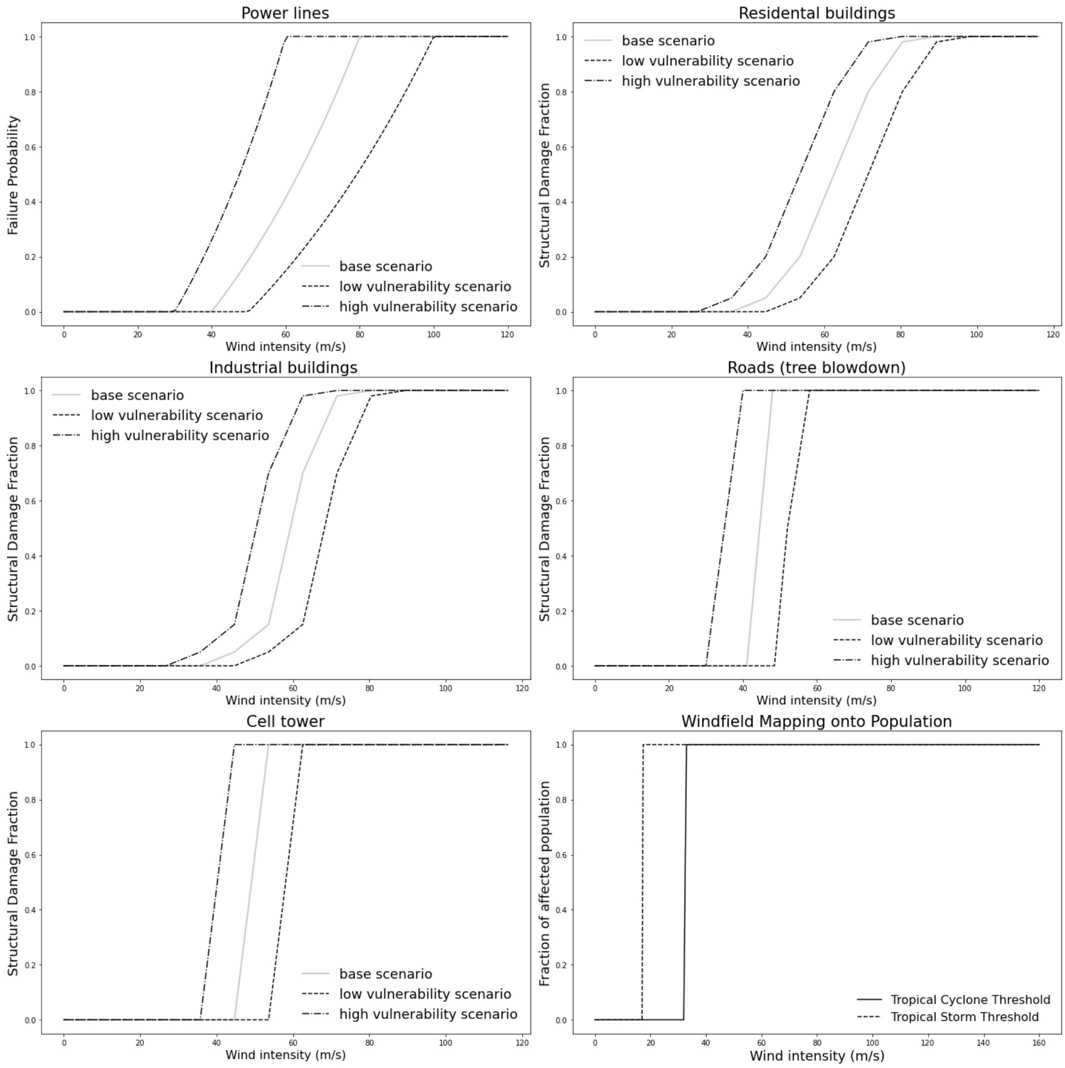

Figure1 Impact functions used for base case (grey, solid), low vulnerability scenario (black, dotted) and high vulnerability scenario (black, dashed). x-axes: hurricane wind strength (m/s), y-axes: failure probability (power lines), structural damage fraction (all other CIs).

ii. Scenario Specifications 'Damage-Functionality Thresholds'

Table 1 Threshold of structural component damage (averaged over length of section for edge-type CIs such as powerlines & roads), which leads to an assignment of internal functional level of 0.

Scenario	**Base**	**Low**	**High**
Threshold	0.05 (power lines) 0.5 (roads) 0.3 (all others)	0.01 (power lines) 0.3 (roads) 0.15 (all others)	0.1 (power lines) 0.7 (roads) 0.5 (all others)

iii. Scenario Specifications 'No CI interdependencies'

Table 2 Dependency conditions used in the scenario w/o inter-CI links.

Dep	**Source**	**Target**	**Redundancy**	**Road access**	**Dep. type**	**Flow type**	**FuncThresh**	**Dist. Thresh. [m]**
7	celltower	people	FALSE	FALSE	end user	logical	1	40000
8	education	people	TRUE	TRUE	end user	logical	1	40000
9	health	people	FALSE	TRUE	end user	logical	1	100000
10	power line	people	TRUE	FALSE	end user	physical	0.6	
11	road	people	FALSE	FALSE	end user	logical	1	30000
12	wastewater	people	TRUE	FALSE	end user	logical	1	

iv. Scenario Specifications 'Lower & higher distance thresholds

Table 3 Dependency conditions for scenario with modified parametrizations compared to base case (lower and higher distance thresholds).

Dep	**Source**	**Target**	**Redundancy**	**Road access**	**Dep. type**	**Flow type**	**Func. Thresh**	**Dist. Thresh. [m]**
1	power line	celltower	TRUE	FALSE	functional	physical	0.6	
2	power line	education	TRUE	FALSE	functional	physical	0.6	

3	waste water	education	TRUE	FALSE	functional	logical	1	
4	power line	health	TRUE	FALSE	functional	physical	0.6	
5	waste water	health	TRUE	FALSE	functional	logical	1	
6	power line	waste water	TRUE	FALSE	functional	physical	0.6	
7	celltower	people	FALSE	FALSE	end user	logical	1	40’000
8	education	people	TRUE	TRUE	end user	logical	1	25'000 / 40’000
9	health	people	FALSE	TRUE	end user	logical	1	70'000 / 130’000
10	power line	people	TRUE	FALSE	end user	physical	0.6	
11	road	people	FALSE	FALSE	end user	logical	1	30’000
12	waste water	people	TRUE	FALSE	end user	logical	1	

Case study validation material

The following paragraphs provide detailed information on the evidence used for validation of the case study results. Official government resources are available for power and telecommunication impacts, in all other cases print media accounts were considered. Search efforts focused both on retrieving information on infrastructure impacts (i.e. structural damages, outages, etc.) and basic service impacts (i.e. healthcare incidents, mobility impairment, etc.).

Structural damages to infrastructure components are only incidentally reported in newspapers and in the National Weather Service’s Post-Tropical Cyclone Report, for all studied sectors. Utility outages are documented on county-level for power and mobile communication by the respective government offices (Office of Cybersecurity, Energy Security, and Emergency Response and Federal Communications Commission), yet unavailable for the water and transport sectors. Hospital closures are documented, while school closures are less complete. People suffering from basic service disruptions can only be inferred indirectly for power and mobile communications based on outage statistics, and are anecdotally reported in newspaper articles for all other services, such as communities being supplied by freshwater tanks or being cut off due to collapsed roadways.

Healthcare facilities impacted and incidents related to inaccessibility of emergency services & healthcare

Universal Health Services' Emerald Coast Behavioral Hospital, Fort Walton Beach; Encompass Health Rehabilitation Hospital, Panama City; George E. Weems Memorial Hospital in Apalachicola; Bay Medical Sacred Heart in Panama City; Calhoun Liberty Hospital in Blountstown; Gulf Coast Regional Medical Center in Panama City; Jackson Hospital in Marianna; Sacred Heart Hospital on the Gulf in Port St. Joe; HCA Healthcare's Gulf Coast Regional Medical Center (Retrieved from

https://www.modernhealthcare.com/article/20181012/NEWS/181019944/eight-hospitals-evacuate-patients-in-wake-of-hurricane-michael ,
https://www.medscape.com/viewarticle/903327, last accessed: 08. Feb '22)

- Springfield: "When is anybody coming to do something?" said Trenisa Smith, 48, a school bus driver in Springfield who had been giving herself insulin treatments in the back of her car.
- Gadsden County: Another was found unresponsive by family members during the storm. They called 911 but were told no one could respond. 3. Charles Ash Sr., 71. Unable to receive dialysis treatment due to the storm.
- Liberty county: 4. Man, 78. Complained of chest pain/shortness of breath during the storm. EMS was unable to respond. Pronounced dead at scene several hours later.
- Bay county: 12. Timothy Clark, 64. Working in yard after storm, collapsed, EMS unable to respond.13. Robert Whitney, 43. After onset of strong winds from storm. Working in yard to secure property, collapsed, EMS unable to respond. 15. Jose Golazo, 52. Complicated medical history, unable to access dialysis due to power outage/ transportation. 16. Judith Cooley, 79. Hospice; complicated medical history which required use of powered devices, no power, no generator. 17. James Stukey, 81. Hospice; complicated medical history which required use of powered devices, no power, no generator. 21. Paul Gilday, 77. Extensive natural disease, found deceased in home after storm, no power. 25. Kurt Bennett, 67. Medical conditions which required use of powered respiratory devices, no power. 28. Dorothy Lawrence, 94. Natural disease, no power, home health less accessible.

Retrieved from https://www.nytimes.com/2018/10/12/us/hurricane-michael-live-updates-florida.html, https://eu.tallahassee.com/story/news/2018/11/29/43-and-counting-deconstructing-death-toll-hurricane-michael/2124902002/, last accessed: 08. Feb '22

Power outages

Retrieved from Hurricane Michael Situation Reports,
https://www.energy.gov/ceser/downloads/hurricane-michael-situation-reports-october-2018 ,
last accessed 08. Mar '22.
County-wise outage statistics are only graphically available, see Figure 2, detailed numbers are reported on a state-basis as displayed in Table 4, from which validation numbers were taken.

Table 4 Number of affected people (col. 3) is estimated by multiplying population census data with % of affected customers (col. 1), since number of affected customers refers to subscribers, not people per household.

State	**% affected**	**# customers affected**	**Estimated # people affected**
Alabama	3.09%	87,706	150'000
Florida	3.68%	400,666	780'000
Georgia	6.44%	424,744	676'000

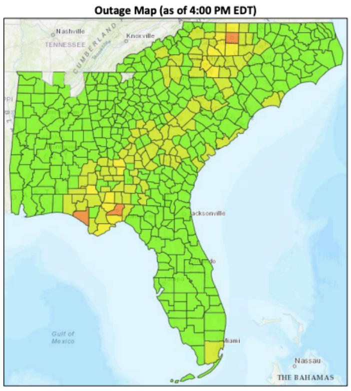

Figure 2 Outage map per county, from Hurricane Michael event summary # 4, for the afternoon of October 11, 2018

Telecommunication impacts

Fractions of cell sites out-of-service per county were reported in the Hurricane Michael Communications Status Reports provided by the Federal Communications Commission, https://www.fcc.gov/michael, accessed 08. Feb '22.

For comparison with the results in this study, fractions of dysfunctional cell towers were aggregated on county levels as defined by TIGER/Line shapefiles provided by the US Census Bureau, Department of Commerce, and contrasted with reported figures. It is to be noted that cell sites and cell towers are not exactly analogous, and county naming was ambiguous in a few cases.

Road and mobility incidents

- Wakulla County : "We had well over a 1000 trees just on lines," Savary said. "We stopped counting after a while." Trees knocked out communications, blocked roads and entangled power lines, cutting power.
- Calhoun & Liberty: Unaccustomed to the destructive rage of hurricanes, inland communities like Calhoun and Liberty counties were cut off for days – roads were blocked and all communication was cut off. Downed trees and debris littered or blocked all the roads. Rural residents were trapped behind their long dirt driveways.
- Jackson County: A big challenge was clearing blocked roads and convincing local motorists to say off the roads to allow the cleanup to proceed more quickly. Jackson County Fire and Rescue Chief Mark Foreman reported a lot of vehicle crashes and injuries at night.
- Eastside, FL: Returning wasn't always easy. Parts of U.S. Highway 98, the coastal highway, was washed out. "It could take several weeks. We're still cleaning roads. A lot of roads have been damaged. There's extensive damage by water and some are washed out.

Retrieved from https://eu.tallahassee.com/story/news/hurricane/2018/10/14/hurricane-michael-arc-ruin-trail-destruction-florida-panhandle-big-bend/1614787002/, accessed 08. Feb '22

Water supply incidents

- When Hurricane Michael tore through Florida's panhandle, the vicious category 4 hurricane toppled the water tower in *Mexico Beach*.
- Nearby, Bay Medical Center in *Panama City* was still running on partial electricity provided by generators, but the facility's toilets were filling up, and they had no water.
- the U.S. Army Corps of Engineers in restoring drinking water and wastewater service to communities in *Bay County* affected by Hurricane Michael. As communities in Florida and Georgia began to rebuild after Hurricane Michael, Anheuser-Busch said it would be shutting down some of its beer lines to get more than 300,000 cans of drinking water to people in need.
- Counter-example: As Hurricane Michael churns toward the Florida Panhandle, *Tallahassee* residents can rest easy that their drinking water is safe and they don't need to amass bottled water. The city has an abundant, safe water supply drawn from the Floridan Aquifer deep in the ground, with enough redundancies built into it that it is unlikely to fail or become contaminated during a hurricane, a city official said Monday.

Retrieved from https://www.meco.com/hurricane-season-impact/, https://response.epa.gov/site/site_profile.aspx?site_id=13982 , accessed 08. Feb '22

School access incidents

"Until further notice, schools are closed in eight counties across the Panhandle, including Bay, Calhoun, Franklin, Gadsden, Gulf, Jackson, Liberty and Washington counties, displacing around 45,000 students."

Retrieved from https://eu.pnj.com/story/news/2018/10/17/hurricane-michael-closes-schools-florida/1660289002/ , accessed 08. Feb. '22

SM3 Supplementary 3

SM3.1 Supplementary Material 1

Modelling Assumptions

S.1 Geo-Spatial Exposure Data: Infrastructure and Population

Table S 1 Data sources for infrastructure component and population data used throughout the study.

Exposure	Source	Details
population	WorldPop	- gridded population count data, 1km^2 resolution, UN adjusted. Post-processing: To decrease memory consumption on the networks, “very sparse” population clusters were dropped. A country-specific population density cut-off was determined such that at most 10% of the population was dropped (see *Figure S 1*). This reduced the amount of population nodes in the network by up to 55%.
roads	OpenStreetMap	- main roads: tags matching highway = motorway, motorway_link, trunk, trunk_link, primary, primary_link, secondary, secondary_link, tertiary, tertiary_link - all roads: main roads plus tags matching highway = residential, road, unclassified For computational reasons during network construction and shortest path searches, preferentially only main roads were taken. However, if a high share (>20%) of road tags were unclassified, all roads were included. In 2 cases of very large and dense main road networks (Italy and Japan), tertiary roads were excluded, too, with no impact on base rate accessibility.
hospitals	OpenStreetMap	- Primary healthcare facilities: tags matching amenity = hospital, clinic, doctors, health_post; healthcare = hospital, clinic, doctors; building = hospital, clinic
schools	OpenStreetMap	- Primary education facilities: tags matching amenity = school, college; building = school, college; education = school
cell towers	OpenCellID / WorldBank	- Cell sites from the OpenCellID, gridded by the World Bank Open Data to a 1km^2 resolution Post-processing: Re-gridded to 5kmx5km resolution.
power lines	Gridfinder	- Global high and medium voltage lines.
power plants	World Resource Institute / OpenStreetMap	- WRI power plant database - OSM tags matching power= plant, generator In cases of no hits in the WRI data base, power plant locations were queried from OSM. Generator locations from OSM were taken as a last resort if this did not yield any hits, either.
power substations	None / (Gridfinder)	OSM was not used for extracting substations due to inconsistent mapping (see Figure S 2). Instead,

		substations locations were inferred by taking end points of power lines, and power line nodes with degrees $>$ 2 (line bifurcations) as proxy.
power poles	None / (Gridfinder	Due to sparse mapping results on OSM, power pole (tower) locations were inferred along the transmission lines, assuming one every 500 m.

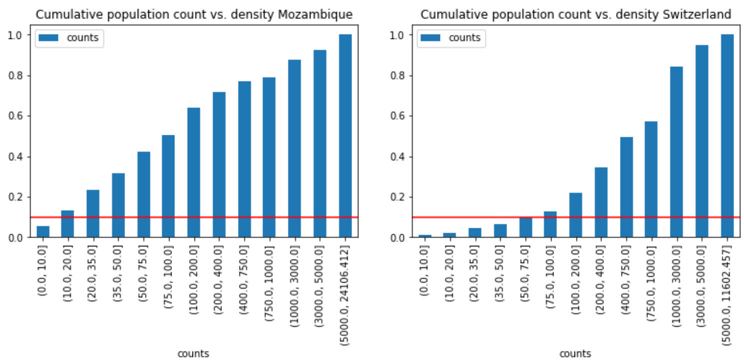

Figure S 1 Population density vs. cumulative population histograms for Mozambique (left) and Switzerland (right). The red line (at 10% of the population) determines the cut-off value below which population clusters were dropped from the analysis (20 people/km2 and 100 people/km2, resp.)

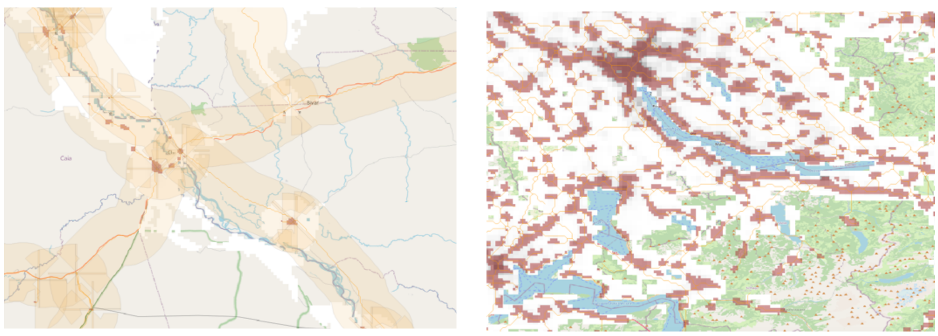

Figure S 2 - left: Population clusters (white) in rural Mozambique (avg. electrification rate is 38%): 10km distance thresholds from power lines (shaded orange) would over-predict access; continuously expanded electrification targets (red) are the best-guess estimate. right: Population clusters (white) in CHE (100% electrification rate): Consideration of electrification targets (red) would unnecessarily under-predict population's access to electricity.

S.2 Dependence Inference Heuristics

Explanation on parametrization decisions

Table S 2 Parametrization of infrastructure and end-user dependencies used within the network model.

Dep	source	target	single link	road access	dependency type	flow type	functional threshold	distance threshold [m]	conditions
1	power line	cell tower	TRUE	FALSE	functional	physical	0.6	inf	
2	power line	school	TRUE	FALSE	functional	physical	0.6	inf	
3	power line	hospital	TRUE	FALSE	functional	physical	0.6	inf	
4	cell tower	people	FALSE	FALSE	end-user	logical	1	20'000	
5	school	people	TRUE	TRUE	end-user	logical	1	*	
6	hospital	people	FALSE	TRUE	end-user	logical	1	*	
7	power line	people	TRUE	FALSE	end-user	physical	0.6	*	electrified=True
8	road	people	FALSE	FALSE	end-user	logical	1	10'000 / 2'000	

No. 1-3: power dependence of cell towers, hospitals and schools: Since those infrastructures need electricity for their functioning, they are assumed to be connected to the single closest node in the power network, irrespective of the resulting link distance. The link fails if power grid capacity falls below 60% of the initial supply level.

No. 4: End-user dependence on cell towers for mobile communication services. Coverage range limits of cell towers vary widely depending on tower design, technology standards and characteristics of the surroundings, with maximal coverage distances reaching up to 26 km (rural cell site range of 4G cells in the US (Holma et al. 2011), yet often revolve around 10km (written communication of an expert in the field). We reverted to a compromise of 20 km, from which end-users can receive mobile phone coverage of any cell tower. The links are binary and fail upon failure of the source.

No. 5: End-user dependence on schools for provision of educational services. People are assigned one single, non-substitutable school at most, as allocations can normally not be switched arbitrarily within a semester. While schools have to be physically reachable to provide service, literature finds that acceptable travel distances to educational facilities vary depending on various factors such as access modality (motorized private and public transport modes tend to be longer than walking (Liao and Dai 2022)), income level (affecting access modality choices) (Malone and Rudner 2011), rural-urban divides (inhabitants of rural areas experience longer travel distances) (Easton and Ferrari 2015), and country standards (Malone and Rudner 2011). Literature agrees, however, that acceptable travel time to educational facilities rarely surpasses 45 minutes across most settings . To account for such large variability, a link between people and an educational facility was established for the closest facility satisfying at least one of the two constraints:

i) it is reachable within 60 minutes at terrain-dependent walking speed, when walking as the crow flies.
ii) it is reachable within 60 minutes of driving over functioning roads using country-specific average road speeds.

Terrain-dependent walking speeds were obtained from the friction surface provided in the supplementary of (Weiss et al. 2020), at a resolution of 1km^2. Road speeds were obtained from tables provided in (Moszoro and Soto 2022).

No. 6: End-user dependence on hospitals for provision of healthcare services. People are linked to all healthcare facilities located within an acceptable travel distance, reflecting a certain level of substitutability among healthcare service providers. As in the case of access to education, typical travel modalities and acceptable travel distances to obtain healthcare service are highly variable. Literature finds a that beyond 30 minutes of travel time and 3 miles of travel distance, respectively, selection attractiveness of healthcare facilities in the US sharply decays (Guagliardo 2004), whereas medical recommendations in Sub-Saharan African countries are to have 80% of the population within a 2-hour travel time radius (Meara et al. 2015). The WHO tends to report people further away than 5 km from a healthcare facility (WHO, 2019). Several studies for effective healthcare access report access thresholds from between 30 minutes up to 6 hours (Hierink et al. 2020; Petricola et al. 2022). Since there is no finite consensus on what defines effective healthcare access, but there is agreement that for emergency healthcare incidents, a critical 'golden hour' of survival chances exist (Hu et al. 2020), we establish links between all healthcare facilities and population that satisfy at least one of the two constraints:

i) it is reachable within 60 minutes at terrain-dependent walking speed, when walking as the crow flies.
ii) it is reachable within 60 minutes of driving over functioning roads using country-specific average road speeds.

Speeds were obtained as mentioned above for educational service links.

No. 7: End-user dependence on power infrastructure for provision of electricity.
In absence of reliable data on the power distribution network (i.e., substations and low-voltage distribution lines), and without global electricity access maps matching the high resolution of gridded population data used in this study, dependence links were established using a two-stage heuristic: For countries with electrification rates of 90% or more (as reported by the World Bank Open Data, indicator EG.ELC.ACCS.ZS Access to electricity (% of population), all population clusters were connected to the respective single closest nodes in the high-and medium voltage transmission line network, irrespective of the resulting link length. For all other countries with low electrification rates, a pre-selection was made on where population clusters with likely electricity access are located. To this end, an electrification target map, estimating locations where people have access (Arderne et al. 2020), was spatially overlaid with population clusters. As these estimates were frequently too conservative, the overlay was consecutively expanded until hence-predicted electrification rates matched the World Bank country statistics. Those population clusters were then linked to the respective single closest nodes in the power network, irrespective of the resulting link length.

No. 8: End-user dependence on roads for access to transport.
The UN SDG indicator 9.1.1 tracks access to transport in rural areas using the Rural Access Index (RAI), which is computed based on the population living within 2 km of an all-season road. Access to transport in an urban context is frequently related to availability of public transport options, which, however, surpasses the scope of this study. We hence implemented the distance-based approach and established a single link between population clusters and the closest road point which is located at most 2 km away, for cases where all roads in a country were considered (i.e., whenever the fraction of 'unclassified' roads on OpenStreetMap surpassed 20%), and between population clusters and road points at most 10 km apart for cases where only main roads in a country were considered (i.e. less than 20% unclassified roads in OpenStreetMap). Reverting to main roads was preferred for computational reasons, yet the distance threshold had to be set larger than the 2 km RAI-threshold as fewer parts of the road network are hence considered. 10 km was judged to be a reasonable limit, as in Ireland (a country with high levels of access to transport), for instance, maximum average residential distance to the main road network is 6.7 km (CSO - Central Statistics Office 2019).

S.3 Impact Functions (Fragility Curves)

Table S3 provides an overview on which infrastructure components were considered to be vulnerable to which types of natural hazards, including sources of the impact functions and further explanations where necessary.
Figure S 3 graphically displays the employed curves.

Table S 3 Overview on infrastructure vulnerabilities to different natural hazard types, as modelled in this study.

Infrastructure Component	Flood	Winds	Sources & Details
Power Lines	-	x	Failure probability of line snapping due to wind stress (Guo et al. 2020). Binary failures are randomly sampled from the resulting probabilities.
Power Poles	-	x	Failure probability of tower blow-down due to wind stress (Panteli et al. 2017). Binary failures are randomly sampled from the resulting probabilities.
Power Substations	x	-	Binary step function for flooding.
Power Plants	-	-	Not designed to fail, hence no impact functions.
Roads	x	x	Binary step function for flooding. Wind impact function for damages from tree and debris blow-down according to (Koks et al. 2019)
Hospitals	x	x	Binary step function for flooding. Wind impact function for structural damages from HAZUS Tropical Cyclone technical manual for industrial buildings (FEMA, 2021)
Schools	x	x	Binary step function for flooding. Wind impact function for structural damages from HAZUS Tropical Cyclone technical manual for residential buildings (FEMA, 2021)
Cell Towers	x	x	Binary step function for flooding. Binary step function for wind impacts, assuming a withstand speed of 110 mph (manufacturer interview).

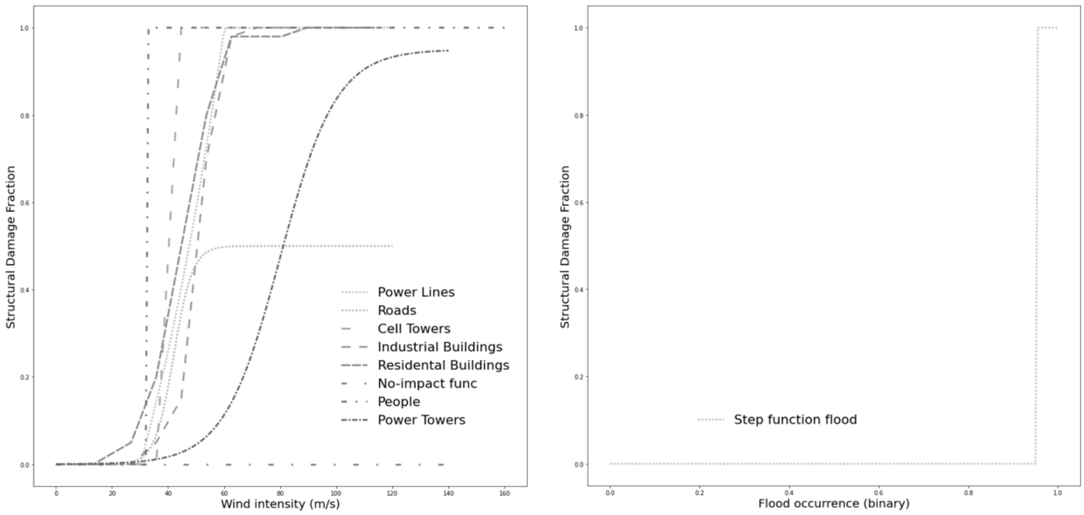

Figure S 3 Impact functions used for structural damage computations on CIs due to wind impacts (left) and flood impacts (right)

Part 2 - Detailed Results

S.4 Selected Regions Overview

Table S 4 Overview on study regions, including geographic area (NAM - North America; LAC - Latin America and the Caribbean, ECA - Europe and Central Asia; EAP East Asia & Pacific; SA - South Asia; SSA - Sub-Saharan Africa), region statistics from the World Bank Open Data repository, Social Vulnerability Risk Index From the WorldRiskReport 21, and access rates to electricity, healthcare, education, telecom and roads in undisrupted base states according to model calculations. Hazard event counts refer to number of events per region which were available from historic records based on IBTrACS for TCs (1980-2020) and the cloud-to-street database for floods (~2002-2018).

Study Region	**Geographic Area**	**WB Inc. Group**	**Pop. Density (ppl/km^2)**	**% Urban**	**Size (' 000 km^2)**	**WorldRisk Index 21**	**electr. access**	**healthc. access**	**educ. access**	**tele. access**	**road access**	**TC Event Count**	**Flood Event Count**
USA - Florida	NAM	1	136	91.5	170	133	100	100	100	100	100	31	4
USA - Texas	NAM	1	43	84.7	695	133	100	100	100	100	100	14	8
USA - Louisiana	NAM	1	41	73.2	135	133	100	100	100	100	100	17	0
Mexico	LAC	2	66	80.7	2000	94	100	99.4	99.6	99.5	99.7	49	5
Haiti	LAC	4	414	57.1	28	21	51	97.6	96.7	95.7	94.6	7	11
Puerto Rico	LAC	1	360	93.6	9	n/a	100	100	100	100	100	7	1
Cuba	LAC	2	109	77.2	110	105	100	99.1	99.2	98.4	99	17	6
Chile	LAC	1	26	87.7	1250	33	99.3	99	99.1	99.3	99.8	0	1
Guatemala	LAC	2	167	51.4	108	10	100	97.6	98	99.9	98.2	2	3
Uruguay	LAC	1	20	95.4	176	27	100	99.4	99.5	99.9	99.2	0	10
Antigua & Barbuda	LAC	1	223	24.4	0	2	100	100	100	100	100	7	0
Switzerland	ECA	1	219	73.9	41	170	100	100	100	100	100	0	2
Netherlands	ECA	1	518	92.2	49	66	100	99.8	99.9	100	99.8	0	1
UK	ECA	1	277	83.9	250	140	100	97.6	97.6	100	97.6	0	11
Serbia	ECA	2	79	56.5	88	111	100	99.5	99.7	100	99.4	0	4

Hungary	ECA	2	107	71.3	93	114	100	100	100	100	100	0	13
Greece	ECA	1	83	79.7	131	82	100	99.9	99.9	100	99.9	0	18
Georgia	ECA	2	65	59.5	70	108	100	99.5	99.5	99.8	99.5	0	1
Tajikistan	ECA	3	67	28	141	99	100	90.2	93.2	92.2	94	0	5
China - Hainan	EAP	2	276	58	33	95	100	83.7	92.6	96.6	92.2	40	0
China - Fujian	EAP	2	349	64.8	121	95	100	99.7	100	97.5	100	35	4
Philippines	EAP	3	376	48	300	8	98.9	97.9	98.4	98.1	98.9	128	41
Viet Nam	EAP	3	313	38	331	43	100	97.1	98.7	99.8	99.6	49	33
Cambodia	EAP	3	95	23.8	181	15	91.2	80.4	83.7	99.8	80.1	1	17
Bangladesh	SA	4	1265	38.2	148	13	100	85.2	66.3	99.9	83.4	14	13
Sri Lanka	SA	3	354	18.7	65	75	100	100	100	100	100	1	8
Pakistan	SA	3	387	37.2	880	85						1	2
Madagascar	SSA	4	48	38.5	587	39	34.2	47.1	51.6	56.1	54.4	45	4
Mozambique	SSA	4	40	37.1	801	50	31.6	63.5	56	66.1	60.5	14	9
Burundi	SSA	4	463	13.7	27	40	18.9	99	60.6	95	98.1	0	7

S.5 General findings on service disruption patterns, per hazard type

Figure S 4 Top: Typical disruption patterns from tropical cyclone events, for Puerto Rico and Florida. Bottom: Typical disruption patterns from flood events, for Cambodia and Serbia. Notable is Great Britain. Figures exemplarily taken from respective study region files

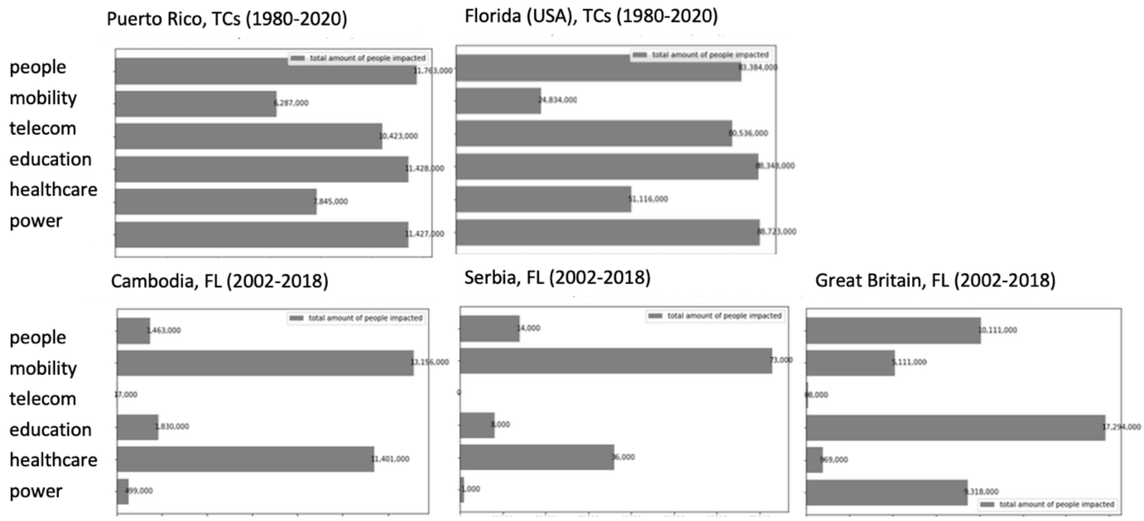

of SM2.

S.6 Contrasting event severity and service disruption patterns

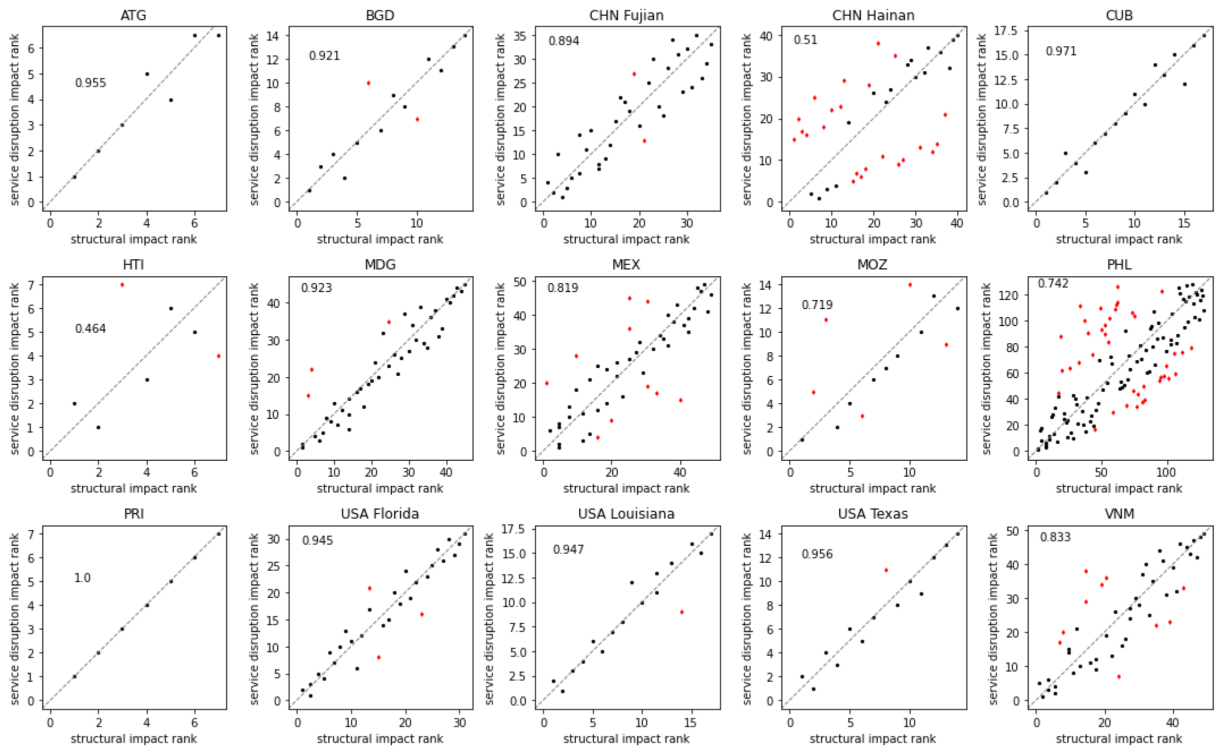

Figure S 5 Event rank plots of structural impact severity (measured in total amount of critical infrastructure components damaged) vs. service disruption impact severity (measured in total amount of people experiencing at least one type of service disruption) for tropical cyclone events across all study regions. Generally, events which cause more structural destruction also cause more service disruptions, but significant individual outliers (here defined as >20% rank difference between structural and service impacts, plotted as red diamonds) and larger-scale patterns of outliers are present in many regions.

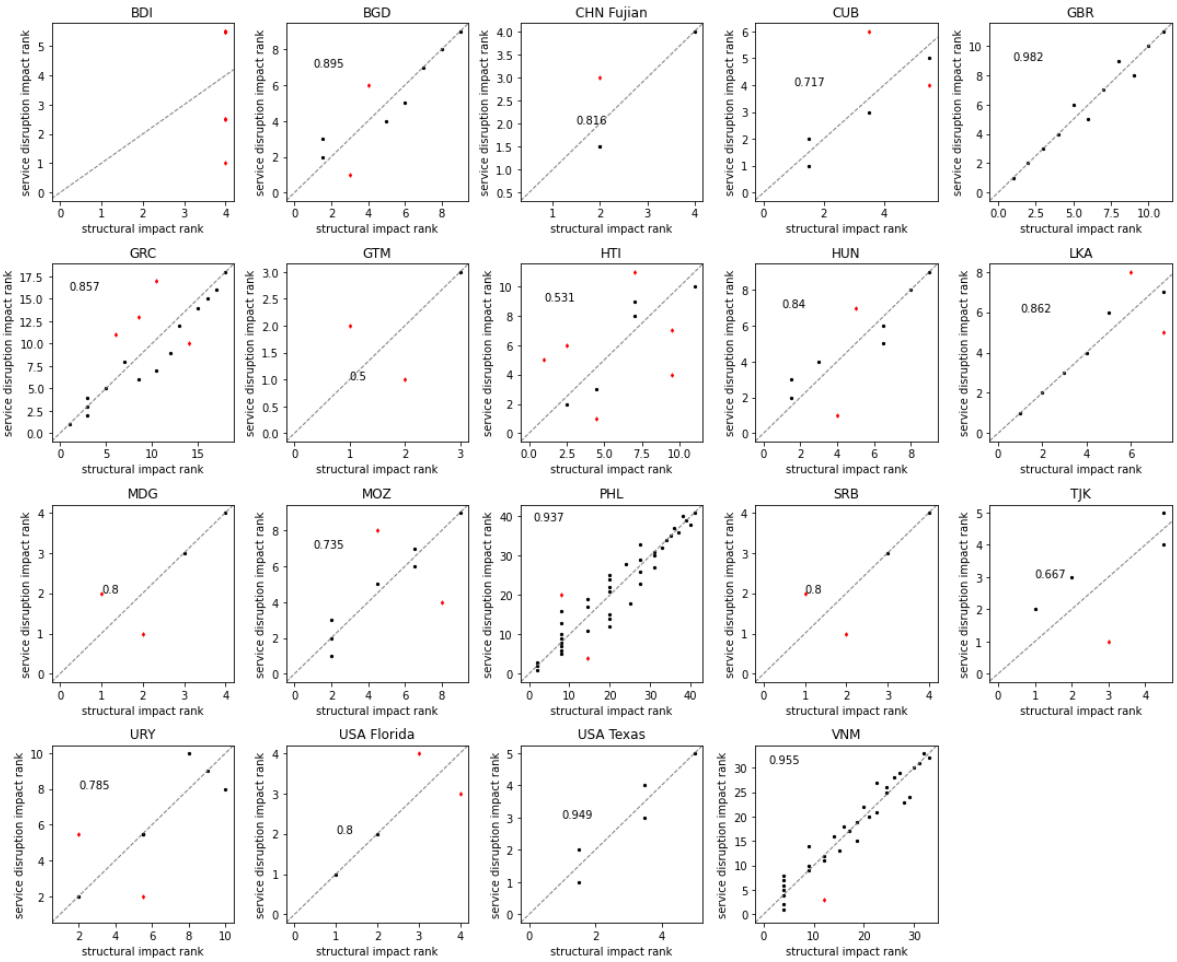

Figure S 6 Event rank plots of structural impact severity (measured in total amount of critical infrastructure components damaged) vs. service disruption impact severity (measured in total amount of people experiencing at least one type of service disruption) for flood events across all study regions. Generally, events which cause more structural destruction also cause more service disruptions, but significant individual outliers (here defined as >20% rank difference between structural and service impacts, plotted as red diamonds) and larger-scale patterns of outliers are present in many regions

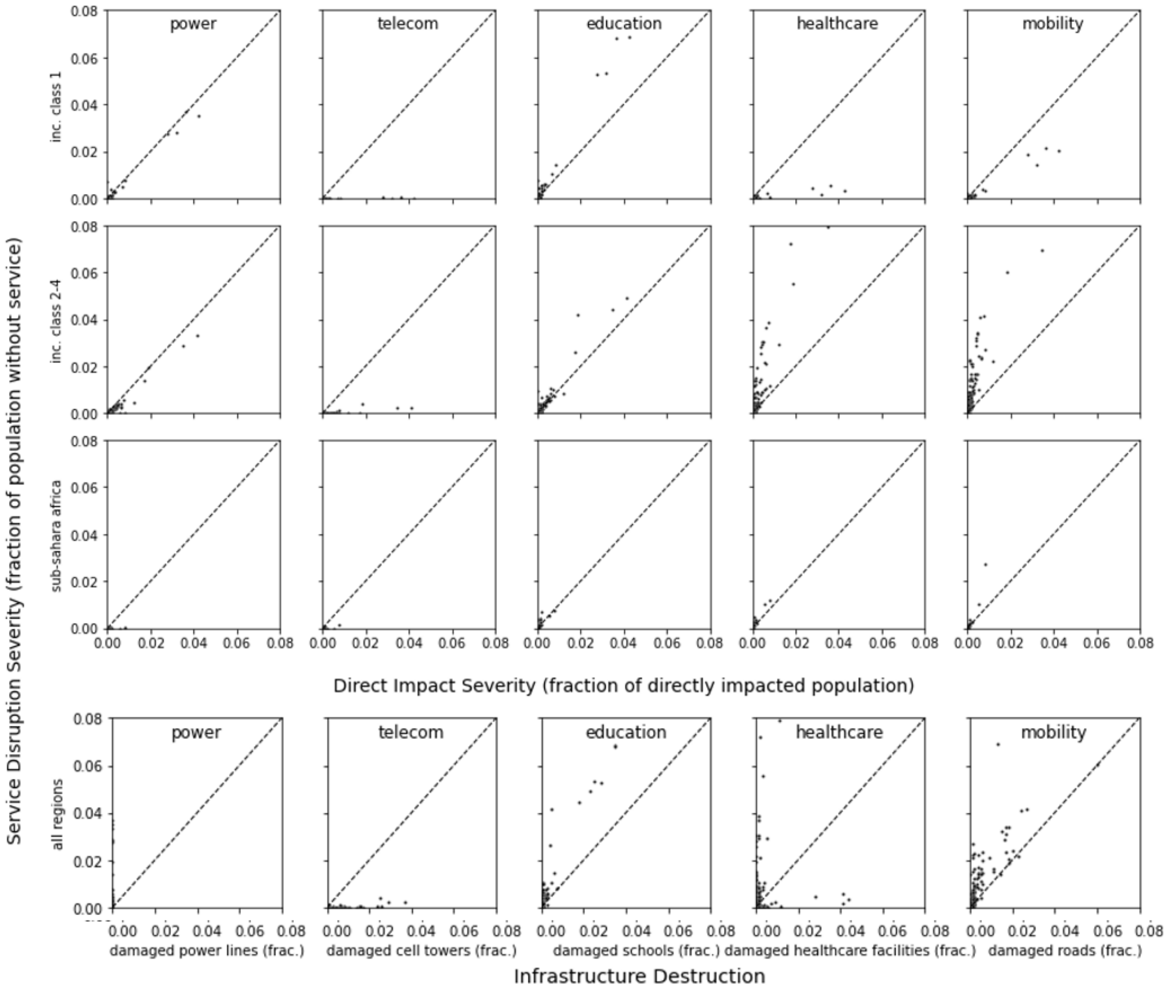

Figure S 7 Disruptions to power, telecom, education, healthcare and mobility access are not concurrent with physical impacts. Upper panel: Fraction of directly affected population (located within the flooded area) vs. fraction of population without access to the respective service, split by income groups; events in sub-Sahara Africa (all income class 4) plotted explicitly. Lower panel: Fraction of destroyed core assets vs. fraction of population without access to the respective service, for all events and region

S.7 Service Resilience Factors

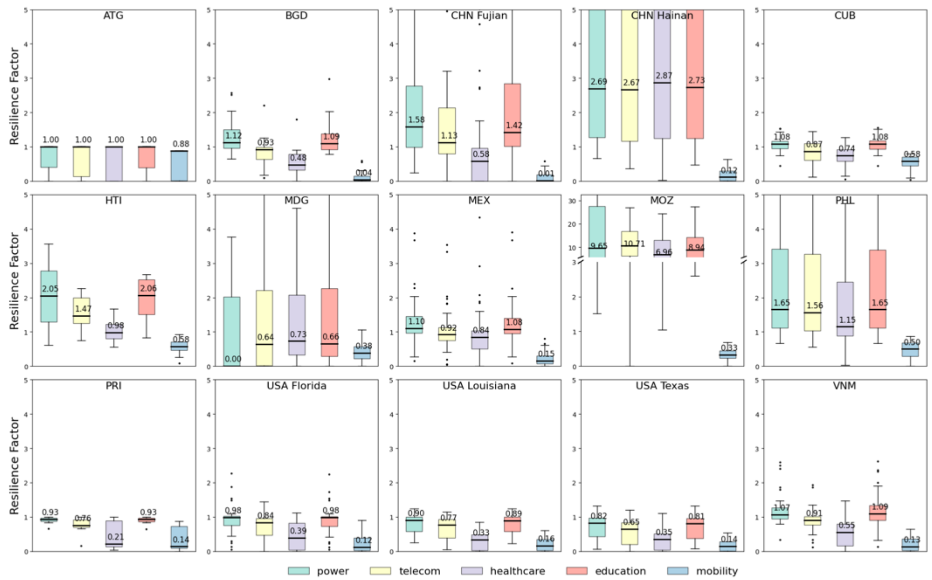

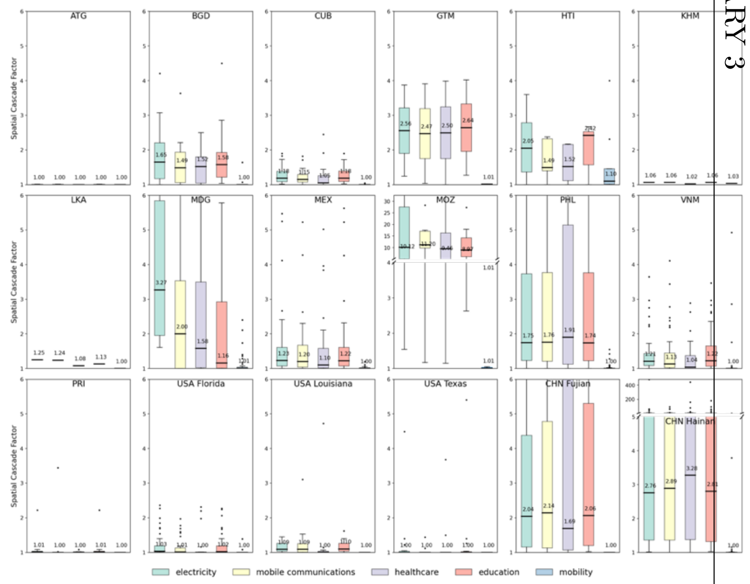

Figure S 8 Right: Distribution of event-and service-wise resilience factor R [0, inf) for tropical cyclone events, defined as the ratio between population without access to service in the entire study region and population with pre-disaster service access in directly affected region). A service is defined to be resilient if R < 1. Study regions with less than 4 events are omitted. Left: spatial cascade factor, which specifically captures the spatial containment of impacts (i.e. the ratio of impacts incurred outside and within the directly affected area).

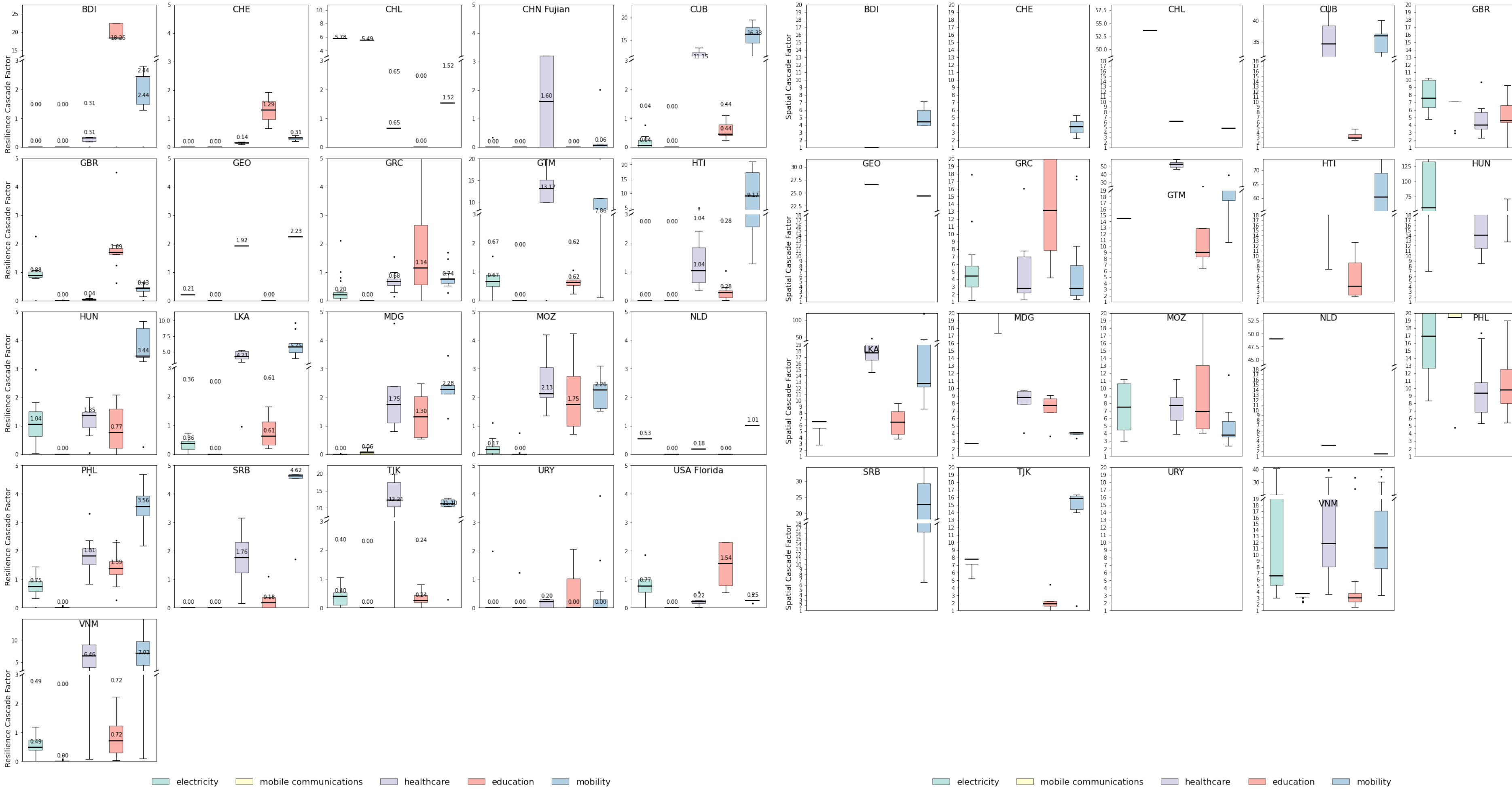

Figure S 9 Right: Distribution of event-and service-wise resilience factor R [0, inf) for flood events, defined as the ratio between population without access to service in the entire study region and population with pre-disaster service access in directly affected region). A service is defined to be resilient if R < 1. Left: spatial cascade factor, which specifically captures the spatial containment of impacts (i.e. the ratio of impacts incurred outside and within the directly affected area).

S.8 Region variables and system resilience

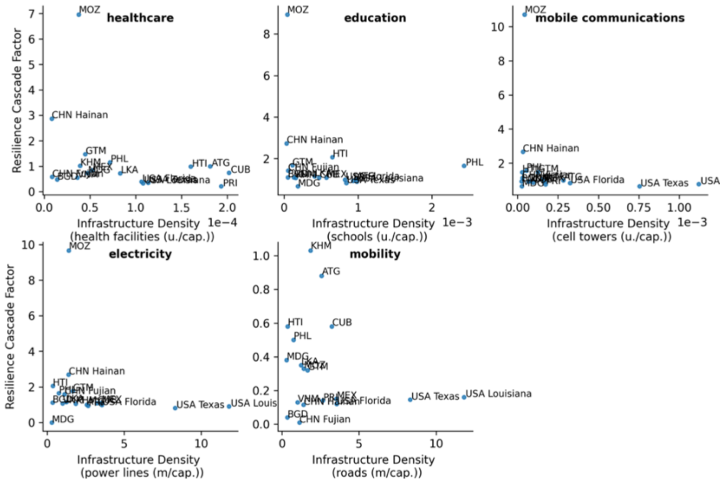

Figure S 10 -Correlations between average resilience cascade factors per service and region's infrastructure density (measured in units or km per capita)

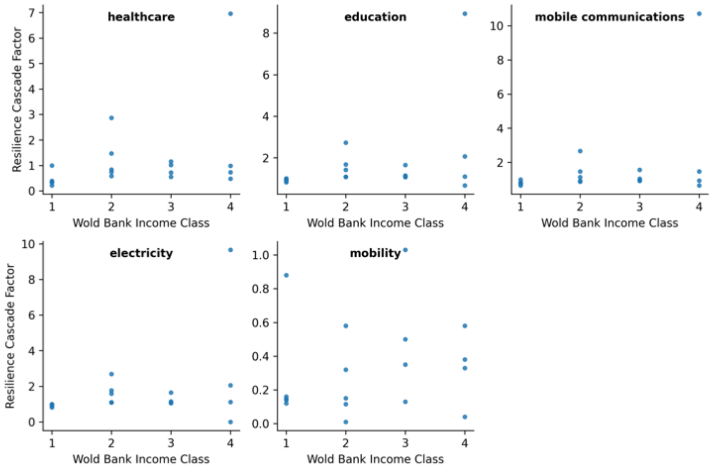

Figure S 11 - Average resilience cascade factors per service, by region's World Bank Income classification (1 - high, 4 - low)

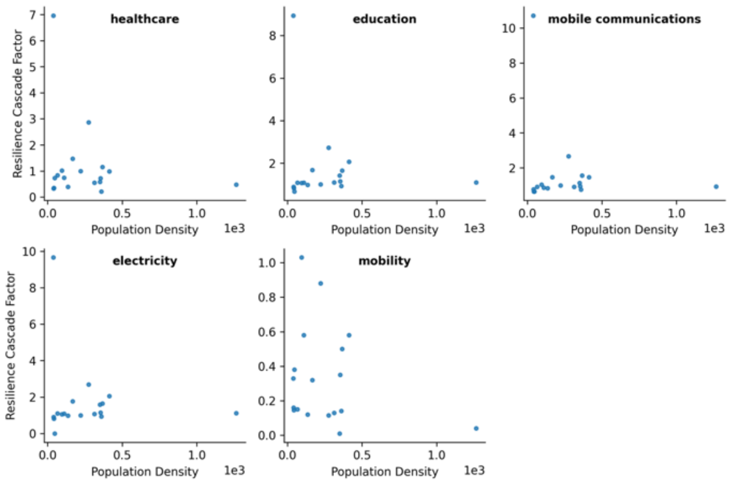

Figure S 12 - Correlations between average resilience cascade factors per service and region's population density (population count / km^2).

S.8 Case Study on Florida - Results

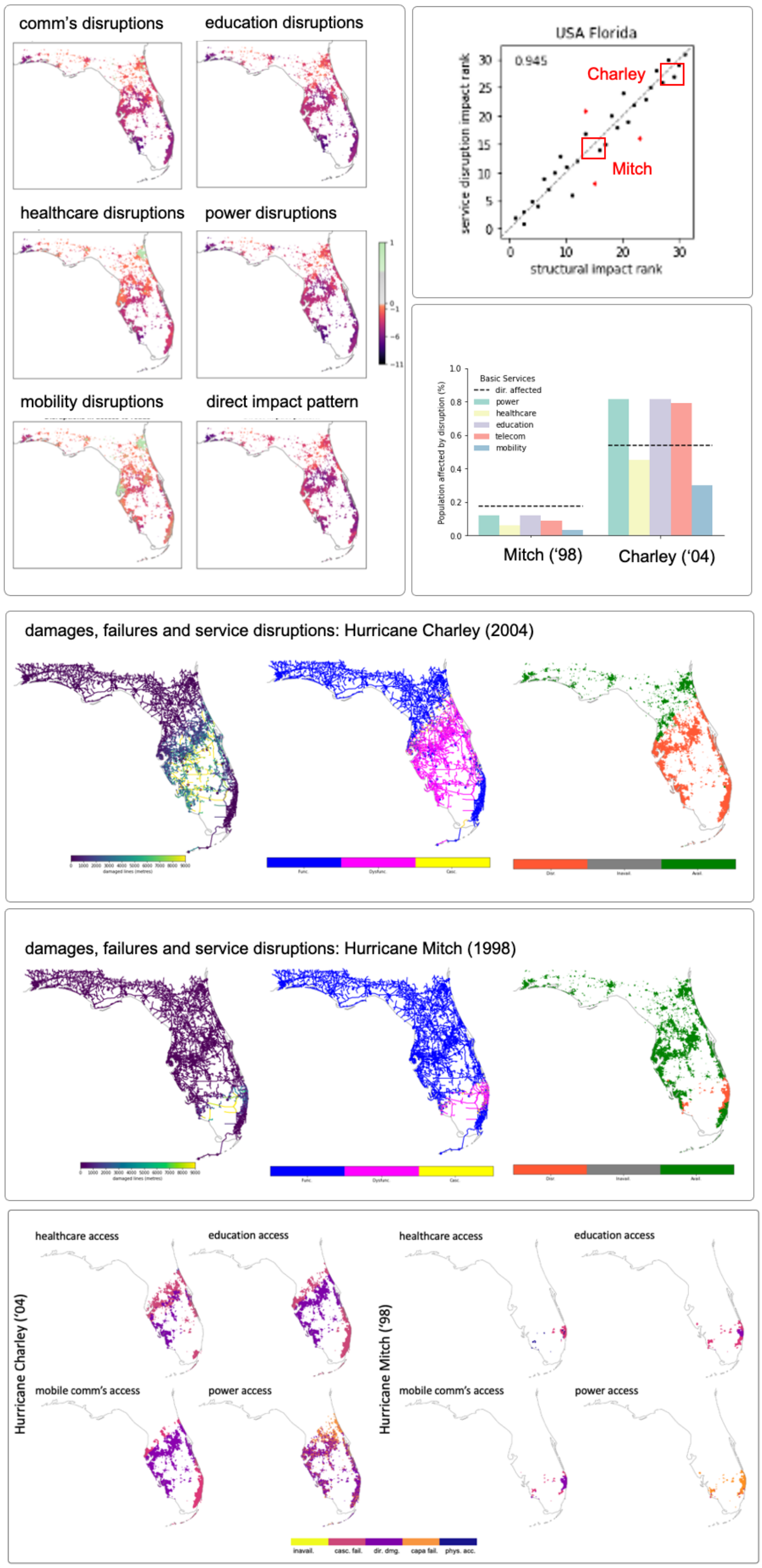

Figure S 13 Case study on the drivers of tropical-cyclone induced service disruption patterns in Florida, United States; analogous to Figure 6 of the manuscript.

S.9 Towards systemic risk metrics: population at risk of basic service disruptions from tropical cyclones

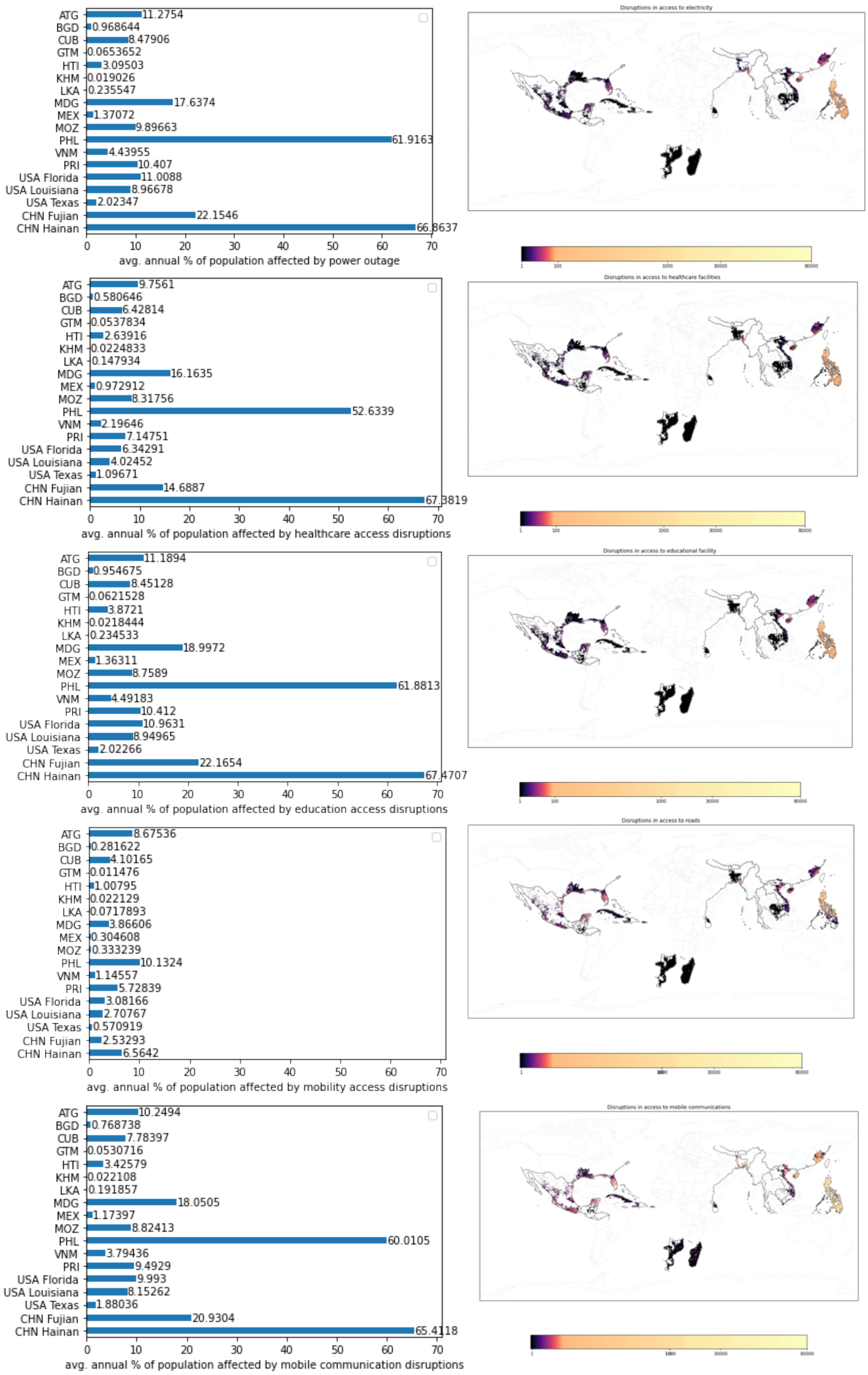

Figure S 14 Service disruption risks from tropical cyclones, by service and study region. Expressed as average annual population (left) and spatially explicit as number of people per cluster (right).

Part 2 - Detailed Results

References

Arderne, C., C. Nicolas, C. Zorn, and E. E. Koks, 2020: Data from: Predictive mapping of the global power system using open data. https://doi.org/10.5281/zenodo.3628142.

CSO - Central Statistics Office, 2019: Measuring Distance to Everyday Services in Ireland. https://www.cso.ie/en/releasesandpublications/ep/p-mdsi/measuringdistancetoeverydayservicesinireland/ (Accessed September 11, 2023).

Easton, S., and E. Ferrari, 2015: Children's travel to school—the interaction of individual, neighbourhood and school factors. *Transport Policy*, **44**, 9–18, https://doi.org/10.1016/j.tranpol.2015.05.023.

Guagliardo, M. F., 2004: Spatial accessibility of primary care: concepts, methods and challenges. *International Journal of Health Geographics*, **3**, 3, https://doi.org/10.1186/1476-072X-3-3.

Guo, J., T. Feng, Z. Cai, X. Lian, and W. Tang, 2020: Vulnerability Assessment for Power Transmission Lines under Typhoon Weather Based on a Cascading Failure State Transition Diagram. *Energies*, **13**, http://dx.doi.org/10.3390/en13143681.

Hierink, F., N. Rodrigues, M. Muñiz, R. Panciera, and N. Ray, 2020: Modelling geographical accessibility to support disaster response and rehabilitation of a healthcare system: an impact analysis of Cyclones Idai and Kenneth in Mozambique. *BMJ Open*, **10**, e039138, https://doi.org/10.1136/bmjopen-2020-039138.

Holma, H., P. Kinnunen, I. Z. Kovács, K. Pajukoski, K. Pedersen, and J. Reunanen, 2011: Performance. *LTE for UMTS*, John Wiley & Sons, Ltd, 257–301.

Hu, W., V. Freudenberg, H. Gong, and B. Huang, 2020: The "Golden Hour" and field triage pattern for road trauma patients. *Journal of Safety Research*, **75**, 57–66, https://doi.org/10.1016/j.jsr.2020.08.001.

Koks, E. E., J. Rozenberg, C. Zorn, M. Tariverdi, M. Vousdoukas, S. A. Fraser, J. W. Hall, and S. Hallegatte, 2019: A global multi-hazard risk analysis of road and railway infrastructure assets. *Nature Communications*, **10**, 2677, https://doi.org/10.1038/s41467-019-10442-3.

Liao, C., and T. Dai, 2022: Is "Attending Nearby School" Near? An Analysis of Travel-to-School Distances of Primary Students in Beijing Using Smart Card Data. *Sustainability*, **14**, 4344, https://doi.org/10.3390/su14074344.

Malone, K., and J. Rudner, 2011: Global Perspectives on Children's Independent Mobility: A Socio-Cultural Comparison and Theoretical Discussion of Children's Lives in Four Countries in Asia and Africa. *Global Studies of Childhood*, **1**, 243–259, https://doi.org/10.2304/gsch.2011.1.3.243.

Meara, J. G., and Coauthors, 2015: Global Surgery 2030: evidence and solutions for achieving health, welfare, and economic development. *Lancet*, **386**, 569–624, https://doi.org/10.1016/S0140-6736(15)60160-X.

Moszoro, M., and M. Soto, 2022: *Road Quality and Mean Speed Score*. International Monetary Fund, https://www.imf.org/en/Publications/WP/Issues/2022/05/20/Road-Quality-and-Mean-Speed-Score-518200 (Accessed October 6, 2022).

Panteli, M., C. Pickering, S. Wilkinson, R. Dawson, and P. Mancarella, 2017: Power System Resilience to Extreme Weather: Fragility Modeling, Probabilistic Impact Assessment, and Adaptation Measures. *IEEE Transactions on Power Systems*, **32**, 3747–3757, https://doi.org/10.1109/TPWRS.2016.2641463.

Petricola, S., M. Reinmuth, S. Lautenbach, C. Hatfield, and A. Zipf, 2022: Assessing road criticality and loss of healthcare accessibility during floods: the case of Cyclone Idai, Mozambique 2019. *International Journal of Health Geographics*, **21**, 14, https://doi.org/10.1186/s12942-022-00315-2.

Weiss, D. J., and Coauthors, 2020: Global maps of travel time to healthcare facilities. *Nat Med*, **26**, 1835–1838, https://doi.org/10.1038/s41591-020-1059-1.

2019: As post-cyclone resettlement, 200 000 people lack access to health services in Mozambique - Mozambique | ReliefWeb. https://reliefweb.int/report/mozambique/post-cyclone-resettlement-200-000-people-lack-access-health-services-mozambique (Accessed September 11, 2023).

2021: *Hazus Hurricane Model Technical Manual*. FEMA, https://www.fema.gov/sites/default/files/documents/fema_hazus-hurricane-technical-manual-4.2.3_0.pdf (Accessed March 10, 2022).

SM3.2 Supplementary Material 2

The documents can be retrieved at `https://www.research-collection.ethz.ch/handle/20.500.11850/648007`.

SM4 Supplementary 4

Exploring Compound Event Impacts on Critical Infrastructures, Cascading Failures and Basic Service Disruptions

Evelyn Mühlhofer, Elco E. Koks, David N. Bresch; published in *JRC Publications Repository: Proceedings of the 61*st *ESReDA seminar*

Abstract. Critical infrastructures such as power lines, roads, telecommunication and healthcare systems are essential for a society's daily functioning. Yet they are also more exposed than ever to the risks of extreme weather events in a changing climate. Damages to interdependent infrastructure systems often lead to failure cascades, and result in catastrophic, yet poorly studied impacts when people are cut off from basic service access. The large spatial extents of infrastructure systems make them a natural target of compound events, and may further even connect seemingly unconnected hazard events, potentially amplifying impacts. We present a consistent and transferable way to study the effects of (spatio-)temporally compounding hazard events on such infrastructure systems and their impacts on disruptions of basic services. Building on an open-source modelling framework which embeds a network-based infrastructure model into the globally consistent and spatially explicit natural hazard risk modelling platform CLIMADA, we simulate failure cascades across power, mobile communications, roads, healthcare and educational infrastructures and the respective service disruptions in Bangladesh from two historic compound flood and tropical cyclone events (Typhoon Sidr 2007 with concurrent storm surges and pluvial floods, and Typhon Giri 2010 followed by a flood). We show that cascading failures are substantial with respect to final impacts, and that the consideration of sub-hazards such as flooding and wind are of utmost importance regarding impact magnitudes. Yet, we find that compound events may not necessarily escalate the level of impact further than if they had occurred in temporally well separated instances, especially if the events are spatially disjoint. The hypothesis remains, however, that such escalations may well happen for more spatially close events and/or high-impact events capable of 'tipping' system performance thresholds.We discuss implications for future connected event research and propose ways forward.

1 Introduction

Critical infrastructures (CIs) such as powerlines, roads, telecommunication and healthcare systems across the globe are more exposed than ever to the risks of extreme weather events in a changing climate [1]. Natural hazard-induced damages to CIs often lead to failure cascades with catastrophic impacts for the population which faces access disruptions for basic services such as energy, mobility and healthcare [8]. Being able to represent the spatial exposure of real-world CI systems to relevant hazards in a realistic manner, to model direct structural impacts of such events, and to capture the dependencies within and between the systems [9], is hence crucial for understanding the risk associated with failure cascades and basic service disruptions at large scales.

Research on CI interdependences has made much progress throughout the last years [10], and especially network (flow) modelling approaches have been demonstrated to lend themselves as illustrative means for hotspot analyses at large system scales (such as entire countries) [7] at which many natural hazards may typically occur.

Within the natural hazard research community, much energy has recently been dedicated to the inquiry of 'compound weather and climate events', which are an "*integral part of almost all climate-related risks and pose significant challenges to many risk-reduction measures*" [2]. Within their seminal paper, Zscheischler *et al.* [2] proposed a typology that identifies four distinct categories of compound events - preconditioned, multivariate, temporally compounding and spatially compounding - which when occurring, may aggravate the impacts of a hazard compared to its isolated treatment, and potentially drive maladaptation.

Developing this predominantly hazard-focused concept of compound events further, Raymond *et al.* [3] coined the term of "*connected events*", incorporating "*'interacting', 'cascading' or 'multi-risk' natural hazards; and systemic risks and complexity science*". Applied to the lens of critical infrastructures, it is suggested that *"[c]onnected extremes can exert forces on these [infrastructure] systems beyond their design specifications, making it imperative to understand and incorporate such effects into infrastructure planning and risk assessments. The relevant interactions are typically poorly constrained, despite the large investments involved, due to the great complexities of the systems and the numerous and widely disparate actors with jurisdiction over them.*"

Our goal is to showcase a practical platform and means to quantitatively study such - often conceptually remaining - compound event phenomena under the aspect of interdependent critical infrastructure systems, and their connections within the (human-centric) impact space. Drawing on an end-to-end risk modelling and infrastructure failure framework, we start out on two case studies in Bangladesh, one of the most vulnerable countries to multiple hazards, involving tropical cyclones and flooding. We explore how temporally, yet not necessarily spatially compounding events may induce failure cascades and disrupt basic services. Using a generalized framework, we aim to draw preliminary conclusions on the adequacy of the approach as such to advance connected event research, and highlight insights, limitations and extension methods for the future.

2 Methods

2.1 Modelling framework - Overview

Critical infrastructure (CI) failure models often operate at local scales, with high data requirements and low transferability. The focus frequently lies on a technical performance side, and (natural) hazards are often not explicitly modelled as a physically consistent disruptive scenario. To handle the scales at which natural hazards occur, and to enable a coherent, transferrable assessment of CI risks and their social impacts, we developed an end-to-end framework [5] that employs a network modelling approach for interdependent CI systems, embedded into the natural hazard risk assessment platform CLIMADA [6], a state-of-the-art tool for impact calculations and adaptation options appraisal. CI component damages are computed from hazard footprints within the natural hazard risk module of the framework, which then initiate CI failure cascades within the CI systems module of the framework, which propagate along dependencies between the different CI systems. Result layers are computed both on a technical (functional) CI systems level and translated into human-centric impacts (basic service disruptions) for the dependent population. The framework is spatially explicit, fully open-source and open-access, allowing for the analysis of geographical regions, CI systems and hazards of interest.

2.1.1 Natural Hazard Risk Modelling with CLIMADA

While several platforms for natural hazard modelling exist, the open-source and -access software CLIMADA (CLImate ADAptation) is the only globally consistent and spatially explicit tool which is freely available to assess the risks of natural hazards and to support the appraisal of adaptation options [6, 14]. The event-based modelling approach of CLIMADA allows for a fully probabilistic risk assessment based on the IPCC risk definition as a function of hazard, exposure and vulnerability. 'Hazard' is a spatial representation of an intensity measure for the respective physical event, such as a wind field computed from the track records of a tropical cyclone, or the flood depth at certain locations within a region. 'Exposure' represents the geo-located critical infrastructures at component level which are potentially at risk (e.g. power plants and power lines, cell towers, etc.), and their associated value (such as Dollars, length or area). 'Vulnerability' is a hazard and infrastructure component-specific function, relating hazard intensity to the degree of expectable structural damage. Risk is computed efficiently in CLIMADA by overlaying these three layers, and obtaining structural damage fractions for each infrastructure component. While data curation is automated for many layers (such as downloading infrastructure shapes from OpenStreetMap, or hazard footprints for several types of natural hazards from a dedicated data API), user-specific data of many geospatial formats can readily be ingested into the platform. More details on the approach can be found in [5] and [6].

2.1.2 Infrastructure Systems Modelling within a System-of-Systems Formulation

CI graphs with directed edges and nodes are generated from the same geo-located component data as used in the risk calculations for each CI system. The individual graphs are combined into one interdependent CI graph through dependencies. Dependencies between components of different CI systems are inferred through a dependency-search algorithm described further in [5]. Population data equally forms part of the interdependent CI graph, where dependencies (representing demand for basic services such as access to power, mobile communication, healthcare, education and mobility) are similarly inferred via the search algorithm, yet additionally involve checking for availability of road access to schools and healthcare facilities. CI failure cascades are triggered through the computed component damages as described above and propagated along CI dependencies in the graph representation of the interdependent CI system until reaching a steady state. Basic service disruptions for the dependent population are calculated accordingly. More details on the approach can be found in [5].

2.2 Case Selection - Two Compound Tropical Cyclone and Flood Events in Bangladesh

Bangladesh was selected due to its frequent exposure to a multitude of hazards, particularly floods and tropical cyclones (TCs). Desk research and data availability revealed two explorative case study combinations: Typhoon Giri in 2010, which brought about strong winds, and was followed by a major flood two weeks later (also termed *case A* henceforth), and typhoon Sidr in 2007, which brought about strong winds, storm surge and flooding due to torrential rainfalls (also termed *case B* henceforth). Impacts were explored for the interdependent power, mobile communications, road, healthcare and educational infrastructure systems, both on a functional basis and in terms of service disruptions to the dependent population. To study the possible increased effects of temporally compounding events, two types of simulations were performed: Once, impact and cascading failure calculations were run separately per hazard (i.e. once per TC wind and once per flooding), following a single-event logic, and once, structural damages on components were first combined from both winds and floods, and then propagated through the failure cascade module.

2.2.1 Data

— Infrastructure component data within Bangladesh is collected for power plants, high-and medium voltage power lines, cell towers, main roads, hospitals and schools (see Figure 1). Data is taken from gridfinder [11], World Bank Open Data and OpenStreetMap. Gridded population count data is extracted from WorldPop [12] at a $1km^2$ resolution.

- Supply and demand data were obtained for the power sector (electricity generation and per capita electricity consumption) from the International Energy Agency IEA.
- Hazard source data is taken from IBTrACS, the International Best Track Archive for Climate Stewardship project [13], providing time and location of TC tracks for typhoons Giri (storm-ID 2010280N17085) and Sidr (storm-ID 2007314N10093). Flood footprints are obtained from the Cloud To Street database, for the two events with identifiers DFO 3713 and DFO 3226. See figure 2.
- Impact functions (also termed vulnerability curves or fragility functions), relating hazard intensity to structural damage extent are taken from FEMA's Hazus MH manuals and literature, as detailed in [5].

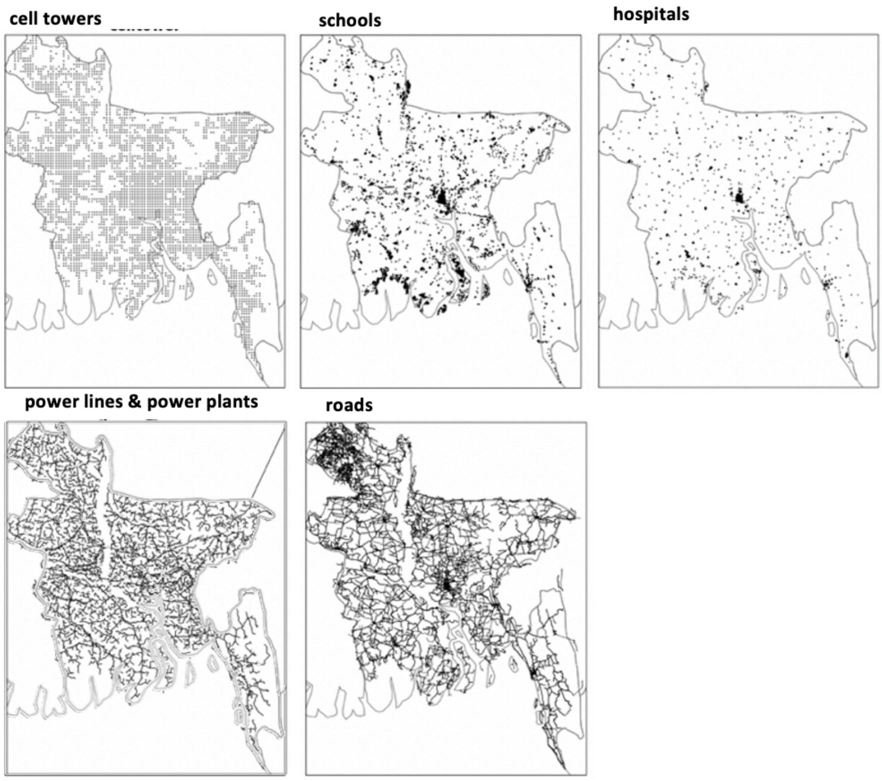

Source: OpenStreetMap, 2022; gridfinder, 2018; World Bank OpenData, 2019.

Figure 1. Critical infrastructure systems within Bangladesh considered in case studies A and B.

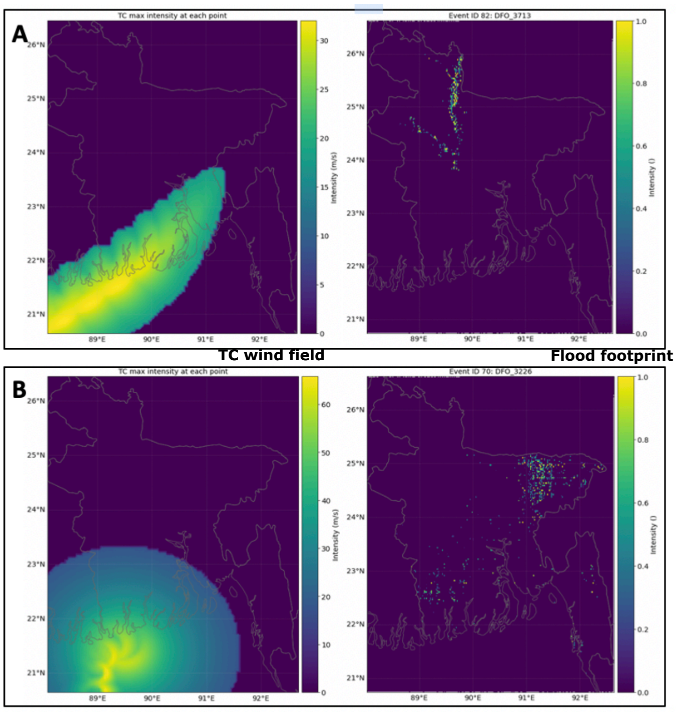

Source: authors, with source data from Cloud to Street flood database and IBTrACS [13].

Figure 2. Hazard pairs considered in compound event computations: A - consecutive TC wind (Giri 2010) and flood event (DFO 3713), B - concurrent TC wind (Sidr 2007) and flood sub-hazards from storm surge and torrential rainfalls (DFO 3226).

3 Results

Figure 3 summarizes the spatial results in terms of people being affected by basic service disruptions due to infrastructure failure cascades induced by temporally compounding hazard events. As visible in the hazard figures in Section 2, the flooding and wind footprints were spatially disjoint, without any geographic overlap in case A. Particularly in this case (Figure 2, left), impacts are clearly attributable to either of the two hazard events - the flooding for disruptions in the northern part of the country, and some minor disruptions due to winds in the southern part of the country. Similar, yet not as pronounced, is case B (Figure 3, right), with flood-induced impacts in the north-east and east part, and wind-induced impacts in the south of the country.

Result tables 1 and 2 confirm the visual impression quantitatively by detailing the number of people affected by service disruptions due to either the wind hazard or the flood hazard individually, following a single-event logic, and for the compound-event logic in comparison: The sums of people experiencing disruptions per individual hazard type (columns 'min-sum'), result in the same impact figures as for the compound event computations (columns 'compound'), without bigger, escalating effects in the latter.

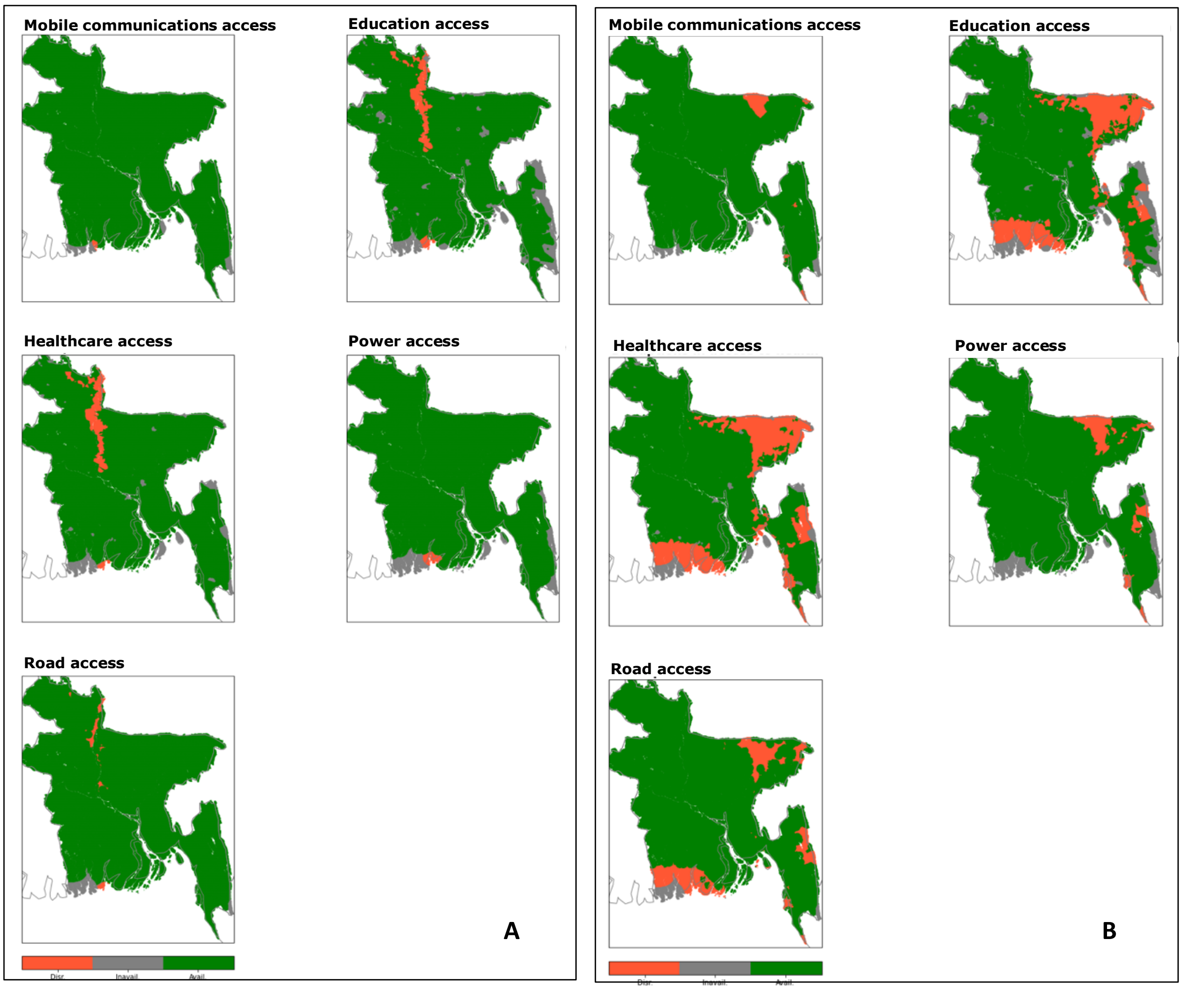

Source: authors' calculations, 2022

Figure 3. Maps of population estimated to experience service disruptions in access to telecommunications, education, healthcare, power and roads, due to (cascading) infrastructure failures induced by compound hazard events as presented above: panel A (consecutive TC Giri and flood events) and panel B (compound TC Sidr and surge/pluvial flooding event). Green - population cluster has access to respective service, red - population cluster lost access to respective service, grey - population cluster never had access to respective service.

Table 1. Total population estimated to experience disruption in access to the respective services from event pair A (TC Giri and a consecutive flood event). *Wind Only* - disruption scenario computed only from the tropical cyclone wind field; *Flooding Only* - disruption scenario computed only from the flood footprint; *Compound* - disruption scenario computed from wind and flood being treated as a single, co-occurring hazard event; Min-Sum - Sum of separately computed disruption scenarios *Wind Only* and *Flooding Only,* avoiding double-counting of potential population clusters which are affected by both scenarios.

	Wind Only	**Flooding Only**	**Compound** (1)	**Min-Sum** (2)
mobile comm's.	5'368	-	5'368	5'368
education	50'953	4'569'298	4'620'251	4'620'251
healthcare	30'878	4'799'014	4'829'892	4'829'892
power	243'593	-	243'593	243'593
road	16'129	653'864	669'993	669'993

Source: Authors' calculations.

Table 2. Total population estimated to experience disruption in access to the respective services from event pair B (concurrent TC wind and flood sub-hazards of Typhoon Sidr, 2007). Columns are as explained in caption of Table 1.

	Wind Only	**Flooding Only**	**Compound** (1)	**Min-Sum** (2)
mobile comm's.	-	1'981'026	1'981'026	1'981'026
education	2'475'998	14'265'789	16'741'787	16'741'787
healthcare	2'579'788	15'398'783	17'978'571	17'978'571
power	-	4'672'555	4'672'555	4'672'555
road	1'717'565	4'536'270	6'253'836	6'253'836

Source: Authors' calculations.

It is important to point out that failure cascades were still triggered due to the networked character of the infrastructure systems under study and their dependencies between each other, and that they are a dominant factor in healthcare and education access disruptions. Cascades did, however, not spread beyond their single-event extent.

The non-occurrence of any detectable ‘connections’ magnifying impacts beyond their initial scopes for the cases studied here may be attributable to two factors: Firstly, due to the different spatial patterns of the wind and flooding occurrence, those hazards were not acting on the same infrastructure components, and hence would not contribute to a joint failure (such as winds weakening a structure, which is rendered fully dysfunctional through the onset of a flood). Secondly, no ‘system thresholds’ were surpassed that would have led to a system-wide failure (such as the power network falling below a certain capacity, which then results in a full blackout). However, the occurrence of such scenarios would in general lie within the ranges of possibility, for instance through the occurrence of more intense or more spatially compounding hazard events.

Lastly, looking particularly at case B, where a tropical cyclone event entailed several compounding sub-hazards (wind, and storm surge and torrential rainfalls producing flooding), the importance of explicitly capturing those becomes obvious despite any secondary escalating effects: While strong winds did cause some basic service disruptions, the resulting floods were the main drivers of impacts. This would have been neglected when proxying the event through the wind field only, as is frequently done.

4 Conclusions and Outlook

In this contribution, we demonstrated a flexible approach to study the systemic impacts of compound events interacting with interdependent critical infrastructure systems. The approach was demonstrated on two tropical cyclone wind and flooding compound events in Bangladesh, for five infrastructure systems and basic services. It demonstrated that an event connection, i.e. the modification of impacts through the multiple interplay of system interdependencies and compounding hazards, may not necessarily occur: If events, though temporally compounding, are spatially disjoint enough, and if the sum of individual impacts are not grave enough to tip the system towards a larger failure scenario (such as a wide-spread blackout), compound events may be considered as multiple single events. Vice-versa, this leaves many possibilities for such magnifying impact scenarios to occur Further to that, the present approach lends itself to explore more extreme counterfactual events in future studies, either be magnifying the intensity of the constituent (sub-)hazards and/or the connections between the systems studied – not least with respect to the appraisal of potentially robust measures to strengthen system resilience [14].

The flexibility of the framework to readily study other regions and hazard pairs allows to explore more such events and their impact characteristics. Further, historic case studies which are known for their escalating behaviour due to compound event impacts (such as Hurricane Harvey 2017 in Texas and Louisiana) could serve as a model calibration and validation source.

Acknowledgements

This project has received funding from the European Union's Horizon 2020 research and innovation programme under grant agreement No 821010 and under grant agreement No 820712.

References

1. Thacker, S. *et al.* (2019) "Infrastructure for sustainable development". *Nature Sustainability*, https://doi.org/10.1038/s41893-019-0256-8.
2. Zscheischler, J., Martius, O., Westra, S. *et al.* A typology of compound weather and climate events. *Nat Rev Earth Environ* **1**, 333–347 (2020). https://doi.org/10.1038/s43017-020-0060-z
3. Raymond, C., Horton, R.M., Zscheischler, J. *et al.* Understanding and managing connected extreme events. *Nat. Clim. Chang.* **10**, 611–621 (2020). https://doi.org/10.1038/s41558-020-0790-4
4. Hillier, J.K., Matthews, T., Wilby, R.L. *et al.* Multi-hazard dependencies can increase or decrease risk. *Nat. Clim. Chang.* **10**, 595–598 (2020). https://doi.org/10.1038/s41558-020-0832-y
5. Mühlhofer, E., E. E. Koks, C. M. Kropf, G. Sansavini and D. N. Bresch. (*in review*). "A Generalized Natural Hazard Risk Modelling Framework for Infrastructure Failure Cascades." https://doi.org/10.31223/X54M17
6. Aznar-Siguan, G. and D.N. Bresch (2019) CLIMADA v1: A Global Weather and Climate Risk Assessment Platform. *Geoscientific Model Development* **2** (7): 3085–9. https://doi.org/10.5194/gmd- 12-3085-2019
7. Thacker, S., R. Pant, and J. W. Hall. 2017. "System-of-Systems Formulation and Disruption Analysis for Multi-Scale Critical National Infrastructures." *Reliability Engineering & System Safety*, 167 (November): 30–41.
8. Zio, Enrico. 2016. "Challenges in the Vulnerability and Risk Analysis of Critical Infrastructures." *Reliability Engineering & System Safety* 152 (August): 137–50.
9. Rinaldi, S. M., J. P. Peerenboom and T. K. Kelly, "Identifying, understanding, and analyzing critical infrastructure interdependencies", *IEEE Control Systems Magazine*, vol. 21, no. 6, pp. 11-25, Dec. 2001, doi: https://doi.org/10.1109/37.969131.
10. Ouyang, Min. "Review on modeling and simulation of interdependent critical infrastructure systems", *Reliability Engineering & System Safety*, Volume 121, 2014, Pages 43-60, https://doi.org/10.1016/j.ress.2013.06.040.

11. Arderne, C., Zorn, C., Nicolas, C. *et al.* "Predictive mapping of the global power system using open data". Sci Data **7**, 19 (2020). https://doi.org/10.1038/s41597-019-0347-4

12. WorldPop (www.worldpop.org - School of Geography and Environmental Science, University of Southampton; Department of Geography and Geosciences, University of Louisville; Departement de Geographie, Universite de Namur) and Center for International Earth Science Information Network (CIESIN), Columbia University (2018). Global High Resolution Population Denominators Project - Funded by The Bill and Melinda Gates Foundation (OPP1134076). https://dx.doi.org/10.5258/SOTON/WP00671

13. Knapp, K. R., H. J. Diamond, J. P. Kossin, M. C. Kruk, C. J. Schreck, 2018: International Best Track Archive for Climate Stewardship (IBTrACS) Project, Version 4. NOAA National Centers for Environmental Information. doi:10.25921/82ty-9e16 [accessed 20.08.2022].

14. Bresch, D. N. and Aznar-Siguan, G., 2021: CLIMADA v1.4.1: towards a globally consistent adaptation options appraisal tool, *Geosci. Model Dev.*, **14**, 351-363, https://doi.org/10.5194/gmd-14-351-2021

List of abbreviations and definitions

CI	Critical Infrastructure
NH	Natural Hazard
TC	Tropical Cyclone

SM5 Supplementary 5

Data for Critical Infrastructure Network Modelling of Natural Hazard Impacts: Needs and Influence on Model Characteristics

Roman Schotten, Evelyn Mühlhofer, Georgios Alexandros Chatzistefanou, Daniel Bachmann, Albert S. Chen, Elco Koks; published in *Resilient Cities & Structures*

Abstract. Natural hazards impact the interdependent infrastructure networks that keep a modern society functional. A variety of critical infrastructure network (CIN) modelling approaches are available to represent CI networks on different scales and analyse the impacts of natural hazards. A recurring challenge for all modelling approaches is the availability and accessibility of sufficiently high-quality input and validation data. The resulting data gaps often require modellers to make a plethora of assumptions for specific technical parameters, functional relationships and system behaviours. In other cases, expert knowledge from one sector is extrapolated to other sectoral structures or even cross-sectorally applied to fill data gaps. Those assumptions and extrapolations lead to uncertainty and can undermine the outcomes of valuable CIN modelling approaches aimed at increasing infrastructure resilience. How to overcome data availability challenges in CIN modelling, and how this influences the quality of results, remains questionable. To approach this challenge, a generic modelling workflow is devised featuring six modelling stages commonly encountered in CIN models. Data requirements of each stage are hence systematically defined, and literature on potential sources is reviewed to enhance data collection and raise awareness of the issue. The workflow represents model generation and validation as well as natural hazard impact assessment, recovery and mitigation. Using this workflow, three case studies on CIN impacted by natural hazards, albeit with different modelling purposes, are assessed for data availability challenges. From this, a generalised reflection on the relation between data availability, model purposes, model performance, and aptness of the approach is derived. Finally, there is a brief discussion of how to overcome the challenges of data scarcity, including the use of participatory methods, anonymized data-sharing platforms for CI operators, and event-based impact datasets.

Introduction

Critical infrastructures (CIs) are responsible for the supply of essential services and goods. They are organised in sectors which have intra- and inter-sectoral dependencies. Due to such dependencies within (intra-sectoral) and across (intersectoral) components of different critical infrastructure sectors, critical infrastructure networks (CINs) are formed. Disruptions in one sector can lead to impacts in other sectors and cause chain effects [1, 2]. The role of CIs for society's safety and security receives increasing acknowledgement due to an increasing number of threats such as extreme natural events, military conflicts, global pandemics or cyberattacks.

The purposes that CIs are serving are versatile, and societies' reliance on them is not conceived easily due to complex arrangements and dependencies between CI sectors. This especially applies to densely populated urban environments which sustain themselves due to an equally dense CIN. One way to capture CIs' supply of essential services and goods is utilising models. Invariably, representing the multifaceted purposes of CIs results in similarly multifaceted modelling approaches, on which comprehensive overviews can be found in literature [1 ,3 ,4]. Such CIN models may analyse direct disruptions, caused for instance by natural hazards, as well as indirect disruptions caused by cascading effects transmitted through dependencies [5]. Next to the analysis of disruptions, CIN models are used to develop and quantify measures for every step of the disaster risk reduction cycle [6 – 8].

Invariably, CIN modelling approaches rely on a range of data and information inputs. Data acquisition for modelling inputs poses a challenge, which is also identified by the United Nations [9]. The challenge of gathering input data hinders the potential utility of CIN modelling techniques in contributing to the evaluation and management of resilience in urban environments facing natural hazards. There are several reasons in the lacking availability or accessibility of this data, such as data protection of CI users, data confidentiality of CI operators, sensitivity of CI and their essential services during conflicts or unawareness for the benefits and data needs of CIN models. Despite the challenge in data and information availability and accessibility, CIN modelling approaches are becoming a popular tool for capturing larger-scale interdependent infrastructures, disruption and cascading effects. Lacking data and information is often complemented by assumptions in all stages and data types of the modelling process, which may compromise the quality of the output and thus the reliability of the decision made based on the CIN model outputs. First component for a solution is to bridge the gap of missing data and information. Categorisation of the data types needed for CIN models is the fundamental step required for filling the gap. [10] and [11] outlined the needs of data and methods to support empirical and predictive assessments for CI resilience. But currently very few systematic reviews are available on the types of data needed. Secondly, a discussion about the implications of data availability and accessibility on model characteristics is needed. Model characteristics are further defined as capabilities, attributes and reliability of CIN modelling approaches and their output. Discussions about the impacts of data scarcity on models in general are given such as [12]. Very few discussions focus on how those assumptions are made to overcome data scarcity and how they affect the quality and aptness of CIN model characteristics to make actual judgements. Those exchanges may lead to more thorough data acquisition practices and enable the dialog with potential data providers and lead to better assessment of CIN model results.

The presented work provides a categorisation and explanation of data input types for a more systematic way of thinking about data needs and assumption implications. For each data input type a definition is given as well as literature references to existing data sets if available or approaches in need of this data type. The categorisation is made based on individual stages within CIN modelling workflow. The presented work is delimited in two important dimensions: The purpose that CIN models fulfil define the specific needs for data. As an example: The vulnerability of CIN to cyber attacks and the identification of maintenance needs of infrastructures requires different information and data. In the presented work the limitation is to only consider extreme natural events as impacts to CIN. The various techniques to derive the features of natural hazards such as numerical modelling, data-driven or empirical methods are not outlined in this work, since the focus is on the impact of extreme natural events on the exposed CIN. Another limitation is to focus explicitly on CIN modelling approaches conventionally termed "network-based approaches" [3] or "graph-based modelling approaches" for the gathering of data needs. The represented modelling approaches are further on referred to as CIN modelling approaches. Those approaches have sub-categories such as flow-based network models, which treat the flow of commodities through the CIN as the driving characteristics. Another sub-category which is also included in this work are topology-based network modelling approaches, which concentrate on the functionality of CI assets considering their location in the network as defining characteristics. Other sub-categories for CIN modelling approaches, such as agent-based or system-dynamics-based approaches must be mentioned in this context but are not considered explicitly further on due to their more specific data needs.

In the introduction chapter, the background and motivation of this work were outlined and a short review of literature was presented. The main purpose of the paper is to provide an overview of data needs for CIN modelling. Therefore, a generalised modelling approach is defined and elaborated in stages. Based on every stage, the required input data types are categorised and literature is presented for each data type. It is not intended to represent a risk management framework but only to concentrate on the modelling workflow and the risk analysis. Subsequently arguments are collected on why the data is important for CIN modelling techniques: Three case studies are introduced with a focus on one missing input dataset per category, the assumptions that are necessary due to the missing data and the resulting effects on the model characteristics. The presented work is then discussed and concluded (cf. section 4 & 5).

CIN Modelling Stages & Data

2.1 A Generalised CIN Modelling Process in Stages

As previously mentioned, a wide range of data needs may be encountered throughout different CIN modelling approaches. To capture these in a systematic manner, a broadly formulated and generic multi-stage modelling process is defined, inspired by work stages frequently encountered in studies about CIN network modelling [1, 3, 7]. Each of the stages form a category which is examined separately for their data needs (cf. section 2.2). It is noted that this categorisation is not exhaustive but serves as a starting point for the development of CIN modelling studies. Figure 1 shows those six stages as well as the two overarching stances. The *definition of the model purpose* drives every single stage in the beginning of the modelling assignment and is not necessarily driven by data but drives the data need. The stage of *validation, calibration and plausibility evaluation* overarches the entire process as well since it can be applied to all modelling stages as well. Validation and model purpose thus have a distinctive role in the graphical representation of Figure 1 pointing to every other modelling stage. Additionally, Figure 1 displays that a model can be compiled already by only following the stages until the stage of Impacts of natural hazards, the two stages hereafter are only optional. This is indicated by an additional arrow branching from the path described by the arrows.

Models are by definition a simplified representation of nature or systems. Thus, the first stage of the modelling is outlining the model purpose, which is defined by the intention that applies to CIN modelling efforts. Rather than requiring much data per se, the purpose of each study focuses on the choice of modelling approach and, consequently, data requirements. The purpose frames expectations on the usability and types of results which the model should eventually provide (for instance decision support for strategic planning, information for disaster management, creation of knowledge, awareness building) and specifies users and target groups (such as academic researchers, utility providers, regulators, etc.). All in all, the model purpose is determining other model characteristics such as system boundaries, potential output and the target group. An in-depth discussion on the relation between model purpose, data needs, data availability and model characteristics is given in section 3.

The next stage is defined as the *mapping of infrastructures assets*. The intention of this stage is to set up a network representation of the CI under study, considering their topological characteristics. This includes the transformation of information on physical infrastructure components into network elements such as nodes and links or vertices and edges. Nodes represent individual entities and links represent the dependencies between those entities.

Consecutive to the asset mapping is the *quantification of dependencies*. In this stage, dependencies within CIN (intra-sectoral) and in between different infrastructure networks (inter-sectoral) are identified, quantified, and included as explicit network model elements.

The next step is the *quantification of CI services* for the network assembled. The objective of this stage is to obtain a quantifiable extent of the service levels provided by the CIs under study, including information on the service area, recipients of the services, and demand patterns for these services.

In the stage of *impacts of natural hazards*, the exposure of infrastructure assets to natural hazards, and their consequences, are considered. Knowledge is needed on the area and type of natural hazards causing structural damages, as well as on the impact-functionality relationships linking infrastructure damage to their ability to provide their services.

The successive stage deals with the *appraisal of adaptation measures*. The target of this stage is to evaluate the effect of measures (designed for adaptation, mitigation, or other purposes), implemented at any potential level of the system under study (i.e. at infrastructure network components, at dependencies, at the network structure, etc.), on a specified target metric.

Approximating the steps of the disaster risk reduction cycle, is done in the following stage *determination of response and recovery*. The objective of this stage is to analyse post-disruption behaviour of the modelled system, and its trajectory until reaching a certain performance state (such as pre-disaster service levels, or a new status quo). Not considering a response and recovery will lead to an inaccurate representation of disruptions and ultimately an incomplete representation of CINs under the impact of natural extreme events.

The final stage is the *validation, calibration and plausibility evaluation* stage of the individual stages before and refers to the examination of the system behaviour with sufficient accuracy. The stage can consist of the calibration of input parameters, the checking for plausibility or the verification of input and output data [13, 14]. Several model validation approaches exist [15, 16], which entail different data requirements. Usually, it is carried out by comparing field or experimental data to the model output, referring to the same (or a sufficiently similar) scenario. Finally, it must be noted that model validation should also be carried out according to the purpose of the model, rather than aiming to achieve a perfect representation of the studied systems.

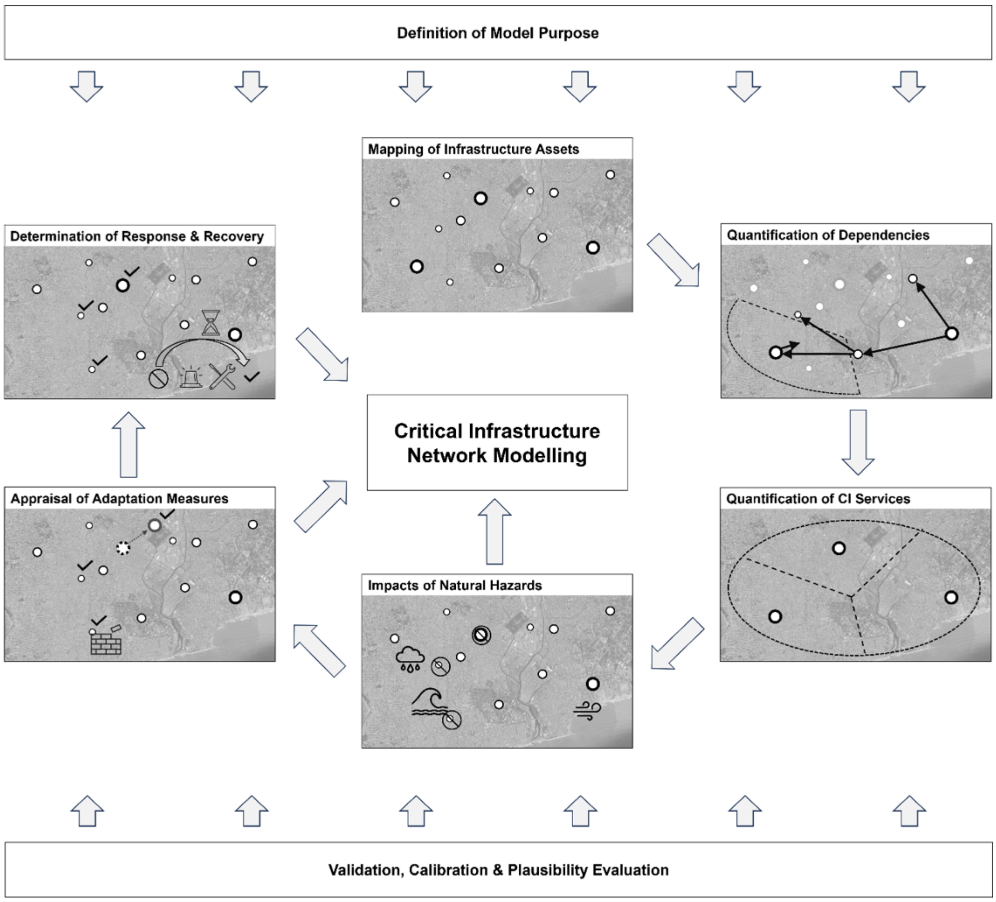

Figure 1: Generalised stages of critical infrastructure network modelling for hazard assessments including overarching stances of model purpose and validation.

2.2 Data Needs Derived from CIN Modelling Process Stages

Grounded in the stages of the generalised modelling process defined in section 2.1, an in-depth literature review is taken to collect frequently occurring data needs, types and if available show potential data sources. Those data types are introduced for every modelling stage as seen in Figure 2. Every icon indicates a type of data and information that can be relevant for the CIN modelling.

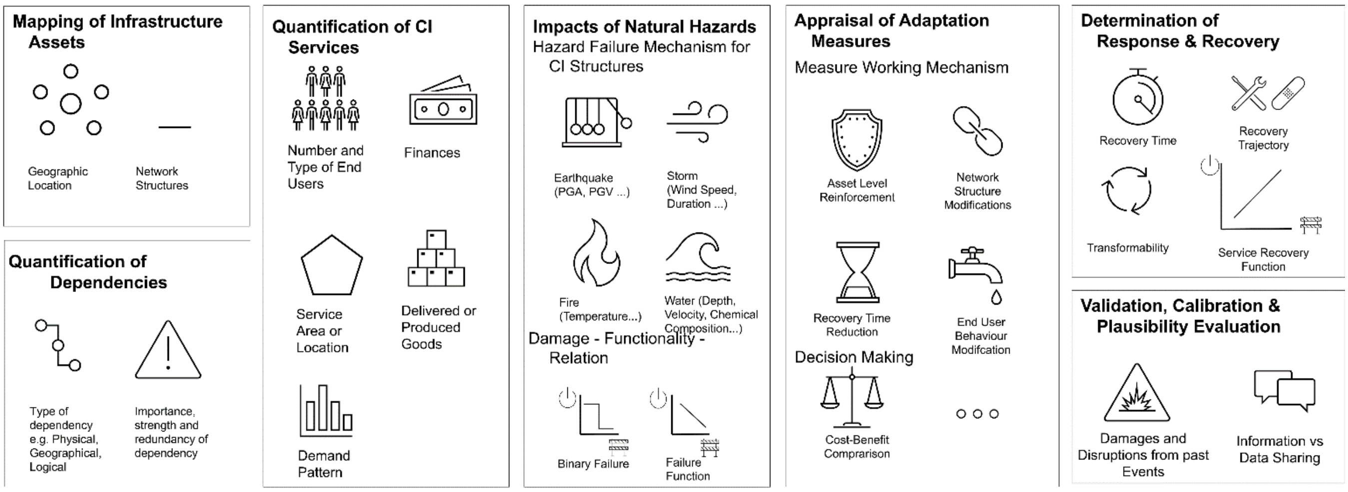

Figure 2: Data types for critical infrastructure network hazard modelling categorised by modelling stages.

2.2.1. Mapping of Infrastructure Assets

Spatially explicit modelling studies start out with a need for geospatial information on CI component locations as point elements and occasionally as polygons as well. Depending on the spatial scale and geographical region of interest, availability of such information is highly varied: While infrastructure location data may be readily accessible, curated and openly provided through official (e.g. governmental) sources - as by the *Homeland Infrastructure Foundation-Level Open Data* of the U.S. Department of Homeland Security [17] or by the *GeoPortal* of the Swiss Federal Administration [18], the only way to obtain infrastructure data in less affluent regions may be reliance on crowd-sourced mapping platforms such as OpenStreetMap, with often unknown quality and completeness ratings [19]. Besides regional differences in data availabilities, certain infrastructure sectors are notorious for data scarcity: Road infrastructure, for instance, is relatively well mapped and available [20] since the availability of its location is a prerequisite for its usage. Many sub-terrain components tend to have mapping gaps, which impedes large-scale risk analysis, as for instance common in the water sector [21]. Further data scarcity concerns arise from resolution issues, i.e. when detailed sub-components of infrastructure networks are required for analyses, as opposed to a more simplistic reliance on high-level components. For instance, when representing the power grid through different types of power plants, substations, transformers, high-and medium voltage transmission lines, power towers, low-voltage distribution lines, poles, etc. instead of mapping simply the most important transmission lines and plants. In case of missing data sources workarounds are applied depending on the model purpose. In case a model is generated to develop and test a modelling framework e.g. the generation of synthetic infrastructure data has been used among others in [22, 23], machine-learning based inference of infrastructure data for the global power transmission grid [24], or even omission from the scope of study [21].

2.2.2. Quantification of Dependencies

Since the seminal work of [1] on the importance of dependencies among critical infrastructures, many frameworks on categorising dependencies have been developed [3, 4]. However, data is needed to identify dependencies in the first place and enable the consideration of potential chain reactions. Empirical approaches have focused on a range of methods such as expert judgement and media coverage [25, 26], yet to date no comprehensive dependency databases exist which thoroughly document these (cf. [27] for a European-wide effort to build one). The level of detail for such identification efforts is often limited by the resolution at which utility providers share data [28]. Deductions of dependencies often remain at a sectoral scale [29, 30], which does not link appropriately to the resolution of many CIN modelling approaches. Further, quantification of the hence-identified dependencies is often summarised under terms such as “coupling behaviour” [1] or “coupling strength”. Ideally dependencies should incorporate a notion of input quantities at the supporting side which relate to output quantities at the dependent side, and of the degree to which certain impacts on a dependency source propagate down to a dependency target. Quantification efforts have proven data-intensive, relying on time-dependent disruption and restoration data [28, 31]. While such coupling behaviours are sometimes implicitly quantified through (lack of) redundancy in the network topology, or through failure tolerance threshold attributes, deterministic and binary dependency formulations still prevail due to a lack of refined enough data to capture more elaborate dependency relationships.

2.2.3. Quantification of CI Services

Per definition, CIs provide essential services to a number of end-users, including population, businesses or other infrastructure. The performance provided by infrastructures can be expressed not only in terms of services but also in terms of goods. However, in presented work, only services will be mentioned. As CIN modelling is usually concerned with impact estimation, a multitude of data regarding CI services are necessary. Firstly, knowledge about the characteristics of the population, including their number, socio-economic status and vulnerabilities, served from a particular infrastructure asset is required. Moreover, data about the characteristics of businesses and other infrastructure assets served could also be needed. In the absence of detailed data, a number of substitute techniques are commonly employed, such as the estimation of a service area using geometric methods e.g. Voronoi decompositions or shortest path algorithms, [32 – 35]. Voronoi polygons can also be used for the dependency quantification as done in [7]. Other options the use of surveys [36], or the use of aggregated customer and census data [37]. Additionally, service demand pattern data may also be required both for asset functionality determination as well as for impact estimation [23], especially when examining societal impacts of disruptions [38]. While sufficiently accurate estimations exist for certain CI services such as water distribution networks [39, 40], they may be more difficult to obtain for other CI services such as emergency services or the financial sector. CI service data as defined herein are usually difficult to obtain either due to legislative restrictions, economic competition or general absence. As a result, most studies in the scientific literature resort to a number of assumptions and inference approaches.

2.2.4. Impacts of Natural Hazards

From a CIN modelling perspective, it is important to capture when and how individual infrastructure assets subject to natural hazards fail and translate this direct asset-level failure to system-level indirect failures. It is noted that failure does not necessarily imply a binary state as commonly used [41], but can also refer to reduced functionality. Asset damage or failure is a product of complex interactions between the characteristics of the asset as well as those of the hazard considered [42], making failure identification a data-intensive task. In practice, asset damage is usually linked to certain hazard parameters (e.g. via appropriate curves) according to the type of asset examined. These parameters may vary according to the infrastructure or hazard considered. For example, in the case of flooding a range of hydrological characteristics can be considered [43], including whether the asset is flooded or not [44], inundation depth [45], water velocity [46], flood duration [47] or water chemical composition, although inundation depth is the most commonly used parameter in practice [48]. In the case of earthquakes, fragility curves linking element damages to ground motion parameters such as peak ground acceleration (PGA), peak ground velocity and peak ground displacement among others [49] are commonly employed. Additionally, insights on how damages translate to service or functionality reduction are needed. Next to the identified hazard failure mechanisms also storms and fire have to be mentioned. Several functionality mechanisms are being considered in practice, such as binary functionality states [50], discrete functionality states [51, 52] or continuous functionality [53]. These mechanisms are infrastructure and hazard specific. A binary state realistically represents the failure of electric power assets under a flood scenario, while a transportation network requires a continuous functionality representation. Consequential is the consideration of multi-hazards which may complicate infrastructure response further [54]. A simple superposition of the previously mentioned response attributes may not suffice for multi-hazard environments since a compound event could either have more severe impacts on the disruption or also be the same compared to a singular event. The disruption functions thus have to be generated individually for each multi-hazard-sector combination.

Finally, the exposure to natural hazards may not be described deterministically only, but under consideration of extrinsic uncertainties e.g. meteorologic uncertainties and intrinsic uncertainties e.g. resulting from a system's inherent variability. Currently, a lack of comprehensive datasets regarding infrastructure failure under a multitude of hazards is a bottleneck for risk and resilience analyses.

2.2.5. Determination of Response & Recovery

Modelling the response and recovery process of interdependent CIs naturally relies on most of the aforementioned data to represent the interdependent infrastructure system itself, yet requires various additional data: component repair times [55]; quantitative relationships between repair state of components and service provision levels [56] - conceptually the inverse of the damage-functionality relationship mentioned above-; data on response actions including work capacities and repair priorities or the rerouting of CI supply flows [57]. In general, this refers to the transformability of infrastructure assets under the stress of natural hazards. Frequently used component repair time tables are partly available through the technical manuals of FEMA's Hazus Program [58], or from ATC-13 data [59] for a wider range of buildings pertaining to different social function classes. Such tables deliver a partial insight in terms of infrastructure components covered and may not always be directly transferable to regions other than the US for which they were designed. Given the complexity of the task, many recovery studies tend to remain at sectoral level rather than at infrastructure component levels, and do not incorporate the multitude of uncertainties involved in these processes [60].

2.2.6. Appraisal of Adaptation Measures

Commonly, the viability of adaptation measures is evaluated by trading off benefits against costs, requiring data on either side and at various scales of a network. Multi-criteria analyses and most commonly cost-benefit analyses are generally performed for many types of hazards and individual infrastructure sectors [61 – 63]. As measures may act on different aspects of the risk chain, such as reducing a component's vulnerability or exposure to a certain hazard, or on the hazard intensity itself, data is needed to parametrise the working mechanism and hence quantify risk aversion benefit adequately. Evaluating measures with regards to their co-benefits and costs on other CI sectors require adequate parametrisation of the above-mentioned dependency relationships. The latter is particularly crucial when evaluating the effect of system-level adaptation measures [56]. These measures for instance aim at enhancing resilience through modifying dependency relationships instead of fortifying individual components. Examples for system-level adaptation measures are increasing redundancies, reducing failure propagation behaviour, etc.), or modification of end-user demands and response capacities. Drawing on the level of destruction and disruption from real-world extreme events, it may however be concluded that the performance of adaptation measures is still rarely evaluated at a system-level, nor do measures tend to target system-level adaptation [55].

2.2.7. Validation, Calibration & Plausibility Evaluation

In the context of modelling CI response under hazard scenarios, studies focus on collecting field data from past events. Such data might include print-media and social media or infrastructure and disruption damage and disruption reports of past events [35], utility providers' service outage statistics and restoration timelines [28, 64] and reports of response measures taken [65]. Methodologies requiring data collected from expert and stakeholder elicitation processes may also be employed [66]. It is important that these datasets are of sufficient quality in terms of reliability, consistency, completeness and detail, which in turn requires additional verification. In general, there is a lack of established CI model validation approaches in the scientific literature and validation of CI models is rarely comprehensive due to the unavailability of relevant, homogeneous data.

Data Scarcity Influencing CIN Model Characteristics

3.1. Introduction of Case Studies with Varying Model Purposes

Three specific case studies are introduced which represent the experience from the authors and will be used to discuss the effect of data scarcity on CIN models. The CIN model case studies are defined by four model characteristics in Table 1:

The first case study briefly summarised in Table 1 concerns a continental-level earthquake risk assessment for Europe with the aim of identifying vulnerable geographical hotspots and to quantify the vulnerabilities that are induced by dependencies between CI sectors. Similar case studies are present in the scientific literature [67]. While CI networks are represented at an asset-level, simplifications regarding the detailed structures of the various networks are made. Similar simplifications are made regarding the ways that the various CI sectors are connected and how their disruptions influence the population.

The model purpose of the second case study is to identify the flood risk as population time disrupted per year for CIs next to other tangible flood consequences such as economic damages and the population affected or endangered. The analysis is based on a CIN model based on [68] and is additionally used to compare the benefits of potential mitigation measures and allow for an improved decision making. The specific model purpose of flood risk management could be generalised by being applied to other natural hazards such as droughts, storms, bushfire etc. Thus, the generalised model purpose would be defined as *hazard risk management*. In terms of abstraction from the real complexity of CIN, this type is more differentiated with regard to the sectors than the first case study, but has a smaller spatial boundary.

The third case study is a sectoral adaptation study, designed to decrease healthcare access disruptions across the population in the face of multi-hazard (particularly strong winds and flooding) events [69]. The analysis is based on an integrated natural hazard risk and CIN modelling approach [35], and evaluates five adaptation measure packages, which are either focused on resilience-enhancing measures to a single CI type, target multiple CIs at once, or modify the dependency relationships among CIs. While real-world data is used to map the interdependent CI systems and hazards, the stylised parametrisation of adaptation measures intends to exemplify trade-offs and benefits of component level against system-level measure packages to prevent service disruptions.

Table 1: Three exemplary case studies using CIN modelling, featuring a wide range of model purposes, system boundaries and outputs. Those case studies serve for the further examination of data

Case Study Area	Case Study I. - European continent	Case Study II. - Accra, Ghana	Case Study III. - Mozambique
Model Purpose	Continental level **earthquake risk-assessment**; identification of **vulnerable** hotspots; quantification of **interdependency**-induced vulnerability	Identifying **flood risk** for critical infrastructures in Accra including a benefit analysis of **potential CI measures**	Evaluate several **adaptation measures** to reduce **healthcare access disruptions** in the face of wind & flood **multi-hazard** events
System Boundary	Spatial: **Continental** level (Europe); CI sectors: **energy, gas, water, telecommunication**	Spatial: **catchment** area of the Odaw river and four surrounding catchments, CI sectors: **energy, water, telecommunication, healthcare, emergency services**	Spatial: **Country** level; CI sectors: **roads, power, telecommunication, education & healthcare**;
Output	Network fragility **curves**; **Geographical** distribution of disruptions and of **affected** population	**Area** of disrupted CI users per sector, **number and time of disrupted CI users** per year and sector, a **comparative overview** of the previous point for **potential CI measures**	Number of **avoided user-disruptions**, incl. co-benefits on other types of service disruptions (power outages, education disruptions, ..)
Target Group	Decision makers; Academics	**Decision makers** from public administration and **CI operators**	Academics; UN Habitat & Ministry of Health

3.2. Repercussions of Data Scarcity for Every Modelling Stage in the presented Case Studies

Exemplifying the introduced modelling stages (cf. section 2.1) and data requirements (cf. section 2.2) on the presented case studies (cf. section 3.1), Table 2 briefly illustrates typical repercussions of data scarcity for the corresponding three generalised model purposes. Table 2 does not claim that the collected repercussions always occur for the generalized model purpose types. It merely serves to highlight that this is one of the possible repercussions. For brevity, only one instance of lacking data and its consequence for the modelling process is discussed per stage and case study. Additionally, it is noted that the three given model purpose types are not a complete picture of all possible model purpose types but only three possibilities. A brief overview is given on the content of Table 2 for every modelling stage. In the stage of assets mapping all case studies receive incomplete or partial information about specific CI sectors. This leads to a coarse representation of the network and its sectoral hierarchy as well as higher uncertainty of the results. In the stage of dependency quantification, the general issue is missing information about dependencies. This materializes in assumptions that need to be made and overlooked redundancies that should not be disregarded. For the stage of quantification of CI services, the level of detail of the input that is necessary for the specific model purposes is a challenge. Additional challenge is to retrieve the same metric for different CI sectors, resulting in challenges for the comparability of scenario calculations.

For all case studies different problems occur in the stage of natural hazard and operational limits and the type of challenges are determined by the model characteristics. First case study mentions that no functionality-impact relation is available for the earthquakes. Second case study is missing sector specific flood-depth-functionality relations and the third case study is missing a combined flood depth and wind speed functionality relation. All missing information are resulting in assumptions that lead to a potential over- or underestimation of the final results. In the response and recovery stage desired metrics are missing to quantify the recovery after a CI disruption. But also the initial information about the mere presence of emergency structures is missing and thus the response is also not represented appropriately. For the measure appraisal stage, the issue concerns the identification of potential measures alone. But in case those measures are identified, as in the second case study, the metrics to quantify the potential costs are missing. For all three case studies the validation stage was hindered by data availability

Table 2: Repercussions of data scarcity in every modelling stage, illustrated on three different model purposes, generalised from exemplary case study experiences in Table 1..

Model Purpose Type	(A) Hazard Hotspot Assessments	(B) Hazard Risk Management	(C) Sectoral Adaptation
(1) Mapping of Infrastructure Assets	**Network structures** *Only partial information available.* Several assets of the examined networks may be missing or not correctly placed, introducing some uncertainties in the results.	**Network structure of electricity grid** *Only substation information available.* Coarse granularity of electricity sector causes inaccurate results because electricity transformers are not represented.	**Healthcare sites and types** *Many unmapped healthcare sites, unclear service offerings.* Faulty baseline system.
(2) Quantification of Dependencies	**Connections or dependencies between infrastructure** *No information regarding connections.* Assumptions made during this stage introduce some uncertainties in the results.	**Redundant connections in between nodes** *No information about redundancies.* The disruptions in the CIN model will be overestimated due to missing redundancies.	**Dependencies between power network and healthcare network** *No information available regarding the extent of dependency on the power sector.* The disruptions in the CIN model will be overestimated due to overestimation of healthcare site dependencies on the power grid.
(3) Quantification of CI Services	**Population served by each considered asset** *No available information regarding detailed numbers of population served.* Only estimations of population affected are possible.	**Metrics to quantify CI sectors in multi-sectoral network** *Not all sectors give the same metric for CI disruption.* Results of the multisectoral CIN model cannot be compared with each other.	**Socio-economic constraints to access healthcare services.** *No available high-resolution information on who is (financially) able to seek healthcare support.* Over/under-estimation of potentially impacted population.
(4) Impacts of Natural Hazards	**Earthquake damage-functionality relation** *Difficulty in obtaining detailed damage-functionality data for the considered assets.* Binary functionality considered via fragility functions, which may differ from real infrastructure response.	**Water depth-functionality relation** *No data or information for the range of sectors available and the area of interest.* The water depth - functionality relation is set to be binary. Disruptions and their sensitivity might be overestimated.	**Parametrization of combined wind- and flood damage - functionality curves for infrastructures.** *No data on the effect of structural damage onto the functionality of local infrastructures.* Binary and arbitrary damage-functionality thresholds for all infrastructure components may under/-over estimate impacts.
(5) Determination of Response & Recovery	**n/a**	**Recovery time of communication towers** *Sector specific recovery times from other survey areas are extrapolated to unsuitable case study areas.* Availability of spare parts differs in this area due to higher frequency of flooding events. The resilience of this sector is underestimated.	**Clarification on the availability of backup generators for response** *The presence of back-up generator and their associated start-up and run times is not available* Potential damages could be overestimated and potential measures could be suggested that might be in place already.
(6) Appraisal of Adaptation Measures	**n/a**	**Effectiveness of potential measures** *No knowledge about the applicability of a potential measure due to missing information about the technical set up of a CI element.* Measures are tested for effectiveness that might not be feasible at the selected network element.	**Applicability and cost of potential measures** *Unclear (financial) means, cost and local fitness for purpose of certain measures.* Measures may be not implementable, or not as effective as modelled.
(7) Validation, Calibration & Plausibility Evaluation	**Documented failures for similar earthquake scenarios** *No available data at the level of examined detail.* Accurate model validation is not possible.	**Area of disrupted people during historic events** *Not available only individual experiences or anecdotal stories.* No Calibration of model parameters possible.	**Documentation of historic events along the entire impact chain.** *Limited availability of exact hazard footprints, structural damages, functionality failures, service disruptions.* Only anecdotal validation or plausibility valuation, no calibration possible.

3.3. Influence of data scarcity on CIN model characteristics

As the compilation in Table 2 illustrates, absence of data impacts model inputs and potential outputs. This invariably affects a range of model characteristics, which should be carefully evaluated under consideration of the model purpose, to critically reflect its fitness for the intended purpose. Without claim of completeness, a few crucial model characteristics and the implications of data scarcity onto those are discussed below, extending the mathematically driven characteristics of networks as introduced by [70].

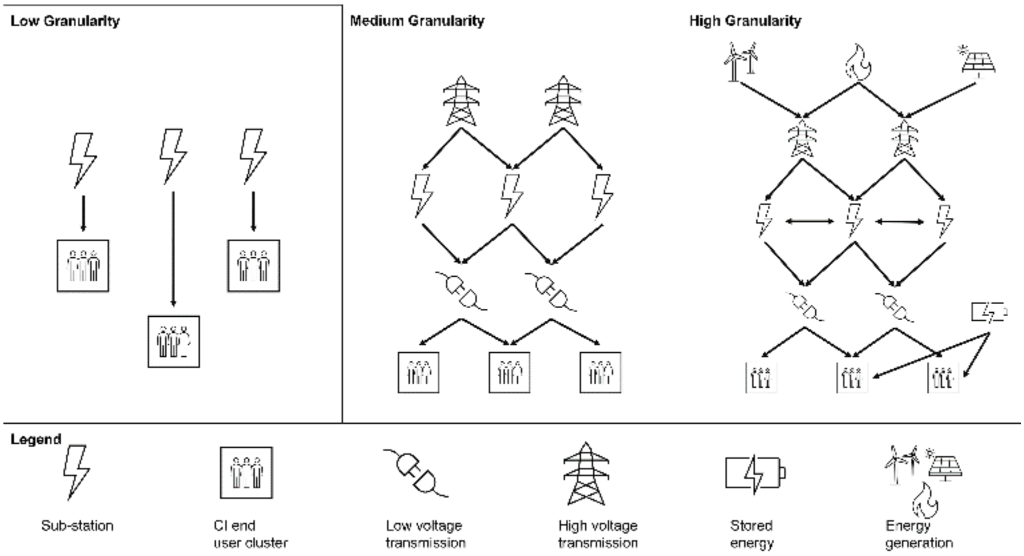

Figure 3: Amount of data and information available affects the resolution (granularity) with which CIs, CI dependencies and services can be modelled.

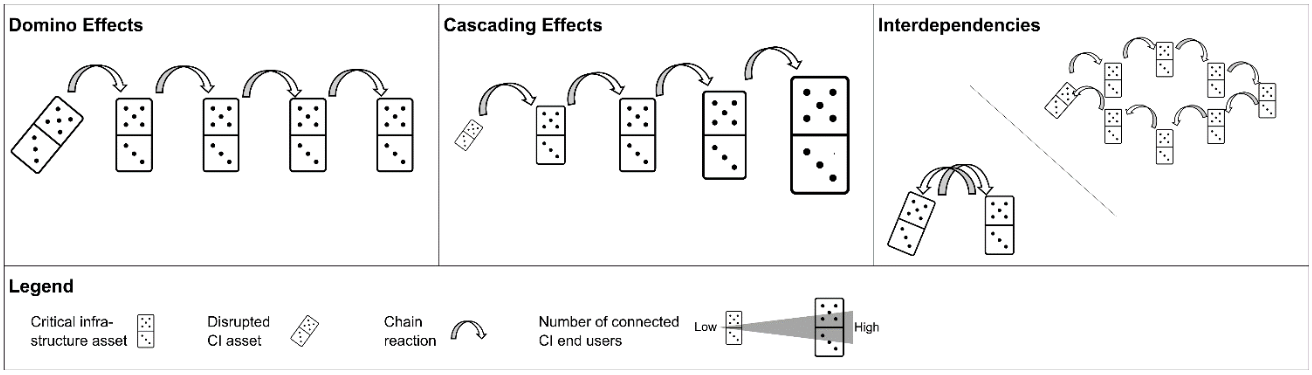

Figure 4: Types of failure mechanisms or chain reactions, which can propagate through disrupted CINs, adapted from definitions in [69]. Depending on data availability, different failure mechanisms / chain reaction types may be captured.

The *granularity* describes how fine or coarse a network model resembles the details of CI supply systems. Figure 3 provides an illustration demonstrating one possible scale from low to high granularity for the electricity sector. The figure does not depict the exclusive approach to coarse granularity; for instance, dynamics encompassed by a coarser granularity can also be cross-sectoral. The granularity is intricately linked to the accuracy and complexity of CIN models. Invariably, the amount of data and information available influences how accurate and complex a model can be and how granular it may or should be resolved. The granularity is adjusted on a precision scale according to the model objectives. Thus, models of type A tend to attain their model purpose using a coarser granularity than e.g. models of type C, which generally may require a finer granularity. When comparing the examples in cell 1A and 1C Table 2 this is underlined as well.

Another CIN model characteristic linked to the granularity as well as the accuracy is the *ability to resemble chain reactions*. The German Federal Office of Civil Protection and Disaster Assistance (BBK) suggests a scale of three types of chain reactions which are elaborated in Figure 4 [71]: First type of chain reaction refers to the *domino effect* where disruptions are propagated through critical infrastructure assets through their dependencies. *Cascading effects* describe a type of chain reaction similar to the domino effect but underline the progressiveness of the consequences of the disruption. The last type of chain reaction features *interdependencies*, which refer to the mutual reliance or connection between different CI assets. Depending on the granularity as well as the level of detail of dependency information those different chain reaction levels are representable in CIN models. Table 2 introduced in cell 2A the fact that all of those dependencies had to be assumed and thus have a lot of uncertainty. The resemblance of chain reaction might thus be inaccurate.

The *communicability* of CIN models describes the ability to transfer the methodology as well as potential outputs to the desired target group. Absence of information and data often leads to the replacement through assumptions and heuristics - which often happen implicitly or may not be kept close track of. More assumptions may lead to lower communicability of how a model was set up and reduce trust in its outputs. This is one factor hindering the process of testing measures in the CIN model environment as described in Table 2 cell 6B.

Existence of many assumptions due to data scarcity may hamper *reproducibility* of a modelling approach by other researchers. Further, data availability and assumptions for certain geographic or system boundaries, for which a model was initially designed, may not extend to other regions and systems, limiting its transferability. Some modelling approaches may be more versatile and flexible with respect to underlying premises than others, which feature a higher level of hard-coded assumptions or which are calibrated against specific, non-widely available datasets.

Discussion & Outlook

Current CIN modelling techniques can already supply advice for the consequence assessment and mitigation planning, but the more accurate, complete, relevant, consistent and accessible data is, the better model results can become. The added value of this work lies in collecting the data requirements of CIN models. This is achieved through the systematic division of data categories and associated data types based on modelling stages. Further possibilities of categorisation, for example based on sectors or importance for models, are conceivable. These new categories have the potential to elicit further data types that have not been considered so far. Therefore, this work does not claim to be a complete collection of data needs but is intended as a propulsion for the discourse about data availability of CIN models.

Wording remains a challenge in the field of hazard modelling for CIN models since two fields of expertise (impact modelling and engineering of CIs) meet and do not share the same established terminology. Although the network models considered in this work have been limited to the area of graph-based CIN models it remains an issue to identify the right terminology for the interaction of data scarcity and CIN models. The characteristics previously defined are a first approach to describe the interface of those fields under consideration of the CIN models capabilities and limitations. More efforts need to be invested in defining a generally accepted terminology for a range of network characteristics such as fidelity, granularity, sensitivity or the representation of cascading effects to close the gap between impact modelling and CIN modelling.

In the surrounding of this work, the category of CIN model purposes has been defined and filled with three examples along a scale from (1) hazard vulnerability hotspot assessment to (2) hazard risk management to (3) sectoral adaptation. These examples seek the representation of network models on a scale comparable to a spatial scale (global, national, regional and local) suggested by [72] for flood risk assessments including typical model characteristics for each scale level. In the future, scales like these need to be defined as well for the other CIN model characteristics with a clear division of levels as well. The definition of these levels is not about setting a better or worse value but about being able to accommodate the subdivisions defined by model purposes and to enable differentiation of the characteristics.

One concomitant of data scarcity are assumptions made by CIN modellers. Those assumptions can be supported by from CI operators and scientists alike through expert knowledge. Nevertheless, assumptions influence the network model's characteristics in their performance. Although commonly used in CIN models, current studies often lack sufficient communication or quantification of the uncertainty resulting from assumptions, unlike other fields where such practices are more prevalent [73]. A range of possibilities are available to modellers to quantify or counter uncertainties, beginning with uncertainty analysis [74], sensitivity analysis, anecdotal verification with expert knowledge or at the least an overview of made assumptions as done in [35]. It must, however, be noted that uncertainty and sensitivity analyses often in turn also rely on more input data, for instance for validation and setting of plausible bounds for the tested parameters as an input. The additional communication and quantification of uncertainties have the potential to enhance trust in CIN model results and, consequently, strengthen CIN modelling methods as a whole. When it comes to presenting the results, uncertainties must be communicated appropriately to establish trust with the intended recipients and allow for robust decision making [75]. In the case studies that were presented, CI stakeholders, particularly CI operators, were involved as recipients or the least CI operators are key partners in the development and implementation of measures. In any case, trust is of significance to ensure sufficient eagerness. An early and ongoing participation of CI stakeholders in the process of the CIN hazard assessments can be beneficial in all stages of the modelling process [26, 56]. Not only will this create a greater identification and trust in the potential results but additionally has a huge potential of acquiring qualitative information or sometimes even quantitative information, in perspective: data.

An issue that persists and needs to be addressed as well in participatory settings is the manner in which data is conveyed or provided. A range of options have been tested by US Federal National Laboratories (e.g. Sandia Lab, Los Alamos Lab etc.) but the knowledge is not publicly accessible for security reasons. Opposite to these options is the openness to share most of its infrastructure data as done in New Zealand for example [76]. Therefore it seems that the willingness to share data varies a lot and discussion is ongoing. The question remains whether the sharing of data or information itself is proven to cause more disruptions on CIN due to physical or cyber-attacks compared to disruptions from natural hazards that cannot yet be recorded or recorded inadequately due to a lack of data exchange.

Even though some data sources were compiled in this work, gaps remain. One suggestion is to collect more impact data in the direct aftermath of disaster events either in person or through social media. Another suggestion is to establish platforms for CIN datasets accessible for research including a range of prerequisites from users and providers: (1) consideration of previously defined data types needed, (2) awareness for the level of detail that needs to be published if this data is used by CIN modellers, (3) sensibility for privacy of CI users. Despite the strong case for more and better data and information in CIN modelling, it is paramount to critically reflect on the need for complexity and detail, depending on the purpose for which a model is built. In many cases, the unavailability of detailed data does not hamper the purpose of the developed CIN models. Whether a model aims to create new knowledge (models for understanding), or to create new capabilities within its user-space (models for action) may require different levels of upfront data availability, since in the latter scenario users may provide those themselves on-the-fly, as deemed necessary. Further, societal context and ethical uncertainties may influence data requirements - some societies and studied problems may require higher levels of resolution and certainty to justify action than others.

Conclusion

CIN modelling offers approaches to better assess and manage natural hazards. Data inputs limit and determine the value of CI modellers' "offerings" to specific assignments. This work identifies overarching similarities in the modelling process and defines eight stages and associates each stage with data types. The typification of those data needs has been documented and the potential data sources for all data types are pinpointed, or if unavailable, gaps are identified. Three purpose-driven classes of CIN models have been distinguished, setting it apart from the pure size-driven classification (e.g. local, regional, national, global). For the model purpose type case studies of CIN models have qualitatively shown the influence of data scarcity and the resulting assumptions at each modelling stage.

This work increased the level of understanding regarding CIN modelling and the difficulties faced by both CI operators and CI modelling experts alike. The modelling stages and data types defined enhance the possibility to communicate about the data needs and assumptions in participatory settings. On the other hand, an orientation is provided for network modellers at an early stage of a model setup including potential data sources. Additionally, CIN modellers are encouraged to disclose uncertainties in their methods by delivering examples on how data scarcity influences network characteristics. In the end, this contribution is advancing the potential of CIN models to be utilised mutually by research and practice.

The work provided, enhances CIN modelling techniques by clearly outlining their data needs based on modelling workflow stages and provides a literature review that identifies potential data sources or examples in practise or research. Ultimately, this leads to the enhancement of analyses and evaluation methods for a resilience-based planning of urban environments under consideration of CI services.

Funding

This research was partially funded by Germany's Federal Ministry of Education and Research within the framework of IKARIM and the PARADeS project, grant number 13N15273, the ARSINOE project (GA 101037424) and the MIRACA (GA 101093854) under European Union's H2020 innovation action programme.

Acknowledgement

Roman Schotten: conceptualisation, methodology visualisation, writing - original draft; Evelyn Mühlhofer: methodology, writing - original draft; Georgios Alexandros Chatzistefanou: methodology, writing - original draft; Daniel Bachmann: writing - review & editing; David N. Bresch: Funding acquisition; Albert Chen: writing - review & editing; Elco Koks: writing - review & editing; During the preparation of this work the authors used GPT-3.5 from OpenAI in order to rephrase specific statements. After using this tool, the authors reviewed and edited the content as needed and take full responsibility for the content of the manuscript.

Relevance to Resilience

Impacts on critical infrastructure (CI) assets cascade through their dependencies from and to other CI assets. CI network modelling methods are one viable tool to consider these cascading effects.

When addressing the resilience of infrastructure, it is essential to consider the dependencies within a network. Different measures, each with a variety of operating principles, need to be tested for their potential to increase resilience. CIN (Critical

Infrastructure Network) modelling methods have proven to be valuable tools for quantifying CI response, reconstruction, protection, and adaptation measures.

This work contributes to unlocking the potential of CIN modelling methods by classifying and identifying data needs and discussing the implications of data scarcity on model performance.

References

[1] S. M. Rinaldi, 'Modeling and simulating critical infrastructures and their interdependencies', in *37th Annual Hawaii International Conference on System Sciences, 2004. Proceedings of the*, Jan. 2004, p. 8 pp.-. doi: 10.1109/HICSS.2004.1265180.

[2] M. Korkali, J. G. Veneman, B. F. Tivnan, J. P. Bagrow, and P. D. H. Hines, 'Reducing Cascading Failure Risk by Increasing Infrastructure Network Interdependence', *Sci. Rep.*, vol. 7, no. 1, Art. no. 1, Mar. 2017, doi: 10.1038/srep44499.

[3] M. Ouyang, 'Review on modeling and simulation of interdependent critical infrastructure systems', *Reliab. Eng. Syst. Saf.*, vol. 121, pp. 43–60, Jan. 2014, doi: 10.1016/j.ress.2013.06.040.

[4] W. Sun, P. Bocchini, and B. D. Davison, 'Overview of Interdependency Models of Critical Infrastructure for Resilience Assessment', *Nat. Hazards Rev.*, vol. 23, no. 1, p. 04021058, Feb. 2022, doi: 10.1061/(ASCE)NH.1527-6996.0000535.

[5] S. Thacker, R. Pant, and J. W. Hall, 'System-of-systems formulation and disruption analysis for multi-scale critical national infrastructures', *Reliab. Eng. Syst. Saf.*, vol. 167, pp. 30–41, Nov. 2017, doi: 10.1016/j.ress.2017.04.023.

[6] United Nations, 'Sendai Framework for Disaster Risk Reduction 2015 - 2030', 2015. Accessed: May 16, 2023. [Online]. Available: https://www.undrr.org/publication/sendai-framework-disaster-risk-reduction-2015-2030

[7] U. D. Ani, J. D. McK Watson, J. R. C. Nurse, A. Cook, and C. Maples, 'A review of critical infrastructure protection approaches: improving security through responsiveness to the dynamic modelling landscape', in *Living in the Internet of Things (IoT 2019)*, London, UK: Institution of Engineering and Technology, 2019, p. 6 (15 pp.)-6 (15 pp.). doi: 10.1049/cp.2019.0131.

[8] R. Schotten and D. Bachmann, 'Integrating Critical Infrastructure Networks into Flood Risk Management', *Sustainability*, vol. 15, no. 6, Art. no. 6, Jan. 2023, doi: 10.3390/su15065475.

[9] UNDRR, 'Addressing the infrastructure failure data gap: A governance challenge', 2021. https://www.undrr.org/publication/addressing-infrastructure-failure-data-gap-governance-challenge (accessed May 09, 2023).

[10] J. Johansson and P. Månsson, 'Data and methods related to major accidents and crises : Empirical and predictive approaches focused on disaster risk management, critical infrastructure resilience & GIS', Swedish Civil Contingencies Agency, 2020. [Online]. Available: https://rib.msb.se/filer/pdf/29975.pdf

[11] V. Ramachandran, S. Long, T. Shoberg, S. Corns, and H. Carlo, 'Post-Disaster Supply Chain Interdependent Critical Infrastructure System Restoration: A Review of Data Necessary and Available for Modeling', *Data Sci. J.*, vol. 15, p. 1, Jan. 2016, doi: 10.5334/dsj-2016-001.

[12] Y. Huang and A. Bardossy, 'Impacts of Data Quantity and Quality on Model Calibration: Implications for Model Parameterization in Data-Scarce Catchments', *Water*, vol. 12, no. 9, Art. no. 9, Sep. 2020, doi: 10.3390/w12092352.

[13] B. A. McCarl, Ed., 'Model Validation: An Overview with some Emphasis on Risk Models', *Rev. Mark. Agric. Econ.*, 1984, doi: 10.22004/ag.econ.12282.

[14] C. A. Aumann, 'A methodology for developing simulation models of complex systems', *Ecol. Model.*, vol. 202, no. 3, pp. 385–396, Apr. 2007, doi: 10.1016/j.ecolmodel.2006.11.005.

[15] R. Sargent, *Verification and validation of simulation models*, vol. 37. 2011, p. 183. doi: 10.1109/WSC.2010.5679166.

[16] A. Farina, A. Graziano, S. Panzieri, F. Pascucci, and R. Setola, 'How to Perform Verification and Validation of Critical Infrastructure Modeling Tools', in *Critical Information Infrastructure Security*, S. Bologna, B. Hämmerli, D. Gritzalis, and S. Wolthusen, Eds., in Lecture Notes in Computer Science, vol. 6983. Berlin, Heidelberg: Springer Berlin Heidelberg, 2013, pp. 116–127. doi: 10.1007/978-3-642-41476-3_10.

[17] United States Department of Homeland Security, 'HIFLD Open Data'. 2021. Accessed: May 28, 2023. [Online]. Available: https://hifld-geoplatform.opendata.arcgis.com/

[18] Coordinating body for federal geoinformation, 'Geoportal of the Swiss Confederation'. 2023. Accessed: May 28, 2023. [Online]. Available: https://www.geo.admin.ch/de/

[19] OpenStreetMap contributors, 'Planet dump retrieved from https://planet.osm.org'. 2017. Accessed: May 16, 2023. [Online]. Available: https://www.openstreetmap.org/

[20] C. Barrington-Leigh and A. Millard-Ball, 'The world's user-generated road map is more than 80% complete', *PLOS ONE*, vol. 12, no. 8, p. e0180698, Aug. 2017, doi: 10.1371/journal.pone.0180698.

[21] C. Stip, Z. Mao, L. Bonzanigo, G. Browder, and J. Tracy, 'Water Infrastructure Resilience', Jun. 2019, doi: 10.1596/31911.

[22] B. R. Ellingwood, H. Cutler, P. Gardoni, W. G. Peacock, J. W. van de Lindt, and N. Wang, 'The Centerville Virtual Community: a fully integrated decision model of interacting physical and social infrastructure systems', *Sustain. Resilient Infrastruct.*, vol. 1, no. 3–4, pp. 95–107, Nov. 2016, doi: 10.1080/23789689.2016.1255000.

[23] R. Guidotti, H. Chmielewski, V. Unnikrishnan, P. Gardoni, T. McAllister, and J. van de Lindt, 'Modeling the resilience of critical infrastructure: the role of network dependencies', *Sustain. Resilient Infrastruct.*, vol. 1, no. 3–4, pp. 153–168, Nov. 2016, doi: 10.1080/23789689.2016.1254999.

[24] C. Arderne, C. Zorn, C. Nicolas, and E. E. Koks, 'Predictive mapping of the

global power system using open data', *Sci. Data*, vol. 7, no. 1, Art. no. 1, Jan. 2020, doi: 10.1038/s41597-019-0347-4.

[25] C. Zorn, R. Pant, S. Thacker, L. Andreae, and A. Y. Shamseldin, 'Quantifying system-level dependencies between connected electricity and transport infrastructure networks incorporating expert judgement', *Civ. Eng. Environ. Syst.*, vol. 38, no. 3, pp. 176–196, Jul. 2021, doi: 10.1080/10286608.2021.1943664.

[26] K. M. de Bruijn *et al.*, 'Flood Resilience of Critical Infrastructure: Approach and Method Applied to Fort Lauderdale, Florida', *Water*, vol. 11, no. 3, Art. no. 3, Mar. 2019, doi: 10.3390/w11030517.

[27] E. Luiijf and M. Klaver, 'Analysis and lessons identified on critical infrastructures and dependencies from an empirical data set', *Int. J. Crit. Infrastruct. Prot.*, vol. 35, p. 100471, Dec. 2021, doi: 10.1016/j.ijcip.2021.100471.

[28] L. Dueñas-Osorio and A. Kwasinski, 'Quantification of Lifeline System Interdependencies after the 27 February 2010 Mw 8.8 Offshore Maule, Chile, Earthquake', *Earthq. Spectra*, vol. 28, no. 1_suppl1, pp. 581–603, Jun. 2012, doi: 10.1193/1.4000054.

[29] R. Zimmerman, 'Decision-making and the vulnerability of interdependent critical infrastructure', in *2004 IEEE International Conference on Systems, Man and Cybernetics (IEEE Cat. No.04CH37583)*, Oct. 2004, pp. 4059–4063 vol.5. doi: 10.1109/ICSMC.2004.1401166.

[30] E. Luiijf, A. Nieuwenhuijs, M. Klaver, M. van Eeten, and E. Cruz, 'Empirical Findings on Critical Infrastructure Dependencies in Europe', in *Critical Information Infrastructure Security*, R. Setola and S. Geretshuber, Eds., in Lecture Notes in Computer Science. Berlin, Heidelberg: Springer, 2009, pp. 302–310. doi: 10.1007/978-3-642-03552-4_28.

[31] C. R. Zorn and A. Y. Shamseldin, 'Quantifying Directional Dependencies from Infrastructure Restoration Data', *Earthq. Spectra*, vol. 32, no. 3, pp. 1363–1381, Aug. 2016, doi: 10.1193/013015EQS015M.

[32] R. Pant, S. Thacker, J. W. Hall, D. Alderson, and S. Barr, 'Critical infrastructure impact assessment due to flood exposure', *J. Flood Risk Manag.*, vol. 11, no. 1, pp. 22–33, Mar. 2018, doi: 10.1111/jfr3.12288.

[33] B. Evans *et al.*, 'Mapping urban infrastructure interdependencies and fuzzy risks', *Procedia Eng.*, vol. 212, pp. 816–823, Jan. 2018, doi: 10.1016/j.proeng.2018.01.105.

[34] O. Pala, D. Wilson, R. Bent, S. Linger, and J. Arnold, 'Accuracy of Service Area Estimation Methods Used for Critical Infrastructure Recovery', in *Critical Infrastructure Protection VIII*, J. Butts and S. Shenoi, Eds., in IFIP Advances in Information and Communication Technology. Berlin, Heidelberg: Springer, 2014, pp. 173–191. doi: 10.1007/978-3-662-45355-1_12.

[35] E. Mühlhofer, E. E. Koks, C. M. Kropf, G. Sansavini, and D. N. Bresch, 'A generalized natural hazard risk modelling framework for infrastructure failure cascades', *Reliab. Eng. Syst. Saf.*, vol. 234, p. 109194, Jun. 2023, doi: 10.1016/j.ress.2023.109194.

[36] S. Dong, A. Esmalian, H. Farahmand, and A. Mostafavi, ‘An integrated physical-social analysis of disrupted access to critical facilities and community service-loss tolerance in urban flooding’, *Comput. Environ. Urban Syst.*, vol. 80, p. 101443, Mar. 2020, doi: 10.1016/j.compenvurbsys.2019.101443.

[37] C. Zorn, A. Shamseldin, R. Pant, and S. Thacker, *Evaluating the magnitude and spatial extent of disruptions across interdependent national infrastructure networks*. 2019. doi: 10.13140/RG.2.2.30146.84163.

[38] A. Stock *et al.*, ‘Household impacts of interruption to electric power and water services’, *Nat. Hazards*, vol. 115, no. 3, pp. 2279–2306, Feb. 2023, doi: 10.1007/s11069-022-05638-8.

[39] E. J. M. Blokker, J. H. G. Vreeburg, and J. C. van Dijk, ‘Simulating Residential Water Demand with a Stochastic End-Use Model’, *J. Water Resour. Plan. Manag.*, vol. 136, no. 1, pp. 19–26, Jan. 2010, doi: 10.1061/(ASCE)WR.1943-5452.0000002.

[40] F. Mazzoni *et al.*, ‘Investigating the characteristics of residential end uses of water: A worldwide review’, *Water Res.*, vol. 230, p. 119500, Feb. 2023, doi: 10.1016/j.watres.2022.119500.

[41] L. Poirier, P. Knox, E. Murphy, and M. Provan, *Flood Damage to Critical Infrastructure*. 2022. doi: 10.4224/40002986.

[42] B. Merz, H. Kreibich, R. Schwarze, and A. Thieken, ‘Review article “Assessment of economic flood damage”’, *Nat. Hazards Earth Syst. Sci.*, vol. 10, no. 8, pp. 1697–1724, Aug. 2010, doi: 10.5194/nhess-10-1697-2010.

[43] M. J. Hammond, A. S. Chen, S. Djordjević, D. Butler, and O. Mark, ‘Urban flood impact assessment: A state-of-the-art review’, *Urban Water J.*, vol. 12, no. 1, pp. 14–29, Jan. 2015, doi: 10.1080/1573062X.2013.857421.

[44] N. Ranger *et al.*, ‘An assessment of the potential impact of climate change on flood risk in Mumbai’, *Clim. Change*, vol. 104, no. 1, pp. 139–167, Jan. 2011, doi: 10.1007/s10584-010-9979-2.

[45] A. S. Chen, M. J. Hammond, S. Djordjević, D. Butler, D. M. Khan, and W. Veerbeek, ‘From hazard to impact: flood damage assessment tools for mega cities’, *Nat. Hazards*, vol. 82, no. 2, pp. 857–890, Jun. 2016, doi: 10.1007/s11069-016-2223-2.

[46] H. Kreibich *et al.*, ‘Is flow velocity a significant parameter in flood damage modelling?’, *Nat. Hazards Earth Syst. Sci.*, vol. 9, no. 5, pp. 1679–1692, Oct. 2009, doi: 10.5194/nhess-9-1679-2009.

[47] S. Kameshwar, H. Park, D. T. Cox, and A. R. Barbosa, ‘Effect of disaster debris, floodwater pooling duration, and bridge damage on immediate post-tsunami connectivity’, *Int. J. Disaster Risk Reduct.*, vol. 56, p. 102119, Apr. 2021, doi: 10.1016/j.ijdrr.2021.102119.

[48] B. Jongman *et al.*, ‘Comparative flood damage model assessment: towards a European approach’, *Nat. Hazards Earth Syst. Sci.*, vol. 12, no. 12, pp. 3733–3752, Dec. 2012, doi: 10.5194/nhess-12-3733-2012.

[49] K. Pitilakis, P. Franchin, B. Khazai, and H. Wenzel, Eds., *SYNER-G: Systemic Seismic Vulnerability and Risk Assessment of Complex Urban, Utility, Lifeline Systems and Critical Facilities: Methodology and Applications*,

vol. 31. in Geotechnical, Geological and Earthquake Engineering, vol. 31. Dordrecht: Springer Netherlands, 2014. doi: 10.1007/978-94-017-8835-9.

[50] W. Sun, P. Bocchini, and B. D. Davison, 'Model for Estimating the Impact of Interdependencies on System Recovery', *J. Infrastruct. Syst.*, vol. 26, no. 3, p. 04020031, Sep. 2020, doi: 10.1061/(ASCE)IS.1943-555X.0000569.

[51] B. Evans, A. S. Chen, S. Djordjević, J. Webber, A. G. Gómez, and J. Stevens, 'Investigating the Effects of Pluvial Flooding and Climate Change on Traffic Flows in Barcelona and Bristol', *Sustainability*, vol. 12, no. 6, Art. no. 6, Jan. 2020, doi: 10.3390/su12062330.

[52] L. S. Vamvakeridou-Lyroudia *et al.*, 'Assessing and visualising hazard impacts to enhance the resilience of Critical Infrastructures to urban flooding', *Sci. Total Environ.*, vol. 707, p. 136078, Mar. 2020, doi: 10.1016/j.scitotenv.2019.136078.

[53] M. Pregnolato, A. Ford, S. M. Wilkinson, and R. J. Dawson, 'The impact of flooding on road transport: A depth-disruption function', *Transp. Res. Part Transp. Environ.*, vol. 55, pp. 67–81, Aug. 2017, doi: 10.1016/j.trd.2017.06.020.

[54] E. E. Koks *et al.*, 'A global multi-hazard risk analysis of road and railway infrastructure assets', *Nat. Commun.*, vol. 10, no. 1, Art. no. 1, Jun. 2019, doi: 10.1038/s41467-019-10442-3.

[55] E. E. Koks, K. C. H. van Ginkel, M. J. E. van Marle, and A. Lemnitzer, 'Brief communication: Critical infrastructure impacts of the 2021 mid-July western European flood event', *Nat. Hazards Earth Syst. Sci.*, vol. 22, no. 12, pp. 3831–3838, Nov. 2022, doi: 10.5194/nhess-22-3831-2022.

[56] H. J. Murdock, K. M. De Bruijn, and B. Gersonius, 'Assessment of Critical Infrastructure Resilience to Flooding Using a Response Curve Approach', *Sustainability*, vol. 10, no. 10, Art. no. 10, Oct. 2018, doi: 10.3390/su10103470.

[57] E. E. Lee II, J. E. Mitchell, and W. A. Wallace, 'Restoration of Services in Interdependent Infrastructure Systems: A Network Flows Approach', *IEEE Trans. Syst. Man Cybern. Part C Appl. Rev.*, vol. 37, no. 6, pp. 1303–1317, Nov. 2007, doi: 10.1109/TSMCC.2007.905859.

[58] Federal Emergency Management Agency, 'Hazus'. 2022. Accessed: May 17, 2023. [Online]. Available: https://www.fema.gov/flood-maps/products-tools/hazus

[59] Federal Emergency Management Agency, 'Estimating Losses From Future Earthquakes Panel Report', 1989. Accessed: May 17, 2023. [Online]. Available: https://www.fema.gov/sites/default/files/documents/fema176_estimating_losses_future_earthquakes_panel_report.pdf

[60] Y. Almoghathawi, K. Barker, and L. A. Albert, 'Resilience-driven restoration model for interdependent infrastructure networks', *Reliab. Eng. Syst. Saf.*, vol. 185, pp. 12–23, May 2019, doi: 10.1016/j.ress.2018.12.006.

[61] M. Davlasheridze *et al.*, 'Economic impacts of storm surge and the cost-benefit analysis of a coastal spine as the surge mitigation strategy in Houston-Galveston area in the USA', *Mitig. Adapt. Strateg. Glob. Change*, vol. 24, no. 3, pp. 329–354, Mar. 2019, doi: 10.1007/s11027-018-9814-z.

[62] A. J. Wild, T. M. Wilson, M. S. Bebbington, J. W. Cole, and H. M. Craig,

'Probabilistic volcanic impact assessment and cost-benefit analysis on network infrastructure for secondary evacuation of farm livestock: A case study from the dairy industry, Taranaki, New Zealand', *J. Volcanol. Geotherm. Res.*, vol. 387, p. 106670, Dec. 2019, doi: 10.1016/j.jvolgeores.2019.106670.

[63] P. C. Ryan and M. G. Stewart, 'Cost-benefit analysis of climate change adaptation for power pole networks', *Clim. Change*, vol. 143, no. 3, pp. 519–533, Aug. 2017, doi: 10.1007/s10584-017-2000-6.

[64] G. P. Cimellaro, D. Solari, and M. Bruneau, 'Physical infrastructure interdependency and regional resilience index after the 2011 Tohoku Earthquake in Japan', *Earthq. Eng. Struct. Dyn.*, vol. 43, no. 12, pp. 1763–1784, 2014, doi: 10.1002/eqe.2422.

[65] C. Briere *et al.*, 'Multi-Hazard Risk Assessment for the Schools Sector in Mozambique', Deltares, 2018. Accessed: May 22, 2023. [Online]. Available: https://www.gfdrr.org/sites/default/files/publication/1230818-002-ZKS-0008-r-Multi-Hazard%20Risk%20Assessment%20for%20the%20Schools%20Sector%20in%20Mozambique%20final.pdf

[66] A. Voinov and F. Bousquet, 'Modelling with stakeholders', *Environ. Model. Softw.*, vol. 25, no. 11, pp. 1268–1281, Nov. 2010, doi: 10.1016/j.envsoft.2010.03.007.

[67] J. Verschuur, E. E. Koks, and J. W. Hall, 'Port disruptions due to natural disasters: Insights into port and logistics resilience', *Transp. Res. Part Transp. Environ.*, vol. 85, p. 102393, Aug. 2020, doi: 10.1016/j.trd.2020.102393.

[68] R. Schotten and D. Bachmann, 'Critical infrastructure network modelling for flood risk analyses: Approach and proof of concept in Accra, Ghana', *J. Flood Risk Manag.*, Apr. 2023, doi: 10.1111/jfr3.12913.

[69] E. Mühlhofer, Z. Stalhandske, J. Schlumberger, D. N. Bresch, E. E. Koks, and M. Sarcinella, 'Supporting robust and climate-sensitive adaptation strategies for infrastructure networks: A multi-hazard case study on Mozambique's healthcare sector.', presented at the 14th International Conference on Applications of Statistics and Probability in Civil Engineering, Dubling, Ireland, 13.07 2023.

[70] M. Arosio, M. L. V. Martina, and R. Figueiredo, 'The whole is greater than the sum of its parts: a holistic graph-based assessment approach for natural hazard risk of complex systems', *Nat. Hazards Earth Syst. Sci.*, vol. 20, no. 2, pp. 521–547, Feb. 2020, doi: 10.5194/nhess-20-521-2020.

[71] (BBK) Federal Office of Civil Protection an Disaster Assistance, 'Definition of CI Hazards - KRITIS-Gefahren', BBK, 2023. https://www.bbk.bund.de/DE/Themen/Kritische-Infrastrukturen/KRITIS-Gefahrenlagen/kritis-gefahrenlagen_node.html (accessed May 30, 2023).

[72] H. de Moel, B. Jongman, H. Kreibich, B. Merz, E. Penning-Rowsell, and P. J. Ward, 'Flood risk assessments at different spatial scales', *Mitig. Adapt. Strateg. Glob. Change*, vol. 20, no. 6, pp. 865–890, Aug. 2015, doi: 10.1007/s11027-015-9654-z.

[73] B. Winter, K. Schneeberger, M. Huttenlau, and J. Stötter, 'Sources of

uncertainty in a probabilistic flood risk model', *Nat. Hazards*, vol. 91, no. 2, pp. 431–446, Mar. 2018, doi: 10.1007/s11069-017-3135-5.

[74] A. Tabandeh, N. Sharma, and P. Gardoni, 'Uncertainty propagation in risk and resilience analysis of hierarchical systems', *Reliab. Eng. Syst. Saf.*, vol. 219, p. 108208, Mar. 2022, doi: 10.1016/j.ress.2021.108208.

[75] S. De Kleermaeker and J. S. Verkade, 'A decision support system for use of probability forecasts', *ISCRAM 2013 Proc. 10th Int. Conf. Inf. Syst. Crisis Response Manag. Baden-Baden Ger. 12-15 May 2013*, 2013, Accessed: Jun. 01, 2023. [Online]. Available: https://repository.tudelft.nl/islandora/object/uuid%3A3dc8f192-25fc-4b9c-a548-fd78eb2caca5

[76] C. Zorn, R. Pant, S. Thacker, and A. Y. Shamseldin, 'Evaluating the Magnitude and Spatial Extent of Disruptions Across Interdependent National Infrastructure Networks', *ASCE-ASME J Risk Uncert Engrg Sys Part B Mech Engrg*, vol. 6, no. 020904, Mar. 2020, doi: 10.1115/1.4046327.

References

Almoghathawi, Yasser and Kash Barker (2019). "Component importance measures for interdependent infrastructure network resilience". In: *Computers & Industrial Engineering* 133, pp. 153–164.

— (2020). "Restoring community structures in interdependent infrastructure networks". In: *IEEE Transactions on Network Science and Engineering* 7.3, pp. 1355–1367.

Almoghathawi, Yasser, Kash Barker, and Laura A. Albert (May 1, 2019). "Resilience-Driven Restoration Model for Interdependent Infrastructure Networks". In: *Reliability Engineering & System Safety* 185, pp. 12–23. ISSN: 0951-8320. DOI: `10.1016/j.ress.2018.12.006`.

Ammann, Michelle (Apr. 27, 2023). "A Global Multi-Hazard Risk View on Social Facilities (Healthcare and Education)". ETH Zurich.

Arderne, C., Conrad R. Zorn, C. Nicolas, and Elco E. Koks (Jan. 15, 2020). "Predictive Mapping of the Global Power System Using Open Data". In: *Scientific Data* 7.1 (1), p. 19. ISSN: 2052-4463. DOI: `10.1038/s41597-019-0347-4`.

Aznar-Siguan, Gabriela and David N. Bresch (July 19, 2019). "CLIMADA v1: A Global Weather and Climate Risk Assessment Platform". In: *Geoscientific Model Development* 12.7, pp. 3085–3097. ISSN: 1991-959X. DOI: `10.5194/gmd-12-3085-2019`.

Banerjee, Joydeep, Kaustav Basu, and Arunabha Sen (Jan. 1, 2018). "Analysing Robustness in Intra-Dependent and Inter-Dependent Networks Using a New Model of Interdependency". In: *International Journal of Critical Infrastructures* 14.2, pp. 156–181. ISSN: 1475-3219. DOI: `10.1504/IJCIS.2018.091938`.

Barrington-Leigh, Christopher and Adam Millard-Ball (Oct. 8, 2017). "The World's User-Generated Road Map Is More than 80% Complete". In: *PLOS ONE* 12.8, e0180698. ISSN: 1932-6203. DOI: `10.1371/journal.pone.0180698`.

Bay District Schools (2022). *Hurricane Michael Recovery Information*. URL: https://www.bay.k12.fl.us/hurricane-michael.

Beven II, John L., Robbie Berg, and Andrew Hagen (May 17, 2019). *Hurricane Michael Tropical Cyclone Report*. AL142018. National Hurricane Center. URL: https://www.nhc.noaa.gov/data/tcr/AL142018_Michael.pdf.

Beyza, Jesus, Hector F. Ruiz-Paredes, Eduardo Garcia-Paricio, and Jose M. Yusta (Feb. 15, 2020). "Assessing the Criticality of Interdependent Power and Gas Systems Using Complex Networks and Load Flow Techniques". In: *Physica A: Statistical Mechanics and its Applications* 540, p. 123169. ISSN: 0378-4371. DOI: 10.1016/j.physa.2019.123169.

Biljecki, Filip, Yoong Shin Chow, and Kay Lee (June 1, 2023). "Quality of Crowdsourced Geospatial Building Information: A Global Assessment of OpenStreetMap Attributes". In: *Building and Environment* 237, p. 110295. ISSN: 0360-1323. DOI: 10.1016/j.buildenv.2023.110295.

Blass, Robert, Chahan M. Kropf, Irina Mahlstein, and David N. Bresch (2022). *Automatic Generation of Winter Storm Warnings*. Technical Report 282. MeteoSwiss. URL: https://doi.org/10.18751/pmch/tr/282.winterstormwarnings/1.0.

Bloemendaal, Nadia, Ivan D. Haigh, Hans de Moel, Sanne Muis, Reindert J. Haarsma, and Jeroen C. J. H. Aerts (Feb. 6, 2020). "Generation of a Global Synthetic Tropical Cyclone Hazard Dataset Using STORM". In: *Scientific Data* 7.1 (1), p. 40. ISSN: 2052-4463. DOI: 10.1038/s41597-020-0381-2.

Bloemendaal, Nadia and Elco E. Koks (2022). "Current and Future Tropical Cyclone Wind Risk in the Small Island Developing States". In: *Hurricane Risk in a Changing Climate*. Ed. by Jennifer M. Collins and James M. Done. Hurricane Risk. Cham: Springer International Publishing, pp. 121–142. ISBN: 978-3-031-08568-0. DOI: 10.1007/978-3-031-08568-0_6.

Bloemendaal, Nadia, Hans de Moel, Jantsje M. Mol, Priscilla R. M. Bosma, Amy N. Polen, and Jennifer M. Collins (Jan. 2021). "Adequately Reflecting the Severity of Tropical Cyclones Using the New Tropical Cyclone Severity Scale". In: *Environmental Research Letters* 16.1, p. 014048. ISSN: 1748-9326. DOI: 10.1088/1748-9326/abd131.

Bloomfield, Robin E., Peter Popov, Kizito Salako, Vladimir Stankovic, and David Wright (Nov. 1, 2017). "Preliminary Interdependency Analysis: An Approach to Support Critical-Infrastructure Risk-Assessment". In: *Reliability Engineering & System Safety*. Special Section: Applications of Probabilistic Graphical Models in Dependability, Diagnosis and Prognosis 167, pp. 198–217. ISSN: 0951-8320. DOI: 10.1016/j.ress.2017.05.030.

Boeing, Geoff (Sept. 1, 2017). "OSMnx: New Methods for Acquiring, Constructing, Analyzing, and Visualizing Complex Street Networks". In: *Computers, Environment and Urban Systems* 65, pp. 126–139. ISSN: 0198-9715. DOI: 10.1016/j.compenvurbsys.2017.05.004.

Bossche, Joris Van den, Kelsey Jordahl, Martin Fleischmann, James McBride, Jacob Wasserman, Matt Richards, Adrian Garcia Badaracco, Alan D. Snow, Jeff Tratner, Jeffrey Gerard, Brendan Ward, Matthew Perry, Carson Farmer, Geir Arne Hjelle, Mike Taves, Ewout ter Hoeven, Micah Cochran, rraymondgh, Sean Gillies, Giacomo Caria, Lucas Culbertson, Matt Bartos, Nick Eubank, Ray Bell, sangarshanan, John Flavin, Sergio Rey, maxalbert, Aleksey Bilogur, and Christopher Ren (June 2023). *geopandas/geopandas: v0.13.2*. Version v0.13.2. DOI: 10.5281/zenodo.8009629. URL: https://doi.org/10.5281/zenodo.8009629.

Bowen, William M. (May 3, 2002). *Environmental Justice Through Research-Based Decision-Making*. Routledge. 292 pp. ISBN: 978-1-135-57815-2. Google Books: C_uOAgAAQBAJ.

Braese, Johannes, Jun Rentschler, and Stéphane Hallegatte (June 20, 2019). *Resilient Infrastructure for Thriving Firms: A Review of the Evidence*. Policy Research Working Papers. The World Bank. 26 pp. DOI: 10.1596/1813-9450-8895.

Bresch, David N. (2016). "Shaping Climate Resilient Development: Economics of Climate Adaptation". In: *Climate Change Adaptation Strategies: An Upstream-downstream Perspective*. Springer, pp. 241–254. ISBN: 978-3-319-40771-5. URL: https://www.research-collection.ethz.ch/handle/20.500.11850/126936.

Bresch, David N. and Gabriela Aznar-Siguan (Jan. 22, 2021). "CLIMADA v1.4.1: Towards a Globally Consistent Adaptation Options Appraisal

Tool". In: *Geoscientific Model Development* 14.1, pp. 351–363. ISSN: 1991-959X. DOI: 10.5194/gmd-14-351-2021.

Bresch, David N., Jaap Berghuijs, Rainer Egloff, and Roland Kupers (2014). "A Resilience Lens for Enterprise Risk Management". In: *Turbulence: A Corporate Perspective on Collaborating for Resilience*. Amsterdam University Press, pp. 49–65. ISBN: 978-90-8964-712-2. URL: https://www.research-collection.ethz.ch/handle/20.500.11850/127039.

Bruijn, Karin M. de, Lydia Cumiskey, Róisín Ní Dhubhda, Micheline Hounjet, and William Hynes (2016). "Flood Vulnerability of Critical Infrastructure in Cork, Ireland". In: *E3S Web of Conferences* 7, p. 07005. ISSN: 2267-1242. DOI: 10.1051/e3sconf/20160707005.

Brunner, L. G., R. A. M. Peer, C. Zorn, R. Paulik, and T. M. Logan (Jan. 1, 2024). "Understanding Cascading Risks through Real-World Interdependent Urban Infrastructure". In: *Reliability Engineering & System Safety* 241, p. 109653. ISSN: 0951-8320. DOI: 10.1016/j.ress.2023.109653.

Buldyrev, Sergey V., Roni Parshani, Gerald Paul, H. Eugene Stanley, and Shlomo Havlin (Apr. 2010). "Catastrophic Cascade of Failures in Interdependent Networks". In: *Nature* 464.7291 (7291), pp. 1025–1028. ISSN: 1476-4687. DOI: 10.1038/nature08932.

Bundesamt für Raumentwicklung ARE (2023). *Flächennutzung*. URL: https://www.are.admin.ch/are/de/home/raumentwicklung-und-raumplanung/grundlagen-und-daten/raumbeobachtung/siedlung/flaechennutzung.html.

Burkhardt, Jakob (Dec. 23, 2022). "Recovery of Critical Infrastructure after Natural Disasters". BA thesis. ETH Zurich.

Burlew, Jeff (Nov. 29, 2018). "43 and Counting: Deconstructing the Florida Death Toll after Hurricane Michael". In: *Tallahassee Democrat*. URL: https://www.tallahassee.com/story/news/2018/11/29/43-and-counting-deconstructing-death-toll-hurricane-michael/2124902002/.

Cardona, O.D., G.A. Bernal, C.P. Villegas, J.F. Molina, S.A. Herrera, M.C. Marulanda, D.F. Rincón, S. Grajales, P.M. Marulanda, D. Gonzalez, and A. Maskrey (n.d.). *Multihazard Disaster Risk Model of Infrastructure and Buildings at the Global Level. (Global Infrastructure Resilience 2023 Position Paper 2.4). Background Report.* INGENIAR: Risk Intelligence for the CDRI Flagship Report. URL: https://cdri.world/biennial-report-position-and-contributing-papers.

Center for International Earth Science Information Network (CIESIN), Columbia University (2017). *Gridded Population of the World, Version 4 (GPWv4): Population Density, Revision 11.* Palisades, NY: Socioeconomic Data and Applications Center (SEDAC). DOI: 10.7927/H49C6VHW.

Cerri, Marco, Max Steinhausen, Heidi Kreibich, and Kai Schröter (Feb. 16, 2021). "Are OpenStreetMap Building Data Useful for Flood Vulnerability Modelling?" In: *Natural Hazards and Earth System Sciences* 21.2, pp. 643–662. ISSN: 1561-8633. DOI: 10.5194/nhess-21-643-2021.

Chang, Stephanie E., Timothy L. McDaniels, and C Beaubien (2009). "Societal impacts of infrastructure failure interdependencies: Building an empirical knowledge base". In: *TCLEE 2009: Lifeline Earthquake Engineering in a Multihazard Environment*, pp. 1–10.

Chang, Stephanie E., Timothy L. McDaniels, Joey Mikawoz, and Krista Peterson (May 1, 2007). "Infrastructure Failure Interdependencies in Extreme Events: Power Outage Consequences in the 1998 Ice Storm". In: *Natural Hazards* 41.2, pp. 337–358. ISSN: 1573-0840. DOI: 10.1007/s11069-006-9039-4.

Chang, Stephanie E., C. Pasion, S. Yavari, and K. Elwood (Apr. 26, 2012). "Social Impacts of Lifeline Losses: Modeling Displaced Populations and Health Care Functionality". In: pp. 1–10. DOI: 10.1061/41050(357)54.

Chawla, Sagar, Shaheen Kurani, Sherry M. Wren, Barclay Stewart, Gilbert Burnham, Adam Kushner, and Thomas McIntyre (Mar. 2018). "Electricity and Generator Availability in LMIC Hospitals: Improving Access to Safe Surgery". In: *The Journal of Surgical Research* 223, pp. 136–141. ISSN: 1095-8673. DOI: 10.1016/j.jss.2017.10.016. pmid: 29433865.

Chmielewski, Hana, Roberto Guidotti, Therese McAllister, and Paolo Gardoni (May 18, 2016). "Response of Water Systems under Extreme Events: A Comprehensive Approach to Modeling Water System Resilience". In: pp. 475–486. DOI: 10.1061/9780784479865.050.

Chou, Chien-Cheng and Ssu-Min Tseng (Nov. 1, 2010). "Collection and Analysis of Critical Infrastructure Interdependency Relationships". In: *Journal of Computing in Civil Engineering* 24.6, pp. 539–547. ISSN: 0887-3801. DOI: 10.1061/(ASCE)CP.1943-5487.0000059.

Cimellaro, Gian Paolo (2016). "A Comprehensive Methodology for the Evaluation of Infrastructure Interdependencies". In: *Urban Resilience for Emergency Response and Recovery: Fundamental Concepts and Applications*. Ed. by Gian Paolo Cimellaro. Geotechnical, Geological and Earthquake Engineering. Cham: Springer International Publishing, pp. 139–223. ISBN: 978-3-319-30656-8. DOI: 10.1007/978-3-319-30656-8_7.

Ciullo, Alessio, Olivia Martius, Eric Strobl, and David N. Bresch (Jan. 1, 2021). "A Framework for Building Climate Storylines Based on Downward Counterfactuals: The Case of the European Union Solidarity Fund". In: *Climate Risk Management* 33, p. 100349. ISSN: 2212-0963. DOI: 10.1016/j.crm.2021.100349.

Ciullo, Alessio, Eric Strobl, Simona Meiler, Olivia Martius, and David N. Bresch (Feb. 17, 2023). "Increasing Countries' Financial Resilience through Global Catastrophe Risk Pooling". In: *Nature Communications* 14.1 (1), p. 922. ISSN: 2041-1723. DOI: 10.1038/s41467-023-36539-4.

Claassen, Judith N, Philip J Ward, James Daniell, Elco E Koks, Timothy Tiggeloven, and Marleen C de Ruiter (2023). "A new method to compile global multi-hazard event sets". In: *Scientific Reports* 13.1, p. 13808.

Colon, Célian, Stéphane Hallegatte, and Julie Rozenberg (June 2019). *Transportation and Supply Chain Resilience in the United Republic of Tanzania. Assessing the Supply-Chain Impacts of Disaster-Induced Transportation Disruptions.* World Bank. URL: http://documents1.worldbank.org/curated/en/203311560795432285/pdf/Transportation-and-Supply-Chain-Resilience-in-the-United-Republic-of-Tanzania.pdf.

Coughlan de Perez, E., B. van den Hurk, M. K. van Aalst, B. Jongman, T. Klose, and P. Suarez (2015). "Forecast-based financing: an approach for catalyzing humanitarian action based on extreme weather and climate forecasts". In: *Natural Hazards and Earth System Sciences* 15.4, pp. 895–904. DOI: 10.5194/nhess-15-895-2015. URL: https://nhess.copernicus.org/articles/15/895/2015/.

CRED / UCLouvain (2023). *EM-DAT. The International Disaster Database.* URL: https://public.emdat.be/.

Cutter, Susan L., Bryan J. Boruff, and W. Lynn Shirley (2003). "Social Vulnerability to Environmental Hazards*". In: *Social Science Quarterly* 84.2, pp. 242–261. ISSN: 1540-6237. DOI: 10.1111/1540-6237.8402002.

— (2006). "Social Vulnerability to Environmental Hazards". In: *Hazards Vulnerability and Environmental Justice*. Routledge. ISBN: 978-1-84977-154-2.

Dargin, Jennifer S and Ali Mostafavi (2020). "Human-centric infrastructure resilience: Uncovering well-being risk disparity due to infrastructure disruptions in disasters". In: *PloS one* 15.6, e0234381.

Dawson, Richard J., David Thompson, Daniel Johns, Ruth Wood, Geoff Darch, Lee Chapman, Paul N. Hughes, Geoff V. R. Watson, Kevin Paulson, Sarah Bell, Simon N. Gosling, William Powrie, and Jim W. Hall (June 13, 2018). "A Systems Framework for National Assessment of Climate Risks to Infrastructure". In: *Philosophical Transactions of the Royal Society A: Mathematical, Physical and Engineering Sciences* 376.2121, p. 20170298. DOI: 10.1098/rsta.2017.0298.

De Leonardis, D., R. Huey, and J. Green (Mar. 2018). *National Traffic Speeds Survey III: 2015*. DOT HS 812 485. Washington, DC: National Highway Traffic Safety Administration.

De Zotti, Giulia (Oct. 2020). *Hainan Clean Energy Island*. Danish Energy Agency. URL: https://ens.dk/sites/ens.dk/files/Globalcooperation/hainan_clean_energy_island_-_modelling_report.pdf.

Deltares (2021). *Multi-Hazard Risk Assessment for the Health Sector in Mozambique*.

De Ruiter, Marleen C., Jens A. de Bruijn, Johanna Englhardt, James E. Daniell, Hans de Moel, and Philip J. Ward (2021). "The Asynergies of Structural Disaster Risk Reduction Measures: Comparing Floods and Earthquakes". In: *Earth's Future* 9.1, e2020EF001531. ISSN: 2328-4277. DOI: 10.1029/2020EF001531.

Devanandham, Henry and Emmanuel-Jose Ramirez-Marquez (Mar. 1, 2012). "Generic Metrics and Quantitative Approaches for System Resilience as a Function of Time". In: *Reliability Engineering & System Safety* 99, pp. 114–122. ISSN: 0951-8320. DOI: 10.1016/j.ress.2011.09.002.

DiStefano, Michael J. and Carleigh B. Krubiner (Aug. 2020). "Beyond the Numbers: A Critique of Quantitative Multi-Criteria Decision Analysis".

In: *International Journal of Technology Assessment in Health Care* 36.4, pp. 292–296. ISSN: 0266-4623, 1471-6348. DOI: 10.1017/S0266462320000410.

Dueñas-Osorio, Leonardo, James I. Craig, and Barry J. Goodno (2007). "Seismic Response of Critical Interdependent Networks". In: *Earthquake Engineering & Structural Dynamics* 36.2, pp. 285–306. ISSN: 1096-9845. DOI: 10.1002/eqe.626.

Dueñas-Osorio, Leonardo and Alexis Kwasinski (June 1, 2012). "Quantification of Lifeline System Interdependencies after the 27 February 2010 Mw 8.8 Offshore Maule, Chile, Earthquake". In: *Earthquake Spectra* 28 (1_suppl1), pp. 581–603. ISSN: 8755-2930. DOI: 10.1193/1.4000054.

Eberenz, Samuel, Samuel Lüthi, and David N. Bresch (Jan. 29, 2021). "Regional Tropical Cyclone Impact Functions for Globally Consistent Risk Assessments". In: *Natural Hazards and Earth System Sciences* 21.1, pp. 393–415. ISSN: 1561-8633. DOI: 10.5194/nhess-21-393-2021.

Eberenz, Samuel, Dario Stocker, Thomas Röösli, and David N. Bresch (Apr. 9, 2020). "Asset Exposure Data for Global Physical Risk Assessment". In: *Earth System Science Data* 12.2, pp. 817–833. ISSN: 1866-3508. DOI: 10.5194/essd-12-817-2020.

Eilander, Dirk, Anaïs Couasnon, Tim Leijnse, Hiroaki Ikeuchi, Dai Yamazaki, Sanne Muis, Job Dullaart, Hessel C. Winsemius, and Philip J. Ward (Apr. 11, 2022). "A Globally-Applicable Framework for Compound Flood Hazard Modeling". In: *EGUsphere*, pp. 1–40. DOI: 10.5194/egusphere-2022-149.

Eilander, Dirk, Anaïs Couasnon, Frederiek C. Sperna Weiland, Willem Ligtvoet, Arno Bouwman, Hessel C. Winsemius, and Philip J. Ward (Oct. 4, 2022). "Modeling Compound Flood Risk and Risk Reduction Using a Globally-Applicable Framework: A Case Study in the Sofala Region". In: *Natural Hazards and Earth System Sciences Discussions*, pp. 1–31. DOI: 10.5194/nhess-2022-248.

Espada, Rodolfo Jr., Armando Apan, and Kevin McDougall (Jan. 1, 2015). "Vulnerability Assessment and Interdependency Analysis of Critical Infrastructures for Climate Adaptation and Flood Mitigation". In: *International Journal of Disaster Resilience in the Built Environment* 6.3, pp. 313–346. ISSN: 1759-5908. DOI: 10.1108/IJDRBE-02-2014-0019.

European Commission (Dec. 23, 2008). *Council Directive 2008/114/EC of 8 December 2008 on the Identification and Designation of European Critical Infrastructures and the Assessment of the Need to Improve Their Protection (Text with EEA Relevance).* URL: http://data.europa.eu/eli/dir/2008/114/oj/eng.

Fang, Yi-Ping, Nicola Pedroni, and Enrico Zio (2016). "Resilience-based component importance measures for critical infrastructure network systems". In: *IEEE Transactions on Reliability* 65.2, pp. 502–512.

Fang, Yi-Ping and Giovanni Sansavini (May 1, 2019). "Optimum Post-Disruption Restoration under Uncertainty for Enhancing Critical Infrastructure Resilience". In: *Reliability Engineering & System Safety* 185, pp. 1–11. ISSN: 0951-8320. DOI: 10.1016/j.ress.2018.12.002.

Fausset, Richard, Alan Blinder, and Matthew Haag (Oct. 12, 2018). "Rescue Teams Scour Ruins as Hurricane Death Toll Rises". In: *The New York Times. U.S.* ISSN: 0362-4331. URL: https://www.nytimes.com/2018/10/12/us/hurricane-michael-live-updates-florida.html.

Fekete, Alexander (2019). "Critical Infrastructure and Flood Resilience: Cascading Effects beyond Water". In: *WIREs Water* 6.5, e1370. ISSN: 2049-1948. DOI: 10.1002/wat2.1370.

FEMA (Apr. 2005). *Hurricane Charley in Florida. Observations, Recommendations, and Technical Guidance.* 488. FEMA. URL: https://www.fema.gov/sites/default/files/2020-08/fema488_mat_report_hurricane_charley_fl.pdf.

Feng, Kairui, Min Ouyang, and Ning Lin (2022). "Tropical cyclone-blackout-heatwave compound hazard resilience in a changing climate". In: *Nature communications* 13.1, p. 4421.

Field, C.B, V.R. Barros, D.J. Dokken, K.J. Mach, M.D. Mastrandrea, T.E. Bilir, M. Chatterjee, K.L. Ebi, Y.O. Estrada, R. C. Genova, B. Girma, E.S. Kissel, A.N. Levy, S. MacCracken, P.R. Mastrandrea, and L.L. White (2014). "IPCC, 2014: Summary for Policymakers." In: *Climate Change 2014: Impacts, Adaptation, and Vulnerability. Part A: Global and Sectoral Aspects. Contribution of Working Group II to the Fifth Assessment Report of the Intergovernmental Panel on Climate Change.* Cambridge: Cambridge University Press, p. 34.

Fotouhi, Hossein, Seksun Moryadee, and Elise Miller-Hooks (July 1, 2017). "Quantifying the Resilience of an Urban Traffic-Electric Power Coupled System". In: *Reliability Engineering & System Safety* 163, pp. 79–94. ISSN: 0951-8320. DOI: 10.1016/j.ress.2017.01.026.

Gaillard, Jean-Michel, Patrick Duncan, Daniel Delorme, Guy Van Laere, Nathalie Pettorelli, Daniel Maillard, and Guy Renaud (2003). "Effects of Hurricane Lothar on the Population Dynamics of European Roe Deer". In: *The Journal of Wildlife Management* 67.4, pp. 767–773. ISSN: 0022-541X. DOI: 10.2307/3802684. JSTOR: 3802684.

Gao, Xin, Yunxia Ye, Shitao Gong, Linyan Chen, and Tong Wang (July 13, 2023). "Empirical Patterns of Interdependencies among Critical Infrastructures in Cascading Disasters: Evidence from a Comprehensive Multi-Case Analysis". In: *International Journal of Disaster Risk Reduction*, p. 103862. ISSN: 2212-4209. DOI: 10.1016/j.ijdrr.2023.103862.

Garschagen, Matthias and Simone Sandholz (Apr. 27, 2018). "The Role of Minimum Supply and Social Vulnerability Assessment for Governing Critical Infrastructure Failure: Current Gaps and Future Agenda". In: *Natural Hazards and Earth System Sciences* 18.4, pp. 1233–1246. ISSN: 1561-8633. DOI: 10.5194/nhess-18-1233-2018.

Gauthier, Pauline, Angelo Furno, and Nour-Eddin El Faouzi (Dec. 1, 2018). "Road Network Resilience: How to Identify Critical Links Subject to Day-to-Day Disruptions". In: *Transportation Research Record* 2672.1, pp. 54–65. ISSN: 0361-1981. DOI: 10.1177/0361198118792115.

GeoFabrik (2023). *GEOFABRIK // Downloads*. URL: https://www.geofabrik.de/data/download.html.

Gerber, Julien-François, Rodríguez-Labajos, B., Yánez, I., Branco, V., Roman, P., Rosales, L., and Johnson, P. (2012). *Guide to Multicriteria Evaluation for Environmental Justice Organisations*. 9. EJOLT.

Ghosn, M., L. Dueñas-Osorio, D. M. Frangopol, T. P. McAllister, P. Bocchini, L. Manuel, B. R. Ellingwood, S. Arangio, F. Bontempi, M. Shah, M. Akiyama, F. Biondini, S. Hernandez, and G. Tsiatas (Sept. 1, 2016). "Performance Indicators for Structural Systems and Infrastructure Networks". In: *Journal of Structural Engineering* 142.9, F4016003. ISSN: 1943-541X. DOI: 10.1061/(ASCE)ST.1943-541X.0001542.

Gnyawali, Kaushal, Kshitij Dahal, Rocky Talchabhadel, and Sadhana Nirandjan (May 10, 2023). “Framework for Rainfall-Triggered Landslide-Prone Critical Infrastructure Zonation”. In: *Science of The Total Environment* 872, p. 162242. ISSN: 0048-9697. DOI: 10.1016/j.scitotenv.2023.162242.

Goldbeck, Nils, Panagiotis Angeloudis, and Washington Y. Ochieng (Aug. 1, 2019). “Resilience Assessment for Interdependent Urban Infrastructure Systems Using Dynamic Network Flow Models”. In: *Reliability Engineering & System Safety* 188, pp. 62–79. ISSN: 0951-8320. DOI: 10.1016/j.ress.2019.03.007.

González, Andrés D., Leonardo Dueñas-Osorio, Mauricio Sánchez-Silva, and Andrés L. Medaglia (2016). “The Interdependent Network Design Problem for Optimal Infrastructure System Restoration”. In: *Computer-Aided Civil and Infrastructure Engineering* 31.5, pp. 334–350. ISSN: 1467-8667. DOI: 10.1111/mice.12171.

Group, ECA Working (2009). *Shaping Climate-Resilient Development – A Framework for Decision-Making*. URL: https://ethz.ch/content/dam/ethz/special-interest/usys/ied/wcr-dam/documents/Economics_of_Climate_Adaptation_ECA.pdf.

Guidotti, Roberto, Hana Chmielewski, Vipin Unnikrishnan, Paolo Gardoni, Therese McAllister, and John van de Lindt (Nov. 28, 2016). “Modeling the Resilience of Critical Infrastructure: The Role of Network Dependencies”. In: *Sustainable and Resilient Infrastructure* 1.3-4, pp. 153–168. ISSN: 2378-9689. DOI: 10.1080/23789689.2016.1254999.

Gultom, Yohanes, Toto Haryanto, and Heru Suhartanto (Oct. 2021). “Route Subnetwork Generation Using OpenStreetMap Data for Emergency Response Problem Modeling in Indonesia”. In: *2021 International Conference on Advanced Computer Science and Information Systems (ICACSIS)*. 2021 International Conference on Advanced Computer Science and Information Systems (ICACSIS), pp. 1–6. DOI: 10.1109/ICACSIS53237.2021.9631340.

Hallegatte, Stephane, Jun Rentschler, and Julie Rozenberg (June 19, 2019). *Lifelines: The Resilient Infrastructure Opportunity*. Washington, DC: World Bank. ISBN: 978-1-4648-1430-3. DOI: 10.1596/978-1-4648-1430-3.

Haque, Anika Nasra (2016). "Application of Multi-Criteria Analysis on Climate Adaptation Assessment in the Context of Least Developed Countries". In: *Journal of Multi-Criteria Decision Analysis* 23.5-6, pp. 210–224. ISSN: 1099-1360. DOI: 10.1002/mcda.1571.

Hasan, Samiul and Greg Foliente (Sept. 1, 2015). "Modeling Infrastructure System Interdependencies and Socioeconomic Impacts of Failure in Extreme Events: Emerging R&D Challenges". In: *Natural Hazards* 78.3, pp. 2143–2168. ISSN: 1573-0840. DOI: 10.1007/s11069-015-1814-7.

He, Xian and Eun Jeong Cha (May 3, 2020). "Modeling the Damage and Recovery of Interdependent Civil Infrastructure Network Using Dynamic Integrated Network Model". In: *Sustainable and Resilient Infrastructure* 5.3, pp. 152–167. ISSN: 2378-9689. DOI: 10.1080/23789689.2018.1448662.

He, Yiyi, Jun Rentschler, Paolo Avner, Jianxi Gao, Xiangyu Yue, and John Radke (May 2022). *Mobility and Resilience: A Global Assessment of Flood Impacts on Road Transportation Networks*. Working Paper. Washington, DC: World Bank. DOI: 10.1596/1813-9450-10049.

Hemingway, Rebecca and Joanne Robbins (2020). "Developing a Hazard-Impact Model to Support Impact-Based Forecasts and Warnings: The Vehicle OverTurning (VOT) Model". In: *Meteorological Applications* 27.1, e1819. ISSN: 1469-8080. DOI: 10.1002/met.1819.

Herfort, Benjamin, Sven Lautenbach, João Porto de Albuquerque, Jennings Anderson, and Alexander Zipf (Feb. 4, 2021). "The Evolution of Humanitarian Mapping within the OpenStreetMap Community". In: *Scientific Reports* 11.1 (1), p. 3037. ISSN: 2045-2322. DOI: 10.1038/s41598-021-82404-z.

— (July 6, 2023). "A Spatio-Temporal Analysis Investigating Completeness and Inequalities of Global Urban Building Data in OpenStreetMap". In: *Nat Commun* 14.1 (1), p. 3985. ISSN: 2041-1723. DOI: 10.1038/s41467-023-39698-6.

Hernandez-Fajardo, Isaac and Leonardo Dueñas-Osorio (Mar. 1, 2013). "Probabilistic Study of Cascading Failures in Complex Interdependent Lifeline Systems". In: *Reliability Engineering & System Safety* 111, pp. 260–272. ISSN: 0951-8320. DOI: 10.1016/j.ress.2012.10.012.

Hoffmann, Sarah and contributors (Jan. 21, 2023). *PyOsmium*. Version 3.6.0. URL: https://osmcode.org/pyosmium/.

Holland, Greg (Sept. 1, 2008). "A Revised Hurricane Pressure–Wind Model". In: *Monthly Weather Review* 136.9, pp. 3432–3445. ISSN: 0027-0644. DOI: 10.1175/2008MWR2395.1.

Holma, Harri, Pasi Kinnunen, István Z. Kovács, Kari Pajukoski, Klaus Pedersen, and Jussi Reunanen (2011). "Performance". In: *LTE for UMTS*. John Wiley & Sons, Ltd, pp. 257–301. ISBN: 978-1-119-99294-3. DOI: 10.1002/9781119992943.ch10.

Iannacone, Leandro, Neetesh Sharma, Armin Tabandeh, and Paolo Gardoni (Jan. 1, 2022). "Modeling Time-varying Reliability and Resilience of Deteriorating Infrastructure". In: *Reliability Engineering & System Safety* 217, p. 108074. ISSN: 0951-8320. DOI: 10.1016/j.ress.2021.108074.

IFRC (May 2022). *IFRC Operational Framework for Anticipatory Action 2021-2025*. URL: https://www.ifrc.org/sites/default/files/2022-05/IFRC_Operational_Framework_for_Anticipatory%20_Action_2021-2025_final_0.pdf.

Jenelius, Erik and Lars-Göran Mattsson (June 1, 2012). "Road Network Vulnerability Analysis of Area-Covering Disruptions: A Grid-Based Approach with Case Study". In: *Transportation Research Part A: Policy and Practice*. Network Vulnerability in Large-Scale Transport Networks 46.5, pp. 746–760. ISSN: 0965-8564. DOI: 10.1016/j.tra.2012.02.003.

Jordahl, Kelsey, Joris Van den Bossche, Martin Fleischmann, James McBride, Jacob Wasserman, Matt Richards, Adrian Garcia Badaracco, Alan D. Snow, Jeffrey Gerard, Jeff Tratner, Matthew Perry, Brendan Ward, Carson Farmer, Geir Arne Hjelle, Mike Taves, Ewout ter Hoeven, Micah Cochran, rraymondgh, Sean Gillies, Giacomo Caria, Lucas Culbertson, Matt Bartos, Nick Eubank, Ray Bell, sangarshanan, John Flavin, Sergio Rey, maxalbert, Aleksey Bilogur, and Christopher Ren (Dec. 10, 2022). *Geopandas/Geopandas: V0.12.2*. Zenodo. DOI: 10.5281/zenodo.7422493.

Jordi, Beat (Apr. 12, 2019). *20 Jahre nach ≪Lothar≫: Der Wald hat sein Terrain zurückerobert*. URL: https://www.bafu.admin.ch/bafu/de/home/themen/thema-wald-und-holz/wald-und-holz--dossiers/

magazin2019-4-der-wald-hat-sein-terrain-zurueckerobert.html.

Kam, Pui Man, Gabriela Aznar-Siguan, Jacob Schewe, Leonardo Milano, Justin Ginnetti, Sven Willner, Jamie W. McCaughey, and David N. Bresch (Mar. 2021). "Global Warming and Population Change Both Heighten Future Risk of Human Displacement Due to River Floods". In: *Environ. Res. Lett.* 16.4, p. 044026. ISSN: 1748-9326. DOI: 10.1088/1748-9326/abd26c.

Kaplan, Stanley and B. John Garrick (1981). "On The Quantitative Definition of Risk". In: *Risk Analysis* 1.1, pp. 11–27. ISSN: 1539-6924. DOI: 10.1111/j.1539-6924.1981.tb01350.x.

Karakoc, Deniz Berfin, Kash Barker, Christopher W. Zobel, and Yasser Almoghathawi (June 1, 2020). "Social Vulnerability and Equity Perspectives on Interdependent Infrastructure Network Component Importance". In: *Sustainable Cities and Society* 57, p. 102072. ISSN: 2210-6707. DOI: 10.1016/j.scs.2020.102072.

Knapp, Kenneth R., H. J. Diamond, J. P. Kossin, M. C. Kruk, and C. J. Schreck (2018). *International Best Track Archive for Climate Stewardship (IBTrACS) Project, Version 4*. NOAA National Centers for Environmental Information. URL: doi:10.25921/82ty-9e16.

Knapp, Kenneth R., Michael C. Kruk, David H. Levinson, Howard J. Diamond, and Charles J. Neumann (Mar. 1, 2010). "The International Best Track Archive for Climate Stewardship (IBTrACS): Unifying Tropical Cyclone Data". In: *Bulletin of the American Meteorological Society* 91.3, pp. 363–376. ISSN: 0003-0007, 1520-0477. DOI: 10.1175/2009BAMS2755.1.

Koks, Elco E. (2022). *DamageScanner: Python tool for natural hazard damage assessments*. DOI: 10.5281/zenodo.2551015. URL: http://doi.org/10.5281/zenodo.2551015.

Koks, Elco E., Ben Dickens, and Tom Russell (Oct. 21, 2022). *Trade and tRAnsport Impact and fLow analysiS (TRAILS)*. Zenodo. DOI: 10.5281/zenodo.7234397.

Koks, Elco E., D. Le Bars, A.H Essenfelder, S. Nirandjan, and P. Sayers (Jan. 30, 2023). "The Impacts of Coastal Flooding and Sea Level Rise on Critical Infrastructure: A Novel Storyline Approach". In: *Sustainable* *and Resilient Infrastructure* 8 (sup1), pp. 237–261. ISSN: 2378-9689. DOI: 10.1080/23789689.2022.2142741.

Koks, Elco E., Julie Rozenberg, Mersedeh Tariverdi, Ben Dickens, Charles Fox, Kees van Ginkel, and Stephane Hallegatte (2023). "A Global Assessment of National Road Network Vulnerability". In: *Environmental Research: Infrastructure and Sustainability*. ISSN: 2634-4505. DOI: 10.1088/2634-4505/acd1aa.

Koks, Elco E., Julie Rozenberg, Conrad R. Zorn, M. Tariverdi, M. Vousdoukas, S. A. Fraser, Jim W. Hall, and S. Hallegatte (June 25, 2019). "A Global Multi-Hazard Risk Analysis of Road and Railway Infrastructure Assets". In: *Nature Communications* 10.1 (1), p. 2677. ISSN: 2041-1723. DOI: 10.1038/s41467-019-10442-3.

Koks, Elco E., Kees C. H. van Ginkel, Margreet J. E. van Marle, and Anne Lemnitzer (Nov. 29, 2022). "Brief Communication: Critical Infrastructure Impacts of the 2021 Mid-July Western European Flood Event". In: *Natural Hazards and Earth System Sciences* 22.12, pp. 3831–3838. ISSN: 1561-8633. DOI: 10.5194/nhess-22-3831-2022.

Kreienkamp, Frank, Sjoukje Y. Philip, Jordis S. Tradowsky, Philip Lorenz, Julie Arrighi, Alexandre Belleflamme, Sarah F. Kew, Andrew Ciavarella22, Lesley De Cruz13, Hylke de Vries2, Norbert Demuth, Andrew Ferrone17, Erich, M. Fischer6, Hayley J. Fowler14, Klaus Goergen16, Dorothy Heinrich, Yvonne Henrichs18, Geert Lenderink, Frank Kaspar, Enno Nilson15, Sonja Seneviratne, Roop K. Singh, , Amalie Skålevåg, Piet Termonia13,19, Lisa Thalheimer11, Maarten van, Aalst7,8,21, Joris Van den Bergh13, Hans Van de Vyver13, Stéphane Vannitsem13, Geert Jan van, Oldenborgh2,3, Bert Van Schaeybroeck13, Robert Vautard5, Demi Von, Niko Wanders, Thomas Bettmann18, Steven Caluwaerts, Steven Chan, Friederike E L Otto, and Francesco Ragone (Aug. 23, 2021). *Rapid Attribution of Heavy Rainfall Events Leading to the Severe Flooding in Western Europe during July 2021*. World Weather Attribution. URL: https://www.worldweatherattribution.org/wp-content/uploads/Scientific-report-Western-Europe-floods-2021-attribution.pdf.

Kröger, Wolfgang and Enrico Zio (2011). "Properties of Critical Infrastructures". In: *Vulnerable Systems*. Ed. by Wolfgang Kröger and Enrico Zio.

London: Springer, pp. 9–31. ISBN: 978-0-85729-655-9. DOI: 10.1007/978-0-85729-655-9_2.

Kropf, Chahan M., Alessio Ciullo, Laura Otth, Simona Meiler, Arun Rana, Emanuel Schmid, Jamie W. McCaughey, and David N. Bresch (Sept. 23, 2022). "Uncertainty and Sensitivity Analysis for Probabilistic Weather and Climate-Risk Modelling: An Implementation in CLIMADA v.3.1.0". In: *Geoscientific Model Development* 15.18, pp. 7177–7201. ISSN: 1991-959X. DOI: 10.5194/gmd-15-7177-2022.

Lan, Charles, Alec Wild, Ryan Paulik, Liam Wotherspoon, and Conrad R. Zorn (July 2023). "Assessing Indirect Impacts of Extreme Sea Level Flooding on Critical Infrastructure". In: *Journal of Marine Science and Engineering* 11.7 (7), p. 1420. ISSN: 2077-1312. DOI: 10.3390/jmse11071420.

Lee, Earl E., John E. Mitchell, and William A. Wallace (2009). "Network Flow Approaches for Analyzing and Managing Disruptions to Interdependent Infrastructure Systems". In: *Wiley Handbook of Science and Technology for Homeland Security*. American Cancer Society, pp. 1–9. ISBN: 978-0-470-08792-3. DOI: 10.1002/9780470087923.hhs686.

Lee II, E.E., J. E. Mitchell, and W. A. Wallace (Nov. 2007). "Restoration of Services in Interdependent Infrastructure Systems: A Network Flows Approach". In: *IEEE Transactions on Systems, Man, and Cybernetics, Part C (Applications and Reviews)* 37.6, pp. 1303–1317. ISSN: 1558-2442. DOI: 10.1109/TSMCC.2007.905859.

Lewin, Chris, Monica Rossi, Evangelia Soultani, and Kumar Sudheer Raj (2023). "Managing infrastructure resilience and adaptation". In: *Sustainable and Resilient Infrastructure*, pp. 1–17.

Li, Daqing, Qiong Zhang, Enrico Zio, Shlomo Havlin, and Rui Kang (2015). "Network reliability analysis based on percolation theory". In: *Reliability Engineering & System Safety* 142, pp. 556–562.

Liévanos, Raoul S and Christine Horne (2017). "Unequal resilience: The duration of electricity outages". In: *Energy Policy* 108, pp. 201–211.

Linkov, Igor, Cate Fox-Lent, Laura Read, Craig R. Allen, James C. Arnott, Emanuele Bellini, Jon Coaffee, Marie-Valentine Florin, Kirk Hatfield, Iain Hyde, William Hynes, Aleksandar Jovanovic, Roger Kasperson, John Katzenberger, Patrick W. Keys, James H. Lambert, Richard Moss, Peter S. Murdoch, Jose Palma-Oliveira, Roger S. Pulwarty, Dale Sands, Edward A. Thomas, Mari R. Tye, and David Woods (2018). "Tiered Approach to Resilience Assessment". In: *Risk Analysis* 38.9, pp. 1772–1780. ISSN: 1539-6924. DOI: 10.1111/risa.12991.

Loggins, Ryan A. and William A. Wallace (Dec. 1, 2015). "Rapid Assessment of Hurricane Damage and Disruption to Interdependent Civil Infrastructure Systems". In: *Journal of Infrastructure Systems* 21.4, p. 04015005. ISSN: 1943-555X. DOI: 10.1061/(ASCE)IS.1943-555X.0000249.

Lonergan, Katherine Emma, Salvatore Francesco Greco, and Giovanni Sansavini (2023). "Ensuring/insuring resilient energy system infrastructure". In: *Environment Systems and Decisions*, pp. 1–14.

Lonergan, Katherine Emma, Nicolas Suter, and Giovanni Sansavini (2023). "Energy systems modelling for just transitions". In: *Energy Policy* 183, p. 113791. ISSN: 0301-4215. DOI: https://doi.org/10.1016/j.enpol.2023.113791. URL: https://www.sciencedirect.com/science/article/pii/S0301421523003762.

Loreti, Simone, Enrico Ser-Giacomi, Andreas Zischg, Margreth Keiler, and Marc Barthelemy (Jan. 28, 2022). "Local Impacts on Road Networks and Access to Critical Locations during Extreme Floods". In: *Scientific Reports* 12.1 (1), p. 1552. ISSN: 2045-2322. DOI: 10.1038/s41598-022-04927-3.

Lu, Xiaoyan, Yanfei Zhong, and Liangpei Zhang (2022). "Open-Source Data-Driven Cross-Domain Road Detection From Very High Resolution Remote Sensing Imagery". In: *IEEE Transactions on Image Processing* 31, pp. 6847–6862.

Ludwig, Christina and Alexander Zipf (2019). "Exploring Regional Differences in the Representation of Urban Green Spaces in OpenStreetMap". In: *Geographical and Cultural Aspects of Geo-Information: Issues and Solutions*. AGILE 2019 Workshop. Cyprus.

Luiijf, Eric, Albert Nieuwenhuijs, Marieke Klaver, Michel van Eeten, and Edite Cruz (2009). "Empirical Findings on Critical Infrastructure Dependencies in Europe". In: *Critical Information Infrastructure Security*. Ed. by Roberto Setola and Stefan Geretshuber. Lecture Notes in Computer Science. Berlin, Heidelberg: Springer, pp. 302–310. ISBN: 978-3-642-03552-4. DOI: 10.1007/978-3-642-03552-4_28.

Lüthi, Samuel, Gabriela Aznar-Siguan, Christopher Fairless, and David N. Bresch (Nov. 25, 2021). "Globally Consistent Assessment of Economic Impacts of Wildfires in CLIMADA v2.2". In: *Geoscientific Model Development* 14.11, pp. 7175–7187. ISSN: 1991-959X. DOI: 10.5194/gmd-14-7175-2021.

Mahmoud, Hussam, Thomas Kirsch, Dan O'Neil, and Shelby Anderson (July 1, 2023). "The Resilience of Health Care Systems Following Major Disruptive Events: Current Practice and a Path Forward". In: *Reliability Engineering & System Safety* 235, p. 109264. ISSN: 0951-8320. DOI: 10.1016/j.ress.2023.109264.

Masoomi, Hassan, Henry Burton, Agam Tomar, and Ali Mosleh (May 1, 2020). "Simulation-Based Assessment of Postearthquake Functionality of Buildings with Disruptions to Cross-Dependent Utility Networks". In: *Journal of Structural Engineering* 146.5, p. 04020070. ISSN: 1943-541X. DOI: 10.1061/(ASCE)ST.1943-541X.0002555.

Mbungu, N. T., K. D. Milambo, M. W. Siti, R. C. Bansal, R. M Naidoo, T. P. Kamabu, F. T. Kiseya, D. H. Tungadio, M. K. Kayembe, and B. B. Banza (Oct. 1, 2023). "Assessing and Mapping Electricity Access Patterns in a Developing Country". In: *Energy Reports*. Proceedings of 2022 7th International Conference on Renewable Energy and Conservation 9, pp. 193–201. ISSN: 2352-4847. DOI: 10.1016/j.egyr.2023.08.080.

McKinsey Global Institute (Jan. 2020). *Climate Risk and Response. Physical Hazards and Socioeconomic Impacts.* URL: https://www.mckinsey.com/~/media/mckinsey/business%20functions/sustainability/our%20insights/climate%20risk%20and%20response%20physical%20hazards%20and%20socioeconomic%20impacts/mgi-climate-risk-and-response-full-report-vf.pdf.

Meiler, Simona, Alessio Ciullo, Chahan M. Kropf, Kerry Emanuel, and David Bresch (Mar. 30, 2023). *Unraveling Unknowns of Future Tropical Cyclone Risks.* DOI: 10.21203/rs.3.rs-2703613/v1. preprint.

Meiler, Simona, Thomas Vogt, Nadia Bloemendaal, Alessio Ciullo, Chia-Ying Lee, Suzana J. Camargo, Kerry Emanuel, and David N. Bresch (Oct. 18, 2022). "Intercomparison of Regional Loss Estimates from Global Synthetic Tropical Cyclone Models". In: *Nature Communications* 13.1 (1), p. 6156. ISSN: 2041-1723. DOI: 10.1038/s41467-022-33918-1.

Merkens, Jan-Ludolf, Lena Reimann, Jochen Hinkel, and Athanasios T. Vafeidis (Oct. 1, 2016). "Gridded Population Projections for the Coastal Zone under the Shared Socioeconomic Pathways". In: *Global and Planetary Change* 145, pp. 57–66. ISSN: 0921-8181. DOI: 10.1016/j.gloplacha.2016.08.009.

Messina, William A. Jr. (Sept. 2004). *An Assessment of Hurricane Charley's Impact on Cuba*. FE494. Department of Food and Resource Economics, Florida Cooperative Extension Service, UF/IFAS, University of Florida. URL: https://journals.flvc.org/edis/article/download/113260/108436/157271.

Met Office, IFRC, and other partners (Sept. 2020). *The Future of Forecasts: Impact-Based Forecasting for Early Actio*. URL: https://www.forecast-based-financing.org/wp-content/uploads/2020/09/Impact-based-forecasting-guide-2020.pdf.

MeteoSwiss, Federal Office of Meteorology and Climatology (2023). *Explanation of the danger levels - Wind*. URL: https://www.meteoschweiz.admin.ch/wetter/gefahren/erlaeuterungen-der-gefahrenstufen/wind.html.

Microsoft (Aug. 25, 2023). *GlobalMLBuildingFootprints*. Microsoft. URL: https://github.com/microsoft/GlobalMLBuildingFootprints.

Mitsova, Diana, Ann-Margaret Esnard, Alka Sapat, and Betty S. Lai (Nov. 1, 2018). "Socioeconomic Vulnerability and Electric Power Restoration Timelines in Florida: The Case of Hurricane Irma". In: *Natural Hazards* 94.2, pp. 689–709. ISSN: 1573-0840. DOI: 10.1007/s11069-018-3413-x.

Mitsova, Diana, Alka Sapat, Ann-Margaret Esnard, and Alberto J. Lamadrid (June 1, 2020). "Evaluating the Impact of Infrastructure Interdependencies on the Emergency Services Sector and Critical Support Functions Using an Expert Opinion Survey". In: *Journal of Infrastructure Systems* 26.2, p. 04020015. ISSN: 1943-555X. DOI: 10.1061/(ASCE)IS.1943-555X.0000548.

Montoya-Rincon, Juan P., Said A. Mejia-Manrique, Shams Azad, Masoud Ghandehari, Eric W. Harmsen, Reza Khanbilvardi, and Jorge E. Gonzalez-Cruz (July 31, 2023). "A Socio-Technical Approach for the Assessment of Critical Infrastructure System Vulnerability in Extreme Weather Events".

In: *Nature Energy*, pp. 1–11. ISSN: 2058-7546. DOI: 10.1038/s41560-023-01315-7.

Mooney, Elyssa L, Yasser Almoghathawi, and Kash Barker (2018). "Facility location for recovering systems of interdependent networks". In: *IEEE Systems Journal* 13.1, pp. 489–499.

Mühlhofer, Evelyn, Elco E. Koks, Chahan M. Kropf, Giovanni Sansavini, and David N. Bresch (June 1, 2023). "A Generalized Natural Hazard Risk Modelling Framework for Infrastructure Failure Cascades". In: *Reliability Engineering & System Safety* 234, p. 109194. ISSN: 0951-8320. DOI: 10.1016/j.ress.2023.109194.

Mühlhofer, Evelyn, Elco E. Koks, Lukas Riedel, and Chahan M. Kropf (June 26, 2023). *Osm-Flex/Osm-Flex: V1.0.1.* Zenodo. DOI: 10.5281/zenodo.8083066.

Mühlhofer, Evelyn, Chahan M. Kropf, Lukas Riedel, David N. Bresch, and Elco E. Koks (June 29, 2023). "OpenStreetMap for Multi-Faceted Climate Risk Assessments". In: *Environmental Research Communications* 6.1, p. 015005. DOI: https://doi.org/10.1088/2515-7620/ad15ab.

Mulholland, Eamonn and Luc Feyen (Jan. 1, 2021). "Increased Risk of Extreme Heat to European Roads and Railways with Global Warming". In: *Climate Risk Management* 34, p. 100365. ISSN: 2212-0963. DOI: 10.1016/j.crm.2021.100365.

Mutasa, Collen (Jan. 1, 2022). "Chapter 11 - Revisiting the Impacts of Tropical Cyclone Idai in Southern Africa". In: *Climate Impacts on Extreme Weather*. Ed. by Victor Ongoma and Hossein Tabari. Elsevier, pp. 175–189. ISBN: 978-0-323-88456-3. DOI: 10.1016/B978-0-323-88456-3.00012-5.

Nan, Cen and Giovanni Sansavini (Jan. 1, 2017). "A Quantitative Method for Assessing Resilience of Interdependent Infrastructures". In: *Reliability Engineering & System Safety* 157, pp. 35–53. ISSN: 0951-8320. DOI: 10.1016/j.ress.2016.08.013.

Naqvi, Asjad and Irene Monasterolo (Apr. 2019). *Natural Disasters, Cascading Losses, and Economic Complexity: A Multi-layer Behavioral Network Approach.* URL: https://epub.wu.ac.at/6914/.

Nicolas, Claire, Jun Rentschler, Albertine Potter van Loon, Sam Oguah, Amy Schweikert, Mark Deinert, Elco E. Koks, Christopher Arderne, Diana Cubas, Jie Li, and Eriko Ichikawa (June 2019). *Stronger Power: Improving Power Sector Resilience to Natural Hazards.* Washington, DC: World Bank. DOI: 10.1596/31910.

Niemeyer, Stefan and Peter Albisser (2001). *Lothar : der Orkan 1999 : Ereignisanalyse.* Birmensdorf: Eidg. Forschungsanstalt WSL. ISBN: 3-905620-93-6. URL: https://www.wsl.ch/de/projekte/sturm-lothar.html.

Nirandjan, Sadhana, Elco E. Koks, Philip J. Ward, and Jeroen C. J. H. Aerts (Apr. 1, 2022). "A Spatially-Explicit Harmonized Global Dataset of Critical Infrastructure". In: *Sci Data* 9.1 (1), p. 150. ISSN: 2052-4463. DOI: 10.1038/s41597-022-01218-4.

O'Neill, B. C., Elmar Kriegler, Keywan Riahi, Kristie L. Ebi, Stephane Hallegatte, Timothy R. Carter, Ritu Mathur, and Detlef P. van Vuuren (Feb. 1, 2014). "A New Scenario Framework for Climate Change Research: The Concept of Shared Socioeconomic Pathways". In: *Climatic Change* 122.3, pp. 387–400. ISSN: 1573-1480. DOI: 10.1007/s10584-013-0905-2.

O'Neill, B. C., M. van Aalst, Z. Zaiton Ibrahim, L. Berrang Ford, S. Bhadwal, H. Buhaug, D. Diaz, K. Frieler, M. Garschagen, A. Magnan, G. Midgley, A. Mirzabaev, A. Thomas, and R. Warren (2022). "Key Risks across Sectors and Regions". In: *Climate Change 2022: Impacts, Adaptation and Vulnerability. Contribution of Working Group II to the Sixth Assessment Report of the Intergovernmental Panel on Climate Change.* Ed. by H. O. Pörtner, D. C. Roberts, M. Tignor, E. S. Poloczanska, K. Mintenbeck, A. Alegría, M. Craig, S. Langsdorf, S. Löschke, V. Möller, A. Okem, and B. Rama. Cambridge, UK and New York, USA: Cambridge University Press, pp. 2411–2538. ISBN: 978-1-00-932584-4. DOI: 10.1017/9781009325844.025.2412.

Oh, Jung Eun, Xavier Espinet Alegre, Raghav Pant, Elco E. Koks, Tom Russell, Roald Schoenmakers, and Jim W. Hall (Sept. 1, 2019). "Addressing Climate Change in Transport". In: *Pathway to Resilient Transport* Volume 2. DOI: 10.1596/32412.

OpenStreetMap contributors (2023a). *OpenStreetMap Wiki.* URL: https://wiki.openstreetmap.org/wiki/Main_Page.

— (2023b). *Osmosis.* Version 0.48.3. URL: https://wiki.openstreetmap.org/wiki/Osmosis.

Otsu, Nobuyuki (Jan. 1979). “A Threshold Selection Method from Gray-Level Histograms”. In: *IEEE Transactions on Systems, Man, and Cybernetics* 9.1, pp. 62–66. ISSN: 2168-2909. DOI: 10.1109/TSMC.1979.4310076.

Otsuka, Akihiro (Oct. 1, 2019). “Natural Disasters and Electricity Consumption Behavior: A Case Study of the 2011 Great East Japan Earthquake”. In: *Asia-Pacific Journal of Regional Science* 3.3, pp. 887–910. ISSN: 2509-7954. DOI: 10.1007/s41685-019-00129-4.

Ouyang, Min (Jan. 1, 2014). “Review on Modeling and Simulation of Interdependent Critical Infrastructure Systems”. In: *Reliability Engineering & System Safety* 121, pp. 43–60. ISSN: 0951-8320. DOI: 10.1016/j.ress.2013.06.040.

Ouyang, Min and Leonardo Dueñas-Osorio (Nov. 1, 2011). “An Approach to Design Interface Topologies across Interdependent Urban Infrastructure Systems”. In: *Reliability Engineering & System Safety* 96.11, pp. 1462–1473. ISSN: 0951-8320. DOI: 10.1016/j.ress.2011.06.002.

Ouyang, Min, Liu Hong, Zi-Jun Mao, Ming-Hui Yu, and Fei Qi (May 1, 2009). “A Methodological Approach to Analyze Vulnerability of Interdependent Infrastructures”. In: *Simulation Modelling Practice and Theory* 17.5, pp. 817–828. ISSN: 1569-190X. DOI: 10.1016/j.simpat.2009.02.001.

Pagani, Marco, Vitor Silva, Anirudh Rao, Michele Simionato, and Kendra Johnson (2022). *The OpenQuake-engine User Manual. OpenQuake Manual for Engine Version 3.17.2*. Global Earthquake Model (GEM) Foundation. URL: 10.13117/GEM.OPENQUAKE.MAN.ENGINE.%203.17.2.

Pant, Raghav (2022). “Advances in Climate Adaptation Modeling of Infrastructure Networks”. In: *Climate Adaptation Modelling*. Ed. by Claus Kondrup, Paola Mercogliano, Francesco Bosello, Jaroslav Mysiak, Enrico Scoccimarro, Angela Rizzo, Rhian Ebrey, Marleen de Ruiter, Ad Jeuken, and Paul Watkiss. Springer Climate. Cham: Springer International Publishing, pp. 159–167. ISBN: 978-3-030-86211-4. DOI: 10.1007/978-3-030-86211-4_19.

Pant, Raghav, Jim W. Hall, and Simon P. Blainey (Jan. 1, 2016). “Vulnerability Assessment Framework for Interdependent Critical Infrastructures: Case-Study for Great Britain’s Rail Network”. In: *European Journal of*

Transport and Infrastructure Research 16.1 (1). ISSN: 1567-7141. DOI: 10.18757/ejtir.2016.16.1.3120.

Pant, Raghav, Jim W. Hall, and Scott Thacker (2017). "System-of-Systems Framework for Global Infrastructure Vulnerability Assessments". In: URL: https://www.greengrowthknowledge.org/sites/default/files/downloads/resource/System-of-systems%20framework%20for%20global%20infrastructure%20vulnerability%20assessments.pdf.

Pant, Raghav, Scott Thacker, Jim W. Hall, D. Alderson, and S. Barr (2018). "Critical Infrastructure Impact Assessment Due to Flood Exposure". In: *Journal of Flood Risk Management* 11.1, pp. 22–33. ISSN: 1753-318X. DOI: 10.1111/jfr3.12288.

Pant, Raghav, Conrad R. Zorn, Scott Thacker, and Jim W. Hall (2018). "Systemic resilience metrics for interdependent infrastructure networks". In: *6th International symposium on reliability engineering and risk management (6ISRERM), Singapore*, pp. 37–42.

Paulik, Ryan, Nick Horspool, Richard Woods, Nick Griffiths, Tim Beale, Christina Magill, Alec Wild, Benjamin Popovich, Glenn Walbran, and Russel Garlick (Sept. 17, 2022). "RiskScape: A Flexible Multi-Hazard Risk Modelling Engine". In: *Nat Hazards*. ISSN: 1573-0840. DOI: 10.1007/s11069-022-05593-4.

Petricola, Sami, Marcel Reinmuth, Sven Lautenbach, Charles Hatfield, and Alexander Zipf (Oct. 12, 2022). "Assessing Road Criticality and Loss of Healthcare Accessibility during Floods: The Case of Cyclone Idai, Mozambique 2019". In: *Int J Health Geogr* 21.1, p. 14. ISSN: 1476-072X. DOI: 10.1186/s12942-022-00315-2.

Pianosi, Francesca, Keith Beven, Jim Freer, Jim W. Hall, Jonathan Rougier, David B. Stephenson, and Thorsten Wagener (May 1, 2016). "Sensitivity Analysis of Environmental Models: A Systematic Review with Practical Workflow". In: *Environmental Modelling & Software* 79, pp. 214–232. ISSN: 1364-8152. DOI: 10.1016/j.envsoft.2016.02.008.

Pittore, M., P. Campalani, K. Renner, M. Plörer, and F. Tagliavini (Sept. 28, 2023). "Border-Independent Multi-Functional, Multi-Hazard Exposure Modelling in Alpine Regions". In: *Natural Hazards*. ISSN: 1573-0840. DOI: 10.1007/s11069-023-06134-3.

Poljansek, Karmen, Montserrat Marín Ferrer, Tom De Groeve, and Ian Clark (2017). *Science for Disaster Risk Management 2017: Knowing Better and Losing Less*. Report. ETH Zurich. DOI: 10.2788/842809.

Pörtner, H.-O., D.C. Roberts, H. Adams, I. Adelekan, C. Adler, R. Adrian, P. Aldunce, E. Ali, R. Ara Begum, B. Bednar- Friedl, R. Bezner Kerr, R. Biesbroek, J. Birkmann, K. Bowen, M.A. Caretta, J. Carnicer, E. Castellanos, T.S. Cheong, W. Chow, G. Cissé G. Cissé, and Z. Zaiton Ibrahim (2022). *Climate Change 2022: Impacts, Adaptation and Vulnerability*. Technical Summary. Cambridge, UK and New York, USA: Cambridge University Press, pp. 37–118. ISBN: 978-1-00-932584-4.

Potapov, Peter, Matthew C. Hansen, Amy Pickens, Andres Hernandez-Serna, Alexandra Tyukavina, Svetlana Turubanova, Viviana Zalles, Xinyuan Li, Ahmad Khan, Fred Stolle, Nancy Harris, Xiao-Peng Song, Antoine Baggett, Indrani Kommareddy, and Anil Kommareddy (2022). "The Global 2000-2020 Land Cover and Land Use Change Dataset Derived From the Landsat Archive: First Results". In: *Frontiers in Remote Sensing* 3. ISSN: 2673-6187. DOI: 10.3389/frsen.2022.856903. URL: https://www.frontiersin.org/articles/10.3389/frsen.2022.856903.

Price, Wayne T. and Caroline Glenn (Oct. 17, 2018). "Schools Closed across the Panhandle, 45,000 Kids Missing Class Due to Hurricane Michael". In: *Pensacola News Journal*. URL: https://www.pnj.com/story/news/2018/10/17/hurricane-michael-closes-schools-florida/1660289002/.

Prothi, Amit, Mona Chhabra Anand, and Ratnesh Kumar (Jan. 30, 2023). "Adaptive Pathways for Resilient Infrastructure in an Evolving Disasterscape". In: *Sustainable and Resilient Infrastructure* 8 (sup1), pp. 3–4. ISSN: 2378-9689. DOI: 10.1080/23789689.2022.2148951.

Raymond, Colin, Radley M. Horton, Jakob Zscheischler, Olivia Martius, Amir AghaKouchak, Jennifer Balch, Steven G. Bowen, Suzana J. Camargo, Jeremy Hess, Kai Kornhuber, Michael Oppenheimer, Alex C. Ruane, Thomas Wahl, and Kathleen White (June 15, 2020). "Understanding and Managing Connected Extreme Events". In: *Nature Climate Change*, pp. 1–11. ISSN: 1758-6798. DOI: 10.1038/s41558-020-0790-4.

Reimann, Lena, Elco E. Koks, Hans de Moel, Marijn Ton, and Jeroen C. J. H. Aerts (June 1, 2023). "An Empirical Social Vulnerability Map

('GlobE-SoVI') for Flood Risk Assessment at Global Scale". In: DOI: 10.5281/zenodo.7993886.

Rentschler, Jun, Johannes Braese, Nick Jones, and Paolo Avner (June 20, 2019). *Three Feet Under: Urban Jobs, Connectivity, and Infrastructure.* Policy Research Working Papers. The World Bank. 30 pp. DOI: 10.1596/1813-9450-8898.

Richter, H., C. Arthur, S. Schroeter, M. Wehner, J. Sexton, B. Ebert, M.A. Dunford, J. Kepert, Maguire, S., R.J. Hay, and M. Edwards (2018). *Impact-Based Forecasting for the Coastal Zone.* Geoscience Australia, Canberra. URL: https://ecat.ga.gov.au/geonetwork/srv/eng/catalog.search#/metadata/121858.

Rinaldi, S. M., J. P. Peerenboom, and T. K. Kelly (Dec. 2001). "Identifying, Understanding, and Analyzing Critical Infrastructure Interdependencies". In: *IEEE Control Systems Magazine* 21.6, pp. 11–25. ISSN: 1941-000X. DOI: 10.1109/37.969131.

Röösli, Thomas and David N. Bresch (Mar. 25, 2020). *Probabilistic Windstorm Hazard Event Set for Europe.* ETH Zurich. DOI: 10.3929/ethz-b-000406567.

Ruckelshaus, Mary, Borja G. Reguero, Katie Arkema, Roberto Guerrero Compeán, Khafi Weekes, Allison Bailey, and Jessica Silver (Dec. 1, 2020). "Harnessing New Data Technologies for Nature-Based Solutions in Assessing and Managing Risk in Coastal Zones". In: *International Journal of Disaster Risk Reduction* 51, p. 101795. ISSN: 2212-4209. DOI: 10.1016/j.ijdrr.2020.101795.

Sandhu, Himmat Singh and Siddhartha Raja (June 2019). *No Broken Link: The Vulnerability of Telecommunication Infrastructure to Natural Hazards.* Washington, DC: World Bank. DOI: 10.1596/31912.

Sauer, Inga J., Ronja Reese, Christian Otto, Tobias Geiger, Sven N. Willner, Benoit P. Guillod, David N. Bresch, and Katja Frieler (Apr. 9, 2021). "Climate Signals in River Flood Damages Emerge under Sound Regional Disaggregation". In: *Nature Communications* 12.1 (1), p. 2128. ISSN: 2041-1723. DOI: 10.1038/s41467-021-22153-9.

Schmid, Emanuel (2023). *CLIMADA Data API.* Version 2.0.0. URL: https://climada.ethz.ch/data-api/v2/docs.

Schotten, Roman and Daniel Bachmann (Apr. 13, 2023a). “Critical Infrastructure Network Modelling for Flood Risk Analyses: Approach and Proof of Concept in Accra, Ghana”. In: *Journal of Flood Risk Management*, e12913. ISSN: 1753-318X. DOI: 10.1111/jfr3.12913.

— (Jan. 2023b). “Integrating Critical Infrastructure Networks into Flood Risk Management”. In: *Sustainability* 15.6 (6), p. 5475. ISSN: 2071-1050. DOI: 10.3390/su15065475.

Severino, Luca G., Chahan M. Kropf, Hilla Afargan-Gerstman, Christopher Fairless, Andries Jan de Vries, Daniela I. V. Domeisen, and David N. Bresch (Feb. 14, 2023). “Projections and Uncertainties of Future Winter Windstorm Damage in Europe”. In: *EGUsphere*, pp. 1–31. DOI: 10.5194/egusphere-2023-205.

Sharma, Neetesh and Paolo Gardoni (Jan. 1, 2022). “Mathematical Modeling of Interdependent Infrastructure: An Object-Oriented Approach for Generalized Network-System Analysis”. In: *Reliability Engineering & System Safety* 217, p. 108042. ISSN: 0951-8320. DOI: 10.1016/j.ress.2021.108042.

Shepherd, Theodore G., Emily Boyd, Raphael A. Calel, Sandra C. Chapman, Suraje Dessai, Ioana M. Dima-West, Hayley J. Fowler, Rachel James, Douglas Maraun, Olivia Martius, Catherine A. Senior, Adam H. Sobel, David A. Stainforth, Simon F. B. Tett, Kevin E. Trenberth, Bart J. J. M. van den Hurk, Nicholas W. Watkins, Robert L. Wilby, and Dimitri A. Zenghelis (Dec. 1, 2018). “Storylines: An Alternative Approach to Representing Uncertainty in Physical Aspects of Climate Change”. In: *Climatic Change* 151.3, pp. 555–571. ISSN: 1573-1480. DOI: 10.1007/s10584-018-2317-9.

Souvignet, Maxime, Florian Wieneke, Lea Mueller, and David N. Bresch (2016). *Economics of Climate Adaptation (ECA) - Guidebook for Practitioners*, p. 100.

Stip, C., Z. Mao, G. Browder, L. Bonzanigo, and J. Tracy (2019). *Water Infrastructure Resilience – Examples of Dams, Wastewater Treatment Plants, and Water Supply and Sanitation Systems.* Sector note for LIFELINES: The Resilient Infrastructure Opportunity. Washington, DC: World Bank. URL: http://documents1.worldbank.org/curated/en/960111560794042138/pdf/Water-Infrastructure-Resilience-

Examples-of-Dams-Wastewater-Treatment-Plants-and-Water-Supply-and-Sanitation-Systems.pdf.

Stritih, Ana, Peter Bebi, Christian Rossi, and Adrienne Grêt-Regamey (Oct. 15, 2021). "Addressing Disturbance Risk to Mountain Forest Ecosystem Services". In: *Journal of Environmental Management* 296, p. 113188. ISSN: 0301-4797. DOI: 10.1016/j.jenvman.2021.113188.

Stürmer, Julian, Anton Plietzsch, Thomas Vogt, Frank Hellmann, Jürgen Kurths, Christian Otto, Katja Frieler, and Mehrnaz Anvari (Jan. 24, 2023). *Protecting the Texas Power Grid from Tropical Cyclones: Increasing Resilience by Protecting Critical Lines*. arXiv: 2301.13793 [physics]. URL: http://arxiv.org/abs/2301.13793. preprint.

SWD(2013)318 (2013). *SWD(2013)318 - COMMISSION STAFF WORKING DOCUMENT on a New Approach to the European Programme for Critical Infrastructure Protection Making European Critical Infrastructures More Secure*. European Commission. URL: https://ec.europa.eu/transparency/regdoc/?fuseaction=list&coteId=10102&year=2013&number=318&version=ALL&language=en.

Tabandeh, Armin, Neetesh Sharma, and Paolo Gardoni (Mar. 1, 2022). "Uncertainty Propagation in Risk and Resilience Analysis of Hierarchical Systems". In: *Reliability Engineering & System Safety* 219, p. 108208. ISSN: 0951-8320. DOI: 10.1016/j.ress.2021.108208.

Tariverdi, Mersedeh, Miguel Nunez-del-Prado, Nadezda Leonova, and Jun Rentschler (Jan. 28, 2023). "Measuring Accessibility to Public Services and Infrastructure Criticality for Disasters Risk Management". In: *Scientific Reports* 13.1 (1), p. 1569. ISSN: 2045-2322. DOI: 10.1038/s41598-023-28460-z.

Tellman, B., J. A. Sullivan, C. Kuhn, A. J. Kettner, C. S. Doyle, G. R. Brakenridge, T. A. Erickson, and D. A. Slayback (Aug. 2021). "Satellite Imaging Reveals Increased Proportion of Population Exposed to Floods". In: *Nature* 596.7870 (7870), pp. 80–86. ISSN: 1476-4687. DOI: 10.1038/s41586-021-03695-w.

Tenkanen, Henrikki (May 11, 2020). *Pyrosm - OpenStreetMap PBF Data Parser for Python*. Version v0.5.1/2. URL: https://pyrosm.readthedocs.io.

Thacker, Scott, Daniel Adshead, Marianne Fay, Stéphane Hallegatte, Mark Harvey, Hendrik Meller, Nicholas O'Regan, Julie Rozenberg, Graham Watkins, and Jim W. Hall (Apr. 2019). "Infrastructure for Sustainable Development". In: *Nature Sustainability* 2.4 (4), pp. 324–331. ISSN: 2398-9629. DOI: 10.1038/s41893-019-0256-8.

Thacker, Scott, Adshead, Daniel, Fantini, C., Palmer, R., Ghosal, R., Morgan G, Stratton-Short S., and Adeoti T. (2021). *Infrastructure for Climate Action*. Copenhagen, Denmark.: UNOPS. URL: https://www.unops.org/news-and-stories/news/infrastructure-for-climate-action.

Thacker, Scott, Raghav Pant, and Jim W. Hall (Nov. 1, 2017). "System-of-Systems Formulation and Disruption Analysis for Multi-Scale Critical National Infrastructures". In: *Reliability Engineering & System Safety*. Special Section: Applications of Probabilistic Graphical Models in Dependability, Diagnosis and Prognosis 167, pp. 30–41. ISSN: 0951-8320. DOI: 10.1016/j.ress.2017.04.023.

Tootaghaj, D. Z., N. Bartolini, H. Khamfroush, T. He, N. R. Chaudhuri, and T. L. Porta (June 2019). "Mitigation and Recovery From Cascading Failures in Interdependent Networks Under Uncertainty". In: *IEEE Transactions on Control of Network Systems* 6.2, pp. 501–514. ISSN: 2325-5870. DOI: 10.1109/TCNS.2018.2843168.

Topf, Jochen (Jan. 19, 2023). *Osmcode/Osmium-Tool*. Version 1.15.0. URL: osmcode.org/osmium-tool/.

Trejo, David and Paolo Gardoni (Jan. 30, 2023). "Special Issue on Adaptive Pathways for Resilient Infrastructure: An Introduction". In: *Sustainable and Resilient Infrastructure* 8 (sup1), pp. 1–2. ISSN: 2378-9689. DOI: 10.1080/23789689.2022.2139564.

UNDRR (2015). *Sendai Framework for Disaster Risk Reduction 2015-2030*. URL: https://www.undrr.org/publication/sendai-framework-disaster-risk-reduction-2015-2030.

— (2022). *Principles for Resilient Infrastructure*. United Nations Office for Disaster Risk Reduction. URL: https://www.undrr.org/publication/principles-resilient-infrastructure.

— (2023). *How to Make Infrastructure Resilient: The Handbook for Implementing the Principles for Resilient Infrastructure*. Office for Disaster

Risk Reduction (UNDRR). URL: https://www.undrr.org/media/87213/download?startDownload=true.

UNSTATS (July 18, 2023). *SDG Indicator Metadata. Indicator 1.4.1: Proportion of Population Living in Households with Access to Basic Services*. URL: https://unstats.un.org/sdgs/metadata/files/Metadata-01-04-01.pdf.

Van Ginkel, Kees C. H., Francesco Dottori, Lorenzo Alfieri, Luc Feyen, and Elco E. Koks (Mar. 15, 2021). "Flood Risk Assessment of the European Road Network". In: *Natural Hazards and Earth System Sciences* 21.3, pp. 1011–1027. ISSN: 1561-8633. DOI: 10.5194/nhess-21-1011-2021.

Velimirović, Lazar Z., Aleksandar Janjić, and Jelena D. Velimirović (2023). "Multi-Criteria Decision-Making Methods Based on Fuzzy Sets". In: *Multi-Criteria Decision Making for Smart Grid Design and Operation: A Society 5.0 Perspective*. Ed. by Lazar Z. Velimirović, Aleksandar Janjić, and Jelena D. Velimirović. Disruptive Technologies and Digital Transformations for Society 5.0. Singapore: Springer Nature, pp. 9–25. ISBN: 978-981-19767-7-3. DOI: 10.1007/978-981-19-7677-3_2.

Verschuur, Jasper, Elco E. Koks, and Jim W. Hall (July 27, 2022). "Ports' Criticality in International Trade and Global Supply-Chains". In: *Nature Communications* 13.1 (1), p. 4351. ISSN: 2041-1723. DOI: 10.1038/s41467-022-32070-0.

Verschuur, Jasper, Elco E. Koks, Sihan Li, and Jim W. Hall (Jan. 12, 2023). "Multi-Hazard Risk to Global Port Infrastructure and Resulting Trade and Logistics Losses". In: *Communications Earth & Environment* 4.1 (1), pp. 1–12. ISSN: 2662-4435. DOI: 10.1038/s43247-022-00656-7.

Virot, E., A. Ponomarenko, É. Dehandschoewercker, D. Quéré, and C. Clanet (Feb. 2, 2016). "Critical Wind Speed at Which Trees Break". In: *Phys. Rev. E* 93.2, p. 023001. DOI: 10.1103/PhysRevE.93.023001.

Wang, Weiping, Saini Yang, H. Eugene Stanley, and Jianxi Gao (May 15, 2019). "Local Floods Induce Large-Scale Abrupt Failures of Road Networks". In: *Nature Communications* 10.1 (1), p. 2114. ISSN: 2041-1723. DOI: 10.1038/s41467-019-10063-w.

Weber, Markus (Mar. 31, 2020). *Osmconvert*. Version 0.8.11. Nuernberg. URL: http://m.m.i24.cc/osmconvert.c.

Welker, Christoph, Thomas Röösli, and David N. Bresch (Apr. 23, 2020). "Comparing an Insurer's Perspective on Building Damages with Modelled Damages from Pan-European Winter Windstorm Event Sets: A Case Study from Zurich, Switzerland". In: *Natural Hazards and Earth System Sciences Discussions*, pp. 1–31. ISSN: 1561-8633. DOI: 10.5194/nhess-2020-115.

Wiher, Annina (Aug. 4, 2021). "The Social Impact of Infrastructure Failures Caused by a Natural Disaster Event". BA thesis. ETH Zurich.

Williamson, Clare, Cameron McCordic, and Brent Doberstein (Feb. 15, 2023). "The Compounding Impacts of Cyclone Idai and Their Implications for Urban Inequality". In: *International Journal of Disaster Risk Reduction* 86, p. 103526. ISSN: 2212-4209. DOI: 10.1016/j.ijdrr.2023.103526.

WorldPop (June 22, 2020). *Global 1km Population Total Adjusted to Match the Corresponding UNPD Estimate*. University of Southampton. DOI: 10.5258/SOTON/WP00671.

WorldPop and Center for International Earth Science Information Network (CIESIN), Columbia University (2020). *Global High Resolution Population Denominators Project*. University of Southampton. DOI: 10.5258/SOTON/WP00660.

Wu, Jie, Yang Chen, Zhen Liao, Xuejie Gao, Panmao Zhai, and Yamin Hu (2022). "Increasing risk from landfalling tropical cyclone-heatwave compound events to coastal and inland China". In: *Environmental Research Letters* 17.10, p. 105007.

Xie, Xuejing, Yi Zhou, Yongyang Xu, Yunbing Hu, and Chunling Wu (2019). "OpenStreetMap Data Quality Assessment via Deep Learning and Remote Sensing Imagery". In: *IEEE Access* 7, pp. 176884–176895. ISSN: 2169-3536. DOI: 10.1109/ACCESS.2019.2957825.

XinhuaNet (Feb. 12, 2019). "China Power Grid to Double Transmission Capacity to Hainan". In: *XinhuaNet*. URL: http://www.xinhuanet.com/english/2019-02/12/c_137816315.htm.

Yamazaki, Dai, Shinjiro Kanae, Hyungjun Kim, and Taikan Oki (2011). "A Physically Based Description of Floodplain Inundation Dynamics in a Global River Routing Model". In: *Water Resources Research* 47.4. ISSN: 1944-7973. DOI: 10.1029/2010WR009726.

Yesudian, Aaron N. and Richard J. Dawson (Jan. 1, 2021). "Global Analysis of Sea Level Rise Risk to Airports". In: *Climate Risk Management* 31, p. 100266. ISSN: 2212-0963. DOI: 10.1016/j.crm.2020.100266.

Yu, Dapeng, Jie Yin, Robert L. Wilby, Stuart N. Lane, Jeroen C. J. H. Aerts, Ning Lin, Min Liu, Hongyong Yuan, Jianguo Chen, Christel Prudhomme, Mingfu Guan, Avinoam Baruch, Charlie W. D. Johnson, Xi Tang, Lizhong Yu, and Shiyuan Xu (Sept. 2020). "Disruption of Emergency Response to Vulnerable Populations during Floods". In: *Nature Sustainability* 3.9 (9), pp. 728–736. ISSN: 2398-9629. DOI: 10.1038/s41893-020-0516-7.

Zhang, Yuheng, Qi Zhou, Maria Antonia Brovelli, and Wanjing Li (July 3, 2022). "Assessing OSM Building Completeness Using Population Data". In: *International Journal of Geographical Information Science* 36.7, pp. 1443–1466. ISSN: 1365-8816. DOI: 10.1080/13658816.2021.2023158.

Zheng, Guoxiong, Simon Keith Allen, Anming Bao, Juan Antonio Ballesteros-Cánovas, Matthias Huss, Guoqing Zhang, Junli Li, Ye Yuan, Liangliang Jiang, Tao Yu, Wenfeng Chen, and Markus Stoffel (May 2021). "Increasing Risk of Glacial Lake Outburst Floods from Future Third Pole Deglaciation". In: *Nat. Clim. Chang.* 11.5 (5), pp. 411–417. ISSN: 1758-6798. DOI: 10.1038/s41558-021-01028-3.

Zhou, Qi, Shuzhu Wang, and Yaoming Liu (Aug. 1, 2022). "Exploring the Accuracy and Completeness Patterns of Global Land-Cover/Land-Use Data in OpenStreetMap". In: *Applied Geography* 145, p. 102742. ISSN: 0143-6228. DOI: 10.1016/j.apgeog.2022.102742.

Zhou, Xiaoxin and Changyou Yan (July 2008). "A Blackout in Hainan Island Power System: Causes and Restoration Procedure". In: *2008 IEEE Power and Energy Society General Meeting - Conversion and Delivery of Electrical Energy in the 21st Century*. 2008 IEEE Power and Energy Society General Meeting - Conversion and Delivery of Electrical Energy in the 21st Century, pp. 1–5. DOI: 10.1109/PES.2008.4596582.

Zimba, Sydney Kadikula, Mário Jotamo Houane, and Alison Makosa Chikova (Aug. 2020). "Impact of Tropical Cyclone Idai on the Southern African Electric Power Grid". In: *2020 IEEE PES/IAS PowerAfrica*. 2020 IEEE PES/IAS PowerAfrica, pp. 1–5. DOI: 10.1109/PowerAfrica49420.2020.9219944.

Zimmerman, Rae and Carlos E. Restrepo (2006). "The next Step: Quantifying Infrastructure Interdependencies to Improve Security". In: *International Journal of Critical Infrastructures* 2.2/3, pp. 215–230. ISSN: 1475-3219. URL: https://econpapers.repec.org/article/idsijcist/v_3a2_3ay_3a2006_3ai_3a2_2f3_3ap_3a215-230.htm.

Zio, Enrico (Aug. 1, 2016). "Challenges in the Vulnerability and Risk Analysis of Critical Infrastructures". In: *Reliability Engineering & System Safety* 152, pp. 137–150. ISSN: 0951-8320. DOI: 10.1016/j.ress.2016.02.009.

Zischg, Andreas Paul, Veronika Röthlisberger, Markus Mosimann, Rahel Profico-Kaltenrieder, David N. Bresch, Sven Fuchs, Martina Kauzlaric, and Margreth Keiler (2021). "Evaluating Targeted Heuristics for Vulnerability Assessment in Flood Impact Model Chains". In: *Journal of Flood Risk Management* 14.4, e12736. ISSN: 1753-318X. DOI: 10.1111/jfr3.12736.

Zorn, Conrad R., Raghav Pant, Scott Thacker, and Asaad Y. Shamseldin (June 1, 2020). "Evaluating the Magnitude and Spatial Extent of Disruptions Across Interdependent National Infrastructure Networks". In: *ASCE-ASME J Risk and Uncert in Engrg Sys Part B Mech Engrg* 6.2. ISSN: 2332-9017. DOI: 10.1115/1.4046327.

Zorn, Conrad R. and Asaad Y. Shamseldin (Aug. 1, 2016). "Quantifying Directional Dependencies from Infrastructure Restoration Data". In: *Earthquake Spectra* 32.3, pp. 1363–1381. ISSN: 8755-2930. DOI: 10.1193/013015EQS015M.

Publications

Articles

Mühlhofer, E., E. E. Koks, C. M. Kropf, G. Sansavini, and D. N. Bresch, 2023: A generalized natural hazard risk modelling framework for infrastructure failure cascades. *Reliability Engineering & System Safety*, **234**, 109 194, doi:10.1016/j.ress.2023.109194

Mühlhofer, E., C. M. Kropf, D. N. Bresch and E. E. Koks, 2023: OpenStreetMap for multi-faceted climate risk assessments. *Environmental Research Communications*, doi:10.1088/2515-7620/ad15ab

Mühlhofer, E., D. N. Bresch and E. E. Koks, under review: Climate-resilient basic services? Unravelling dynamics of natural hazard-induced infrastructure disruptions across the globe. *One Earth*, url: `http://ssrn.com/abstract=4575341`

Conference Papers

Mühlhofer, E., E. E. Koks, and D. N. Bresch, 2022: Exploring Compound Event Impacts on Critical Infrastructures, Cascading Failures and Basic Service Disruptions, 61st ESReDA Seminar On Technological disruptions triggered by natural events: identification, characterization, and management, September 22 – 23 , 2022, Politecnico di Torino, Italy, doi:

Mühlhofer, E., Z. Stalhandske, M. Sarcinella, J. Schlumberger, D. N. Bresch, E. Koks, Supporting robust and climate-sensitive adaptation strategies for infrastructure networks: A multi-hazard case study on Mozambique's healthcare sector, 14th International Conference on Applications of Statistics and

Probability in Civil Engineering (ICASP14), Dublin, Ireland, 2023. doi: `https://doi.org/10.25546/103336`

Software

Mühlhofer, E., E. Koks, L. Riedel, and C. M. Kropf, 2023: osm-flex/osm-flex: v1.0.1. Zenodo, doi:10.5281/zenodo.8083066

Mühlhofer, E., under development: climada_petals/networks. `https://github.com/CLIMADA-project/climada_petals/tree/feature/nw_minimal`

Co-authored Articles

Schotten, R., E. Mühlhofer, G. A. Chatzistefanou, D. Bachmann, A. S. Chen, E. Koks, under review: Data for Critical Infrastructure Network Modelling of Natural Hazard Impacts: Needs and Influence on Model Characteristics. *Resilient Cities & Structures*

Verschuur, J., A. Fernandez Perez, E. Mühlhofer, S. Nirandjan, E. Borgomeo, O. Becher, A. Voskaki, E. J. Oughton; A. Stankovski, S. F. Greco, E. E. Koks, R. Pant, J. W. Hall, under review: Quantifying climate risks to infrastructure systems: a comparative review of developments across infrastructure sector. *PLOS Climate*

Bachmann, L., R. Lex, F. Regli, S. Voegeli, D. N. Bresch, E. Mühlhofer, C. M. Kropf, in preparation: Climate-resilient strategy planning using the SWOT methodology: A case study of the Japanese wind energy sector.

Friebel, F., P. Lobo, D. Neubauer, U. Lohmann, S. Drossaart van Dusseldorp, E. Mühlhofer, A. A. Mensah, 2019: Impact of isolated atmospheric aging processes on the cloud condensation nuclei activation of soot particles, *Atmos. Chem. Phys.*, **19**, 15545–15567, https://doi.org/10.5194/acp-19-15545-2019.

Talks & Posters

13-15 Jan. 2021	**Workshop on Compound Weather and Climate Events**	Critical infrastructures risk - a spatially explicit connected events perspective on crucial networks (Lightning Talk)
19–30 Apr. 2021	**EGU General Assembly**	Critical infrastructures in a multi-hazard environment: identifying globally consistent heuristics to model interdependencies (PICO presentation)
5-6 Oct. 2021	**Second International Conference on Natural Hazards and Risks in a Changing World**	Critical infrastructure failure cascades & basic service losses: A globally consistent model. (Poster)
8-9 Feb. 2022	**RISK KAN Workshop on Understanding and Modeling Complex Risks in Coupled Human-Environment Systems**	When the lights go out. Capturing basic service disruptions in a globally consistent natural hazard impact model (Talk)
23–27 May 2022	**EGU General Assembly**	Modelling Basic Service Disruptions from Post-Disaster Failure Cascades (Talk)
2 Jun. 2022	**Thematic focus group of Swiss NGOs on climate resilience**	Weather & Climate Risks – an (applied) academic view (Talk)
28 Aug. - 1. Sep. 2022	**32nd European Safety and Reliability Conference**	A Risk Modeller's Approach to Infrastructure Failure Cascades: From Natural Hazards to Basic Service Disruptions (Talk)
22-23 Sep. 2022	**61st ESReDA Seminar On Technological disruptions triggered by natural events**	Cascading Failures and Basic Service Disruptions - a Critical Infrastructure Perspective on Compound Events (Talk)
30 Mar. 2023	**Networking Event Series - Sustainable Finance Technology**	Open-source climate risk assessments – state of the art & challenges (Talk)
23–28 Apr. 2023	**EGU General Assembly**	Flood and Wind-Induced Basic Service Disruptions across the Globe - A Modelling Approach (Poster)
10-13 Jul. 2023	**ICASP14**	Adaptation strategies for infrastructure networks: A multi-hazard case study on Mozambique's healthcare sector (Talk)

CV

Evelyn Mühlhofer
PhD Candidate | MSc ETH MTEC

Ottikerstr. 4, 8006 Zürich, Switzerland +41 (0)79 919 95 36 *05.04.1994, Swiss & German citizen
eve.muehlhofer@gmail.com linkedin.com/in/evelyn-muehlhofer github.com/Evelyn-M

I'm a researcher with a strong quantitative background, interested in social and secondary impacts of weather and climate events. I enjoy developing open-source GIS tools as much as connecting scientific findings to the needs of stakeholders in public institutions and humanitarian organisations.

Education

Jun. 2020- Dec. 2023 — **Doctorate, Weather & Climate Risks Group (WCR), ETH Zurich**
Investigating cascading failures of infrastructure systems due to severe weather events and resulting basic service disruptions. Based on a globally consistent, spatially explicit complex network model combining open-source hazard, exposure and vulnerability data.
- Publication of scientific articles (see below)
- Development of GIS software (see below)

Sept. 2016 - Jan. 2019 — **Master of Science, Management, Technology and Economics (MTEC), ETH Zurich**
Expanding my studies on natural sciences (atmospheric and climate sciences) with lectures on risk modelling, micro and macroeconomics, econometrics and data science / Machine Learning. 5.5/6
- Master thesis: *Global Adaptation to Natural Hazards in NDCs: Quantifying the extent of adaptation actions and their alignment with global natural hazard risk using disaster data and probabilistic risk modelling*. 5.75/6

Sept. 2013 - Aug. 2016 — **Bachelor of Science, Interdisciplinary Sciences (phys.-chem.), ETH Zurich**
Fundamentals of mathematics, physics and chemistry, with a strong focus on interdisciplinary research and applied lab work. 4.8/6
- Semester projects in atmospheric physics and physical chemistry: *Assessing aerosol growth under atmospheric conditions; Programming an HSQC-NMR pulse sequence for measuring N-H coupling strength of fenols*
- Bachelor thesis in organic environmental chemistry: *Fate of antibiotics under photo-chemical degradation in aquatic areas* 5.75/6

Sept. 2011 - Aug. 2012 — **Assessment year, Law and Economics, University of St. Gallen (HSG)**
Fundamentals of civil, penal and constitutional law, micro and macro-economics and business management . 4.9/6
- Discontinued in favor of studies at ETH Zurich.

Sept. 2007 - Jun. 2011 — **Swiss Matura Diploma, , Kantonsschule Heerbrugg, St. Gallen**
Bilingual track (Spanish and English), specialization in mathematics. 5.6/6
- Honours for Maturity thesis and final exam grades.

Work Experience

Feb. 2024 - | **Scientific Collaborator, MeteoSwiss, Federal Office of Meteorology and Climatology**
- Implementation of an impact-based warning chain for severe weather events

Jun. 2020 - Dec. 2023 | **Scientific Assistant, WCR, ETH Zurich**
- Thesis supervision of students at Master and Bachelor level in the areas of impact-based warnings, natural hazard risks to the healthcare and education sectors, and restoration of services after disasters.
- Code review and active development of the CLIMADA risk assessment software.

Aug. 2019 - Jan. 2020 | **Scientific Intern, APPP, MeteoSwiss, Federal Office of Meteorology and Climatology**
- Contributing to the IT framework project *Data4Web*.
- Improving the scientific accuracy and computational efficiency of meteorological modules required for the public weather forecasting application of MeteoSwiss.
- Embedding micro-services, unit and integration testing into the processing pipeline.

Python | R | Docker | git

Feb. 2019 - Jul. 2019 | **Research Assistant, WCR, ETH Zurich**
- Parametrization of adaptation measures.
- Development of a landslide hazard module and a high-resolution exposure module for the CLIMADA risk modelling platform.
- Exchange with international organisations (GCF, UNFCCC) on the use of natural hazard risk modelling for climate information and early warning services.
- Invited speaker & UNFCCC-sponsored participant at the UN NAP Expo 2019 in Incheon, Korea.

Jun. 2017 - Dez. 2018 | **Monitoring & Evaluation Officer, HEKS/EPER, (NGO)**
- Design, evaluation and dissemination of learnings from impact attribution studies on development aid projects using semi-structured longitudinal survey data and statistical methods.
- Contributing to the internal project monitoring manual and statistical methods standards.
- Conducting a field study in Cluj, Romania, on the effectiveness of a social inclusion project.

Jan. 2015 - Jul. 2018 | **Research & Teaching Assistant, Env. Org. Chem & Development Economcis, ETH Zurich**
- Lead-TA for exercises classes in organic chemsistry (Prof. K. McNeil)
- Supporting the Center for Development & Cooperation (NADEL) and the chair of Development Economics (DEC, Prof. I. Günther) in teaching, research and administration.

Dec. 2016 - Feb. 2022 | **Teacher, German & Mathematics, Logos Lehrerteam**
- Giving preparatory classes for the high school entry exams to primary and secondary school children.

Publications & Supervision Activities

Mühlhofer, E., E. E. Koks, C. M. Kropf, G. Sansavini, and D. N. Bresch. 2023. *"A generalized natural hazard risk modelling framework for infrastructure failure cascades."* Reliability Engineering & System Safety, 234: 109194. `https://doi.org/10.1016/j.ress.2023.109194`

Mühlhofer, E., C. M. Kropf, L. Riedel, D. N. Bresch and E. E. Koks, in rev. *"OpenStreetMap for Multi-Faceted Climate Risk Assessments."* Environmental Research Communications: `https://doi.org/10.31223/X5SQ2J`

Mühlhofer, E., D. N. Bresch and E. E. Koks, in rev. *"Climate-resilient basic services? Unravelling dynamics of natural hazard-induced infrastructure disruptions across the globe."* One Earth: `http://ssrn.com/abstract=4575341`

OSM-flex — Software

github.com/osm-flex/osm-flex Documentation

A flexible and lightweight Python-based tool for data extraction from OpenStreetMap.

Python | Jupyter Notebook | git | html | PyPI

Master Thesis Dew Westra — Supervision

Including social vulnerability in critical infrastructure failure
A case study of the longest blackout in U.S. history

Bachelor Thesis Annina Wiher — Supervision

The Social Impact of Infrastructure Failures caused by a Natural Disaster Event

Bachelor Thesis Jakob Burkhardt — Supervision

Recovery of Critical Infrastructure after Natural Disasters

Master Thesis Michelle Ammann — Supervision

A Global Multi-Hazard Risk Assessment On Healthcare and Education Facilities

Master Thesis Gabriela Espejo — Supervision

Impact-Based Forecast for Critical Infrastructure During Tropical Cyclones

Language Skills

German	●●●●●
English	●●●●●
Spanish	●●●●○
French	●●●○○
Italian	●●○○○

IT Skills

Programming	Python, R, Matlab
Operating systems	Linux, Mac OS, Windows
Development tools	git, Visual Studio Code
Office	LaTeX, Microsoft Office

Extracurricular Activities

Sep. 2012 - Jun. 2013 | **Primary School Teacher, Cofradia Bilingual School, Cofradia, Honduras**
Voluntary teaching of a 3rd grade (all subjects) and development of a teaching curriculum.

Sep. 2014 - Sep. 2015 | **German Teacher, Solinetz, Zurich**
Voluntary German classes for refugees.

Hobbies

Sport: Climbing, Mountaineering, Road-Cycling
Other: Chess, Tango, Piano

References

Will be provided upon request.